Technical University of Crete
School of Chemical and
Environmental Engineering

FORTH
INSTITUTE OF GEOENERGY

Microbial communities of the Eastern Mediterranean and their hydrocarbon degradation capability

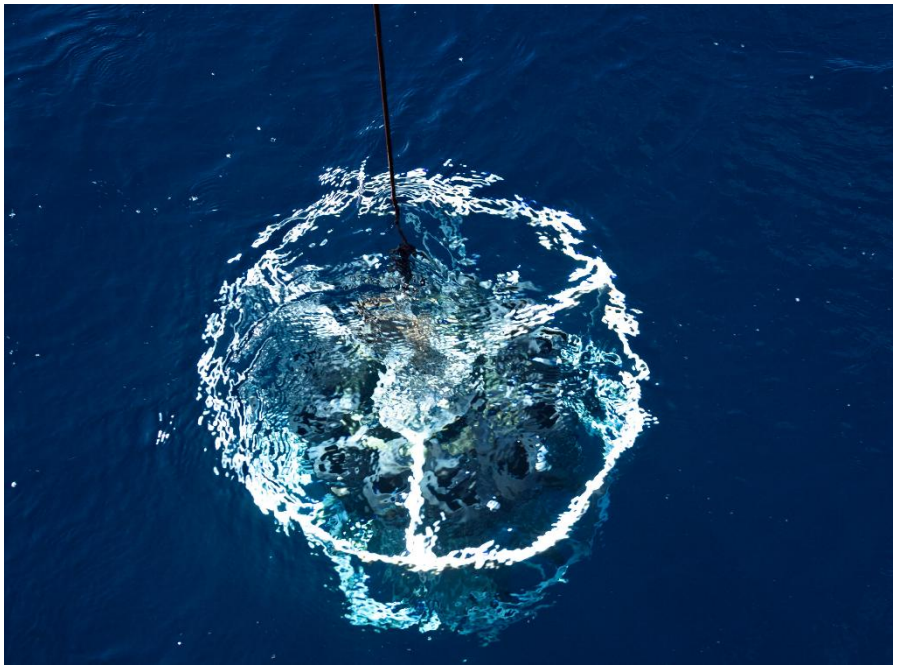

Charalampous Georgia

Biologist, MSc

H.F.R.I.
Hellenic Foundation for
Research & Innovation

GSRT
GENERAL SECRETARIAT FOR
RESEARCH AND TECHNOLOGY

July 2024

MICROBIAL COMMUNITIES OF THE EASTERN MEDITERRANEAN AND THEIR HYDROCARBON DEGRADATION CAPABILITY

ΜΙΚΡΟΒΙΑΚΕΣ ΚΟΙΝΟΤΗΤΕΣ ΤΗΣ ΑΝΑΤΟΛΙΚΗΣ ΜΕΣΟΓΕΙΟΥ ΚΑΙ Η ΔΥΝΑΤΟΤΗΤΑ ΤΟΥΣ ΣΤΗΝ ΑΠΟΔΟΜΗΣΗ ΥΔΡΟΓΟΝΑΝΘΡΑΚΩΝ

"This research was funded by the General Secretariat for Research and Technology (G.S.R.T.) and the Hellenic Foundation for Research and Innovation (H.F.R.I.) projects HEALMED (Grant No 1874) and DEEPSEA (Grant No 1510) under the "1st Call for H.F.R.I. Research Projects to support Post-Doctoral Researchers". Further funding was provided by the GSRT and HFRI project X-PRESS (Grant No 3604) under the "2nd Call for H.F.R.I.'s Research Projects to Support Faculty Members & Researchers."

School of Chemical and Environmental Engineering

Technical University of Crete

This PhD is dedicated to my daughter Zoi,

born and raised in a very challenging period for me.

Thesis committee

Nicolas Kalogerakis (Supervisor)

Professor Emeritus
School of Chemical and Environmental Engineering
Technical University of Crete

Konstantinos Kormas (Advisory Committee)

Professor
Department of Ichthyology and Aquatic Environment
University of Thessaly

Evangelia Gontikaki (Advisory Committee)

Assistant Researcher (Researcher, grade C)
Institute of Geoenergy
Foundation for Research and Technology Hellas

Nikos Pasadakis

Professor
School of Mineral Resources
Technical University of Crete

Danae Venieri

Professor
School of Chemical and Environmental Engineering
Technical University of Crete

Andreas Giotis

Assistant Professor
School of Mineral Resources
Technical University of Crete

Daniele Daffonchio

Professor
Biological, Environmental Sciences and Engineering Division
King Abdullah University of Science and Technology

Acknowledgements

First, I would like to express my gratitude to my supervisor, Professor Emeritus Nicolas Kalogerakis who gave me the opportunity to be a part of the BEEB lab since 2016, trusting me at my very early steps as a postgraduate researcher. Even though things did not always worked-out, the experience gained at his side was invaluable for this PhD thesis. It was an honour to work with him.

I would also like to thank my advisor, Professor Kostas Kormas for his valuable feedback, comments and advice on microbial ecology and our continuous communication even from the other side of the Atlantic.

A special gratitude must be given to Evina Gontikaki who was more than just a member of the advisory committee. For trusting me and giving me the opportunity to work in the HEALMED project as her PhD student. For her continuous guidance, support and patience all these years. Without her this PhD thesis would not be possible.

I would also like to thank the rest of my thesis committee, Professors Danae Venieri, Nikos Pasadakis, Andreas Giotis and Daniele Daffonchio for accepting the invitation to evaluate this dissertation.

A special thanks to the rest of the team. Eleftheria Antoniou and Dimitris Marinakis for all their help in the engineering part of high-pressure sampling and experimentation. To my partner in (PhD) crime, Voula Fragkou, for performing all the GC-MS analysis for all these experiments and for all her support and help wherever it was needed. This PhD thesis would be much more difficult without all of you.

A huge thank to all the members of the BEEB lab. Ariadni Pantidou for all the technical help she provided all these years. Life in the lab wouldn’t be equally fun without Evi Syranidou, Petroula Seridou and Katerina Karkanorachaki. Thank you for all your help and for the time spent together.

Furthermore, I should not miss to express the importance of the Hellenic Center for Marine Research (HCMR), the crew and members of R/V Aegaeo for the field expeditions and all their help in seawater sampling.

I must express my gratitude to the Hellenic Foundation for Research and Innovation (H.F.R.I.) and the General Secretariat for Research and Technology (G.S.R.T.) for their financial support through the projects HEALMED, DEEPSEA and X-PRESS.

Finally, I would like to thank my family and friends for all their support in any way they could all these years. Being abroad has not been easy yet I could always count on them. My life partner, Nikos, for his patience and tolerance with all the stressed-out moments and outbreaks I had. For always being supportive and trying to make things easier for me.

Abstract

The Eastern Mediterranean Sea (EMS) is a semi-enclosed basin, usually referred to as a "miniature ocean" because of the complex oceanic activities that take place there. Increased bottom sea temperatures, salinity levels and ultraoligotrophic conditions are some of its unique characteristics that shape microbial communities. This sub-basin of the Mediterranean Sea has become a hotspot for oil and gas activities in the recent decades. Large reservoirs have already been discovered and exploited in depths reaching ~1500m while several others, including ultra-deep marine areas, have been committed and are currently under exploration (South-Southwest Crete). In the aftermath of Deepwater Horizon (DWH) blowout in 2010, deep-sea oil biodegradation studies flourished providing the scientific community with valuable information about the fate of hydrocarbons (HC) in the deep sea, microbial succession patterns and key oil-degrading taxa. One of the major lessons learned from the DWH accident was the importance of conducting site-specific research under *in situ* conditions to provide policy makers with realistic data for the construction of efficient bioremediation protocols. The ongoing activities, which are progressing in deeper and more challenging waters, increase the risk for a potential oil spill accident in the deep EMS with many environmental and financial consequences for the surrounding countries.

This PhD thesis attempts to evaluate the microbial response and self-healing capability (natural attenuation) in the event of an accidental hydrocarbon release scenario in the deep EMS. For this purpose, seawater was retrieved from the EMS water column, down to 1000 m below sea level, in stations south of Crete (Cretan Passage) using Niskin bottles (decompressed) and a high-pressure sampling apparatus (*in situ* pressure). Hydrocarbon-biodegradation experiments were conducted in Erlenmeyer flasks and in high-pressure bottles or high-pressure bioreactor for incubations at 0.1MPa and 10MPa respectively, using Iranian light crude oil as carbon source. Data on microbial community analysis and hydrocarbon-degradation rates were produced via high throughput sequencing and GC-MS analysis.

Prior to any hydrocarbon exposure experiments, the synthesis of the pristine microbial community along with interspecies associations were analysed across the water column in this understudied marine region and background levels of known hydrocarbon degraders were recorded. Interestingly, even though natural seepages were not present near the sampling stations, notable abundances of taxa involved in oil bioremediation were found, especially in the

deep-water layers. The known hydrocarbonoclastic genus, *Alcanivorax*, was included in the significant nodes of the deep network.

Comparison of a timeseries hydrocarbon-degradation experiment at *in situ* temperature conditions between surface and deep EMS-collected microbial communities indicated that the latter (deep community) responded faster to oil contamination than the surface one despite the incubation at lower *in situ* temperature of 14 ºC. Furthermore, incubation of the deep consortium at a higher temperature of 25 ºC (for direct comparison with the surface community) did not affect oil biodegradation levels suggesting a microbial community that is acclimatized for HC biodegradation at the lower *in situ* temperature. Monitoring of microbial succession patterns resulted in different key hydrocarbon-degrading taxa in each treatment. The deep consortium at 14 ºC, was dominated primarily by the generalist *Vibrio* and substituted later on by the slow-growing specialist *Alcanivorax* whereas incubation at 25 ºC led to the dominance of *Pseudomonas* and *Pseudoalteromonas* in the deep community. On the other hand, the surface consortium was enriched in *Thalassospira*, *Halomonas*, *Alteromonas* and *Idiomarina* genera.

The efficacy of the deep EMS consortia in hydrocarbon bioremediation, was further tested under *in situ* high-pressure conditions. In particular, the impact of decompression was evaluated during deep-sea sampling and in enrichment incubations for the isolation of oil degraders. Decompression upon sampling resulted in a drastic decrease in deep microbial diversity. In addition, subjection of HC-degrading consortia for enrichment in ONR7 medium caused further decrease in biodiversity and taxa correlated with HC removal were outcompeted by *Pseudoalteromonas*, *Halomonas*, *Thalassomonas* and *Alcanivorax* which were favored under all treatments tested. Dispersant application had no significant effect in microbial community composition at any stage of the experimental process. Biodiversity loss impacted the community functionality in terms of biodegradation of the more recalcitrant oil compounds (PAHs, Heavy Alkanes). A strains of *Alcanivorax venustensis* (recently emended as *Alloalcanivorax venustensis*) that dominated the communities was isolated.

Furthermore, a deep EMS hydrocarbon plume emulation experiment was conducted under *in situ* EMS conditions to address primary microbial responders and succession patterns in the absence and presence of dispersant. Genera belonging to Gammaproteobacteria (*Oleispira*, *Thalassomonas*, *Thalassotalea*, *Ralstonia*) were among the first responders to oil-only contamination similarly to studies in the aftermath of the DWH accident. Those were then succeeded by *Alcanivorax* and *Methylophaga*, followed by *Marinobacter* and *Thalassospira* in the late phases of exposure to crude oil. The presence of dispersant favored members of

Bacteroidota along with *Hyphomonas* and *Alcanivorax*, with the latter dominating the community.

In conclusion, marine areas of interest for oil and gas exploration and exploitation (off-Crete) present a microbial “seed bank” of species related to hydrocarbon removal especially in deep-water layers. This could explain why the deep EMS community responds faster to oil contamination even though at lower temperature conditions than the surface consortium. Moreover, the results of this dissertation suggest an important role for *Alcanivorax* in hydrocarbon bioremediation in the deep EMS along with other known obligate oil degraders such as *Oleispira* and *Marinobacter*. Overall, this PhD thesis underlines the importance of maintaining *in situ* pressure and temperature conditions during sampling and experimentation when conducting experiments with deep-seawater microbial communities.

Περίληψη

Η Ανατολική Μεσόγειος (ΑΜ) είναι μια ημίκλειστη θαλάσσια λεκάνη με πολύπλοκες ωκεάνιες διεργασίες. Η αυξημένη θερμοκρασία στα βαθιά της νερά, τα υψηλά επίπεδα αλατότητας και οι υπερολιγοτροφικές συνθήκες είναι μερικά από τα μοναδικά χαρακτηριστικά της ΑΜ τα οποία επηρεάζουν την σύνθεση και τις μεταβολικές διεργασίες των μικροβιακων κοινοτήτων. Τις τελευταίες δεκαετίες, αυτή η περιοχή έχει αποκτήσει ιδιαίτερο ενδιαφέρον λόγω των ερευνών-εξορύξεων πετρελαίου και φυσικού αερίου. Μεγάλα υποθαλάσσια κοιτάσματα βρίσκονται ήδη υπό εκμετάλλευση σε βάθη ~1500 μέτρων από την επιφάνεια της θάλασσας, ενώ άλλες περιοχές, σε ακόμα μεγαλύτερα βάθη, έχουν δεσμευτεί και βρίσκονται ήδη υπό εξερεύνηση (Νότια-Νοτιοδυτικά της Κρήτης). Στον απόηχο του ατυχήματος του Deepwater Horizon (DWH) το 2010, πραγματοποιήθηκαν πολλές μελέτες βιοαποδόμησης πετρελαίου στα βαθιά νερά παρέχοντας πολύτιμες πληροφορίες σχετικά με την τύχη των υδρογονανθράκων (Υ/Α), τα μοτίβα μικροβιακής διαδοχής και ανέδειξαν σημαντικά είδη ως προς την αποδόμηση πετρελαίου. Ένα από τα σημαντικότερα διδάγματα του ατυχήματος DWH είναι η ανάγκη διεξαγωγής πειραμάτων αποδόμησης Υ/Α στις περιβαλλοντικές συνθήκες της περιοχής ενδιαφέροντος προκειμένου να καταγράφονται ρεαλιστικά δεδομένα που να μπορούν να χρησιμοποιηθούν για την δημιουργία αποτελεσματικών πρωτοκόλλων βιοαποκατάστασης. Οι συνεχιζόμενες δραστηριότητες στην ΑΜ, οι οποίες προχωρούν σε ολοένα και βαθύτερα ύδατα με αυξανόμενες τεχνικές δυσκολίες, ενισχύουν τον κίνδυνο για ένα ατύχημα έκλυσης υδρογονανθράκων με πολλές περιβαλλοντικές και οικονομικές συνέπειες για τις γύρω χώρες.

Αυτή η διδακτορική διατριβή επιχειρεί να αξιολογήσει την μικροβιακή απόκριση και την ικανότητα αυτοεξυγίανσης μέσω φυσικής εξασθένησης σε ένα ενδεχόμενο ατύχημα απελευθέρωσης υδρογονανθράκων στα βαθιά νερά της ΑΜ. Για το σκοπό αυτό, ανακτήθηκε θαλασσινό νερό από τη στήλη νερού της ΑΜ, μέχρι τα 1000 m, σε σταθμούς νότια της Κρήτης (Κρητικό Πέρασμα) με τη χρήση φιαλών Niskin (αποσυμπιεσμένο) και με συσκευή δειγματοληψίας υψηλής πίεσης (διατήρηση *in situ* πίεσης). Πειράματα βιοαποδόμησης υδρογονανθράκων διεξήχθησαν σε φλάσκες Erlenmeyer και σε δοχεία ή σε βιοαντιδραστήρα υψηλής πίεσης για επωάσεις στα 0,1 MPa και 10 MPa αντίστοιχα, χρησιμοποιώντας ελαφρύ Ιρανικό αργό πετρέλαιο ως πηγή άνθρακα. Δεδομένα σχετικά με την ανάλυση μικροβιακής κοινότητας και τους ρυθμούς αποδόμησης υδρογονανθράκων παρήχθησαν μέσω αλληλούχισης υψηλής απόδοσης και ανάλυσης αέριας χρωματογραφίας (GC-MS).

Πριν από οποιαδήποτε πειράματα έκθεσης σε υδρογονάνθρακες, η σύνθεση της φυσικής μικροβιακής κοινότητας και οι συσχετίσεις μεταξύ των ειδών αναλύθηκαν σε όλη τη στήλη του νερού σε αυτήν την θαλάσσια περιοχή που δεν έχει μελετηθεί σχεδόν καθόλου ενώ καταγράφηκαν και οι συγκεντρώσεις υπόβαθρου γνωστών αποδομητών Υ/Α. Ενδιαφέρον αποτελεί το γεγονός πως, παρόλο που δεν υπάρχουν φυσικές πηγές διαρροής Υ/Α κοντά στους σταθμούς δειγματοληψίας, εντοπίστηκαν αξιοσημείωτες αφθονίες μικροοργανισμών που εμπλέκονται στη βιοαποδόμηση του πετρελαίου ειδικά στα βαθύτερα ύδατα. Το είδος *Alcanivorax* εντοπίστηκε ανάμεσα στους σημαντικούς κόμβους του δικτύου συσχετίσεων στα βαθιά νερά της ΑΜ.

Η σύγκριση ενός πειράματος αποδόμησης Υ/Α σε συνθήκες *in situ* θερμοκρασίας μεταξύ επιφανειακών και βαθιών μικροβιακών κοινοτήτων της ΑΜ έδειξε ότι η βαθιά κοινότητα αποκρίθηκε ταχύτερα από την επιφανειακή στη μόλυνση του πετρελαίου παρά την επώαση της σε χαμηλότερη θερμοκρασία (14 ºC). Επιπλέον, η επώαση της βαθιάς μικροβιακής κοινότητας στους 25 ºC (για άμεση σύγκριση με την επιφανειακή) δεν επηρέασε τα επίπεδα βιοαποδόμησης πετρελαίου υποδηλώνοντας μια εγκλιματισμένη κοινότητα με ικανότητα βιοαποδόμησης Υ/Α στη χαμηλότερη *in situ* θερμοκρασία. Η ανάλυση των μοτίβων μικροβιακής διαδοχής ανέδειξε διαφορετικά είδη σε κάθε πειραματική επεξεργασία. Στη βαθιά κοινότητα που επωάστηκε στους 14 ºC, κυριάρχησε αρχικά το γένος *Vibrio* που αντικαταστάθηκε αργότερα από το *Alcanivorax*, ενώ η επώαση στους 25 ºC οδήγησε στην κυριαρχία των *Pseudomonas* και *Pseudoalteromonas* στη βαθιά κοινότητα. Από την άλλη, η επιφανειακή κοινότητα εμπλουτίστηκε στα γένη *Thalassospira, Halomonas, Alteromonas* και *Idiomarina*.

Η αποτελεσματικότητα της μικροβιακής κοινότητας από τα βαθιά νερά της ΑΜ στη βιοεξυγίανση υδρογονανθράκων, ελέγχθηκε περαιτέρω σε *in situ* συνθήκες υψηλής πίεσης. Ειδικότερα, αξιολογήθηκε ο αντίκτυπος της αποσυμπίεσης κατά τη δειγματοληψία από τα βαθιά ύδατα όπως και σε πειράματα εμπλουτισμού για την απομόνωση αποδομητών πετρελαίου. Η αποσυμπίεση κατά τη δειγματοληψία οδήγησε σε δραστική μείωση της μικροβιακής ποικιλότητας από τα βαθιά νερά. Επιπλέον, η υποβολή των εγκλιματισμένων κοινοτήτων στο μέσο ONR7 για τον εμπλουτισμό και την απομόνωση αποδομητών Υ/Α προκάλεσε περαιτέρω μείωση της ποικιλομορφίας της κοινότητας και την κυριαρχία των *Pseudoalteromonas, Halomonas, Thalassomonas* και *Alcanivorax* σε όλες τις πειραματικές επεξεργασίες. Η εφαρμογή του διασκορπιστικού μέσου δεν είχε σημαντική επίδραση στη μικροβιακή σύνθεση της κοινότητας σε οποιοδήποτε στάδιο της πειραματικής διαδικασίας. Η απώλεια βιοποικιλότητας επηρέασε την ικανότητα της κοινότητας ως προς την αποδόμηση των πιο

ανθεκτικών ενώσεων του πετρελαίου. Στέλεχος του είδους *Alcanivorax venustensis* (πρόσφατα τροποποιήθηκε σε *Alloalcanivorax venustensis*) που κυριαρχούσε στις κοινότητες απομονώθηκε στο τέλος του πειράματος.

Επιπλέον, διεξήχθη ένα πείραμα εξομοίωσης πλουμίου υδρογονανθράκων στη βαθιά θάλασσα σε *in situ* συνθήκες της ΑΜ για την διερεύνηση των μικροβιακων ειδών που αποκρίνονται πρώτα στην παρουσία πετρελαίου στη βαθιά θάλασσα καθώς και των μοτίβων διαδοχής απουσία και παρουσία διασκορπιστικού μέσου. Τα γένη που ανήκουν στα γ-Proteobacteria (*Oleispira, Thalassomonas, Thalassotalea, Ralstonia*) ήταν μεταξύ των πρώτων που αποκρίθηκαν στη μόλυνση, αντίστοιχα με τις μελέτες που πραγματοποιήθηκαν στον απόηχο του DWH. Στη συνέχεια, η κοινότητα εμπλουτίστηκε στα είδη *Alcanivorax* και *Methylophaga,* ενώ έπειτα ακολούθησε η ενίσχυση στα γένη *Marinobacter* και *Thalassospira* στις όψιμες φάσεις της έκθεσης στο αργό πετρέλαιο. Η παρουσία του διασκορπιστικού μέσου ευνόησε μικροοργανισμούς που ανήκουν στο φύλο Bacteroidota μαζί με τα γένη *Hyphomonas* και *Alcanivorax*, με το τελευταίο να κυριαρχεί στην κοινότητα.

Συμπερασματικά, οι θαλάσσιες περιοχές ενδιαφέροντος για εξερεύνηση και εκμετάλλευση πετρελαίου και φυσικού αερίου (νότια της Κρήτης) παρουσιάζουν φυσική παρουσία μικροβιακών ειδών που σχετίζονται με την απομάκρυνση υδρογονανθράκων ειδικά στα βαθιά νερά. Αυτό θα μπορούσε να ερμηνεύσει και το γεγονός πως η βαθιά μικροβιακή κοινότητα αποκρίνεται ταχύτερα στη ρύπανση πετρελαίου ακόμα και σε συνθήκες χαμηλότερης θερμοκρασίας από την αντίστοιχη επιφανειακή κοινότητα. Επιπλέον, τα αποτελέσματα αυτής της μελέτης υποδηλώνουν τον σημαντικό ρόλο του γένους *Alcanivorax* στη βιοξυγίανση υδρογονανθράκων στη βαθιά θάλασσα της Ανατολικής Μεσογείου μαζί με τα *Oleispira* και *Marinobacter*. Συνολικά, αυτή η διατριβή υπογραμμίζει τη σημασία της διατήρησης των περιβαλλοντικών συνθηκών πίεσης και θερμοκρασίας τόσο κατά τη δειγματοληψία όσο και κατά την διεξαγωγή πειραμάτων με μικροβιακές κοινότητες από τα βαθιά νερά.

Table of Contents

List of Figures

List of Tables

List of Abbreviations

Abbreviation	Definition
AIC	Akaike Information Criterion
ANOVA	Analysis of Variance
API	American Petroleum Institute
ASV	Amplicon Sequence Variant
AW	Atlantic Water
BN	Levin's niche breadth
BP	British Petroleum
CO	Crude Oil
CSS	Cumulative Sum Scaling
CTAB	Cetyltrimethylammonium bromide
CTD	Conductivity-Temperature-Depth
dbRDA	Distance-based Redundany Analysis
DCM	Dichloromethane
D-CO	Dispersed Crude Oil
DI	Deionized water
DISPOIL	Dispersed Oil experimental treatment
DMSO	Dimethyl sulfoxide
DNA	Deoxyribonucleic Acid
DO	Dissolved Oxygen
DOC	Dissolved Organic Carbon
DOR	Dispersant to Oil Ratio
DOSS	Dioctyl Sodium Sulfosuccinate
DWF	Deep Water Formation
DWH	Deepwater Horizon
EDTA	Ethylenediaminetetraacetic acid
EEZ	Exclusive Economic Zone
EIHE	Ecological Index of Hydrocarbon Exposure
EMDW	Eastern Mediterranean Deep Water
EMS	Eastern Mediterranean Sea
EMT	Eastern Mediterranean Transient
EPS	Exopolysaccharides
eSNCM	Endo-symbiotic non-constitutive mixotroph
EU	European Union
GA	Glutaraldehyde
GC-MS	Gas Chromatography-Mass Spectrometry
HC	Hydrocarbons
HCMR	Hellenic Center for Marine Research
HHP	High Hydrostatic Pressure
HP	Undisturbed high-pressure experimental treatment
HTS	High Throughput Sequencing

LIW	Levantine Intermediate Water
LO	Levin's Overlap
LOQ	Limit of Quantification
LSW	Levantine Surface Water
MA	Marine Agar
MAW	Modified Atlantic Water
MB	Marine broth
MEOR	Microbial Enhanced Oil Recovery
MOS	Marine Oil Snow
MOSSFA	Marine Oil Snow Sedimentation and Flocculent Accumulation
MP	Megapascal
MR	Mediterranean Ridge
NE	North-East
N:P	Nitrogen to Phosphate ratio
NSO	Nitrogen-Sulfur-Oxygen
OD	Optical Density
OHCB	Obligate Hydrocarbonoclastic Bacterium
OIL	Oil-only experimental treatment
OM	Organic Matter
ONR7	Artificial Seawater medium
OSCAR	Oil Spill Contingency and Response model
PAH	Polycyclic Aromatic Hydrocarbons
PCoA	Principal Coordinate Analysis
PCR	Polymerase Chain Reaction
PD	Phylogenetic Diversity
PERMANOVA	Permutational Analysis of Variance
PES	Polyethersulfone
PFA	Paraformaldehyde
PH	Phytane
PK	Proteinase K
PR	Pristane
REPRESS	Decompressed high-pressure experimental treatment
RNA	Ribonucleic acid
rRNA	ribosomal-Ribonucleic Acid
SDS	Sodium dodecyl sulfate
SPE	Solid-Phase Extraction
SSC	Side-scatter threshold
SSDI	Subsea Dispersant Injection
TCA	Trichloroacetic Acid
TE	Tris-Edta
TMH	Total Measured Hydrocarbons
TOC	Total Organic Compounds
TPH	Total Petroleum Hydrocarbons
VOC	Volatile Organic Compounds

WMDW	Western Mediterranean Deep Water
WMS	Western Mediterranean Sea

CHAPTER 1.

Introduction

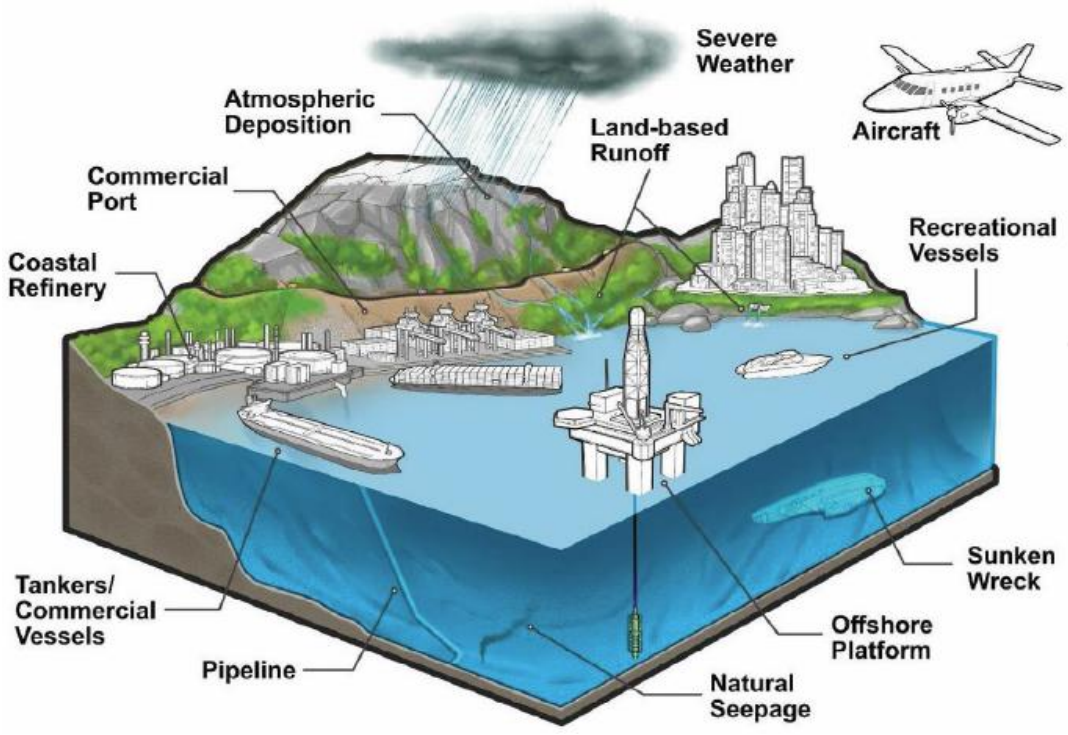

Figure 1. *Sources of hydrocarbon inputs in the marine environment* [1].

1.1 Hydrocarbon inputs in the marine ecosystem

1.1.1 Composition and properties of crude oil

Crude oil or petroleum is a very complicated liquid mixture of thousands or even millions of hydrocarbon (aliphatics and aromatics) and non-hydrocarbon (nickel, sulfur, oxygen, trace metals) substances [2]. It is formed by the long-term deposition and decomposition of organic material (plant, algae etc.), under anoxic conditions in the subsurface. Through diagenesis and catagenesis procedures, under the influence of geothermal heat flow and high pressure, this material is transformed into oil and gas migrating deeper in reservoirs (impermeable geological formations) [3, 4]. It consists of similar types of molecular compounds however, their exact chemical composition and quantities vary depending on location, depth, age and initial organic material [4]. The main crude-oil compound classes are described below [2].

- **Saturates:** this category includes alkanes with simple linear chains of CH_2 groups (n-alkanes), branched and isoprenoid alkanes (one or more alkyl groups) as well as cyclic and polycyclic alkanes (one ring or more). Some of the polycyclic alkanes are used as biomarkers (hopanes, steranes), because of their stability during weathering, in order to gather information on the origin of the oil. The simplest saturated hydrocarbon is methane (CH_4).

- **Aromatics:** these are categorized in single-ring (e.g. xylene, toluene, benzene) and multi-ring (e.g. naphthalene, phenanthrene, anthracene) aromatics. The simplest aromatic compound is benzene (C_6H_6). Single-ring or monoaromatics contain one hexagonal six-carbon ring with three double covalent bonds while multi-ring aromatics are generally known as polycyclic aromatic hydrocarbons (PAHs) that contain two or more fused aromatic rings. Both monoaromatics and PAHs are generally considered as toxic, mutagenic and carcinogenic and they are relatively persistent in nature. A typical crude oil comprises of ~1% aromatic compounds.

- **Resins and Asphaltenes:** Resins are high molecular weight non-hydrocarbon aromatic compounds that include nitrogen, sulfur or oxygen in their molecular structure, known as NSO compounds. Resins are soluble in light alkanes and polar (toluene, methanol)

solvents while Asphaltenes are the heaviest and most polar substances of the oil. Which are insoluble in alkane solvents but soluble in aromatic (e.g. benzene, toluene).

The chemical composition of crude oil determines its physical properties and categorizes it into light or heavy. The most common physical properties used to describe petroleum are density, viscosity, and boiling point. Typical classification of oils is based on density, expressed in American Petroleum Institute (API) gravity (Table 1).

Table 1. *Crude oil classification in API gravity* [3].

OIL TYPE	API GRAVITY*	EXAMPLES (API)	REFERENCES
Condensate	>45°	Agbami, Nigeria (48°)	Speight (2015)
Light oil	35°–45°	West Texas Intermediate (40°), Macondo (40°)	Speight (2015) Reddy et al. (2012)
Medium oil	25°–35°	Alaska North Slope (32°)	Speight (2015)
Heavy oil	15°–25°	Venezuela Heavy (17°)	Speight (2015)
Extra heavy oil	<15°	Tar sands: Orinoco, Venezuela (8°–12°), Athabasca, Canada (6°–10°)	Tissot and Welte (1984)

1.1.2 Routes of hydrocarbon flow in the sea

Crude oil enters the marine ecosystem through various routes as seen in Figure 1. A report of the National Academies of Sciences, Engineering and Medicine, *Oil in the Sea IV* estimates that land-based runoffs are the major source of oil input in the marine environment, 20-fold higher than two decades ago [1]. Hydrocarbons also enter the marine ecosystem naturally, through oil and gas natural seepages located in faults and fractures on the seabed [5]. The improvement of estimation methods and remote sensing suggests that approximately 100.000 metric tonnes of oil and 2-9 teragrams of gas are natively and slowly released in the deep sea [1]. However, a major input of hydrocarbons in the sea is attributed to accidental oil discharges from oil and gas activities (tankers, offshore platforms etc). As opposed to natural sources of hydrocarbons in the sea where oil flow is slow and the ecosystem has acclimatized to utilise these substances, in the case of an accidental oil spill, rapid discharge of hydrocarbons leads to sudden biodiversity loss and restoration occurs only after excess oil is removed [6]. Several such incidents have occurred in the past decades due to oil rig blowouts resulting in the release of extreme amounts of hydrocarbons in the sea (Deepwater Horizon, Ixtoc1) [7, 8]. In the aftermath of these disasters, significant progress in terms of regulations and advances in prevention and safety measures has been made to reduce the risk of such accidents to occur [9]. However, sea-

level rise and the intensification of weather phenomena due to climate change impact the offshore drilling platforms and aging infrastructure [10]. Furthermore, offshore drilling is progressing towards greater depths due to reservoir depletion in shallow waters with each 100 feet of added depth increasing the probability of an incident by 8.5% [11]. Taken together, the inherent risk for catastrophic well blowouts is increasing [12].

In the Mediterranean Sea, the busiest sea in the world, oil and gas inputs involve both natural and anthropogenic sources with shipping considered as the major source of oil pollution due to the intense use of this marine area in trading and transport [13]. From the total oil spilled in the Mediterranean Sea, the 2/3 have been estimated to occur in the eastern part of this basin, the Eastern Mediterranean Sea (EMS) [14]. Accidental spills from offshore oil and gas exploration and exploitation activities in the Mediterranean Sea were estimated to be less than 1% of the total oil pollution [15]. However, these activities have intensified through the years, with nearly half of the Mediterranean basin being licensed for offshore oil and gas operations [16].

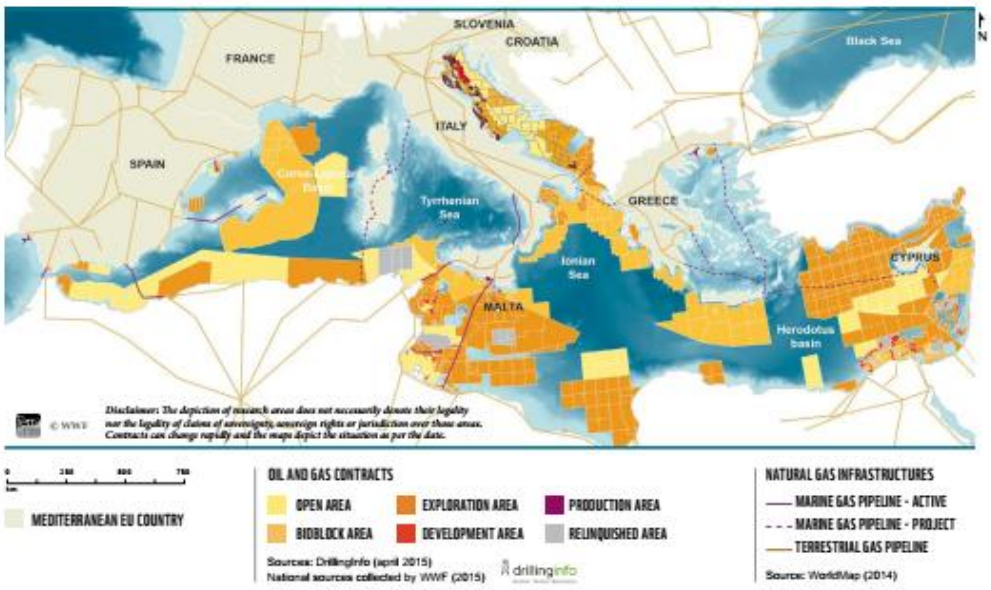

***Figure 2**. Offshore marine areas licensed for oil and gas exploration and exploitation* (2015) [16].

The identification of significant natural gas deposits in the EMS like those near Cyprus, Egypt and Israel (Tamar, Leviathan, Aphrodite, Zohr) in the past decade in combination with the necessity for a more sustainable and cleaner energy source as part of climate regulations for energy transition, have made the EMS an area of high interest for natural gas activities [15, 17, 18]. In this aspect, further marine areas in the EMS (Ionian Sea, South-Southwest Crete) have

been committed for exploration in extreme depths (>3000 meters). This generates a challenging condition for both exploration and production phases in these areas as they are highly seismogenic and in combination with large depths, the risks for accidental oil releases in the deep waters of the EMS are increasing.

1.2 Combating oil releases in the marine environment

Despite the technological advancements in offshore drilling operations and the improvements in the regulatory framework, accidents will continue to occur especially when these activities take place in more and more challenging waters [19]. A variety of response strategies have been developed through the years to mitigate oil releases in the sea [20]. Those include mechanical containment of the oil (booming, skimming), *in situ* burning and chemical application (dispersants) [21]. In the case of an oil spill accident, the most effective response measures are selected based on physical and chemical parameters of the oil as well as on the environmental conditions of the impacted area. For example, mechanical recovery of the oil might not be very effective in offshore waters due to high winds and waves in the sea. In addition, it involves more personnel and logistics and is therefore more suitable for coastal spills and marine areas sensitive to *in situ* burning and dispersants application [22].

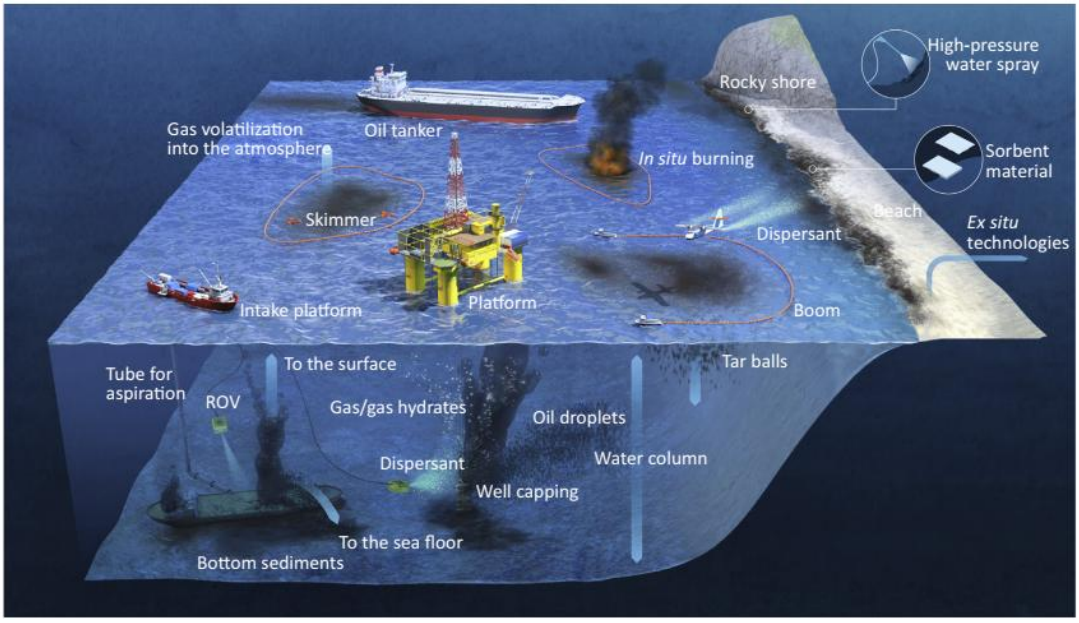

Figure 3. *Response technologies for combating oil releases in the sea* [21].

1.2.1 Chemical dispersants

Dispersants are considered an effective mitigation tool for combating hydrocarbon releases especially in remote marine areas [23]. This mixture of surfactants and solvents induces the natural dissolution of oil in seawater by decreasing the surface tension of the oil/water interface and thus generating small droplets (70-100uM) [20, 24]. Those can then migrate in the water column and depending on the oil composition, oil droplet size, microbial community composition and other environmental parameters (salinity, temperature, nutrients), affect oil biodegradation [25, 26]. However, despite their effectiveness in the field, their use is still controversial and their impact on microbial communities remains unclear [25, 27, 28].

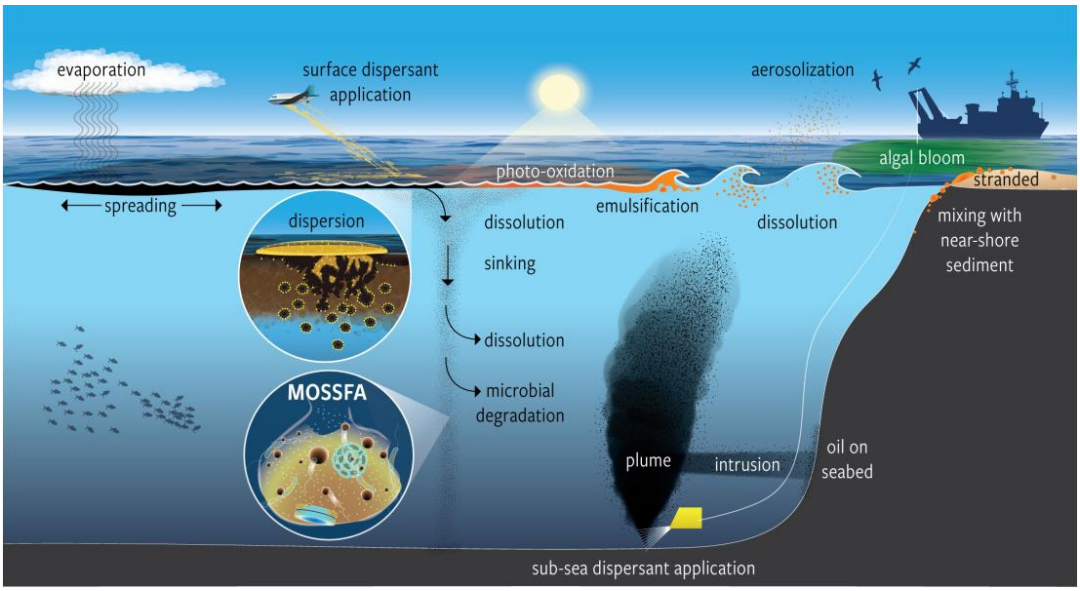

Figure 4. *Dispersant application and an overview of hydrocarbons fate in the marine environment* [27].

1.2.2 Natural Attenuation

The release of hydrocarbons in the sea triggers also natural processes (abiotic and biotic) that in the absence of human intervention, contribute to the decrease of the pollutant's concentration in the sea [29, 30]. Abiotic weathering procedures involve photo-oxidation, dissolution, spreading and evaporation that do not actually remove the oil but rather participate in its transformation, dissolution and transport. Microbial biodegradation on the other hand, is a slow yet very important bioremediation process that can eventually lead to the complete mineralization of hydrocarbons in the marine environment [31–33]. Furthermore, until today, it is the only available (bio)technology for the clean-up of hydrocarbons from the deep sea and its importance was highlighted during the deep oil spill accident of DWH. All these abiotic and

biotic natural processes can take from hours to years depending on the oil properties and environmental conditions [29, 34].

1.3 Microbial biodegradation: The ultimate fate of the oil

The release of hydrocarbons in the marine environment, either naturally or accidentally, triggers the bloom of microbial taxa that have the ability to grow on oil compounds. Those microorganisms belong to Bacteria, Archaea and Fungi and are part of the "rare biosphere" that becomes competitive upon exposure to hydrocarbons [35–37]. Their identification is crucial in order to understand how oil bioremediation, the ultimate mechanism for the cleanup of hydrocarbon pollutants, works and therefore assist policy makers in the build-up of response strategies in the case of an oil spill [38]. Bioremediation of crude oil occurs in all marine environments, aerobically (water column) or anaerobically (sediments) and involves the collective action of several microbes to completely mineralize the oil compounds [36]. Under anoxic conditions, HC biodegradation is feasible by the use of other electron acceptors (iron, sulfate, nitrate) yet it is considered to be a much more slower procedure than the one followed in the aerobic degradation pathway [39]. Biodegradation rates also vary depending on various physical parameters such as nutrient and oxygen availability, temperature and pressure as well as on the chemical characteristics of the oil [40]. For example, a light crude oil such as the one discharged from the Macondo well in the DWH accident (Light Luisiana Sweet crude oil), is more easily biodegraded by microorganisms than a heavier one that has more recalcitrant compounds like PAHs and asphaltenes.

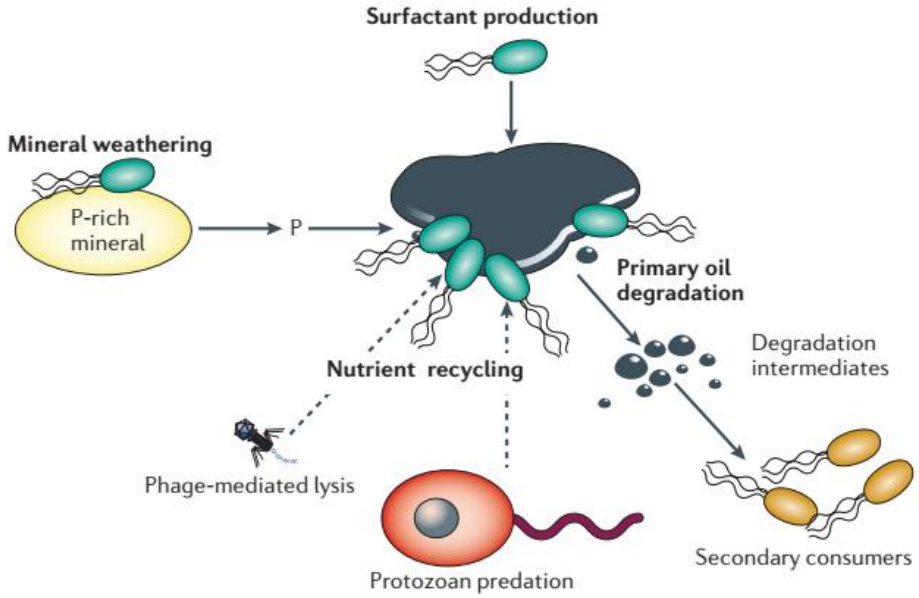

Figure 5. *A schematic representation of a microbial network involved in hydrocarbon degradation* [38].

1.3.1 Microorganisms capable of hydrocarbon degradation

Upon exposure to oil, hydrocarbon degraders flourish depending on the concentration and availability of the oil substrate they utilize and upon its depletion, other taxa are enriched that are capable of metabolizing the remaining oil compounds or secondary metabolites, thus building a functional microbial network that enhances oil bioremediation [36, 41]. Our insight on the diversity of HC-degraders increased dramatically after the DWH accident and due to the advancement of molecular techniques that allowed the identification of oil-degrading species in a culture-independent manner [42]. Common HC-degraders have been identified as members of the phyla Proteobacteria, Bacteroidetes and Actinobacteria while some of those were proposed by Yakimov et al to be specialized obligate hydrocarbon utilizers, the so-called OHCBs (Obligate Hydrocarbonoclastic Bacteria), like *Alcanivorax, Marinobacter, Oleispira, Oleiphilus, Cycloclasticus* and *Thalassolituus,* all members of the Gammaproteobacteria [42, 43]. Moreover, marine fungi have also been identified as efficient oil degraders like *Aspergillus* and *Cladosporium* however, they are far less studied than hydrocarbon-degrading bacteria [44, 45].

1.3.2 Metabolic pathways and enzymes involved in crude-oil degradation

Several enzymes and metabolic pathways are triggered upon exposure to hydrocarbons. Light has been shed on alkanes and aromatics aerobic degradation pathways that involves several oxygenases and peroxidases [46, 47]. The necessary primary breakdown of C-H bonds for low weight n-alkanes involves strong oxidizers like methane monoxygenases (particulate and soluble) and their homologues (propane monooxygenase, butane monooxygenase) that transform the alkane into a primary alcohol. Methane monooxygenases can oxidize up to C_5 n-alkanes (particulate) whereas their soluble form can act on linear alkanes up to C_8, branched alkanes and cycloalkanes [36]. Mid-chain alkanes (C_5-C_{16}) are oxidized by AlkB monooxygenases and P450 cytochrome enzymes both highly diverse and commonly found together in hydrocarbon-degrading bacteria. Whereas the long-chain alkanes involve other monooxygenases like AlmA found in *Acinetobacter, Alcanivorax, Marinobacter* and *Parvibaculum* and can oxidize n-alkanes >C_{32}. LadA enzyme is also another long-chain alkane monooxygenase that can act on C_{15}-C_{36} n-alkanes [48, 49]. An alcohol dehydrogenase oxidizes the alcohol into an aldehyde which is then oxidized into fatty acids via an aldehyde dehydrogenase. The fatty acids are then subjected to beta-oxidation pathway that leads to the formation of phospholipids to be incorporate in the cellular membrane or to be used in the secondary metabolism for the synthesis of biosurfactants.

In the case of aerobic aromatic degradation toluene mono-/di- oxygenases as well as xylene, benzene monooxygenases and naphthalene, pyrene dioxygenases participate in the primary oxidation steps for ring cleavage and the formation of substrates that are subsequently fed in the TCA cycle [36, 47].

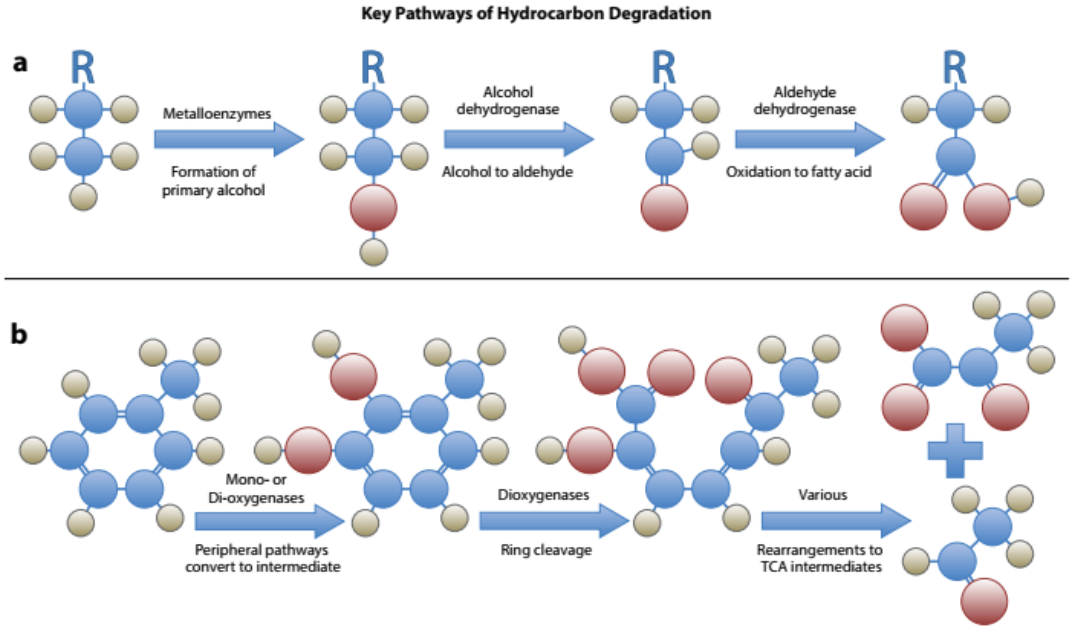

Figure 6. *Microbial degradation pathways followed for (a) alkanes and (b) the aromatic compound, toluene* [36].

1.3.3 Bioremediation technologies

Natural attenuation is considered an intrinsic bioremediation technology that can be enhanced by biostimulation and bioaugmentation, two known engineered bioremediation approaches used for the clean-up of oil-polluted sites [50]. Biostimulation involves the addition of inorganic nutrients (nitrogen, phosphorus, biosurfactants) whereas bioaugmentation contributes in the increase of hydrocarbon-removal rates via inoculation of specialised oil-degrading microorganisms and thus gene pools to mitigate pollution [51, 52]. Autochthonous bioaugmentation (ABA) has been proposed as a bioremediation technology that utilizes exclusively microbial species that are indigenous to the site of pollution and thus limiting the environmental adaptation effects of the contaminated site [53, 54]. Research studies indicated that the use of a microbial consortium instead of a single strain has a better hydrocarbon-removal capacity [55, 56]. However, there are also studies that challenge bioaugmentation as an efficient bioremediation approach [57].

1.4 The disaster of DWH deep-sea oil spill

On the 20th of April 2010, British Petroleum (BP) offshore oil drilling platform exploded in the Gulf of Mexico, 66km off the Louisiana coast, resulting in the death of 11 individuals and in the most catastrophic oil spill ever recorded in the deep sea until today [58]. Live crude was jetting uncontrollably at 1500m depth for a total of 87 days till the wellhead was fully capped and by that time, unprecedented amounts of hydrocarbons were released in the marine ecosystem [59]. In particular, approximately 700,000 metric tonnes of crude oil and 250,000 metric tonnes of natural gas were released impacting in total 11,000 km^2 of ocean surface and 2,000 km of coastline [60, 61]. Twenty-five days after the blowout, Corexit 9527A and Corexit 9500A were applied as a response measure, at sea surface and for the first time, chemical dispersants were introduced in the deep sea, directly at the damaged well. It has been estimated that a total of $4{,}1\times10^6$ and $2{,}9\times10^6$ litres of dispersant were sprayed to the sea surface and injected at the wellhead, respectively [62]. Overall, the DWH blowout presented unique aspects compared to other marine oil spills. Research on the fate of released hydrocarbons and microbial responses flourished making this the most studied oil spill in the world [61, 63].

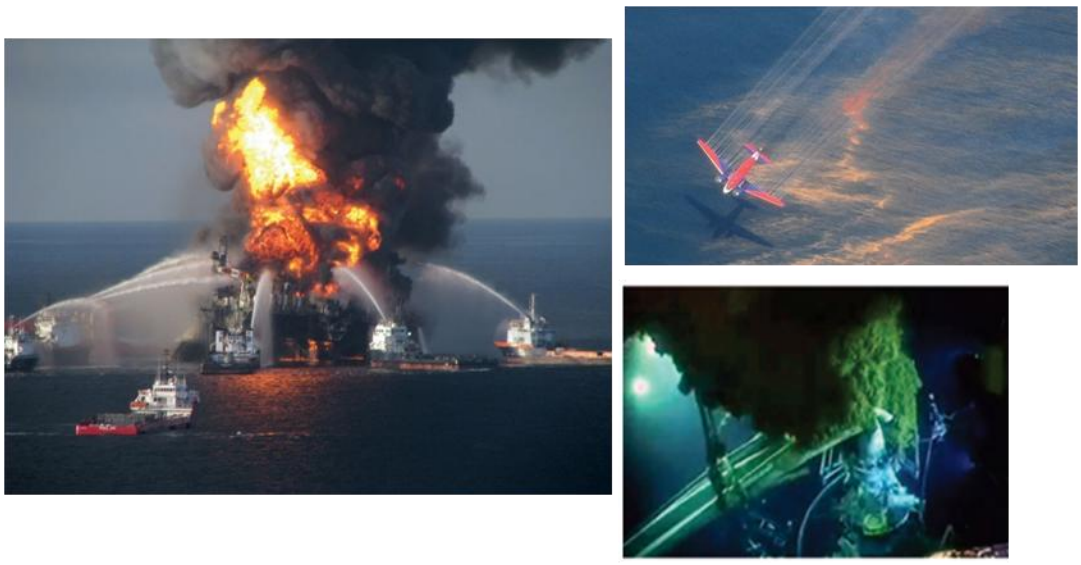

Figure 7. *The accident of Deepwater Horizon and dispersant application (aerial and subsea.)*

1.4.1 The fate of discharged oil in the aftermath of DWH

The discharged oil (Luisiana Light Sweet crude oil) mixture from the Macondo well consisted of 74% saturated hydrocarbons, 16% aromatics (including PAHs) and 10% polar compounds. Light hydrocarbons (C_1-C_5) comprised the 24% of the oil and from those the 60% was methane [59, 64]. From the total hydrocarbons released during DWH, 25% was recovered or

burned, 5-15% was evaporated and the rest was dissolved, spread or sedimented [65]. Research studies suggested that approximately all of the discharged gas (methane) and half of the released crude oil (alkanes, low molecular weight aromatics) were entrained in the water column [66–68]. Subsea application of dispersants reduced the emerging of oil by ~7% and the vaporization of volatile hydrocarbons by ~26% as estimated in a modelling study by French-McKay [69]. The *in situ* environmental conditions existing in the jetting area in combination with dispersant application resulted in the formation of hydrocarbon plumes which expanded at several depths of the water column, with the deepest found at 1000-1200m [70]. Due to the lack of actual field data, microbial oxidation of hydrocarbons was based mainly on deepwater oxygen anomalies [71–73]. Estimations suggested that the 43-61% of the total released oil was removed through biodegradation, underlining the important role of microbial communities in bioremediation of the DWH oil spill [60, 74]. Moreover, microbial attachment on the surface oil slick and on naturally or chemically dispersed oil droplets in the deep plume led to the secretion of exopolymeric substances (EPS) and the formation of biofilms by microorganisms. This mixture of oil, dispersant, microbes and EPS, termed marine oil snow (MOS), migrated deeper in the water column and reached the seabed due to gravitational forces [27, 75]. This marine oil snow sedimentation and flocculent accumulation (MOSSFA) event accounted for the 14% of the total oil released [76].

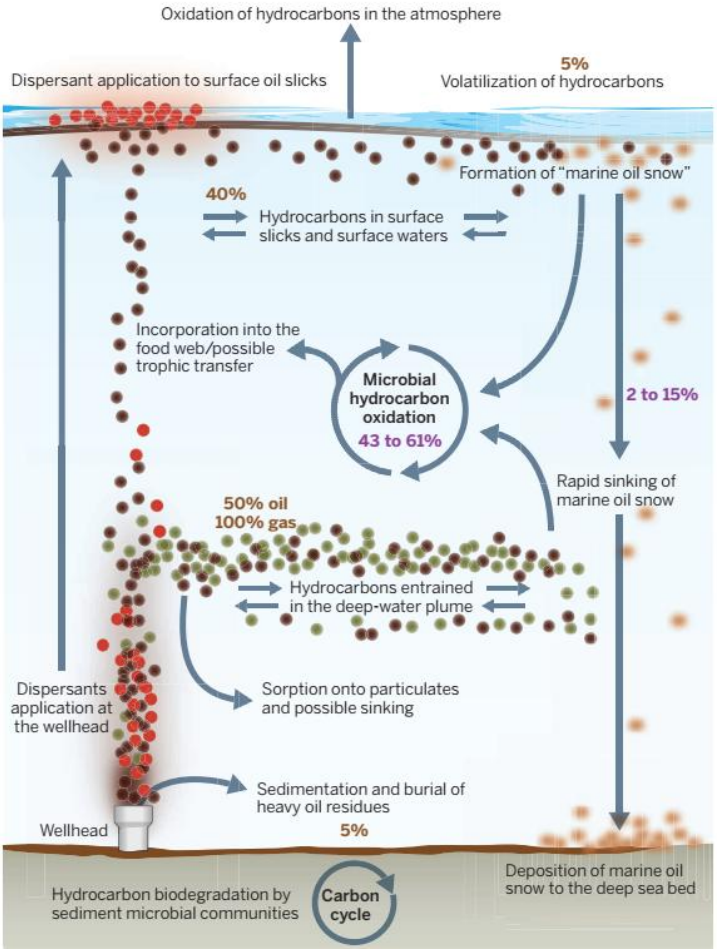

Figure 8. *Fate of hydrocarbons released during Deepwater Horizon in 2010* [60].

1.4.2 Microbial response to oil contamination in the Gulf of Mexico

The novelty of a deep-sea oil plume formation in DWH incident, drove the majority of studies to investigate the microbial response in the subsurface intrusion layer and comparatively fewer studies were conducted at the surface layer [61]. Nonetheless, these studies suggest that a small oil fraction at the sea surface was biodegraded however, the lack of nutrients and particularly of phosphorus in these waters prevented the formation of blooms [77, 78]. Moreover, the surface microbial community was significantly different to that in the deep plume during the same time frame (May-June 2010) [42, 79, 80]. In particular, the surface consortium was abundant in photosynthetic taxa like Cyanobacteria and members of Alphaproteobacteria (Rhodospirillales, Rhodobacterales) in the presence of oil sheens. Instead, in thicker oil surface layers microbial taxa that belong to Gammaproteobacteria (*Pseudomonas*, *Pseudoalteromonas*, *Alteromonas* etc) were favored [79].

Unlike surface waters in the Gulf of Mexico, the deep plume has increased levels of nutrients and thus microbial blooms occurred in the presence of hydrocarbons [61]. Elevated microbial densities were recorded compared to pristine waters adjacent to the plume and metagenomic-metatranscriptomic analysis revealed the microbial succession patterns in the deep oil-intrusion layer linking their abundance with the availability of hydrocarbon compounds [81–83]. The entrapment of methane in the water column led to the rapid response of methanotrophic populations (*Methylococcaceae*) that reduced methane concentrations and contributed significantly in the plume's oxygen anomaly [73]. Moreover, the early response phase of the DWH spill, involved members of Oceanospirillales, known in alkane degradation, followed later on by *Cycloclasticus* and *Colwellia* [81–83]. Laboratory experiments simulating the DWH plume, identified *Bermanella*, a member of Oceanospirillales that utilizes low- and mid- chain n-alkanes [84, 85]. *Bermanella* comprised more than 33% of the microbial community during the first week of the incubation however, when alkane levels dropped, the microbial community shifted to *Cycloclasticus* and *Colwellia* that correlated with the degradation of aromatic compounds [85]. *Cycloclasticus* have been found to utilize BTEX and some PAHs whereas other studies identified *Colwellia* participating in the degradation of natural gas hydrocarbons (ethane,

butane, and propane) and of dispersant compounds (DOSS) [80, 86]. After complete capture of the well in July 2010 and the termination of oil flow in the sea, the deep plume community was enriched in Flavobacteria, *Alteromonadaceae, Rhodobacteraceae* and *Methylophaga* commonly involved in secondary metabolism and organic matter degradation possibly due to the presence of marine oil snow [73, 80, 83, 87].

1.4.3 Subsea dispersant injection and its influence on microbial communities

Dispersants have been applied more than 200 times worldwide at the sea surface, prior to the Deepwater Horizon (DWH) accident [88]. However, the DWH blowout in 2010 marked the first application of dispersants in the deep sea (~1500 meters) to reduce the emergence of oil at the sea surface, minimize the exposure of emergency responders to volatile organic compounds (VOCs) and thus allow vessel operations to close the jetting well [89, 90]. This technique termed as subsea dispersant injection (SSDI), in combination with the rapid jetting rate of the well facilitated the formation of hydrocarbon plumes in the water column, the deepest found near the jetting well and extending for more than 35km [70, 91]. The COREXIT class of dispersants which were applied during the DWH incident comprised of anionic (DOSS) and non-ionic (Tween 80, Tween 85 and Span 80) surfactants mixed with propylene glycol and hydrocarbon solvents [86, 92].

Corexit 9500A, the dispersant which was applied in the deep sea, affected the microbial response however until today, its impact remains unclear [23]. For example, dispersants may enhance biodegradation physically by decreasing the oil droplet size and therefore favor microbial attachment however, their direct application might inhibit microbial response to oil or might cause antagonistic effects between oil and dispersant degradation and thus decrease HC removal [24, 65]. Some studies found the use of dispersants to be beneficial by inducing hydrocarbon-degradation rates such as that of Baelum et al which even in the presence of very high dispersant to oil ratio (DOR), HC removal was increased from 25% to 60% without any significant changes in microbial community structure [93]. Nonetheless, the same study refers to the slow degradation of DOSS compound indicating its persistence in seawater at these dispersant concentrations. Similarly, in microcosm experiments where DOR was lower (1:25) and similar to that applied during the DWH, alkane degradation was enhanced and DOSS was efficiently removed at 25 ºC [94].

Other studies suggested that dispersant had no significant effect or that their application exerts a negative impact on HC degradation rates [86, 95]. According to Kujawinski et al, the application of dispersants in the deep sea led to the accumulation of DOSS in the water column that led to its transport up to 300km from the wellhead and was present in high concentrations even after 64 days from the termination of SSDI indicating its slow biodegradation [62]. Overall, the contradictory results are attributed to the challenges and limitations that both field studies and laboratory experiments face when evaluating the effect of dispersants and their fate in the marine environment [96].

1.4.4 More than a decade from the DWH accident: What was learned?

The collective effort made by the scientific community in the aftermath of the DWH oil spill deepened our understanding in microbial biodegradation of hydrocarbons and contributed in new knowledge for many unique aspects (dispersant effect and fate in the deep sea, MOSSFA event etc) which are necessary for oil spill response [61, 63]. It has been acknowledged that the presence of natural seeps in the GoM was critical in the rapid microbial response to the oil spill due to their role in structuring adapted-to-oil communities. Moreover, the combination of jetting from the wellhead, due to pressure and temperature differences between the reservoir and the surrounding environment, and SSDI led to increased oil solubility and thus bioavailability of the oil substrates with most studies suggesting a positive effect of dispersant application [24, 42, 93, 97, 98]. In addition, the advancement of molecular tools and particularly of high-throughput sequencing led to the unraveling of microbial diversity that responded to oil contamination in real-time [81–83, 99]. However, one of the most important lessons learned from the DWH incident was the necessity of performing site-specific research at *in situ* environmental conditions (pressure, temperature) in order to produce realistic data on microbial response and hydrocarbon-degradation rates, underlining the lack of a significant parameter from deep-sea HC bioremediation studies, the absence of high pressure. [6, 63, 100].

1.5 The Deep-sea piezosphere

High hydrostatic pressure (HHP) is a key physical parameter in the deep sea that structures microbial communities and influences their growth and metabolic rates [101–104]. Based on the importance of HHP, deep-sea microorganisms have been classified as piezophilic, piezotolerant and piezosensitive according to their growth rate under high-pressure conditions. Surface microbes usually grow better under atmospheric conditions (piezosensitive) however some can

grow equally well under pressure (piezotolerant). Likewise, microorganisms isolated from the deep sea or the deep subsurface have an optimum growth at high pressure (piezophilic). Piezotolerant taxa are able to grow at a pressure range of 0.1-10 MPa and piezophiles at 10-50 MPa whereas hyperpiezophilic strains grow at >50 MPa [105]. The majority of isolated piezophiles and microbial community analysis results were obtained following decompression [101, 106]. The reason lies in the technical difficulties and challenges met in maintaining high pressure during sampling and experimentation that may lead to results that do not reflect the *in situ* microbial conditions [6, 101].

1.5.1 Microbial oil bioremediation studies at in situ pressure

Despite the vast number of hydrocarbon-bioremediation studies conducted after the deep oil spill accident of DWH, only a handful of the *ex situ* experiments applied high pressure during incubations [6, 107–110]. Results by Marietou et al were obtained using decompressed deep samples from the GoM and proposed that high pressure acts synergistically with low temperatures to slow microbial growth and thus HC biodegradation in the deep sea [107]. This synergistic effect was also observed by Fasca et al on microbial community structure however their methodology did not respond to realistic conditions as they used surface seawater samples in their experiments [108]. Perez-Calderon et al used decompressed sediments incubated both at *in situ* temperature and pressure conditions (5 ºC, 30MPa) and at 20 ºC and 0.1MPa addressing temperature as more influential on community structure followed by pressure, yet distinct taxa were identified at each pressure treatment indicating the importance of this variable [109]. Whereas, in another study with decompressed sediments, an inhibitory effect was observed on oil biodegradation from the deepest-collected samples incubated at *in situ* pressure and temperature [110].

The effect of high pressure was also tested on isolated hydrocarbon-degrading strains like *Marinobacter, Alcanivorax*, *Rhodococcus* and *Sphingobium* [111–115]. In particular, *Marinobacter hydrocarbonoclasticus* isolated from deep seawater grew well on hexadecane at *in situ* high pressure of 35 MPa. On the other hand, the three *Alcanivorax* species (*A. dieselolei, A. borkumensis, A. jadensis*) tested under high pressure by Scoma et al presented either impaired growth rates either lower metabolic rates at 5-10 MPa [112–114]. Similarly, *Rhodococcus* was capable of growing at 15 MPa however, at lower rates than at 0.1 MPa while the growth of *Sphingobium* was severely decreased at 12 MPa and naphthalene degradation was reduced compared to atmospheric conditions [111]. Nonetheless, a positive impact of high pressure was

observed on hydrocarbon-degradation rates by another *Rhodococcus* strain isolated from deep-sea sediments in the GoM [116].

Elevated pressures impact also the oil dispersion as they can reduce dispersant effectiveness from a few percent to even 50% depending on the dispersant used [117]. That in turn can affect microbial communities and thus hydrocarbon rates. The combination of high pressure and dispersant (DOR 1:100), resulted in a higher negative impact of dispersant on the growth rate of *Rhodococcus* at 15 MPa than at 0.1 MPa [116]. This synergistic effect between high pressure and dispersant application was also observed in HC bioremediation experiments using microbial communities from decompressed sediments where the inhibitory effect of dispersant (DOR 1:25) was decreased on *Cycloclasticus* under high pressure [118].

However, all the aforementioned research results have been obtained with microbial consortia or isolates that were collected under decompressed conditions. The effect of decompression can impact the microbial community diversity, growth rates and therefore the metabolic activities including hydrocarbon degradation [100, 104, 119]. Amano et al observed an overestimation (100-fold increase) in the metabolic activity caused by the revival of piezosensitive taxa upon depressurization of deep-sea samples [104]. Furthermore, a negative effect of decompression was observed on the growth of two model sulfate reducers commonly found in the subsurface [119]. Overall, these studies underscore the importance of maintaining *in situ* pressure levels during sample retrieval from deep-sea environments and in laboratory experiments.

1.6 The Mediterranean Sea

The Mediterranean Sea represents the 0.82% of surface water of all oceans however it is one of the busiest seas of the world. The 1/5 of the seaborne trade as well as the 10% of the world's container throughput and the transportation of 200 million passengers occurs here [120].

1.6.1 Physical and Chemical properties

This semi-enclosed basin connects to the Atlantic Ocean via the Gibraltar straits and is divided into two sub-basins, the Western Mediterranean Sea (WMS) and the Eastern Mediterranean Sea (EMS) separated by the straits of Sicily. Due to the excess heat, evaporation rates surpass precipitation and river inputs to the Mediterranean Sea thus generating a concentration basin [121, 122]. Salinity increases eastwards with the low salinity Atlantic Water

(AW) of 36.2 psu being modified to 37.0 psu near the straits of Sicily and reaching 38.6 psu in the eastern-most part of the EMS. This modified Atlantic Water (MAW), or Levantine Surface Water (LSW), is the primary source for the formation of the Levantine Intermediate Water (LIW), a denser water mass. This salinity difference drives the anti-estuarine thermohaline circulation of the intermediate LIW layer which moves in a westward direction through the Cretan Passage and exits through the Gibraltar straits back to the Atlantic Ocean [123]. Deep Water Formation (DWF) occurs in the Gulf of Lions in the WMS while the Eastern Mediterranean Deep Water (EMDW) is formed in the Adriatic Sea. However, a climatic shift, attributed to hydrological and meteorological factors, termed as the Eastern Mediterranean Transient (EMT) let to the establishment of the Aegean Sea in deep-water formation [124]. According to these processes, water stratification in the EMS occurs at certain depths. In particular, the surface AW occupies depths down to 150 m whereas the intermediate LIW layer extends from 150-400 m and the deepest EMDW is found below 400 m [125].

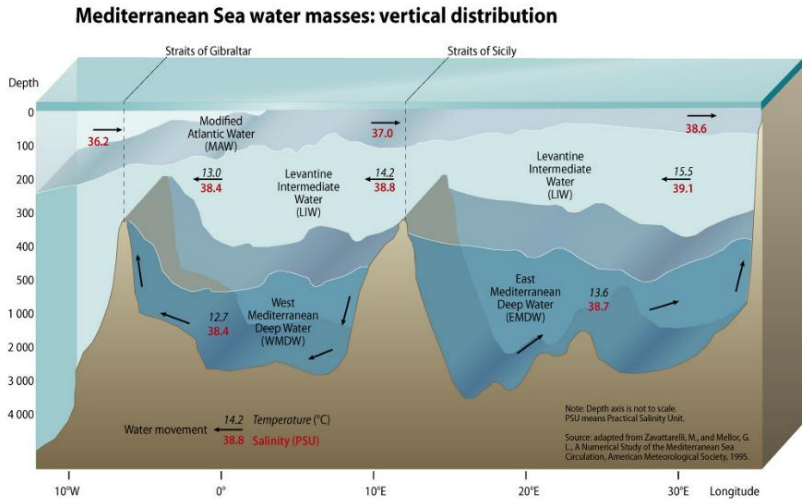

Figure 9. *Water mass stratification of the Mediterranean Sea. Image taken from https://www.grida.no/resources/5885 (Credits: GRID-Arendal)*

Higher bottom sea temperatures of 14 ºC, ultraoligotrophic conditions and low primary productivity characterise the Mediterranean basin [122, 126]. Despite the high anthropogenic activity and river run-offs, the latter two traits (oligotrophy and primary productivity) are more intense especially in the EMS [127, 128]. The Nitrate:Phosphorus (N:P) ratio is higher in the deep-water layers of the EMS (25-28:1) compared to the WMDW (23:1) and with the other oceans (16:1). The concentration of dissolved nutrients in the deep EMS (6 μmol×kg^{-1} N, 0.25 μmol×kg^{-1} P, 11 μmol×kg^{-1} Si) are much lower than any other marine basin [126]. The lower

nutrient concentration is attributed to the high N:P external inputs in combination with the low denitrification levels, due to the absence of blooms and thus the lack of anoxic conditions for denitrification to occur [127]. Moreover, the photic zone of the EMS is P-starved in all nutrient species (organic, inorganic and particulate) as mineralization of phosphorous is more efficient than nitrogen [129]. Phytoplankton bloom occurs with winter mixing of waters due to the transport of nutrients from the deep layers to the surface and ceases once phosphorus level are diminished [127]. Overall, the combination of thermohaline circulation and vertical mixing is crucial for the Mediterranean Sea and the predicted effect of climate change on these processes is expected to cause major issues to the trophic chain.

1.6.2 Microbial ecology of the EMS

The unique conditions of the EMS influence the microbial community structure and diversity. Yet, literature on microbial ecology has been scarce and limited in this marine region with most studies applying non-molecular techniques such as chlorophyll-a measurements, ^{3}H-leucine incorporation methods and flow cytometry to assess microbial growth and activity [130–133]. Studies that applied high throughput sequencing are few and do not provide a comprehensive analysis of the microbial structure as they were either performed for specific microbial groups or they were applied for specific marine areas or water layers. For example, Haber et al applied 16S analysis of bacterial communities but only on surface waters off-Israel to evaluate the spatial and seasonal effect on these communities [134]. In another study, Techtmann et al used seawater samples across the water column providing insight in the prokaryotic community structure and addressing distinct taxa according to the water mass from which they were retrieved [135]. Their results indicated that the surface water mass (AW) was abundant in Cyanobacteria (*Synechococcus*, *Prochlorococcus*), Bacteroidetes (Flavobacteria) and Proteobacteria (alpha-, gamma-), the LIW was enriched in Archaea (Thaumarchaeota, Euryarchaeota) and Chloroflexi whereas the deepest EMDW was enriched in Gammaproteobacteria related to Oceanospirillales and Methylococcales as well as in SAR406 and Nitrospira. A molecular study by Santi et al addressed only the eukaryotic diversity in the water column of stations within the Cretan Passage indicating also the distribution of eukaryotic taxa with depth as well as the presence of high percentages of unassigned species in the deepest sampling layer [136]. Overall, the knowledge gap is still vast in microbial ecology of the EMS and more studies are necessary to understand the basis of our trophic chain, in an area that has been predicted it will be largely affected by climate change [137–139].

1.6.3 Hydrocarbon-degradation studies in the EMS

The deep EMS has been characterised as a hotspot for microbial activity due to the elevated water temperatures of 14 ºC that drive the rapid response to carbon input [140]. Hazen et al however, hypothesised that offshore oil biodegradation rates will be slow in this basin due to the oligotrophic conditions that are present compared to the deep GoM [42]. Despite the intensification of oil and gas activities in the EMS, there are no site-specific studies to provide hydrocarbon-biodegradation rates whereas research on microbial community composition and response is extremely limited [141]. A single study by Liu et al in 2017 is the only that applied 16S rRNA amplicon sequencing to examine the prokaryotic succession patterns in the presence of crude oil or dispersed oil. Their results indicated a rapid response to HC contamination with a drastic drop of the archaeal population and the dominance of *Oceanospirillaceae* in the oil-enriched community after 72 hours. Moreover, they observed a positive effect of dispersant application on relative abundance of HC-degraders (Gammaproteobacteria).

CHAPTER 2.

Innovation and Thesis Objectives

Oil and gas exploration and exploitation activities are progressing at a fast pace in the Eastern Mediterranean sub-basin while at the same time, hydrocarbon-bioremediation studies performed in this marine environment are extremely few. The main aim of this work is to explore the microbial community composition across depths in areas of interest for hydrocarbon exploration in the Eastern Mediterranean Sea and perform site-specific research to evaluate its self-healing capability through natural attenuation in the case of an accidental hydrocarbon release scenario in the deep sea. In particular, this dissertation seeks to:

1) Analyse the pristine microbial community structure across the water masses of the Eastern Mediterranean Sea, compare microbial associations between surface and deep-water layers and record any notable background levels of hydrocarbon degraders across depths down to 1000 m below sea level **(Chapter 1)**. More specifically, in this chapter, the natural community structure of both prokaryotes and unicellular eukaryotes was assessed in the understudied marine areas South of Crete (Cretan Passage). The following questions were attempted to be addressed:

    a. What is the synthesis of prokaryotic and unicellular eukaryotic communities across the three water masses of the EMS?
    b. Are microbial networks structured differently between the two life domains at the surface and deep-water layers?
    c. Do the natural microbial communities comprise of any known hydrocarbon degrading taxa?

2) Evaluate the oil-degradation potential between surface and deep EMS microbial communities, monitor microbial succession patterns and identify differences in key hydrocarbon-degrading taxa under atmospheric conditions and *in situ* temperature **(Chapter 2)**. This timeseries experiment involved oil-acclimatised consortia collected from near-surface and deep-water layers of the EMS incubated in the presence of crude oil. In particular, questions that were desired to be answered in this chapter are presented below:

    a. Do surface and deep microbial communities of the EMS respond similarly to an oil contamination?
    b. Does the increase of temperature enhance oil biodegradation potential of the deep microbial community?
    c. Which key microbial taxa respond to an oil contamination at the different depths under the applied temperature conditions?

3) Assess the impact of decompression on deep EMS microbial communities during seawater retrieval, address the resilience of oil-degrading species to the effect of decompression, the concomitant effect on hydrocarbon degradation rates and isolate HC-degraders under HHP **(Chapter 3)**. This study used pristine deep-water communities from 1000 m depth, collected in Niskin bottles (decompressed) and at *in situ* pressure using a high-pressure sampling apparatus. Acclimatisation and subsequent enrichment experiments were performed under undisturbed or disturbed *in situ* pressure conditions and in the presence and absence of chemical dispersant. In this chapter, the following questions were sought to be addressed:

    a. How severe is the effect of decompression upon deep water retrieval on microbial diversity? Can it be restored by repressurising the samples in the lab?
    b. Which hydrocarbon degraders are favored during sequential enrichments in ONR7 medium under the different pressure and oil treatments?
    c. Does dispersant application influence the microbial community structure under the applied conditions?
    d. Are hydrocarbon degradation rates impacted by decompression and dispersant application?

4) Emulate a deep hydrocarbon plume at *in situ* pressure and temperature conditions of the Eastern Mediterranean basin, monitor the microbial succession patterns and identify key hydrocarbon-degrading taxa in the presence and absence of chemical dispersant **(Chapter 4)**. In this chapter, a timeseries experiment was conducted under undisturbed conditions of the deep Eastern Mediterranean Sea. Questions aimed to be addressed are given below:

    a. Which microbial species act as primary hydrocarbon degraders in the deep plume of the EMS?
    b. What are the microbial succession patterns following exposure to oil and after the application of dispersant?
    c. Are there any similarities in community succession patterns with the microbial response in the deep plume formed during the DWH accident?

All these objectives and research questions were addressed using high-throughput sequencing and GC-MS analysis. This is the first study that applies molecular analysis to assess the microbial ecology of both prokaryotic and unicellular eukaryotic communities in this marine region. Moreover, this is also the first time that direct hydrocarbon degradation rates are provided for the EMS.

The main novelty of this dissertation lies in the performance of experiments under high-pressure using un-decompressed deep microbial communities therefore, at *in situ* conditions of the deep EMS. High-pressure, hydrocarbon-bioremediation studies found in the literature have been conducted using depressurized water samples and thus having the risk of underestimating or overestimating HC removal capacity while for the EMS no high-pressure study exists.

The experimental design for the high-pressure experiments **(Chapters 3 and 4)** involved the use of a high-pressure sampling unit (HP-Sampler) to retrieve and maintain seawater under *in situ* environmental conditions of the deep EMS, pressure vessels (HP-vessels) and a high-pressure reactor (HP-Reactor) for the experimental incubations depicted in Figure **10**-11.

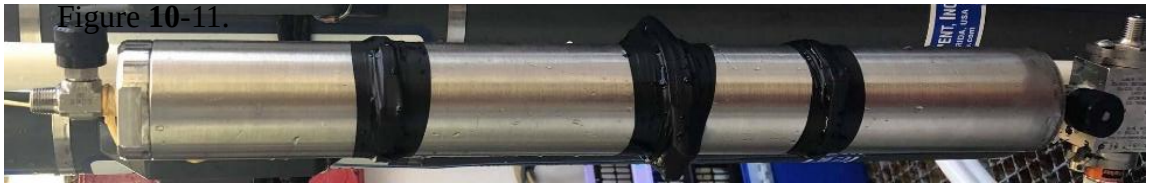

Figure 10. *The engineered high pressure sampling apparatus used for deep seawater retrieval. The unidirectional check valve is attached on the right end of the stainless-steel bottle.*

This engineered apparatus (HP-Sampler) comprises of a 1L stainless-steel bottle equipped with a unidirectional check valve set to open at a ΔP of 0.2 MPa and allow the flow of seawater inside the HP-Sampler. To avoid seawater collection from the upper parts of the water column, the HP-sampler is pressurized with nitrogen gas so that the check valve would open at the desired depth. For these experiments, the HP-Sampler was compressed at 60 MPa (set to open at 600 m depth). The ΔP would allow the check valve to open and close for about every 20 m.

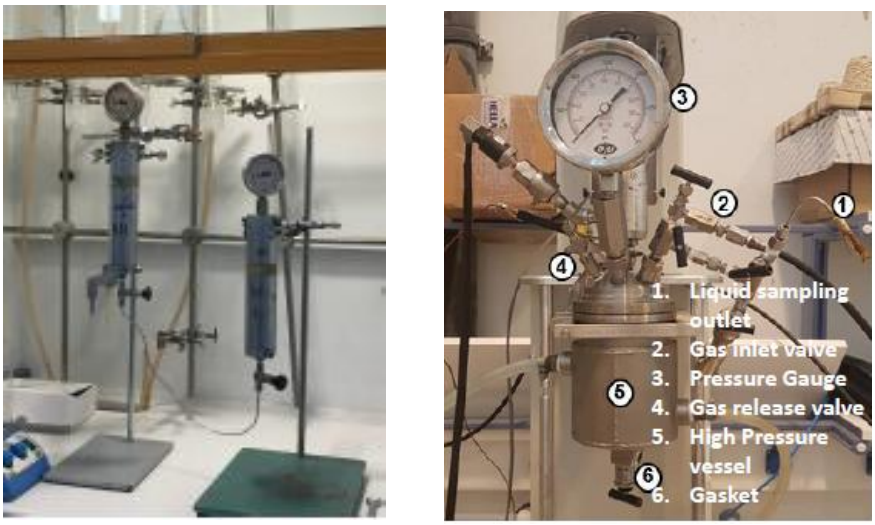

Figure 11. *The high-pressure vessels (left) and the high-pressure reactor (right) used in the experiments.*

Overall, this doctoral thesis attempts to provide, for the first time, site-specific results at *in situ* conditions on hydrocarbon bioremediation capability of the Eastern Mediterranean and particularly of its deep waters, which can serve in the structure of a mitigation response strategy in the case of an accidental release of hydrocarbons in this basin.

CHAPTER 3.

Background prokaryotic and eukaryotic communities of the Eastern Mediterranean Sea

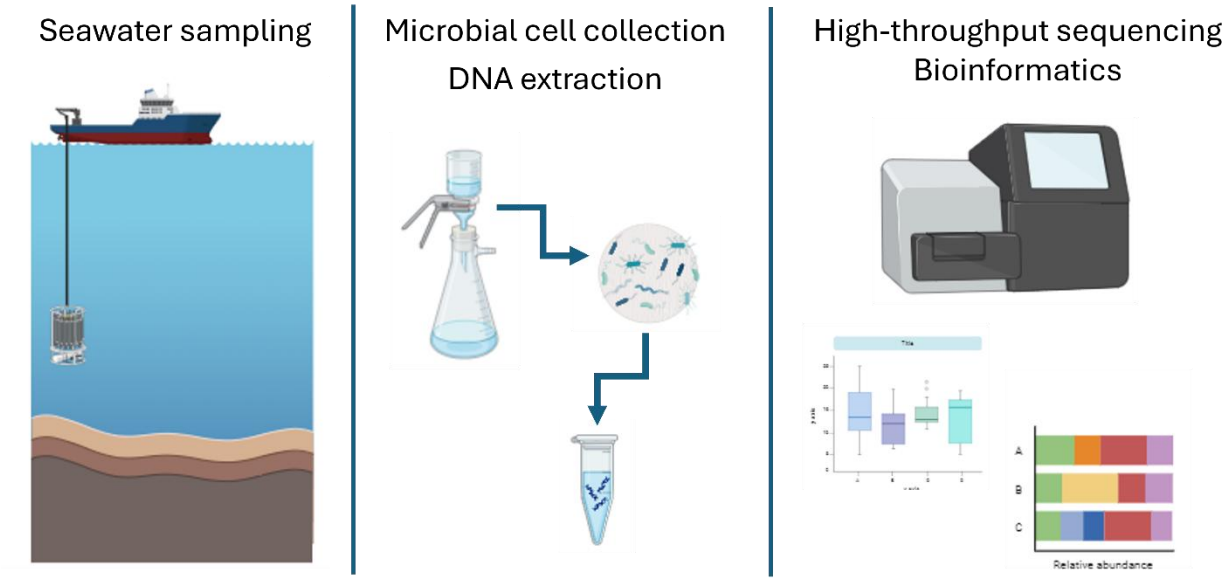

Part of this Chapter is currently Under Review in Current Microbiology Journal under the title:

"Distinct communities of Bacteria and unicellular eukaryotes in the different water masses of Cretan Passage water column (Eastern Mediterranean Sea)"

3.1 Abstract

Understanding marine microbiota diversity and dynamics holds significant importance due to their role in maintaining vital ecosystem functions and services including climate regulation. Here, we studied the diversity and associations between Bacteria and unicellular eukaryotes in the different water masses of the Cretan Passage water column in the Eastern Mediterranean Sea. Samples were collected from two stations during two sampling expeditions in August 2019 and February 2020 and analysed using high throughput 16S and 18S rRNA gene sequencing. Additionally, interspecies co-occurrence patterns were evaluated between the top and bottom water masses. Our results unveiled vertical variations in microbial diversity with species fluctuations indicative of seasonality recorded in the surface water mass. Heterotrophic taxa and grazers related to organic matter degradation and nutrient cycling were enriched in the deepest water layers. In addition, common hydrocarbon-degrading taxa were identified in significant amounts especially in the deep-water layers of both stations. Finally, the higher number of microbial associations in the surface network indicates abundant ecological niches compared to the deepest network, possibly related to the lack of bottom-up resources in the oligotrophic deep ocean. To our knowledge, this is the first study to combine molecular biology tools to understand the ecology and networking of both planktic prokaryotes and unicellular eukaryotes in the different water masses of one of the world's most understudied marine regions.

3.2 Introduction

Deterministic procedures of bottom-up and top-down selection affect the diversity and composition of marine microbial communities and drive the relationships among microorganisms structuring the microbial food web [142, 143]. Despite their importance, the ocean's microbial biosphere remains vastly unexplored. However, the advancement of culture-independent methods and the growing DNA and RNA sequence databases, contributed significantly to our knowledge regarding the ecological roles and trophic connections among photo-autotrophic, phago-heterotrophic and mixotrophic marine microbes [144, 145].

The Eastern Mediterranean Sea (EMS), a sub-basin of the semi-enclosed Mediterranean Sea, expands eastwards from the Straits of Sicily and is of great importance both ecologically and geographically. This aquatic system presents complex oceanic processes and is one of the most oligotrophic, saltier, and warmer basins of the world [121, 122]. The EMS thermohaline, anti-estuarine circulation leads to stratification into three distinct water masses. Here, the surface

Atlantic Water (AW) presents variable salinity (< 38.9 psu) due to evaporation and mixing with the local Levantine Surface Waters (LSW) accumulating in depths down to 150 m. Reaching the eastern-most part of the EMS, the AW/LSW is transformed into the Levantine Intermediate Water (LIW), a more saline (>38.9 psu) and denser water mass, expanding between 150-400 meters in depth and moving in the opposite direction. Finally, the deepest Eastern Mediterranean Deep Water (EMDW) of lower salinity (< 38.9), occupies depths below 400m [121, 125].

One of the most important characteristics of the EMS is the high deep-water temperature (13-15 ^{o}C), lower than the overlying water masses but significantly warmer than any other marine system at respective depths, providing a favorable condition for microbial growth and activity [146]. Even though it is a land-locked basin with increasing anthropogenic activity, the EMS waters have been characterised as ultraoligotrophic. Nutrient levels increase with depth having a high nitrate to phosphate ratio (N:P=28:1), exceeding by far the Redfieldian 16:1, making the system P-starved [129]. Furthermore, primary productivity is one of the lowest observed in oceanic systems globally, three times lower than the western Mediterranean and other similar oligotrophic ecosystems (10-143 g C m^{-2} y^{-1}) [127].

Under these unique conditions, microbial life thrives, occupying different ecological niches. This low-nutrient and low-primary production environment provides an ecological advantage for mixotrophy, triggering the feeding on microbial prey to sustain carbon and inorganic nutrient budgets and to ensure the functioning of the biological pump and biomass transfer to higher trophic levels [147]. Transmediterranean offshore epipelagic cruises have provided significant insights in terms of longitudinal distribution and analysis for plankton, nanoflagellates and ciliates [137, 148, 149]. In the EMS, most studies have been performed in the eastern part of the Levantine basin, recording microbial variations from a temporal, vertical and spatial point of view [131–135, 150]. Whereas studies in the western region of the Levantine Sea, have predominantly used approaches such as flow-cytometry and ^{3}H-leucine incorporation methods to determine microbial growth and activity with only a few employing molecular biology tools for the analysis of community composition [130, 136, 140, 151]. Nonetheless, microbiome exploration in marine areas off-Crete has been limited [152].

Besides water column stratification und other unique traits, the EMS is also known for the numerous presence of active mud volcanoes, capable for the release of methane and other hydrocarbons that influence microbial community structure, like those in the Mediterranean Ridge (MR) [135]. Currently, areas within the Greek Exclusive Economic Zone (EEZ), west and south-west of Crete, have been licensed for geophysical exploration for future hydrocarbon

exploitation. Therefore, evaluation of natural microbial community and preparedness against an accidental release of hydrocarbons in this deep marine basin is urgent.

In this study, we explored the microbial community composition across depths, down to 1000 m, in the Cretan Passage water column using the 16S and 18S rRNA gene diversity. We hypothesised that associations between bacteria and unicellular eukaryotes are different between the surface (AW/LSW) and deep (EMDW) water samples, and we tested this hypothesis through co-occurrence networks. To our knowledge, no study so far has combined DNA metabarcoding for both bacteria and unicellular eukaryotes to investigate community composition and networking between microorganisms in this marine habitat [134–136]. Furthermore, the relative abundance of known hydrocarbon degraders was examined to assess the potential of background microbial communities to respond to oil contamination in an area of interest for oil and gas exploitation.

3.3 Materials and Methods

3.3.1 Seawater sample collection

Seawater samples were collected in marine areas off South Crete (Cretan Passage) onboard HCMR's R/V Aegaeo during two oceanographic cruises. Station A (Koufonisi) was sampled in August 2019 and station B (Gavdos) in February 2020 (Figure 12). The two stations are approximately 183 km apart and are considered to be in the same ecoregion [153]. Water samples were collected from the surface to 1000 m depth with a SBE911 plus CTD unit, equipped with a 12-bottle SBE32 carousel water sampler. The water density at AW/LSW ranged from approximately 26-29 kg m^{-3} in summer and was ~28.8 kg m^{-3} in winter respectively while at EMDW the density ranged between 29.1-29.2 kg m^{-3} for both seasons (Figure S1). Temperature, salinity, and dissolved oxygen profiles were also built indicating a winter vertical mixing down to 300 m in winter (Figure S2). Two litres of seawater from each depth were immediately filtered through a 0.2 μM PES membrane filter and were stored frozen in cryotubes for subsequent DNA extraction.

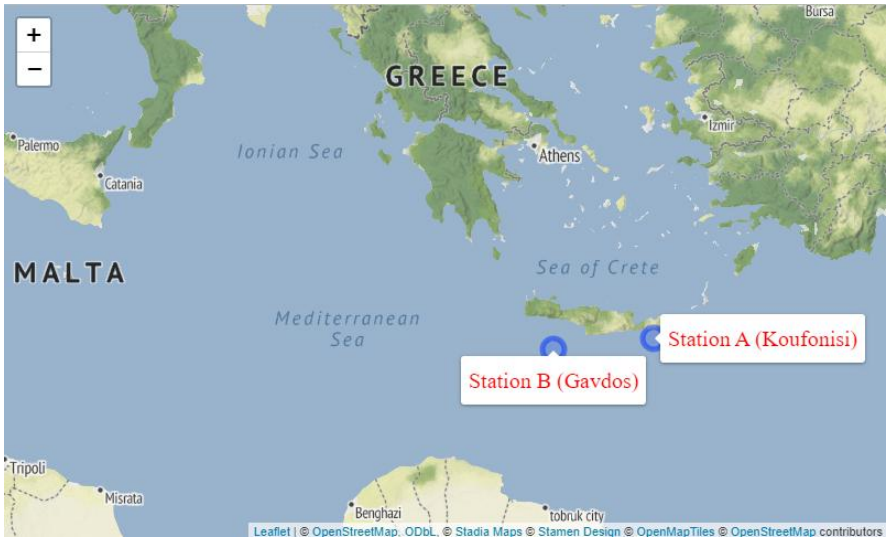

Figure 12. *Map pinpointing the two sampling stations.*

3.3.2 DNA extraction and sequencing

The method followed for DNA extraction has been previously described in Charalampous et al [154]. In summary, membrane filters were vortexed in CTAB extraction buffer, followed by three freeze-thaw cycles. Subsequently, lysozyme and Proteinase K were added, and the mixture was incubated at 37 ^{o}C for 30 min. After treatment with SDS, centrifugation, and extraction with phenol:chloroform:isoamylalcohol, DNA was left to precipitate overnight in isopropanol. The DNA pellet was washed with ethanol, dried, and resuspended in TE buffer. DNA concentration was quantified using Qubit (Invitrogen, Thermo Fisher Scientific, USA) and samples were subjected to high-throughput sequencing. Bacterial and unicellular eukaryotic samples (Table 2) were analysed using the universal primers U341F-U806R for the amplification of the 16S rRNA gene and E572F-E1009R primers for the amplification of the 18S rRNA gene respectively [155, 156]. Sequencing was performed on the Illumina Miseq platform by Biosearch Technologies (LGC Genomics GmbH, Berlin, Germany).

Table 2. *Summary of location, depth and water mass of seawater samples retrieved during the oceanographic expeditions. 16S rRNA sequencing was performed on all samples. In bold are the samples subjected to 18S rRNA sequencing.*

Sampling station	ID	Depth (m)	Water mass
Station A (Koufonisi)	**K10**	**10**	**AW/LSW**

	K75	75	AW/LSW
	K300	**300**	**LIW**
	K500	**500**	**EMDW**
	K800	800	EMDW
	K1000	**1000**	**EMDW**
Station B (Gavdos)	**G2**	**2**	**AW/LSW**
	G50	50	AW/LSW
	G150	150	AW/LSW
	G300	**300**	**LIW**
	G400	**400**	**LIW**
	G500	**500**	**EMDW**
	G700	**700**	**EMDW**
	G1000	1000	EMDW

3.3.3 Bioinformatic analysis

DNA sequencing data were analysed using the DADA2 package in Rstudio (version 2022.12.0) [157] in the R programming environment (version 4.2.2) [158]. Bacterial and eukaryotic datasets were created from primer-clipped reads, filtered, and trimmed for consistent length based on quality profiling. Amplicon sequence variants (ASVs) underwent dereplication, denoising, and merging, followed by chimera screening and taxonomy assignment using SILVA SSU (version 138) and PR2 SSU (version 4.14.0) databases for 16S and 18S rRNA sequences, respectively [159, 160]. Two phyloseq objects were constructed for downstream analysis for each microbial domain. Uncharacterised phyla, Chloroplasts, and Archaea were removed from the bacterial dataset, while uncharacterised supergroup taxa, Metazoa, and Streptophyta species were discarded from the eukaryotic dataset. In the end of all downstreaming processes, the bacterial dataset obtained from 14 samples, consisted of 179,556 reads with an average of 12,868 reads per sample (min: 4234, max: 34227) and a total of 2113 ASVs which were distributed among 30 phyla. Whereas, the eukaryotic dataset retained from 9 samples, consisted of 255,508 reads with an average of 28,390 reads per sample (min: 17,305, max: 39,662) and a total of 1678 ASVs were organised into 25 divisions.

3.3.4 Statistical analysis

All statistical analysis was performed in the R environment using the Rstudio software [158]. Alpha-diversity analysis was performed on ASV abundances prior to normalisation. ANOVA followed by Tukey's HSD test were used to find statistically significant differences in alpha diversity between water masses and sampling stations (seasonality). Beta-diversity was

analysed using PCoA analysis on Bray-Curtis dissimilarity distances after cumulative sum scaling (CSS) normalisation [161]. PERMANOVA (999 permutations) was used to test significant differences using the *adonis2* function of the *vegan* package [162]. ANOVA was also applied to test the significance in relative abundance of bacterial taxa between the surface (AW/LSW) and deep (EMDW) water layers. The Ecological Index of Exposure to Hydrocarbons (EIHE) was calculated according to Lozada et al [163]. All figures were generated using the *ggplot2* package in R [164].

3.3.5 Co-occurrence network analysis

Co-occurrence network analysis was performed separately for samples collected from surface (AW/LSW) and deep (EMDW) water layers. For each water mass, ASV abundance tables were filtered to keep taxa which were present more than 5 times in at least 50% of the samples for both bacterial and unicellular eukaryotes. Following filtering, the two ASV tables were merged for the correlation process in R. The AW/LSW table consisted of 51 ASVs (31 unicellular eukaryotes, 20 bacteria) and the EMDW consisting of 69 ASVs (57 unicellular eukaryotes, 12 bacteria). Spearman's correlation was calculated separately for each water mass table using the *Hmisc* package [165]. Networks were constructed in Cytoscape (version 3.9.1) and included only the statistically significant correlations (p<0.05) with R>0.6 or R<-0.6.

3.4 Results

3.4.1 Beta-diversity

Principal coordinate analysis (PCoA) on Bray-Curtis dissimilarity distances was performed for both bacterial and unicellular eukaryotic datasets indicating that samples were primarily separated according to the water mass from which they were retrieved from (Figure 13, Figure S3). AW/LSW samples clustered together while the deepest EMDW samples formed a second group. The microbial communities from the intermediate layer (LIW) clustered together with those from the upper-EMDW depths (G500, K500) besides LIW-G300 sample which grouped along with the AW/LSW samples (Figure 13, Figure S3). PERMANOVA analysis indicated statistically significant differences between the microbial communities with water mass ($p_{\text{bacterial}}$ = 0.001, $p_{\text{eukaryotic}}$ = 0.017) but not with sampling season ($p_{\text{bacterial}}$ = 0.102, $p_{\text{eukaryotic}}$ = 0.367). Pairwise PERMANOVA analysis indicated significantly different bacterial communities between the top (AW/LSW) and the bottom (EMDW) water masses ($p_{\text{AW/LSW-EMDW}}$ = 0.006).

Differences between AW/LSW-LIW and LIW-EMDW were less pronounced, yet statistically significant ($p_{AW/LSW-LIW} = 0.045$, $p_{LIW-EMDW} = 0.033$).

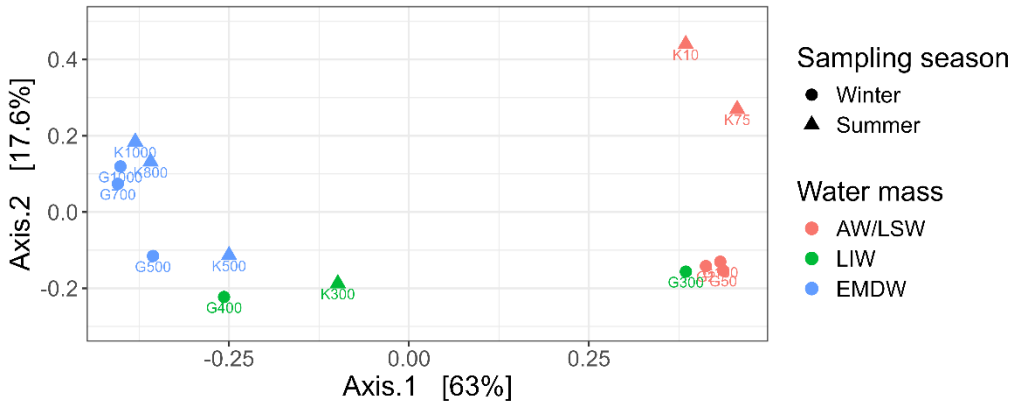

Figure 13. *Principal coordinate analysis of bacterial samples using the Bray-Curtis dissimilarity distances. Samples are clustered according to the water mass from which they were retrieved.*

3.4.2 Alpha diversity

Bacterial and unicellular eukaryotic diversity were assessed using Shannon, Simpson, and Phylogenetic Diversity (PD) indices. Bacterial analysis revealed lower diversity in the AW/LSW layer compared to LIW and EMDW, with the latter having slightly higher diversity (Figure 14A, Figure S4). ANOVA, applied to each metric, revealed only Shannon and PD metrics having a significant difference with water mass ($p<0.05$). Tukey HSD post-hoc test indicated that AW/LSW differed significantly from LIW and EMDW (

Table S1). Moreover, sampling season had no effect on the overall bacterial diversity in contrast to unicellular eukaryotic communities where ANOVA identified significant differences

Diversity metric	ANOVA		Tukey HSD test		
	p-value	F-value	AW/LSW-LIW	LIW-EMDW	AW/LSW-EMDW
Shannon	0.00189	11.69	0.01994	0.79	0.00181
Simpson	0.0777	3.25	0.22189	0.97	0.07825
PD whole tree	0.00226	11.14	0.01382	0.97	0.00264

in Shannon and Simpson metrics (Figure 14B-D, Table S2). Further analysis of eukaryotes showed that alpha diversity was higher in winter samples across all three water layers, with the intermediate water mass (LIW) exhibiting the greatest difference compared to the respective summer samples. (Figure S4). Finally, significant eukaryotic diversity between water masses was observed only in Simpson index (Table S2).

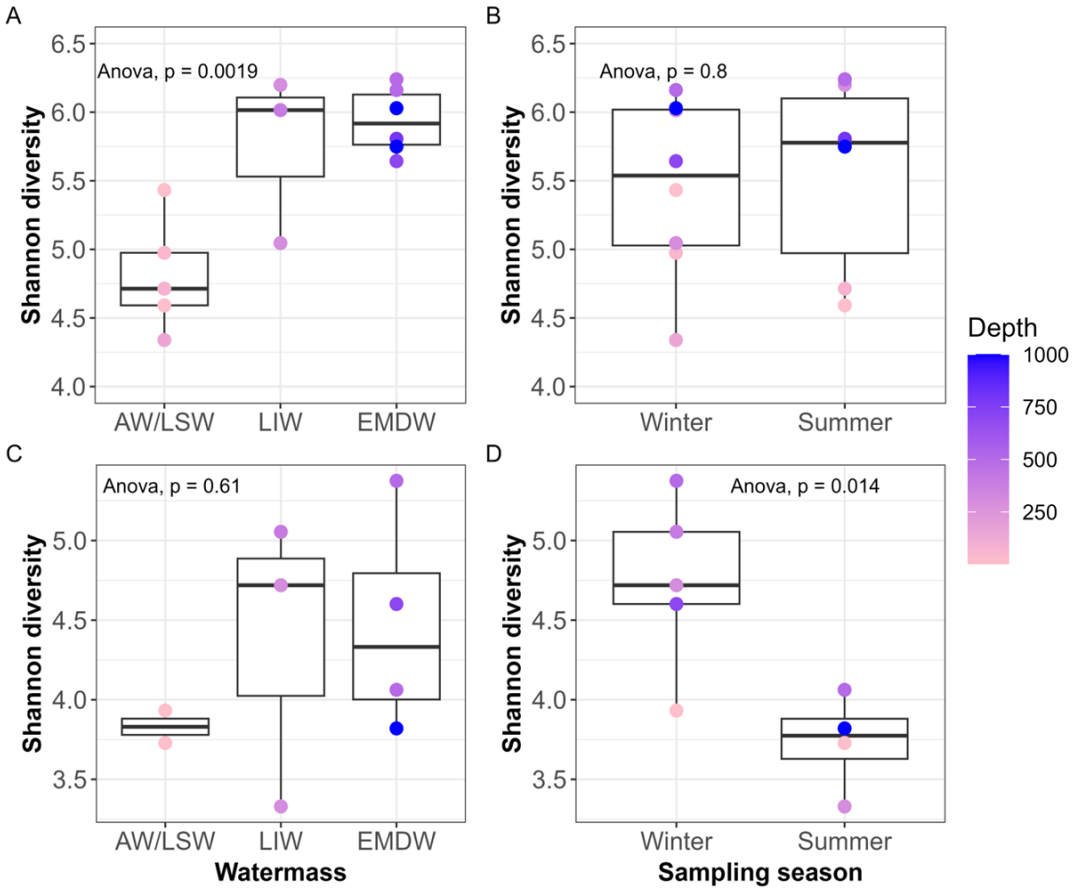

Figure 14. *Boxplot of Shannon diversity for bacterial (A-B) and unicellular eukaryotic (C-D) communities in each water mass and sampling location. Bacterial diversity is significantly influenced by Water mass whereas unicellular eukaryotic diversity is significantly affected by sampling location. Gavdos: winter sampling, Koufonisi: summer sampling.*

3.4.3 Bacterial community structure

Relative abundance analysis revealed water mass-specific bacterial taxa. ANOVA identified 14 phyla with significant differences in abundance between the upper (AW/LSW) and the deepest (EMDW) water layers. Among them were Cyanobacteria (p=0.009) and Bacteroidota (p=0.012) which were significantly enriched in AW/LSW (Figure 15). *Synechococcus* dominated Cyanobacteria in AW/LSW, especially in Gavdos (winter), while Bacteroidota were favored in

summer comprising 9% of surface ASVs, nearly 20 times higher than EMDW. Flavobacteriales were the dominant Bacteroidota in all samples however, in summer Rhodothermales, Balneolales and Sphingobacteriales were also present. Nitrospinota were favored in intermediate depths (LIW) while Chloroflexi (SAR202 clade) were enriched in the deepest water layers (LIW, EMDW), regardless of seasonality having their highest relative abundance in LIW-G400. Deltaproteobacteria (SAR324 clade), Marinimicrobia (SAR406 clade), Actinobacteriota (Microtrichales) and Nitrospirota were also favored in bottom water masses and their relative abundance increased with depth (Figure 15). For example, Marinimicrobia at 1000m depth comprised approximately the 11% of the bacterial community, twice the average levels present in intermediate depths. Overall, rare taxa (<1% abundance, "Other") increased with depth in the water column (Figure 15).

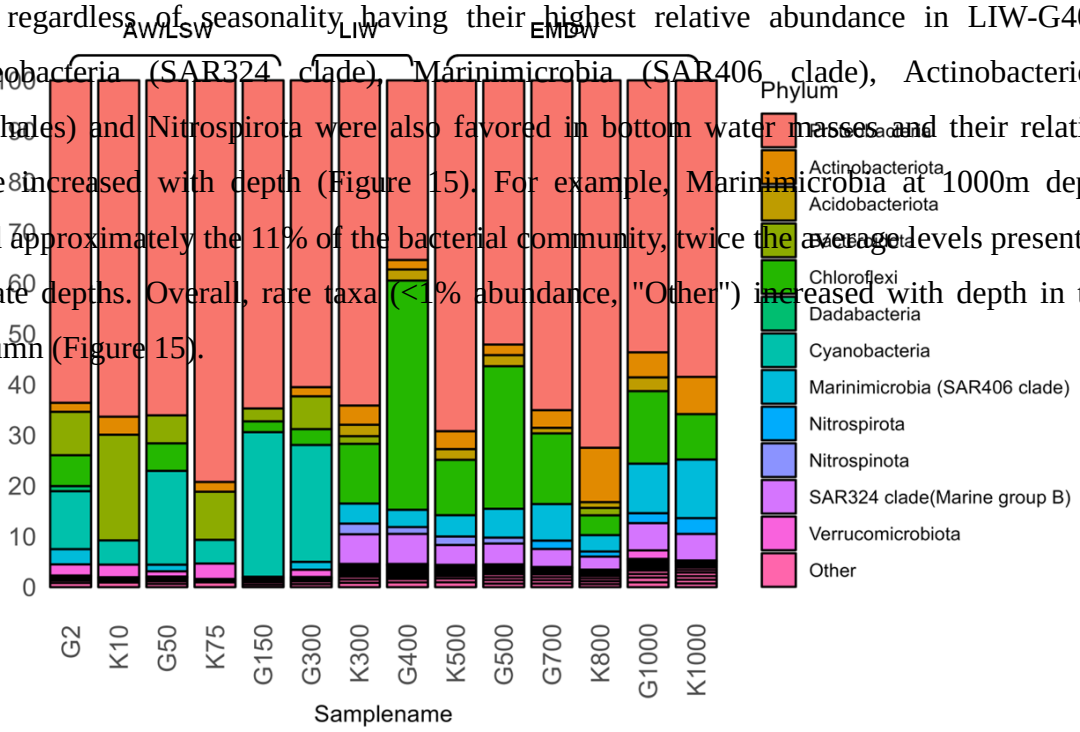

Figure 15. *Relative abundance of bacterial taxa at the Phylum level. The three water masses are annotated on top of the barplot (AW/LSW: Surface Water, LIW: Intermediate Water, EMDW: Deep Water). Rare taxa below 1% are classified as "Other" increase with depth. Species variations between the surface samples are indicative of seasonality. Distinct taxa are present in each water layer.*

3.4.4 Eukaryotic community structure

Unicellular eukaryotic communities differed with both water mass and sampling location (season) (Figure 16). Prymnesiophyceae (Haptophyta) comprised about 35% of total ASVs in winter surface microbial community (Figure 16; G2), five times higher than in summer (Figure

16; K10). Similar fluctuations occurred in other taxa (Dinophyceae, Syndiniales, and Ascomycota) between the two AW/LSW samples, with Syndiniales being fourfold more abundant in winter while Fungi (Ascomycota) and Dinophyceae were higher in summer. Microbial composition in LIW-G300 sample was more similar to the AW/LSW than the other LIW samples. Radiolaria (Acantharea and Polycystinea) were favored in intermediate waters and decreased with depth in contrast with RAD-B members of Radiolaria which preferred deeper waters and comprised ~13% of ASVs at 1000m (Figure 16). Moreover, the relative abundance of Syndiniales and deep-sea acclimated Fungi was elevated in the deepest EMDW samples (Figure 16; G700, K1000).

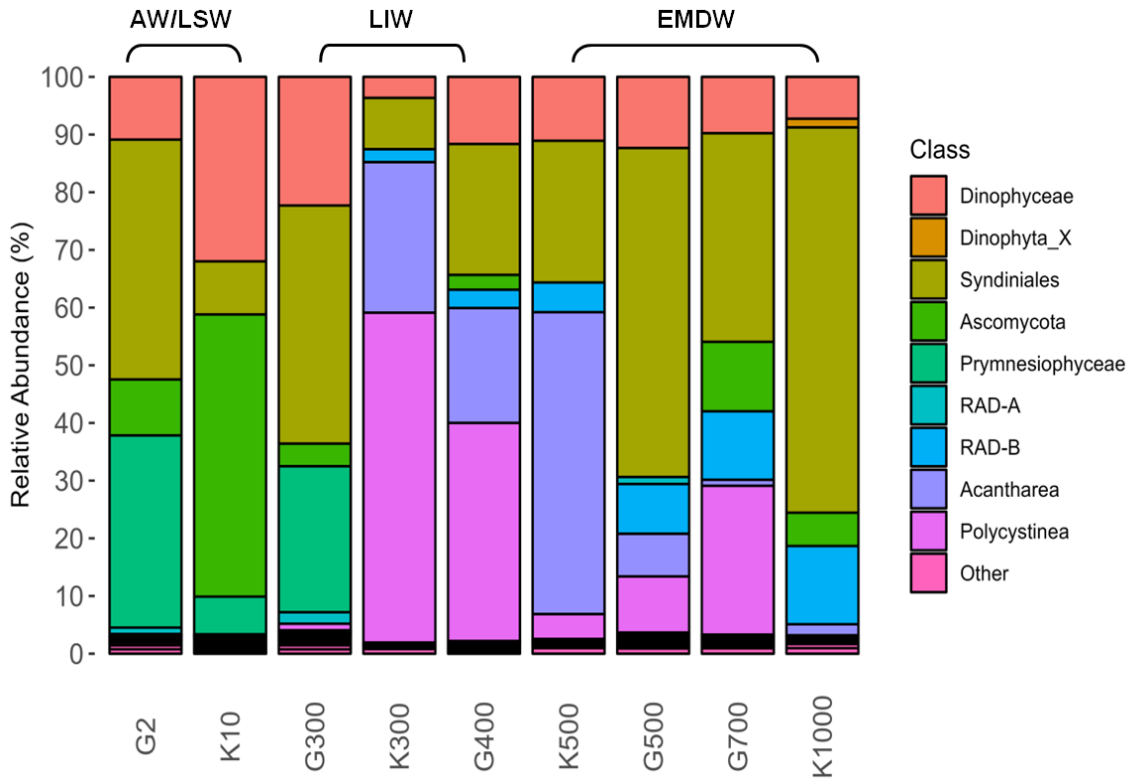

Figure 16. *Relative abundance of eukaryotic taxa at the Class level. The three water masses are annotated on top of the barplot (AW/LSW: Surface Water, LIW: Intermediate Water, EMDW: Deep Water). Rare taxa below 1% are classified as "Other". Species variations between the surface samples are indicative of seasonality. Distinct taxa are present in each water layer.*

3.4.5 Network analysis

The surface AW/LSW co-occurrence network had approximately five times more associations (edges) than the deep EMDW, despite that the latter comprised more ASVs (nodes) (Figure 17-18, Table S3). Both networks exhibited more positive than negative correlations (Table S3). In the AW/LSW network, Dinoflagellata and Haptophyta were positively correlated

with most members of Bacteroidota and Proteobacteria while Fungi (Ascomycota, excluding *Sarocladium*) had exclusively positive correlations with Cyanobacteria, Actinobacteriota, and Verrucomicrobiota (Figure 17). Additionally, Cyanobacteria were negatively related with eukaryotic Haptophytes and Dinoflagellates and were positively associated with Proteobacteria. In EMDW network, approximately 30% of all edges were between Radiolaria and Dinoflagellata, with ~60% being positive (Figure 18). Deep-sea fungal ASVs were positively correlated with Dinoflagellata in contrast to the AW/LSW network while Radiolaria exhibited exclusively negative connections with Proteobacteria, Nitrospinota (*LS-NOB*), and Picozoa, but positive relationships with Cercozoa and Fungi. Nitrospira was only associated with RAD-B taxa of Radiolaria, while Dinoflagellata and Actinobacteriota were negatively correlated, mirroring the surface water mass.

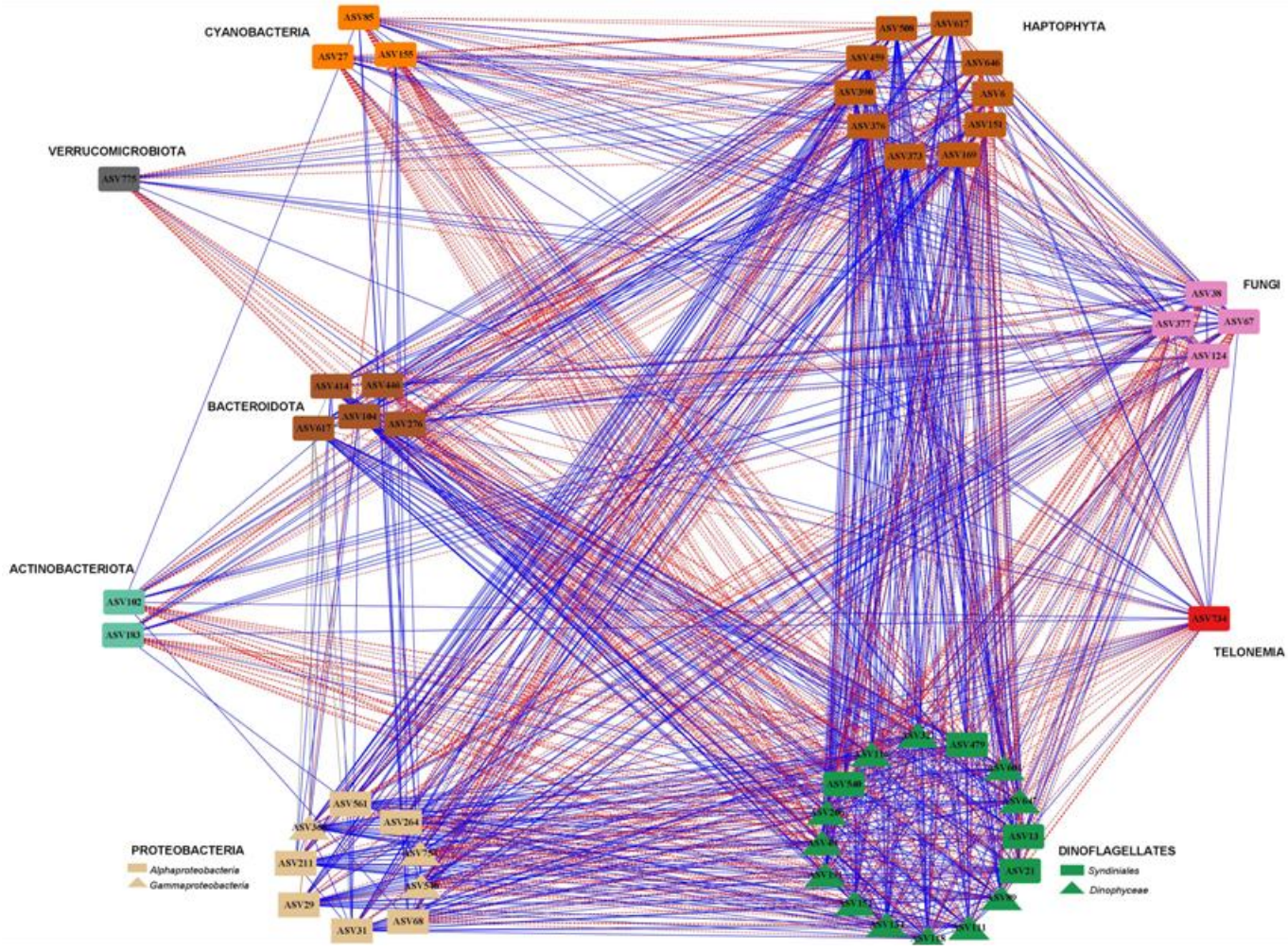

Figure 17. *Co-occurrence network diagram of Spearman's correlations (edges) between the bacterial and unicellular eukaryotic ASVs, (nodes) of the surface water mass. The edges present the statistically significant ($p<0.05$) correlations between ASVs, based on their relative abundance. Blue and red colour indicates positive and negative associations respectively.*

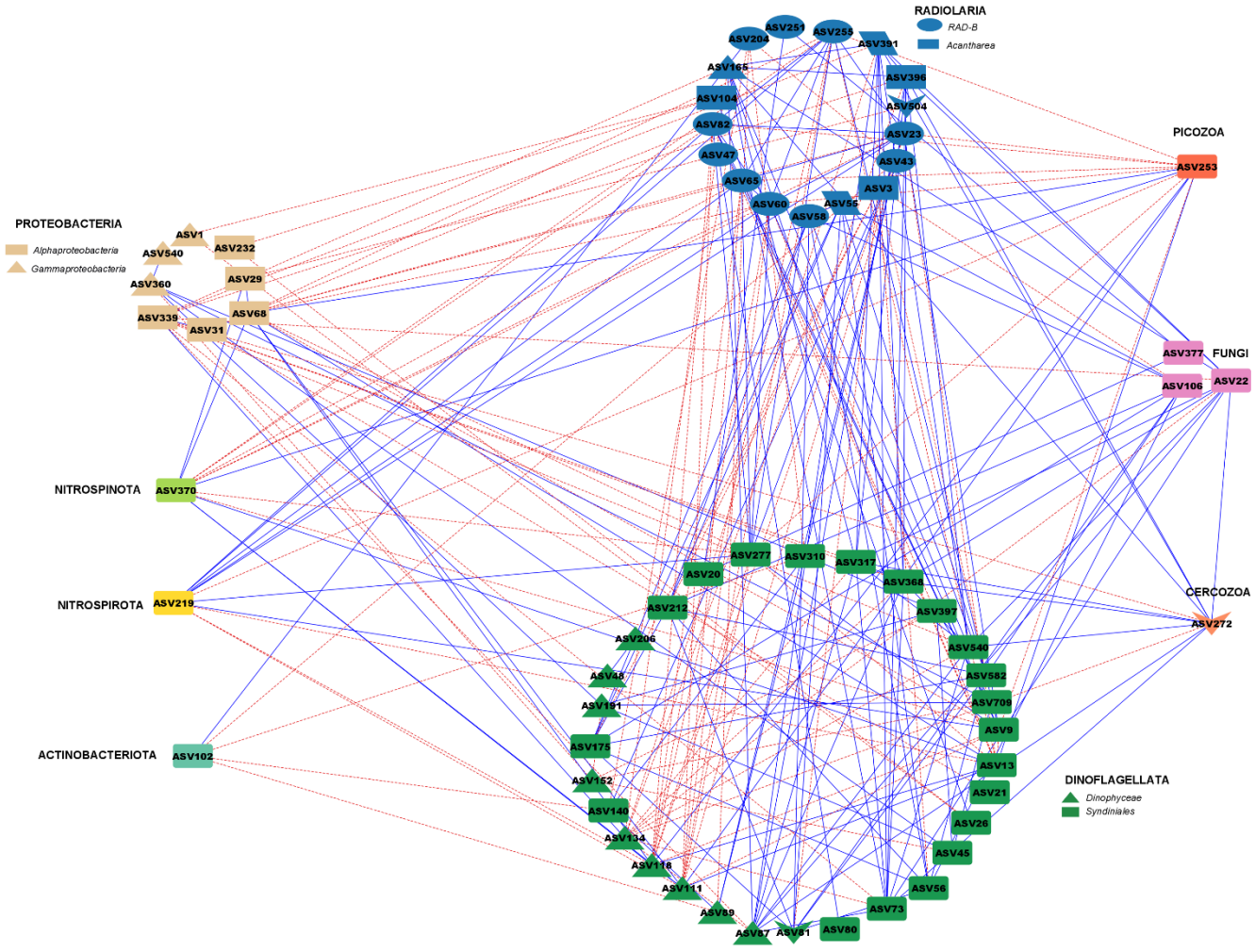

Figure 18. *Co-occurrence network diagram of Spearman's correlations (edges) between the bacterial and unicellular eukaryotic ASVs, (nodes) of the deep-water mass. The edges present the statistically significant ($p<0.05$) correlations between ASVs, based on their relative abundance. Blue and red colour indicates positive and negative associations respectively. Up to 5-fold more associations are present between microorganisms in the surface than in the deep network.*

3.4.6 Background levels of hydrocarbon degraders

Notably, known hydrocarbon degraders (*Alcanivorax*, *Alteromonas*, *Pseudoalteromonas*, *Halomonas*, *Idiomarina*, *Erythrobacter*) were present throughout the water column in summer

and in the deeper waters during winter sampling (Figure S6). Using the relative abundance data of microbial community composition, Ecological Index of Exposure to Hydrocarbons (EIHE) was calculated according to Lozada et al [163]. This index reflects the percentage of the bacterial community that is potentially capable of biodegrading hydrocarbons. EIHE index analysis of our dataset indicated that on average the 3.9% and 9.78% of ASVs were assigned to bacterial genera with hydrocarbon-degradation potential in the winter and summer EMDW layers, respectively (Figure 19).

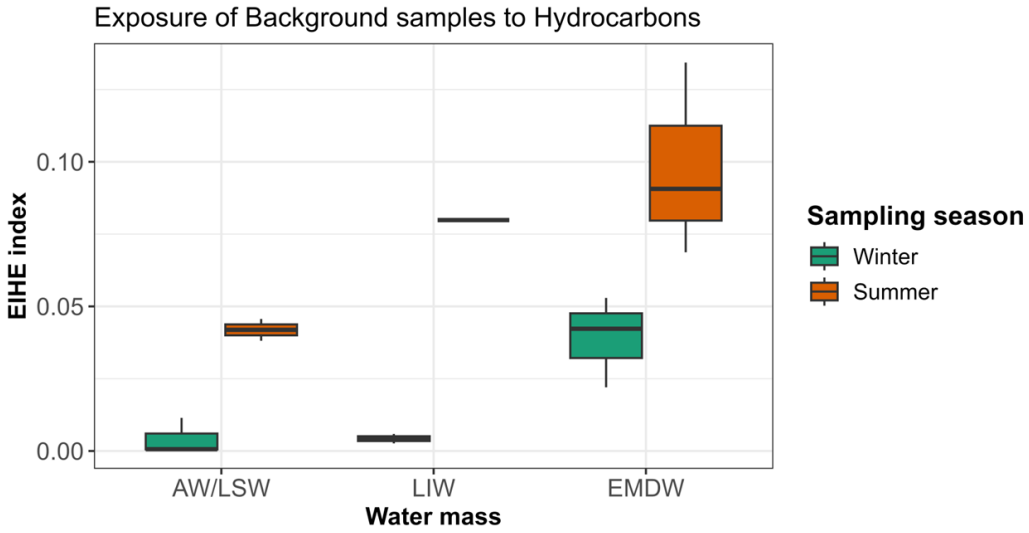

Figure 19. *Ecological Index of Hydrocarbon Exposure (EIHE) representing the proportion of the bacterial community with hydrocarbon-degradation potential. Water mass is on the x-axis while the EIHE values are depicted on the y axis. Different colouring of boxplots indicates the two sampling stations.*

3.5 Discussion

This study investigated microbiota structure and relationships between bacterial and unicellular eukaryotic microorganisms in the western part of the Levantine Sea (Cretan Passage) of the poorly investigated Eastern Mediterranean Sea (EMS). Depth-profiled seawater samples were collected from two different stations located within the Hellenic EEZ, that belong to the same marine ecoregion [153]. As a result, variations in microbial community composition were thought to be attributed on seasonal differences rather than spatial heterogeneity. High-throughput sequencing (HTS) unravelled the bacterial and unicellular eukaryotic diversity and microbial associations were assessed at surface and deep-water layers.

Our findings confirmed that the EMS maintains well-oxygenated conditions throughout its water column with stratified water masses in summer. However, in winter sampling, vertical convection led to water mixing between the surface water (AW/LSW) and intermediate water

(LIW) masses down to depths of 300 m, yet uniformal deep (EMDW) waters were observed in both sampling seasons (Figure S1-Figure **S2**).

3.5.1 Microbial community distribution and diversity

The distribution of bacterial and unicellular eukaryotic communities was linked to the seawater layer of origin. Seasonal effects were evident in AW/LSW communities, but the limited number of samples prevented significant testing. Induced winter vertical mixing caused the LIW-G300 sample to exhibit more environmental and biological similarities to the surface than the intermediate water layer. Microbial communities collected from 500m depth clustered with LIW samples, indicating a deeper LIW stratification in the central EMS basin [121, 125]. Sampling location was insignificant for the overall bacterial diversity however, single-cell eukaryotic communities showed significantly higher a-diversity in winter in all three water masses (Figure 14D, Figure S5). This was attributed to the lower number of observed species recorded in summer samples in combination with the dominance (lower evenness in the community) of certain eukaryotic groups (Fungi, Dinoflagellates, Radiolaria) probably because of feeding and biomass transfer to higher trophic levels in the EMS during this period [166]. Furthermore, the deepest EMDW water mass displayed the highest diversity in both microbial datasets in this part of the EMS, in contrast with studies in the easternmost Levantine region where LIW layer exhibited higher Shannon values [135].

3.5.2 Photosynthetic community composition and associations in the western Levantine basin (Cretan passage)

Unlike other oceans, highest primary production in the EMS occurs in winter however, the oligotrophic nature of this habitat favors the dominance of picophytoplankton and blooms do not occur [127, 167]. The bacterial fraction of picoplankton, Cyanobacteria, were identified in our AW/LSW samples, with *Synechococcus* consistently dominant, especially in winter when primary production is higher [127]. *Prochlorococcus* and *Cyanobium* were present only in winter samples in lower abundance than *Synechococcus*, yet they preferred lower AW/LSW depths confirming that, despite their close relation, picocyanobacteria differ ecologically and occupy diverse niches [168, 169]. In contrast to other EMS studies, where seasonal and depth-related variations were observed in the distribution of Cyanobacteria species, in our samples, *Prochlorococcus* was never the dominant Cyanobacteria [132, 135].

In our surface co-occurrence network, Cyanobacteria were exclusively negatively correlated with the mixotrophic Dinophyceae, previously associated with phytoplankton grazing [170]. Moreover, Syndiniales, the most diverse parasitic group responsible for top-down regulation of *Gyrodinium* (Dinophyceae), exhibited a positive relationship with Cyanobacteria confirming that their parasitism is mainly on other marine protists [171]. The bacterial picoplankton was also correlated with haptophytes (Prymnesiophyceae) which have been linked with mixotrophy in oligotrophic waters accounting for up to 40% of bacterial grazing [172]. It is worth noting that, unassigned members of Prymnesiophyceae (ASV376, ASV646) and *Gephyrocapsa* (ASV6) were the sole representatives of Haptophytes showing a positive association with Cyanobacteria. In contrast, other less prevalent Prymnesiophyceae such as *Phaeocystis* (ASV169), *Prymnesium* (ASV373), *Algirosphaera* (ASV459) and *Chrysochromulina* (ASV151) exhibited negative connections, likely attributable to their distinct ecological roles. For instance, *Chrysochromulina*, has been previously linked to increased bacterivory rates, indicating the importance of heterotrophy for its growth, whereas *Gephyrocapsa* may rely more on photoautotrophy than phagotrophy [173].

3.5.3 Microbial composition and networking in the surface waters of the western Levantine basin (Cretan Passage)

In line with other studies, the heterotrophic SAR11 (Alphaproteobacteria), major players in carbon fixation, dominated across samples, confirming their high prevalence in oligotrophic environments [174]. As previously mentioned, temperature and nutrients are strong predictors of SAR11 ecospecies distribution [175]. In our dataset, members of SAR11 occupied diverse niches, influencing their relationships with Haptophytes and Dinoflagellates, with *Clade Ia* (ASV29) being the predominant ecotype in both sampling seasons but only in the surface-collected samples whereas *Clade Ib* (ASV68) expanded throughout the water column, having a preference for colder waters (Figure S6). In agreement to our results, a spatiotemporal analysis of coastal to offshore surface microbial communities in the eastern Levantine basin found *Clade Ia* more abundant in the summer months while *Clade Ib* was lowered in abundance during that season [134].

Other Alphaproteobacteria (*Erythrobacter*, *OM75*) and Gammaproteobacteria (*OM60*, *SAR86*, and *SAR92*) presented similar seasonal patterns. Despite their common niche for warmer waters, *OM60* (ASV366) and *SAR92* (ASV754) interacted with different eukaryotic groups in our samples. For example, *OM60* was positively associated with phagotrophic Haptophytes,

Dinophyceae and Syndiniales, while *SAR92* was correlated with Ascomycota (excluding *Sarocladium*). Moreover, *Pseudohongiella*, another γ-proteobacterium, preferred colder waters and positively interacted with *Prochlorococcus* and *Cyanobium*. Furthermore, the major Bacteroidota, *NS4* and *NS5 marine groups*, were more abundant in summer samples following the picoplankton bloom in winter, confirming their association with the degradation of high molecular weight organic matter (OM) [176]. Marine mycobiome diversity and ecology is generally understudied however they seem to be involved in OM decomposition, nutrient metabolism, and parasitism on picoeukaryotic algae [177]. In our samples, marine fungi (Ascomycota), mainly represented by *Aspergillus*, were prominent in summer AW/LSW sample yet they were not among the significant nodes in our surface network. However, the negative edges between fungal ASVs, dinoflagellates and haptophytes are in accordance with studies suggesting that marine fungi commonly infect these protists [178].

3.5.4 Microbial composition and networking in the deeper waters of the EMS basin (Cretan Passage)

The deeper waters of the EMS exhibited high microbial diversity yet associations between species were limited, as evidenced from the fewer number of edges compared to the AW/LSW microbiota network. Below 150 m, taxa linked to nitrogen cycling (*Nitrospinaceae*, Chloroflexi, SAR324, SAR406, *Nitrospiraceae*) were identified, indicating the significance of nitrogen cycling process taking place here, in alignment with previous EMS studies [135]. Chloroflexi, previously associated with recalcitrant OM degradation as well as with deep-sea carbon and sulphur cycling, was particularly abundant in winter LIW waters where OM deposition is higher due to vertical mixing [179].

Prokaryotes like the chemolithoautotroph Microtrichales (Actinobacteriota), comammox Nitrospira, the sulfur oxidizing SUP05 cluster and members of the microbial dark matter Marinimicrobia (SAR406) were most abundant in the deepest water layers. ASVs of Dinoflagellates and Radiolaria that often dominate microzooplankton communities, comprised the majority of nodes in our EMDW network [145]. In particular, the Radiolaria species of Acantharea and Polycystinea dominated the LIW and upper EMDW while unclassified RAD-B taxa were increased in deeper waters. In oligotrophic habitats, like the EMS, Radiolaria are considered as important players in the biological carbon pump even thought their trophic role is unclear [180]. However, they have been categorized as non-constitutive mixotrophs ingesting specific algal prey (eSNCM) like Dinoflagellates and Haptophytes [181]. This ecological role is

in agreement with our findings explaining the high number of positive edges between Dinoflagellata and Radiolaria. In our findings, Nitrospinota and Proteobacteria seem to act as prey for Radiolaria based on the exclusively negative associations between them. Moreover, the uncultivated Syndiniales, which comprised 60% of the total abundance in the deepest samples, are considered a black box in protistology [182]. Dinoflagellates seem to act as predators for the prokaryotic Nitrospira and Microtrichales based on our results while deep-sea fungal taxa were also observed (*Aspergillus*, *Lecanicillum*, *Cladosporium*) in accordance with previous studies [183]. Finally, positive relationships of deep-sea fungi with Radiolaria and Dinoflagellates might suggest a symbiotic-mutualistic or commensalistic relationship between these species.

3.5.5 Hydrocarbon-bioremediation potential of background EMS communities

Taxonomic profiling and calculation of hydrocarbon exposure index highlighted the potential for hydrocarbon degradation in the EMS, particularly in deep-water layers. Known hydrocarbon-degrading species were identified in both sampling seasons, thus forming a background community with potential to respond rapidly to an oil spill similar to that of Deepwater Horizon (DWH) in the Gulf of Mexico (GoM). The elevated presence of HC-degraders throughout the water column in summer as opposed to winter (only in EMDW layer) might be attributed to the increased maritime traffic which is considered as the major input source of hydrocarbons in the EMS [13]. Pre-spill microbial community in plume depths near the Macondo well in the GoM, recorded in March 2010, presented an α-/γ-proteobacteria ratio <1 indicating the increased presence of Gammaproteobacteria in the background community [184]. In our dataset, this ratio was higher (>1) in all water masses, including the deepest EMDW layer, where the highest EIHE index was recorded, indicating that lower levels of Gammaproteobacteria are present here compared to the GoM. This may be attributed to the absence of natural hydrocarbon seepages near our sampling stations, the closest being located in the Mediterranean Ridge tens of kilometers away, in contrast to the GoM where natural seepages were near the Macondo well. [185, 186]. Nonetheless, members of γ-proteobacteria and common HC degraders, *Alteromonadales* and *Oceanospirillales*, previously found in 800 m depth in GoM's pre-spill microbial community, were also identified in deep EMDW in both sampling seasons [84]. Moreover, our results find *Alcanivorax* among the significant nodes of the deep network having negative interactions with eukaryotes thus suggesting the low predation effect by this microbial group. Based on its mean *rrn* copy number (2.4) and according to Roller et al, *Alcanivorax* is expected to be a slow grower specialist that becomes antagonistic under certain

environmental conditions [187, 188]. Taken together, our data underline the presence of a microbial “seed” bank of taxa capable for oil bioremediation in the deep EMS.

3.6 Conclusion

Overall, our study aims to investigate that in the oligotrophic EMS basin, microbial communities can be differentially shaped according to distinct water masses. Through analysing samples from two sampling stations in this highly oligotrophic oceanic region, we observed distinct bacterial and unicellular eukaryotic communities with water mass. The eukaryotic community appeared to be more diverse throughout the water column, having the greatest differentiation in LIW layer, in winter than in summer. However, more interseasonal sampling expeditions are required for this to be statistically verified. The microbial network analysis revealed interspecies associations, indicating the increased number of ecological niches present in the surface layer compared to the deeper water mass. Finally, background levels of known hydrocarbon degraders were recorded indicating the capacity for oil bioremediation, particularly in the deep EMDW layer. These findings underline the necessity for further exploration and understanding of microbial ecology and associations in one of the world’s most understudied marine habitats, especially if we consider the heavy anthropogenic stress and the prediction of climate change impact in this basin.

CHAPTER 4.

Hydrocarbon-degrading consortia from Surface and Deep waters of the Eastern Mediterranean Sea

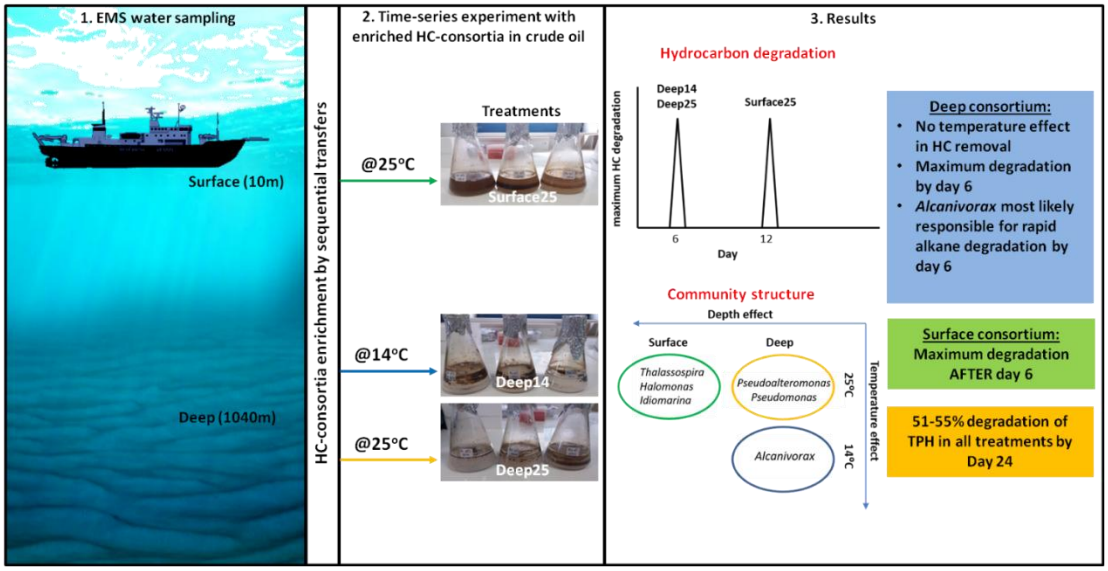

This Chapter has been published as:

Charalampous, G.; Fragkou, E.; Kormas, K.A.; Menezes, A.B.D.; Polymenakou, P.N.; Pasadakis, N.; Kalogerakis, N.; Antoniou, E.; Gontikaki, E. Comparison of Hydrocarbon-Degrading Consortia from Surface and Deep Waters of the Eastern Mediterranean Sea: Characterization and Degradation Potential. Energies 2021, 14, 2246. https://doi.org/10.3390/en14082246

4.1 Abstract

The diversity and degradation capacity of hydrocarbon-degrading consortia from surface and deep waters of the Eastern Mediterranean Sea were studied in time-series experiments. Microcosms were set up in ONR7 medium at *in situ* temperatures of 25 ºC and 14 ºC for the Surface and Deep consortia, respectively, and crude oil as the sole source of carbon. The Deep consortium was additionally investigated at 25 ºC to allow the direct comparison of the degradation rates to the Surface consortium. In total, ~50% of the alkanes and ~15% of the polycyclic aromatic hydrocarbons were degraded in all treatments by Day 24. Approximately ~95% of the total biodegradation by the Deep consortium took place within 6 days regardless of temperature, whereas comparable levels of degradation were reached on Day 12 by the Surface consortium. Both consortia were dominated by well-known hydrocarbon-degrading taxa. Temperature played a significant role in shaping the Deep consortia communities with *Pseudomonas* and *Pseudoalteromonas* dominating at 25 ºC and *Alcanivorax* at 14 ºC. Overall, the Deep consortium showed a higher efficiency for hydrocarbon degradation within the first week following contamination, which is critical in the case of oil spills, and thus merits further investigation for its exploitation in bioremediation technologies tailored to the Eastern Mediterranean Sea.

4.2 Introduction

The Eastern Mediterranean Sea (EMS) presents unique physical-chemical characteristics, with high salinity levels of approximately 39 psu (compared to 35 psu in the open ocean), elevated bottom seawater temperatures of 14 ºC (as opposed to 4 ºC on the average at similar depths and latitudes in the Atlantic Ocean) and ultra-oligotrophic conditions owing to extreme phosphorus limitation throughout the water column [126]. The waters of the EMS are stratified, with distinct water masses of unique physical and chemical properties present at different depths, each harboring distinct microbial communities in terms of properties, activity levels and metabolic capacities [135].

Oil pollution in the Mediterranean Sea has been attributed mainly to intense shipping activities resulting in a number of surface oil spills [13]. Oil contamination from shipping has been greatly reduced in recent years; however, the EMS is now facing a greater challenge: the intensification of offshore oil and gas exploration activities in deep and ultra-deep waters [189]. In the past two decades, exploration for oil and gas is moving towards increasingly deeper waters

due to the depletion of easily accessible hydrocarbon reserves on land, in combination with the increasing demand for fossil fuels. An empirical analysis of company-reported incidents (e.g., well blowouts, injuries and oil spills) in the Gulf of Mexico (GoM) has identified a positive correlation between platform incidents and water depth [11]. An oil spill in the semi-enclosed basin of the Mediterranean Sea, similar to the Deepwater Horizon (DWH) in the GoM, would have severe consequences for the marine ecosystem and the economic life of the surrounding countries [190].

The DWH blowout is considered the world's largest offshore oil spill so far, with unprecedented quantities of hydrocarbons (oil and gas) being released at 1500 m below sea level in the northern GoM [32]. Approximately half of the total oil released, along with all the gas, remained in the water column, creating a deep hydrocarbon plume [60]. Another 40% reached the surface with an important percentage of it (14%) sinking back at depth in the form of marine oil snow (MOSSFA event) [75, 76]. Several studies have been conducted in the aftermath of DWH, which focused on the microbial response to oil contamination [81, 82, 191, 192]. Gammaproteobacteria dominated both surface and subsurface waters but selected for different microbial populations [193]. In offshore surface waters, the microbial community shifted drastically and became enriched in *Cycloclasticus* with *Alteromonas*, *Pseudoalteromonas* and *Halomonas* increasing in abundance to a lesser extent [84]. Oceanospirillales, *Cycloclasticus* and *Colwellia* were the three most dominant taxa present in the deep plume during the different phases of the spill [80].

The extended research performed in the GoM following DWH revealed several unexpected aspects of hydrocarbon dynamics in the event of a deep-sea release of live crude oil. One of the major lessons learned from the DWH accident was the necessity of area-specific data on the microbial composition and activity, pre and post the event of an accidental oil release, in order to predict the fate of the oil spill in simulation models and assess the recovery of the ecosystem [63]. In the EMS, the future exploitation of recently discovered oil and gas reserves in deep waters may be translated into an increased risk of accidental oil spills. Nevertheless, our current knowledge regarding the response of microbial life to oil contamination in the EMS is extremely limited [140, 141]. This study aims to contribute towards that direction by assessing the biodegradation capacity of two hydrocarbon-degrading consortia enriched from surface and deep waters of the EMS. Key hydrocarbon degraders and succession patterns during crude-oil degradation were identified in time-series microcosm experiments containing crude oil as the sole source of carbon and energy. To our knowledge, this is the first study to provide quantitative

data on the capacity of microbial communities from the Eastern Mediterranean for oil-spill remediation in surface and deep-water layers and sets the baseline for site-specific bioremediation solutions and oil-spill monitoring.

4.2 Materials and Methods

4.2.1. Sample Collection

The circulation of the Eastern Mediterranean can be described as a three-layer system: Modified Atlantic Water (MAW) flows in along the surface through the Straits of Sicily (~upper 150 m). This water flows in an easterly direction getting more saline under the hot and dry conditions extant in the region, particularly in summer. The Levantine Intermediate Water (LIW), formed in the Levantine basin at intermediate depths (150–400 m), is characterized by temperatures around 15 ºC, higher nutrient concentrations and high salinity (39 psu), and forms the major part of the return flow of water out of the basin through the Straits of Sicily. The Eastern Mediterranean Deep Water (EMDW), occupying depths below 400 m, is characterized by particularly warm temperatures (compared to similar depths and latitudes in the Atlantic), stabilizing at approximately 13.5 ºC [125, 126].

Seawater samples were collected on board the R/V Aegaeo (Hellenic Centre for Marine Research) on 23–28 August 2019. The sampling station was located off Southern Crete, Greece (Koufonisi station: 26.131288 E, 34.815447 N). Surface (10 m) and deep (1040 m) seawater samples were collected in 12 L Niskin bottles mounted on a CTD rosette and stored (within 1 h) in acid-washed plastic containers in the dark until use in laboratory experiments. Seawater temperature and salinity at each sampling depth were 27 ºC/39.6 psu at 10 m and 14 ºC/38.8 psu at 1040 m. Two liters of seawater from each sampling depth were filtered onboard through 0.2 µM polyethersulfone (PE) membrane filters (Rephile, USA) and stored frozen until DNA extraction.

4.2.2. Enrichment of Hydrocarbon-Degrading Microbial Consortia

Hydrocarbon-degrading microbial consortia originating from Eastern Mediterranean surface and deep-seawater samples, hereafter referred to as Surface and Deep consortia, respectively, were produced through sequential enrichments in ONR7 medium (DSMZ medium 950, accessed on 18 October 2019) and 0.5% v/v filter-sterilized Iranian light crude oil (CO, density ~0.7821 g mL^{-1}). The enrichment cultures were initially inoculated with 20% v/v aged

seawater (maintained in the dark at 14 ºC for 4 months) and subsequently by transferring 10% v/v of culture to new ONR7+CO medium. Microbial biomass was measured daily as optical density (OD) at 600 nm. Transfers took place when the culture growth entered the early exponential phase (OD 0.2–0.3). The cultures were incubated at room temperature (23–25 ºC) for Surface and at 14 ºC for Deep enrichments. Following each transfer, part of the remaining volume of the culture was stocked in 25% glycerol aliquots and the rest was filtered through 0.2 µM PES filters (Rephile, USA) for DNA extraction. Glycerol stocks and filters were stored at −80 ºC. The community composition of background and aged seawater, as well as that of each transfer step, is given in Appendix I (Figure S7). The 2nd transfer (S2, D2) from both enrichments was selected for the timeseries biodegradation experiment.

4.2.3. Time-Series Biodegradation Experiment

Batch microcosms were set up in 250 mL Erlenmeyer flasks containing 125 mL ONR7 medium and 0.5% v/v filter-sterilized CO. The microcosms were inoculated with thawed glycerol stocks of the enriched consortia (S2 and D2 for Surface and Deep microcosms, respectively). Three treatments were examined in triplicate microcosms: the Surface consortium at 25 ºC (Surface25) and the Deep consortium at 14 ºC (Deep14) and 25 ºC (Deep25). Sub-samples for microbial community analysis were collected after 6, 12, 18 and 24 days on 0.2 µM PES filters, as described above. A parallel set of triplicate flasks per treatment and sampling points at 6, 12 and 24 days were prepared for destructive sampling for gas chromatography–mass spectrometry (GC-MS) analysis of hydrocarbon concentrations. Abiotic hydrocarbon losses were assessed in triplicate flasks prepared without inoculum and sampled on Day 24.

4.2.4. Hydrocarbon Extraction and GC-MS Analysis

Liquid–liquid extraction was performed to obtain the microbial activity extract, free from the aqueous culture medium (ONR7). For the extraction of the organic compounds, an equal volume of dichloromethane (DCM Suprasolv®, Merck KGaA, Darmstadt, Germany) was used (3 × 20 mL for each extraction), in 100 mL Erlenmeyer flasks with a glass spout at the bottom. The flasks were shaken manually to assist the dissolution of the organic compounds in the solvent and the extract was filtered through columns of anhydrous sodium sulfate and fiberglass to remove any water residues. Following solvent removal on a rotary evaporator, the dried samples were transferred to 4 mL vials with a small amount of DCM Suprasolv® and concentrated by evaporation at low heat on a hot plate (~40 ºC) with simultaneous nitrogen blow.

The solid extracts that occurred were then separated in saturated and aromatic hydrocarbon fractions by elution through SPE columns (Bond Elute TPH, Agilent Technologies, Inc., Santa Clara, CA, USA) with n-hexane Suprasolv® (Merck KGaA, Darmstadt, Germany) and DCM Suprasolv®, respectively. GC-MS analysis was performed on an Agilent GC-MS HP 7890/5975C system, with an Agilent HP-5MS 5% phenyl methyl siloxane column (60 m × 250 µm × 0.25 µm). The hydrocarbon mixture consisted of an Oil Analysis Standard (Absolute Standards Inc.®, Hamden, CT, USA) containing 44 compounds, and a 17a(H),21b(H)-hopane (Chiron AS®, Trondheim, Norway). The standard composition of the hydrocarbon mixture was normal alkanes from C_{10} to C_{35}, pristane and phytane and 16 polycyclic aromatic hydrocarbons (PAHs) (naphthalene, phenanthrene, anthracene, fluorene, dibenzothiophene, fluoranthene, pyrene, chrysene, benzo(b)fluoranthene, benzo(k)fluoranthene, benzo(e)pyrene, benzo(a)pyrene, perylene, indeno(g,h,i)pyrene, dibenzo(a,h)anthracene and benzo(1,2,3-cd)perylene).

4.2.5. DNA Extraction

DNA was extracted according to [194], with modifications. Briefly, each PES membrane filter was cut in smaller pieces and divided into two Eppendorf tubes containing 670 µL of CTAB extraction buffer (1 M Tris-HCl (pH 8), 0.5 M EDTA (pH 8), 1 M NaH2PO4 (pH 8), 5 M NaCl and 5% cetyltrimethylammonium bromide) and mixed using a high-speed vortex for 2 min. The samples were then subjected to 3 freeze–thaw cycles in liquid nitrogen (1–2 min) to 65 ºC (10 min) followed by addition of 100 µL (10 mg mL^{-1}) lysozyme and 10 µL (20 mg mL^{-1}) Proteinase K and incubation at 37 ºC for 30 min. After incubation, 60 µL of 20% sodium dodecyl sulfate (SDS) were added and the samples were left at 65 ºC for 2 h with gentle mixing every 10 min. The supernatant was collected after centrifugation at 10,000× g for 10 min and transferred into a new 2 mL microcentrifuge tube where it was mixed with an equal amount of phenol:chloroform:isoamylalcohol (25:24:1). The aqueous phase obtained after centrifugation (15,000× g for 15 min) was subjected to a second purification step with 700 µL chloroform:isoamylalcohol solution (24:1). DNA was precipitated overnight at 4 ºC by addition of a x0.7 volume of ice-cold isopropanol to the aqueous phase. The precipitated DNA was centrifuged at room temperature (13,000× g, 45 min) and the supernatant was discarded. The DNA pellet was washed with ice-cold 70% molecular-grade ethanol and centrifuged again for 30 min at 13,000× g. Finally, the ethanol was removed, and the pellet was left to dry for 15 min in a laminar flow hood. Genomic DNA was resuspended in 50 µL TE buffer. DNA concentration was measured on a Qubit 4.0 fluorometer (Invitrogen, Thermo Fisher Scientific, Waltham, MA,

USA) using the Qubit dsDNA high sensitivity assay. All chemical reagents were purchased from Sigma-Aldrich Inc. (Merck KGaA, Darmstadt, Germany).

4.2.6. 16S rRNA Amplicon Sequencing and Bioinformatic Analysis

The V3-V4 regions of the 16S rRNA gene was sequenced on the Illumina MiSeq (2 × 300 bp) platform by Biosearch Technologies, LGC Genomics GmbH (Berlin, Germany) using the universal primers 341F and 806R [195]. Bioinformatic analysis was performed in the "R" programming environment (version 4.0.2) [158] using the DADA2 R package and pipeline for microbiome data analysis [157]. The SILVA SSU taxonomic training data for DADA2 (Silva version 138) was employed for taxonomy assignment [159]. A neighbor-joining phylogenetic tree was constructed in the *phangorn* R package (version 2.5.5) [196] following multiple alignment of ASVs using the *DECIPHER* R package [197]. The DADA2 pipeline resulted in a single object containing the sample-by-sequence feature table, the experimental metadata, the sequence taxonomies and the phylogenetic tree, which was subsequently imported into the *phyloseq* R package for further analysis [198]. A total of 1,563,382 reads were obtained from 49 samples after Illumina paired-end sequencing of 16S rRNA gene amplicons (V3-V4 region) with 1,082,378 total reads remaining after quality filtering and chimera removal. The number of sequences per sample ranged from 4993 to 43,902, with an average of 22,083 sequences. One feature for which a taxonomic rank could not be assigned at the phylum level was removed. The remaining dataset consisted of 1415 unique ASVs. Supervised prevalence filtering was further applied, with five more phyla removed from the dataset. Following prevalence filtering, 1404 unique ASVs remained, distributed among 19 Phyla.

4.2.7. Statistical Analysis

Statistical analysis was performed in the "R" programming environment [158]. All plots were produced using the R package *ggplot2* unless otherwise specified [164]. Linear regression was used to test the effect of treatment (Deep14, Deep25 and Surface25) and time (categorical variable, levels: 0, 6, 12, 18 and 24) on alpha diversity (richness, Shannon– Weaver, Simpson and Chao1 indices). The optimal models were identified based on AIC (*step* function) by forward and backward selection. In case the optimal model included non-significant regression parameters, further model selection steps were undertaken using the F-test (*drop1* function) [199]. Model validation was applied to check that the underlying statistical assumptions were not

violated. Post-hoc multiple comparisons were carried out using Tukey's honest significant difference test.

Principal coordinate analysis (PCoA) and distance-based redundancy analysis (dbRDA) on weighed Unifrac distance were used to explore similarities between microbial communities and assess the effect of depth, temperature and time using the *vegan* R package [162]. Count data were normalized by the cumulative sum scaling (CSS) method prior to multivariate analysis [161]. Negative binomial regression on DESeq2-transformed count data was used to identify differentially abundant taxa related to explanatory variables using the *DESeq2* package [200, 201]. DESeq2 was run using the Wald test, with automatic filtering of low abundance ASVs, automatic calculation of adjusted p-values and an alpha of 0.01. Levin's niche breadth and niche overlap indices of ASVs were measured with the *MicroNiche* R package [202]. Prior to niche breadth analysis, the dataset was rarefied to 4993 sequences per sample. The *MicroNiche* functions were applied to the ASV count table after genus taxa assignment. A limit of quantification (LOQ) was applied, defined as a threshold calculated from the distribution of microbial taxa within the dataset and a 95% certainty that these taxa will fall within a null distribution, where the mean taxon abundance is zero. In our case study this was set to 1.3× standard deviations from zero in order to exclude any false-positive taxa that are misclassified as specialists/generalists. Levin's Overlap values (LO12 and LO21) are plotted as heatmaps using the *gplots* R package [203].

4.3. Results

4.3.1. Hydrocarbon Degradation

The results from the GC-MS analysis revealed an effective degradation of CO by Day 24 in all three treatments (Surface25, Deep14 and Deep25), achieving a total of 51%, 53% and 55% reduction in the total petroleum hydrocarbon (TPH) concentration, respectively (Figure 20A). More than 85% of the TPH degradation by the Deep consortium at both temperatures (Deep14 and Deep25) was achieved by Day 6. The Surface consortium presented a lag phase until Day 6 but reached a comparable TPH reduction by Day 12. The crude-oil fractions, examined by GC-MS analysis, consisted of about 99% saturated components, out of which 89% were short-chain (C14-C25) and 11% were long-chain alkanes (C26-C35), and 1% PAHs. The light alkanes fraction was rapidly degraded by the Deep consortium regardless of temperature; 50% of light

alkanes were degraded by Day 24, of which 86–88% were removed by Day 6 (43–44% of total light alkanes) (Figure 20B).

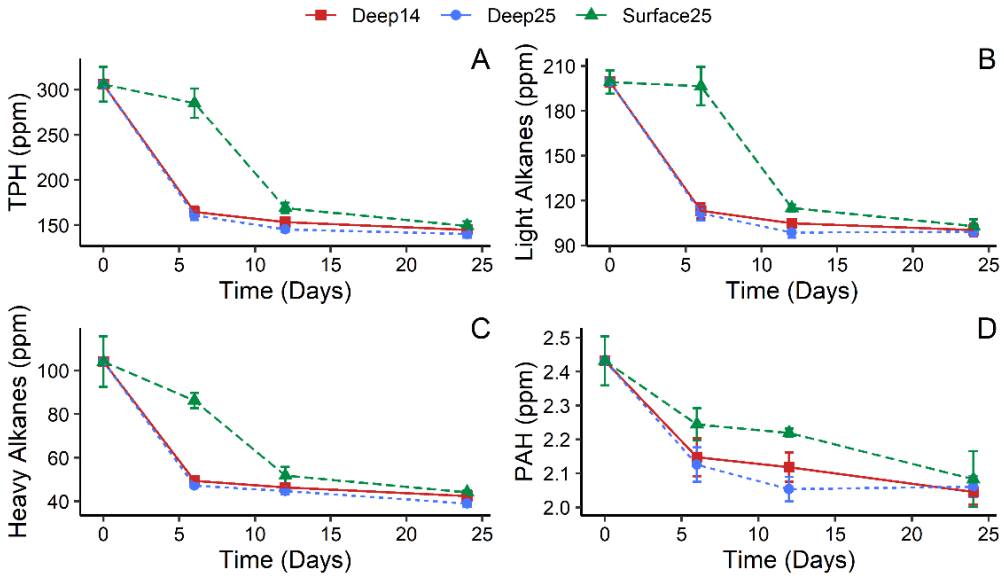

Figure 20. *Hydrocarbon biodegradation over time for the Deep14, Deep25 and Surface25 treatments for (A) total petroleum hydrocarbons (TPH), (B) light alkanes (C14-C25), (C) heavy alkanes (C26-C35) and (D) PAHs. Values on the y-axis correspond to the concentration range of each hydrocarbon group to aid visualisation. Error bars represent the standard deviation (n = 3).*

Light alkanes degradation reached 47% and 50% by Day 12 in the Deep14 and Deep25 treatments, respectively, but was negligible between 12 and 24 days. Almost no degradation of light alkanes occurred within the first 6 days in the Surface25 treatment, yet a 48% reduction in the concentration of light alkanes was achieved by Day 24 (85% of total reduction between 6 and 12 days) (Figure 20B). Long-chain alkanes degradation was proportionally higher than that of light alkanes and ranged between 58 and 63% of the total heavy alkanes concentration on Day 24 in all treatments (Figure 20C). The maximum degradation rate of this hydrocarbon group was observed in the 0–6 time interval for both Deep treatments and 6–12 for Surface25. Unlike light alkanes, the Surface consortium immediately started degrading the heavier compounds of the oil. Deep25 presented the highest degradation of the heavier compounds (17% reduction) followed by Deep14 and Surface25 (13% and 12%, respectively).

PAH degradation was initiated immediately in all three consortia, reaching a total PAH reduction of ~15% by Day 24 (Figure 20D). Both Deep consortia performed better than Surface25 at the early stages, similar to the pattern observed for saturated hydrocarbons. The majority of PAHs were consumed by Day 6 in Deep14 and Deep25, after which the degradation slowed down until Day 24. PAH degradation in Surface25 occurred in the 0–6 and 12–24 time intervals; between 6 and 12 days, when the maximum degradation of alkanes is observed, PAH degradation in Surface25 stalled. Supporting data for the hydrocarbon degradation and the different components can be found in the Supplementary Materials section (Figures Figure **S8**-Figure **S10**,Table S4).

4.3.2. Microbial Diversity Analysis

4.3.2.1. Microbial Community Structure

The Deep consortium at 14 ºC (Deep14 treatment) was highly enriched in *Vibrio* up to Day 6. *Alcanivorax* replaced *Vibrio* as the most abundant taxon between Days 12 and 24, reaching a relative abundance of 40–60%. *Alteromonas* and *Pseudoalteromonas* were also present in the Deep14 treatment but maintained constant relative abundance throughout the experiment (Figure 21). The Deep consortium at 25 ºC (Deep25) was similar to that of the Deep14 samples up to Day 6. Changes in the dominant taxa due to increased temperature became prevalent on Day 12 onwards, with *Pseudomonas* and *Pseudoalteromonas* collectively reaching 80–90% in relative abundance (Figure 21). Alphaproteobacteria of the order Rhodospirillales (genus *Thalassospira*) were significantly enriched in Surface samples, reaching up to 40% of the total abundance (Figure 21 and Figure S11). *Halomonas* and *Alteromonas* were also highly abundant in Surface samples. *Idiomarina* became enriched through time, reaching approximately 15% of the microbial abundance on Day 24 (Figure 21).

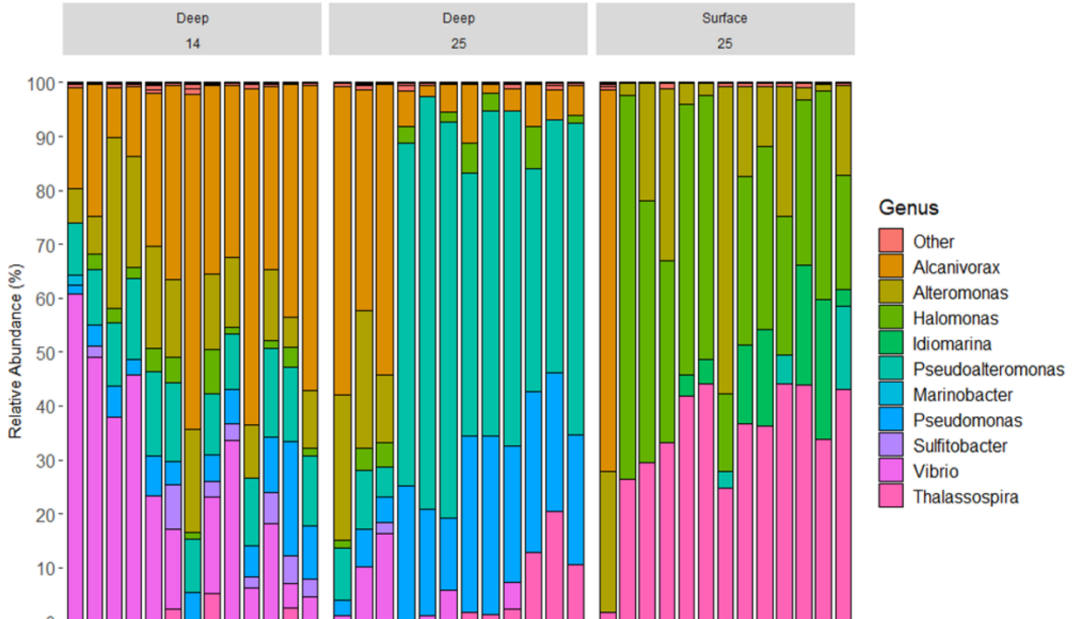

Figure 21. *Relative abundance of bacterial taxa at the genus level plotted against time (days) and grouped by treatment (Deep14, Deep25 and Surface25). Taxa that are less than 1% in abundance are grouped as "Other". Brackets on the x-axis correspond to the triplicate samples for the given timepoint. Day zero corresponds to the original D2 and S2 consortia and is common for the Deep14 and Deep25 treatments.*

4.3.2.2. Alpha Diversity

A steep drop in alpha diversity was observed with seawater storage, i.e., between the background (fresh) and aged seawater (Figure 22, Figure S7). Alpha diversity decreased further with oil contamination (starting consortium Day 0) but did not change further with time during the incubation experiment. Statistical analysis to test for differences between treatments and time effects on alpha diversity metrics was performed for Days 6, 12, 18 and 24, in which triplicate samples were collected. Alpha diversity, as measured by the Shannon index, differed significantly between treatments (F = 42.09, d.f.2, $p < 0.001$) but did not change with time (F = 1.41, d.f.3, $p = 0.257$). The same pattern was observed using other diversity metrics (ASV richness, Simpson index and Chao1 index). Pairwise comparisons with Tukey's post-hoc test showed consistently higher ASV richness and diversity in the Deep14 treatment (Figure 22, Table S5), with the exception of the Chao1 index; the diversity estimator Chao1 index, which calculates the expected ASVs based on the low abundance species (singletons and doubletons), was not significantly different between the Deep14 and Deep25 treatments (t-value = −1.81, $p = 0.181$).

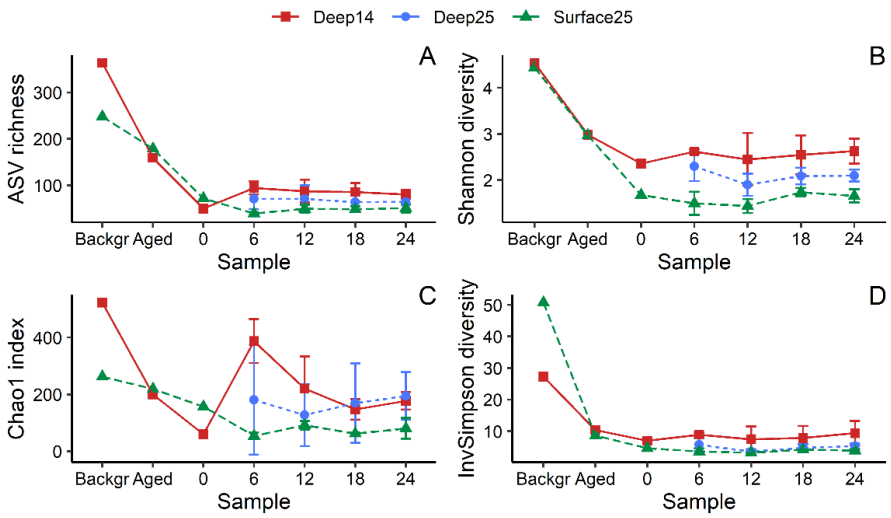

Figure 22. *Measures of alpha diversity: (A) richness, (B) Shannon's diversity index, (C) Chao1 index and (D) Inverse Simpson index. "Backgr" corresponds to the background microbial community in seawater at a 10 and 1040 m water depth. "Aged" is the seawater that was used as inoculum for the enrichment of consortia. Day 0 corresponds to consortia S2 and D2, which were selected for the microbial succession experiment.*

4.3.2.3. Beta Diversity

Microbial communities clustered into three groups according to the treatment (Figure 23A). Samples of the same treatment clustered together except for Deep25 samples on Day6, which clustered with Deep14, reflecting the gradual shift of the Deep community due to increased temperature. Treatments were significantly different to each other based on PERMANOVA multilevel pairwise comparisons (R2: Surface25-Deep25: R2 = 0.88, p = 0.003; Surface25-Deep14: R2 = 0.91, p = 0.003; Deep25-Deep14: R2 = 0.15, p = 0.012). Depth, temperature and time explained 69% of the variation in the structure of microbial communities based on dbRDA analysis using weighed Unifrac distances (Figure 23B). The distribution of the samples on the dbRDA triplot indicated clustering based on depth along the first axis, explaining 60% of the variance in the data, and on temperature and time along the second axis (Figure 23B). The ANOVA-like permutation testing for dbRDA (*anova.cca* function in *vegan* R package) indicated that all explanatory variables were significant at the 5% level (depth: F = 58.12, d.f.1,34, p = 0.001; temperature: F = 4.99, d.f.1,34, p = 0.007; time: F = 4.88, d.f.1,34, p = 0.011).

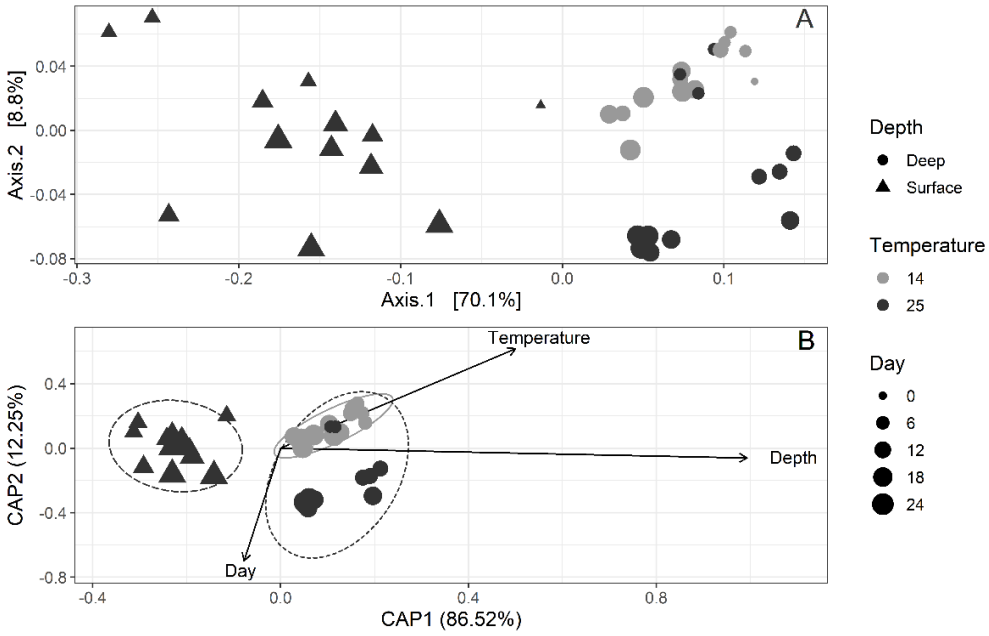

Figure 23. *(A) Principal coordinate analysis (PCoA) of the weighted UniFrac distances. (B) Distance-based redundancy analysis (dbRDA) of the weighted UniFrac distances quantifying the impacts of depth, temperature and time on microbial community composition. Cumulative sum scaling (CSS) normalization was applied to the data prior to ordination analysis to account for differences in library size.*

4.3.3. Identification of Influential Taxa Based on DESeq2 Analysis

Differential abundance analysis was conducted to identify ASVs that were strongly influenced by depth, temperature, and time. DESeq2 analysis by depth identified 20 influential ASVs that were strongly enriched in the Surface25 treatment (Figure 24A, Table S6). Characteristic taxa of the Surface25 treatment belong to the Gammaproteobacteria families *Halomonadaceae* (genus *Halomonas*) and *Idiomarinaceae* (genus *Idiomarina*), and the Alphaproteobacteria *Thalassospiraceae* (genus *Thalassospira*). *Halomonas* and *Thalassospira* became enriched within the first 6 days while *Idiomarina* became influential after Day 12 (Table S4). DESeq2 analysis by temperature revealed influential ASVs in the Deep14 treatment (negative log2FC) (Figure 24B, Table S6), namely, *Rhodobacteraceae* (*Sulfitobacter*), *Alcanivoracaceae* (*Alcanivorax*), *Vibrionaceae* (*Vibrio*) and *Marinobacteaceae* (*Marinobacter*). DESeq2 analysis per treatment at each time interval (Table S7) identified common aspects in the behavior of *Alcanivorax* and *Sulfitobacter* to temperature, which both became depleted in Surface25 at 0–6 days and in Deep25 between 6 and 18 days. On the other hand, *Thalassospira* was favored by higher temperature, as evidenced by enriched ASVs in the Deep25 treatment between 12 and 24 days (Table S7).

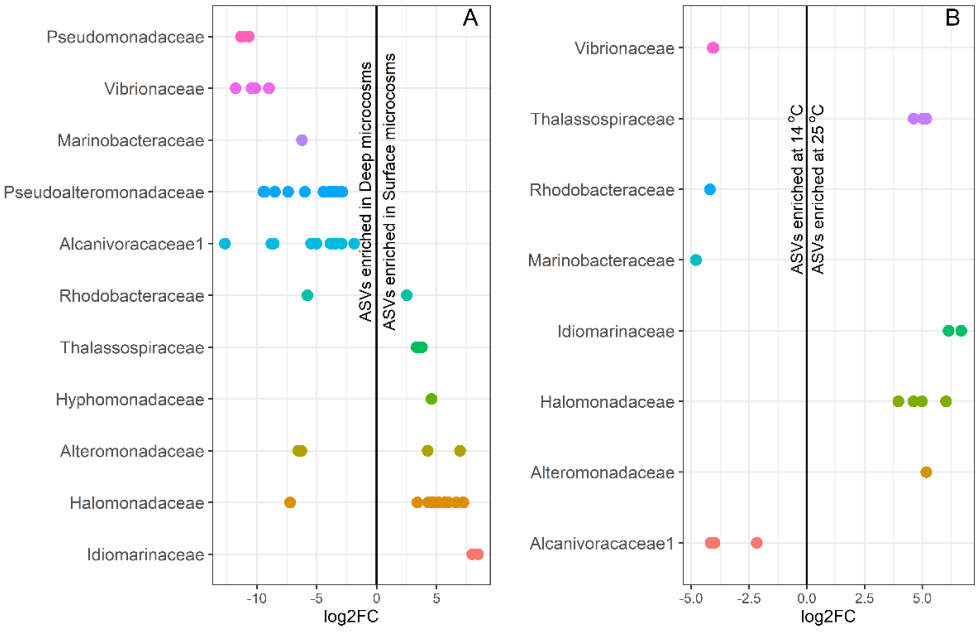

Figure 24. *ASVs strongly influenced by depth (A) and temperature (B) based on DESeq2 analysis. Log2FC is the logarithmic fold change of taxa abundance between two conditions (Surface–Deep and 14–25 ºC).*

4.3.4. Levin's Niche Analysis

Levin's niche analysis can provide valuable quantitative information as to which genera are considered specialists or generalists and assess taxon–taxon relationships [202]. This is achieved by using Levin's niche breadth (BN) and Levin's overlap (LO), respectively [202]. We performed niche analysis of bacterial genera identified in the three treatments of the experiment (Deep14, Deep25 and Surface25). A limit of quantification (LOQ) threshold was employed on rarefied data to exclude any taxa with low, random abundance from being falsely characterized as specialists/generalists (Figure S12). Levin's BN values indicate which taxa are present under any environmental conditions (generalists) and which are restricted in a unique environment, in this case, a treatment (specialists). Generalists have BN values closer to 1 while specialists have values closer to 0 (Figure S13, Table 3). *Idiomarina*, *Marinobacter*, *Vibrio*, *Thalassospira* and *Sulfitobacter* were the strongest specialists classified in our samples ($p < 0.001$, Table 3). In addition, *Pseudoalteromonas* and *Pseudomonas* were also classified as significant specialists ($p < 0.05$), resulting in BN values below the 0.05 quantile threshold (BN < 0.57) (Table 3, Figure S13). *Alcanivorax*, *Alteromonas* and *Halomonas* presented BN indices that are neither proportionally equal (generalists), neither associated with a unique environment (specialists). Identified specialists are shown in boxplots indicating the treatment they were enriched in (Figure S14).

Table 3. *Taxa that pass the limit of quantification (LOQ) threshold and can be characterized with confidence as specialists or generalists by their Levin's BN indices. Taxa with values closer to 0 are considered specialists while those closer to 1 are considered generalists.*

Genus	Levin's B_N	*p*-Value
Alcanivorax	0.691	0.2537
Alteromonas	0.858	0.5606
Halomonas	0.664	0.1560
Idiomarina	0.342	0.0000 **
Marinobacter	0.447	0.0002 **
Pseudoalteromonas	0.565	0.014 *
Pseudomonas	0.559	0.013 *
Sulfitobacter	0.427	0.0001 **
Thalassospira	0.425	0.0001 **

Vibrio	0.417	0.0001 **

Levin's Overlap (LO) takes into account the species abundance across environments and indicates which taxa coexist on a heatmap plot (Figure 25). LO12 and LO21 axis values do not necessarily have the same indices as that depends on the distribution of the compared taxa and their classification as specialists or generalists [202]. For example, a strong overlap between *Alcanivorax* and *Sulfitobacter* was observed on the LO12 axis but not on LO21 (Figure 25). This indicates that *Sulfitobacter* co-occurred with *Alcanivorax* but the absence of *Sulfitobacter* did not entail absence of *Alcanivorax*. In addition, *Idiomarina* depended on the presence of *Halomonas* but not the opposite (LO12 overlap only). On the other hand, *Halomonas* and *Thalassospira*, as well as *Pseudomonas* and *Pseudoalteromonas*, overlap on both LO12 and LO21 axes, meaning that both species coexist in specific environments. Finally, *Marinobacter* depended on the presence of *Vibrio* (LO12 overlap only) (Figure 25)

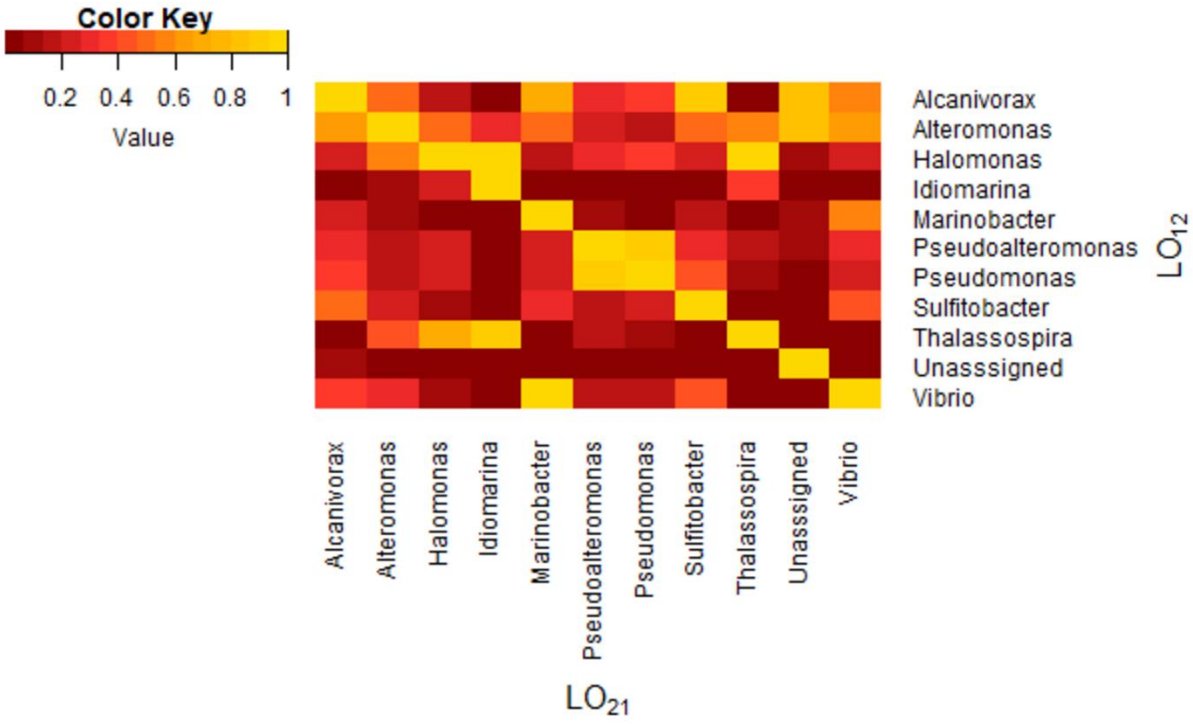

Figure 25. *Heatmap of Levin's Overlap (LO) indicating coexistence of species taking into account their environmental distribution in the three different treatments (Deep14, Deep25 and Surface25). Only taxa that pass the LOQ line are included. The scale bar shows values between 0 for poor overlap (dark red) and 1 for complete overlap (yellow).*

4.4. Discussion

Hydrocarbon-degrading bacterial consortia were enriched from surface and deep waters of the EMS with the aim to investigate the degradation capacity of indigenous microorganisms and the potential use of enriched consortia in bioremediation. We did not observe a significant temperature effect on the degradative capability of the Deep consortium, which responded rapidly to hydrocarbon contamination, removing 47% of the alkanes and 12% of the PAHs within 6 days at both tested temperatures (25 ºC and 14 ºC). In comparison, the Surface consortium had a lower degradative capability, removing only 8% of the total alkanes and 8% of the PAHs during the same period with close to zero degradation of the low molecular weight alkanes. Despite the response lag, both the Deep and Surface consortia removed similar amounts of TPH by Day 24, ranging from 51% (Surface25) to 55% (Deep25).

Between-study heterogeneity in experimental conditions hampers direct comparison of the degradative characteristics of consortia. Temperature, nutrient levels, the geographic origin of microbial communities and previous exposure to hydrocarbon sources as well as the composition and concentration of the hydrocarbon substrate are part of a nonexhaustive list of factors affecting hydrocarbon-degradation rates [81, 204, 205]. In the GoM, a surface-water consortium removed almost 90% of total the alkanes and 77% of the PAHs after 8 days, while the deep-water consortium at 5 ºC was equally capable in hydrocarbon removal albeit with a considerable lag phase [97]. The high degradation rates by GoM consortia in the aforementioned study may be attributed to the low concentration of crude oil used in the experiments that is known to result in more efficient hydrocarbon removal [81, 204, 206]. At comparable, to this study, crude-oil concentrations (400 mg L^{-1}), Bacosa et al. measured 65% degradation of alkanes after 50 days in surface waters of the GoM [206]. Microbial consortia originating from shallow and deep sub-arctic sediments of the NE Atlantic were less efficient in diesel and model oil degradation (1% v/v concentration; 50–58% and 33–42% TPH removal by the shallow and deep consortia, respectively) at 20 ºC [207].

Temperature often emerges as the major environmental parameter determining the composition of oil-degrading microbial communities and the rate of hydrocarbon degradation [208]. Deep-sea microbial communities exhibit a lower hydrocarbon-degradation potential than shallower communities when incubations are performed at *in situ* conditions primarily due to the low temperatures prevailing in the deep sea [109, 209, 210]. At equivalent incubation temperatures, there is not enough evidence to support an intrinsically lower potential of deep-

water microbial communities for hydrocarbon degradation compared to shallow-water counterparts although the latter seem to perform better in most cases [205, 207]. The Deep consortium, in this study, performed better in terms of response time and overall performance even at 14 ºC although differences with the Surface consortium were negligible by Day 24. Remarkably, raising the incubation temperature of the Deep consortium by 11 ºC (from 14 to 25 ºC) did not produce the expected increase in biodegradation rate based on a Q10 (change in metabolic rates with a 10 ºC increase) range of 2–3, which is widely accepted for temperature compensation in biodegradation rate calculations (e.g., a Q10 of 2 is applied in the OSCAR Oil Spill Contingency and Response model) [211]. Based on the Q10 approach, the hydrocarbon-biodegradation rate in Deep25 should be at least double that in the Deep14 treatment. Yet, Q10 remains close to 1 for all hydrocarbon fractions, demonstrating the adaptation of deep-water microbes in the Eastern Mediterranean to ambient conditions and their ability to degrade hydrocarbons at comparable, if not greater, rates to surface communities. Our results confirm findings of faster-than-expected hydrocarbon-degradation rates in deep waters of the GoM following DWH [212].

The narrow temperature gradient between surface and deep waters in the Mediterranean, selecting for mesophilic microorganisms throughout the water column, may partly explain why temperature is of secondary importance in this environment compared to other oceanic locations where the temperature of deep waters is typically 4 ºC or less [109, 205]. The origin of the consortium from surface or deep waters was the most important variable in shaping the structure of the bacterial community, followed by temperature. These two factors selected for different dominant oil-degrading taxa within each treatment. *Thalassospira* and *Halomonas* were characteristic of the Surface consortium throughout the incubation period. *Idiomarina*, identified as a strong specialist based on the Levin's BN index, appeared solely in the surface consortium after Day 12 and increased in relative abundance thereafter. Several members of the *Thalassospira* and *Idiomarina* genera are known PAH degraders [213, 214]. In the Eastern Mediterranean, *Idiomarina* emerged as a potential PAH degrader in surface sediments of contaminated sites following the Agia Zoni II oil spill in Greece [215]. Although highly abundant in the original S2 consortium, *Alcanivorax* was not present in the Surface25 treatment at any time point. It is not clear why *Alcanivorax* was not competitive at the given experimental conditions, but its absence may well explain the response lag in the degradation of light alkanes by the Surface25 community. In the Deep consortium incubations, *Alcanivorax* and *Vibrio* dominated at 14 ºC but were replaced by the cosmopolitan *Pseudoalteromonas* and

Pseudomonas at 25 ºC after Day 6. The role of *Alcanivorax* species in deep-sea oil-spill remediation is ambiguous; several species of *Alcanivorax* have been isolated from the deep sea [216–218] yet *Alcanivorax* was not reported among the dominant taxa in the deep hydrocarbon plume during DWH and, based on ex-situ experiments, this genus is not considered as characteristic of the microbial community response to oil contamination in the deep sea [81, 85, 210, 219]. Nevertheless, *Alcanivoraceae* were identified as key players in crude-oil degradation in deep waters of the EMS [141], in agreement with the results of this study. However, the importance of *Alcanivorax* as a key taxon in hydrocarbon degradation in the deep Eastern Mediterranean needs to be confirmed under high hydrostatic pressure conditions.

The genus *Vibrio* was characteristic of the deep consortium at 14 ºC. Members of the genus are capable of alkane and PAH degradation [220, 221], and *Vibrio* has been found at high concentrations in oil-contaminated sites, particularly in association with biofilms [215, 222–224]. Nevertheless, *Vibrio* strains isolated from oil-contaminated beach sands in the Gulf of Mexico following DWH showed little-to-no oil consumption [99]. In, similar to ours, oil-enriched microcosms from GoM, *Vibrio* represented ~80% of the total community (DNA) abundance in surface water consortia, but only 25% of the active community (RNA) [97]. Here, monitoring the community structure in each enrichment step allowed us to observe that *Vibrio* was not consistently present in all transfers of the deep consortium. The presence of *Vibrio* in high concentration was restricted to the second transfer consortium (D2), which introduces a random element in the outbursts of this genus. Further biologically relevant conclusions can be extracted from hierarchical testing (DESeq2), in conjunction with Levin's niche analysis, both of which are useful for gaining insight on influential low-abundance taxa. Of interest in this study were *Marinobacter* and *Sulfitobacter* (family *Rhodobacteraceae*), both of which were associated with the Deep consortium at 14 ºC and are common encounters in oil-contaminated sites under various environmental conditions [99, 225]. Interestingly, the presence of *Sulfitobacter* was tightly coupled to that of *Alcanivorax* both spatially and temporally. The preference of *Sulfitobacter* for lower temperatures has been previously reported [205]. Little is known about the degradative capability of *Sulfitobacter* although utilisation of crude oil as a carbon source has been previously reported [219] and draft genome sequences of *Sulfitobacter* have revealed the presence of genes involved in aromatic hydrocarbon degradation [226].

4.5. Conclusions

Over the last few years, the area south of Crete has drawn attention concerning its oil and gas reservoirs that, if proven financially exploitable, will result in the development of a number of oil and gas production platforms in waters exceeding 1000 m in depth and in close proximity to land. This investment would increase the risk of oil-spill accidents in the area. The unique physical-chemical properties and the distinct microbial communities of the EMS require site-specific data to improve oil-spill preparedness and develop appropriate mitigation measures in the event of an accident. This study generated enriched hydrocarbon-degrading bacterial consortia from deep waters of the EMS that proved to be readily effective in the biodegradation of crude-oil constituents within the first week following contamination, which is even more critical in the case of oil spills. This fundamental finding sets the foundations for further study on the efficacy of the Deep consortium under field environmental conditions, i.e., high pressure and low nutrient levels, with possible applications in bioremediation technologies tailored to the EMS.

CHAPTER 5.

Enrichment and isolation of Hydrocarbon Degraders under high-pressure from Deep-Water Communities of the Eastern Mediterranean Sea

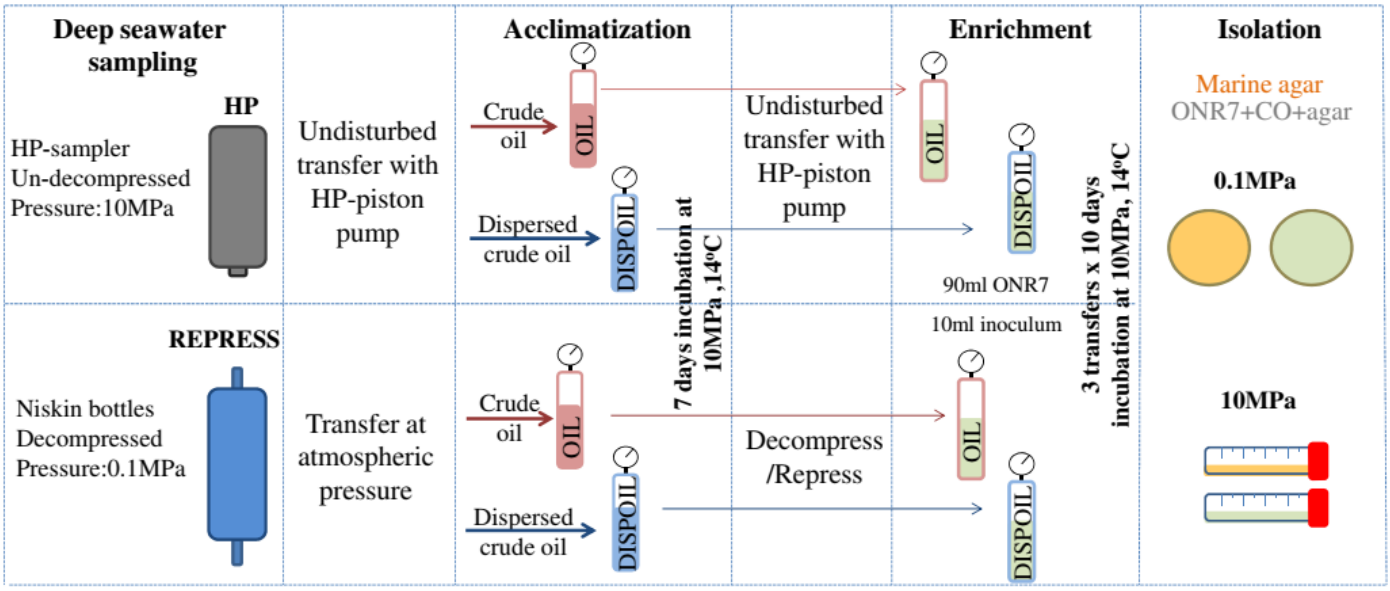

A modified version of this chapter has been published as:

Charalampous, G.; Fragkou, E.; Kalogerakis, N.; Antoniou, E.; Gontikaki, E. Diversity links to functionality: Unraveling the impact of pressure disruption and culture medium on crude oil-enriched microbial communities from the deep Eastern Mediterranean Sea, Marine Pollution Bulletin, 2024, 202, 116275. https://doi.org/10.1016/j.marpolbul.2024.116275.

5.1. Abstract

Mesopelagic water from the deep Eastern Mediterranean Sea (EMS) was collected under disrupted (REPRESS) or undisturbed (HP) pressure conditions and was acclimated to oil (OIL) or dispersed oil (DISPOIL) under *in situ* pressure and temperature (10 MPa, 14 ºC). Decompression resulted in oil-acclimatised microbial communities of lower diversity despite the restoration of *in situ* pressure conditions during the 1-week incubation. Further biodiversity loss was observed when oil-acclimatised communities were transferred to ONR7 medium to facilitate the isolation of oil-degrading bacteria. Microbial diversity loss impacted the degradation of recalcitrant oil compounds, especially PAHs, as low-abundance taxa, linked with PAH degradation, were abolished due to decompression upon sample retrieval or outcompeted in the enrichment process. *Thalassomonas*, *Pseudoalteromonas*, *Halomonas* and *Alcanivorax* were enriched in ONR7 under all experimental conditions. No effect of dispersant application on the microbial community structure was identified. *A. venustensis* was isolated under all tested conditions suggesting a potential key role of this species in hydrocarbons removal in the deep EMS.

5.2. Introduction

The Eastern Mediterranean Sea (EMS) has become a hotspot for oil and gas exploration activities in recent years [15]. Large natural gas reservoirs have been discovered and are currently being exploited at depths close to that of the Macondo well where the Deepwater Horizon (DWH) blowout occurred, in Israel (Tamar-1700 m, Leviathan-1800 m), Cyprus (Aphrodite-1700 m) and Egypt (Zohr-1450 m) [17]. In addition, ultradeep (>3000 m depth) marine areas have been licensed for exploration in Greece (Ionian Sea, Southern Crete). The risk of a potential oil spill is increasing as drilling operations move towards deeper and more challenging waters [11]. The advancement of drilling technologies and the reviewed EU regulatory framework on the safety of oil and gas operations [227] diminish the risk of an accident in the EMS however oil spill preparedness is still required to limit the environmental and financial impacts in such an event.

The DWH accident, the first recorded deep-sea oil spill, resulted in the release of a total of 530,000 t of live crude oil and 170,000 t of natural gas at a depth of 1500 m [61]. As a response measure, unprecedented amounts of chemical dispersants were applied for the first time in the deep sea, at 1500 m below sea level, in order to reduce the emergence of oil to the surface,

the formation of oil slicks and the subsequent transport of oil to coastal ecosystems [27, 92]. The chemically dispersed oil created neutrally buoyant droplets which accumulated in plumes within the water column with the deepest being located at 900-1300 m depth and expanding over 35 km from the jetting site [66, 69, 91]. Considering deep-sea environments, biodegradation is the only mechanism to remove oil however bioremediation strategies targeted at these frail ecosystems are not advancing at the same pace as drilling technologies [21, 228, 229].

The physical, chemical and biological properties of a deep-sea basin affect oil biodegradation and thus site-specific research is required for the development of efficient bioremediation protocols for the EMS [40, 113]. This semi-enclosed basin presents unique deep-sea characteristics compared to the oceans [121, 126, 135] with the most striking being the warmer temperatures of ~14 ºC compared to colder waters in the oceans at equivalent depths (0-4 ºC). The deep EMS presents also high salinity levels (~39 psu), a remarkable phosphorus limitation (N:P ratio 28:1 instead of 16:1 in the oceans) and low amounts of organic carbon [40, 126, 140].

The ultraoligotrophic, saline conditions of the EMS basin in combination with the high hydrostatic pressure (HHP) form an extreme environment in which deep-water microbial communities have adapted to survive. HHP affects the physiology, metabolic response, and enzymatic function of microbes [6, 101–103, 230, 231] however it has been largely overlooked in oil biodegradation experiments with deep-water samples due to technical challenges in retaining pressure levels during retrieval and experimentation [6, 101]. The few studies performed at HHP had several weaknesses in their methodology and inconclusive results [107, 109, 110, 232]. To our knowledge, all hydrocarbon (HC) biodegradation studies under HHP were performed with deep-water microbial communities which had experienced depressurisation during retrieval. Thus, the effect of HHP on oil-degradation rates is still unclear, underlining that this critical parameter needs to be considered in HC degradation experiments for obtaining realistic and unbiased data. Decompression may cause substitution of piezotolerant with piezosensitive taxa that can become highly active resulting in biodiversity loss and altered microbial activity rates [100, 104]. For example, the metabolic activity levels of bathypelagic communities incubated under atmospheric conditions was several-fold overestimated due to the revival of piezosensitive prokaryotes which were inhibited at HHP [104]. The majority of isolated oil-degrading bacteria are actually considered piezosensitive [40, 233, 234].

In the aftermath of DWH, several lab-based studies focused on the capacity of deep-water microbial communities to alleviate the consequences of oil entrainment in deep-water layers, but were mainly conducted at atmospheric pressure [36, 77, 80, 83, 94, 97, 191, 192, 205, 235]. In regards to the response of microbial communities to HC releases in the deep EMS, despite the ongoing intensification of oil and gas activities, site-specific research studies are extremely few [140, 141, 154]. Thorough research on the application of chemical dispersants as a bioremediation response measure has been conducted but their effectiveness remains debated [24, 96, 236]. Some studies suggest a positive effect of dispersant application, others that dispersants suppress the microbial activity of natural HC-degraders or cause no change on oil biodegradation rates [86, 93, 94, 97, 210]. In addition, the effect of elevated pressure in combination with dispersant application on microbial communities or isolated strains has been limited. Hackbush et al. tested these two variables on a HC-degrading *Rhodococcus* strain isolated from deep-sea sediments in the Gulf of Mexico and found an increasing inhibitory effect of dispersant when elevated pressure was applied [116]. On the contrary, Noirungsee et al., indicated that the inhibitory effect of dispersant on *Cycloclasticus* was reduced at HHP [118].

In this study, a high-pressure sampling and experimentation system was employed for the collection of mesopelagic seawater from the EMS in order to preserve the *in situ* pressure conditions. Un-decompressed (HP) and decompressed (REPRESS) microbial communities were collected from the deep sea with the high-pressure sampler or Niskin bottles respectively. The REPRESS community was re-pressurised in the lab at *in situ* pressure while the respective HP was transferred into incubation vessels under undisturbed pressure conditions. Both were then acclimatised in oil (OIL) and dispersed oil (DISPOIL) prior to enrichment in ONR7, a selective medium for HC-degraders. Three sequential enrichment transfers were performed in the presence of oil or dispersed oil, each incubated for 10 days at 14 ºC under undisturbed (HP) or disturbed (REPRESS) pressure conditions. This work aims to assess the tolerance of deep EMS hydrocarbon degraders to pressure disruption and whether the effect of depressurisation during retrieval could be surpassed by re-pressurising the microbial communities in the lab. We compare the results of this study to our previous work, which was performed under atmospheric pressure [154], to investigate if different oil-degrading strains are favored under *in situ* vs. atmospheric pressure conditions and the presence of dispersant. Finally, we present HC-degrading strains isolated at HHP which could be employed as bioremediation tools in the future.

5.3. Materials and Methods

5.3.1. Field sampling

Seawater samples were collected on board the R/V Aegaeo, in March 2019 in southern Crete, Greece (Gavdos station: coordinates 34º41′58.6″N 24º07′36.2″E). A high-pressure sampling unit (HP Sampler), attached to a CTD rosette, was deployed to obtain deep water from 600 to 1000 m depth [237]. The seawater was maintained in the HP-Sampler at *in situ* pressure and temperature until use in lab incubations within 6 days. Depressurised seawater samples were also collected from 1000 m depth in Niskin bottles and were immediately stored at 14 ºC in the dark. Seawater temperature and salinity at the sampling depth was on average 13.83 ºC/38.81 psu while total phosphorus concentration was approximately 0.28μM.

5.3.2. Preparation of acclimatised communities

Deep seawater retrieved with the HP-Sampler, hereafter HP treatment, was transferred, via a piston pump, in two pressure vessels without depressurisation in any stage of the process. The pressure vessels were pre-filled with 20 mL of filter-sterilized Niskin-collected deep seawater amended with oil (100 ppm; OIL treatment) or dispersed oil (450 ppm of crude oil and a 1:25 ratio of the dispersant Corexit 9500A; DISPOIL treatment) and were pressurised with nitrogen gas up to 10 MPa. A pressure difference between the piston pump and the pressure vessels allowed the transfer of seawater in the latter (~90 mL). Iranian light crude oil (CO; density ~ 0.7821 g mL^{-1}) was used for our experiments. The oil concentration for the OIL and DISPOIL was determined in preliminary experiments as the amount of dissolved or dispersed oil remaining in the water phase after mechanical agitation for 10 min at 600 rpm and 10 MPa followed by 10 min of rest (initial oil amount 0.5 % v/v). Identical treatments in high-pressure vessels at 10 MPa were set up with depressurised deep seawater (REPRESS treatment). All 4 pressure vessels (OIL-HP, OIL-REPRESS, DISPOIL-HP, and DISPOIL-REPRESS) were incubated at 14 ºC for 7 days (Figure 26). At the end of incubation, no visible oil was observed floating on the surface. Subsequently, samples were taken for GC–MS analysis, microbial cell counts and DNA extraction.

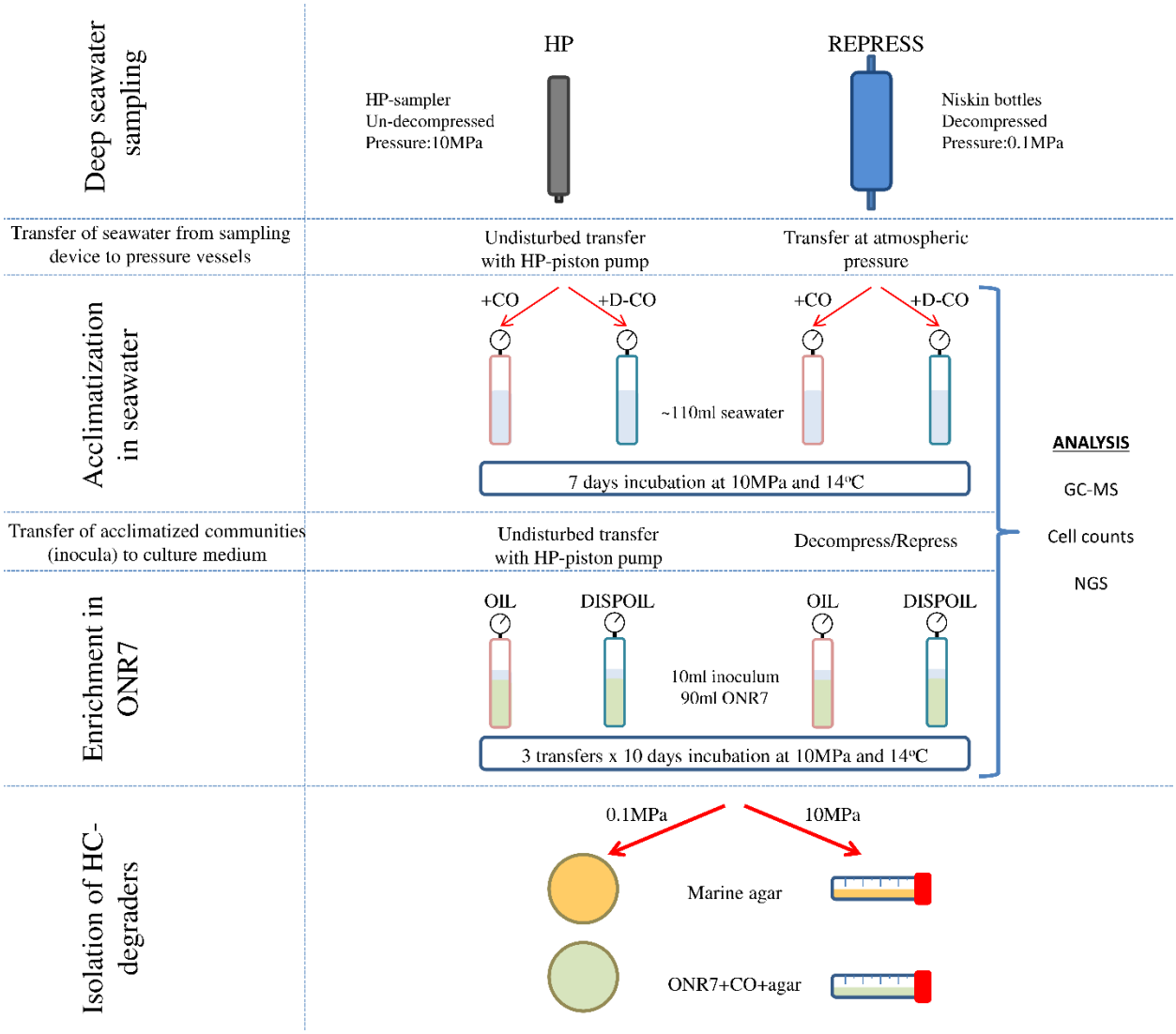

Figure 26. *Schematic representation of experimental workflow for deepwater sampling, acclimatisation and enrichment of microbial communities and the subsequent isolation of microbial strains. CO: crude oil, D-CO: dispersed crude oil, OIL: Oil only treatment, DISPOIL: Dispersed Oil treatment.*

5.3.3. Enrichment of HC-degrading consortia at undisturbed vs disturbed conditions

Artificial seawater (ONR7) was prepared in-house according to Dyksterhouse et al. [238]. This medium is commonly used for the enrichment and isolation of HC-degrading bacteria. The HP and REPRESS microbial communities acclimatised to oil in deep seawater at 10 MPa, were used as inocula for the respective enrichment cultures (OIL-HP, OIL-REPRESS, DISPOIL-HP, and DISPOIL-REPRESS) in ONR7 medium. Prior acclimatisation of the collected

deep-water microbial communities in oil/dispersed oil before enrichment in ONR7 served to form lower-diversity consortia by excluding unrelated to oil-degradation taxa and thus promote the selection of HC-degraders during the enrichment phase later on. Ten ml of inoculum from each culture was transferred in the respective pressure vessel containing 90 mL of ONR7 and 450 ppm crude oil (OIL) or an equal amount of dispersed crude oil (DISPOIL). A total of three sequential transfers were performed for every treatment combination, each incubated for 10 days at 10 MPa and 14 ºC. In the REPRESS incubations, the microbial communities were decompressed and recompressed in each transfer. In the case of HP treatments, 10 mL were transferred via a piston pump to the next pressure vessel without decompression (Figure 26). Following transfer, the remaining volume was collected for GC–MS analysis of HC concentration and the determination of microbial cell counts with flow cytometry. In addition, 70–75 mL were filtered through a 0.2 μM PES filter (Rephile, USA) for DNA extraction and 16S rRNA amplicon sequencing to determine the microbial community structure in the enrichment cultures. The pH was measured at the end of every incubation step using a HQD portable meter (HQ30d) and IntelliCAL PHC101 pH probe (Hach-LANGE).

5.3.4. Isolation and identification of bacterial strains

At the end of the 3rd transfer, 10^{-5} dilutions were plated on solid media to isolate and identify bacterial strains from the enrichments. Marine agar (MA) and ONR7 + crude oil (CO) agar mediums were prepared in both petri dishes and 50 mL falcon tubes for incubation at 0.1 and 10 MPa respectively (Figure 26). ONR7 + CO agar medium was prepared by autoclaving first the ONR7 with agar. Once the medium cooled down to ~50 ºC, 15 mL of solution containing DMSO (1 %) + CO (0.5 %) were inoculated in 1 litter of ONR7 + agar while stirring and then poured onto plates and falcons. Individual colonies were subsequently picked and inoculated in the respective broth medium in culture tubes (0.1 MPa) or 5 ml syringes (10 MPa) for biomass production. DNA extraction from the liquid cultures was performed using the DNeasy PowerLyzer kit (QIAGEN). The extracted DNA was subjected to PCR amplification of the 16S rRNA gene using the 27F and 1492R universal primers, which amplify nearly full-length of the 16S rRNA gene [239]. The amplification was performed with the FastGene Taq ReadyMix PCR kit (Nippon Genetics) and the result was visualized by electrophoresis on a 1.2 % agarose gel and the remaining PCR product was purified using the NucleoSpin Gel and PCR clean-up kit (Mackerey-Nagel). The purified DNA eluate was measured on a Qubit 4.0 fluorometer (Invitrogen, Thermo Fisher Scientific, Waltham, MA, USA) using the Qubit dsDNA high

sensitivity assay. A total of 10 isolated strains from all treatments were selected and submitted for Sanger sequencing (Eurofins Genomics, Germany). Consensus sequences from matching forward and reverse trace files, filtering of low-quality base calls and end trimming of finished sequences were performed using the SeqTrace software [240].

5.3.5. GC–MS analysis of HC degradation

The separation of organic compounds from the aqueous cultivation medium was performed using liquid-liquid extraction as described in Antoniou et al. [237]. Briefly, dichloromethane (DCM Suprasolv®, Merck KGaA, Darmstadt, Germany) was used (3× the sample volume), in 100 mL Erlenmeyer flasks with a glass spout at the bottom. Any further moisture was removed by filtering the extract through columns of anhydrous sodium sulphate and fiberglass. The solvent (DCM) was removed on a rotary evaporator and the dried samples were transferred to 4 mL vials with a small amount of DCM Suprasolv®. The samples were once again concentrated by evaporation on a hot plate (~50 ºC) with simultaneous nitrogen blow. DCM Suprasolv® and n-hexane Suprasolv® (Merck KGaA, Darmstadt, Germany) were used to separate the solid extracts in aromatic and saturated HC fractions respectively by elution through SPE columns (Bond Elute TPH, Agilent Technologies, Inc., Santa Clara, CA, USA). GC–MS analysis was performed on an Agilent GC–MS HP 7890/5975C system, with an Agilent HP-5MS 5 % phenyl methyl siloxane column (60 m × 250 μm × 0.25 μm). The HC mixture consisted of an Oil Analysis Standard (Absolute Standards Inc.®, Hamden, CT, USA) containing 44 compounds, and 17a(H),21b(H)-hopane (Chiron AS®, Trondheim, Norway). The standard composition of the HC mixture was normal alkanes from C10 to C35, pristane and phytane and 16 polycyclic aromatic hydrocarbons (PAHs).

5.3.6. Cell count determination-flow cytometry

Microbial cell counts were determined on a CytoFlex Flow Cytometer (Beckman Coulter Inc., USA). The cells were fixed with 1% paraformaldehyde (4 % stock) and 0.025% glutaraldehyde (25% stock). The samples were diluted with filter-sterilised deionized water to a final concentration 106–107 cells and were stained with 1× thiazole green stain (1000× stock in DMSO, BIOTIUM, USA) for 15 min in the dark at room temperature. For the analysis of samples, side-scatter (SSC) threshold was set to automatic (10,000) with a slow flow rate of 10 $\mu L\ min^{-1}$.

5.3.7. DNA extraction and next-generation sequencing

DNA extraction from PES membranes was performed according to Charalampous et al.[154]. Briefly, the membranes were soaked in CTAB extraction buffer (1 M Tris-HCl (pH 8), 0.5 M EDTA (pH 8), 1 M NaH2PO4 (pH 8), 5 M NaCl and 5 % cetyltrimethylammonium bromide) and vortexed thoroughly for 2 min. The samples were then subjected to three freeze-thaw cycles (liquid nitrogen to 65 ºC). Lysozyme and Proteinase K (PK) were subsequently added, and the samples were incubated for 30 min at 37 ºC prior to SDS addition and further incubation at 65 ºC. The supernatant obtained after centrifugation (10,000g, 10 min) was mixed with an equal volume of phenol:chloroform:isoamylalcohol (25:24:1) followed by another centrifugation step. Further purification was performed by mixing the aqueous phase with chloroform:isoamylalcohol (24:1) and the DNA was left to precipitate overnight by adding ice-cold isopropanol. The precipitated DNA obtained after centrifugation was washed with 70 % molecular-grade ethanol. Finally, after another spin, the supernatant was discarded, and the DNA pellets were left to dry at room temperature. TE buffer was used for resuspending the DNA pellets and Qubit dsDNA high-sensitivity assay was used to measure the DNA concentration on a Qubit 4.0 fluorometer. The V3-V4 region of 16S rRNA gene sequence was amplified using the universal primers 341F and 806R [155, 241]. Sequencing was done on an Illumina MiSeq using V3 Chemistry at Biosearch Technologies, LGC Genomics GmbH (Berlin, Germany).

The PCRs included 1–10 ng of DNA extract (total volume 1 µL), 15 pmol of each forward primer and reverse primer in 20 µL volume of 1 × MyTaq buffer containing 1.5 units MyTaq DNA polymerase (Bioline GmbH, Luckenwalde, Germany) and 2 µL of BioStabII PCR Enhancer (Sigma-Aldrich Co.). For each sample, the forward and reverse primers had the same 10-nt barcode sequence. PCRs were carried out for 30 cycles using the following parameters: 1 min 96 ºC pre-denaturation; 96 ºC denaturation for 15 s, 55 ºC annealing for 30 s, 70 ºC extension for 90 s and hold at 8 ºC. DNA concentration of amplicons of interest was assessed by gel electrophoresis. About 20 ng amplicon DNA of each sample were pooled for up to 48 samples carrying different barcodes. The amplicon pools were purified with one volume Agencourt AMPure XP beads (Beckman Coulter, Inc., IN, USA) to remove primer dimer and other small mispriming products, followed by an additional purification on MiniElute columns (QIAGEN GmbH, Hilden, Germany). About 100 ng of each purified amplicon pool DNA was used to construct Illumina libraries using the Ovation Rapid DR Multiplex System 1–96

(NuGEN Technologies, Inc., CA, USA). Illumina libraries (Illumina, Inc., CA, USA) were pooled and size selected by preparative gel electrophoresis.

5.3.8. Bioinformatic analysis of 16S rRNA sequences

The bioinformatic analysis of the primer-clipped V3-V4 16S rRNA sequences was performed using the DADA2 package in R [157]. This microbiome data analysis pipeline includes dereplication of reads, denoising, merging of reads to generate amplicon sequence variants (ASVs) and chimeric screening. Taxonomy assignment up to Genus level was performed using the SILVA 16S rRNA gene database (Silva version 138) [159]. A single object including the ASV abundance and taxonomy tables, the experimental metadata and a neighbor-joining phylogenetic tree was created with the *phyloseq* package [198] and was used in downstream analysis. A total of 11 ASVs that could not be taxonomically ranked at the phylum level were removed. After discarding zero abundance ASVs and single singletons (ASVs occurring only once in one sample), we applied a filtering step to a prevalence threshold of 10% to exclude any ASVs with low biological meaning.

5.3.9. Statistical analysis

All statistical analysis was performed with Rstudio software (version 1.4.1106) in R version 4.3.2 [158]. All figure plots were created using the *ggplot2* package [164] unless otherwise stated. Alpha-diversity was calculated on the data prior to normalisation. The effect of oil treatment (OIL, DISPOIL) and pressure (HP, REPRESS) on the beta diversity of microbial communities was evaluated via Principal Coordinate Analysis (PCoA) on the Bray-Curtis distance of cumulative sum-scaling (CSS)-normalized data using the *phyloseq* package (*ordinate* function) [161, 198]. Significant differences were assessed via permutational multivariate ANOVA (PERMANOVA) based on Bray-Curtis dissimilarity matrix using the *vegan* package (*adonis* function) [162]. The significance of variable fitting was determined using 999 permutations. Venn diagram was created using the *Venndiagram* and *gplot* package [203].

5.4. Results

5.1. Microbial community analysis

5.1.1. Alpha diversity

Low diversity levels were observed in the REPRESS inocula (i.e., microbial community after acclimatisation with oil) compared to the respective HP inocula that were not subjected to

depressurisation during sample retrieval, based on all diversity metrics (Figure 27, Inoc). Alpha diversity decreased further upon transfer to ONR7 medium (1st transfer period) and remained low in subsequent transfers under all treatment combinations. No major differences in biodiversity were observed between OIL and DISPOIL samples. It is worth mentioning that the Simpson diversity index which takes into account both species evenness and richness was two-fold higher for the DISPOIL-HP sample compared to the respective REPRESS at the end of the experiment (i.e. 3rd transfer). The Simpson index gives more weight to common or dominant species meaning that taxa are more evenly distributed in DISPOIL-HP than in the REPRESS treatment even though their ASV richness is the same.

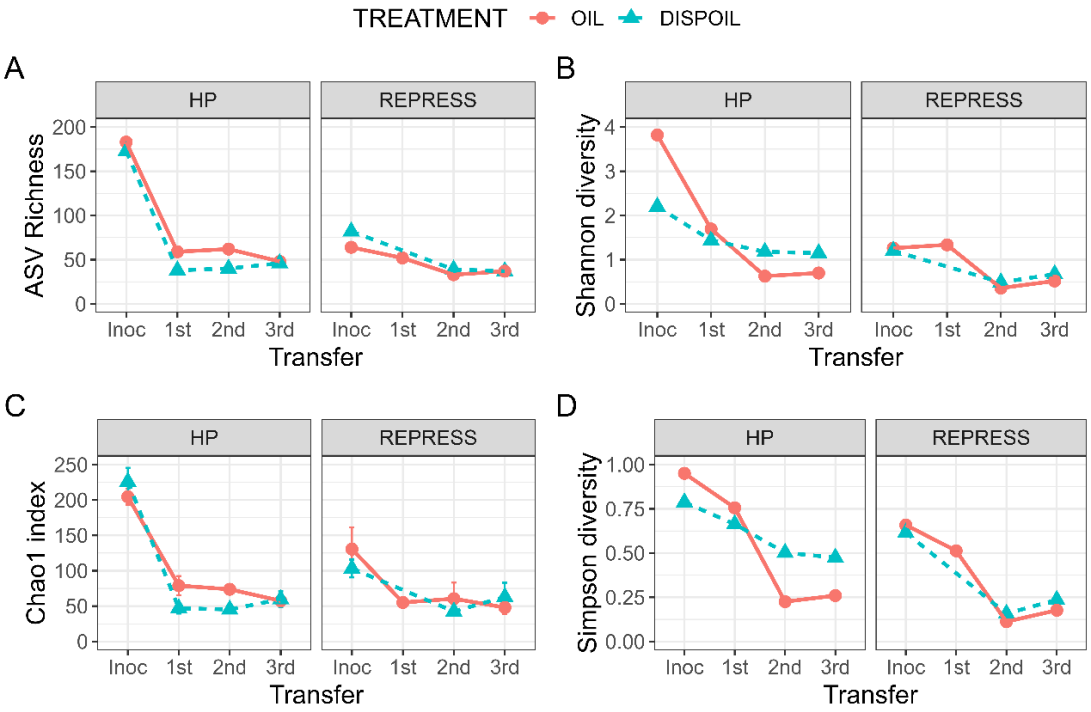

Figure 27. *Alpha diversity indices of OIL and DISPOIL treatments under HP and REPRESS conditions. A) ASV richness, B) Shannon index (H), C) Chao1 index and D) Simpson index (D). "Inoc" samples represent the acclimatised communities used to inoculate the respective enrichment cultures.*

5.1.2. Beta diversity

Principal Coordinate Analysis (PCoA) was performed using the Bray-Curtis distance metric for enrichments and their inocula (Figure 28). Differences in the microbial community structure were primarily explained by the cultivation medium used for the incubations. In particular, the acclimatised microbial communities (inocula) which were incubated in seawater were separated on the x-axis from the enrichment samples which were incubated in ONR7. The samples clustered within each pressure treatment regardless of dispersant application while the

non-significant effect of dispersant was confirmed by PERMANOVA which was conducted after the removal of inocula from the dataset (pressure: R2 = 0.46, p = 0.001, oil treatment: R2 = 0.10, p = 0.071).

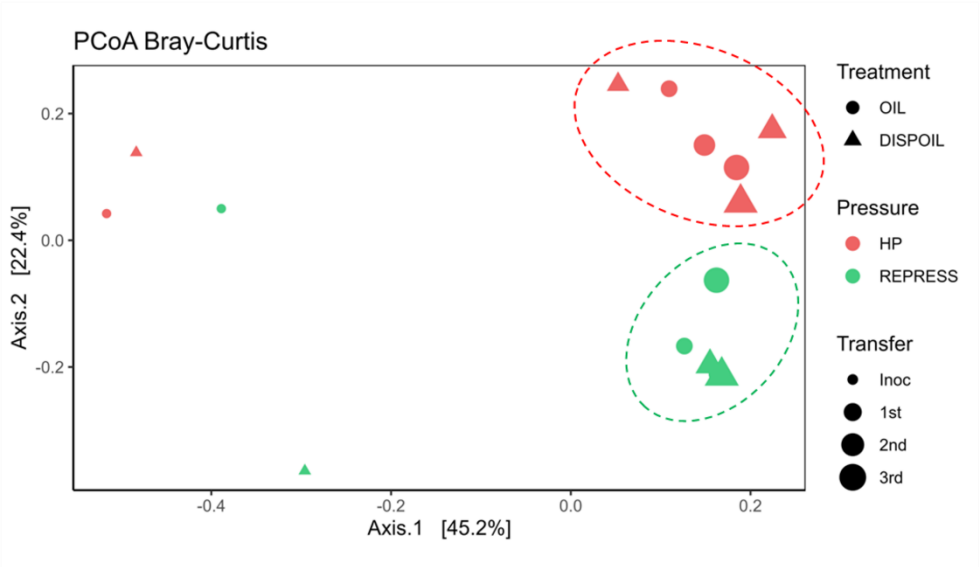

Figure 28. *Principal Coordinate Analysis (PCoA) based on the Bray-Curtis dissimilarity matrix of the enrichments and their respective acclimatised inocula. Ellipses encircle the enrichment samples which are grouped by the pressure treatment.*

5.1.3. Identification of unique and common community members between tested conditions

Venn diagram analysis was performed to identify common and unique community members between pressure and oil treatment (Figure 29). This analysis is based on the presence/absence of ASVs and was applied on the enrichment samples only (i.e., inocula not included). As observed by beta-diversity, pressure is the factor that determines the microbial community structure. Of primary interest were the HP-unique taxa regardless of oil treatment (OIL or DISPOIL) which comprised approximately 32 % of the identified ASVs (Table S11). Among the 101 ASVs in the dataset, 32 were exclusively found under HP conditions while 59 ASVs were common between the two tested pressure treatments (HP-REPRESS). This is an indication of which taxa were sensitive to pressure disruption (HP-unique) and which were

resistant (HP-REPRESS). The list of resistant species consisted mainly of Gammaproteobacteria and in particular of *Alcanivorax*, *Halomonas*, *Thalassomonas*, *Aestuariicella* and *Pseudoalteromonas* (Table S12). The HP-unique taxa belonged to members of *Sphingomonadaceae*, *Caulobacteraceae* and *Burkholderiaceae* families (Table S11). Out of the 32 HP-unique ASVs, 18 were identified exclusively in OIL-HP and 6 were specific to DISPOIL-HP however their combined abundance was low in both cases (0.14 % and < 0.10 % respectively). In addition, 8 ASVs were present under constant high pressure and were common between the two treatments (OIL and DISPOIL). The distinct ASVs from the oil-only enriched HP samples (OIL-HP) belonged to genera such as *Ralstonia*, *Hephaestia*, *Alteromonas*, *Marinobacter* and others, while the list is much narrower for the dispersed oil treated samples under HP (DISPOIL-HP) comprised of *Novosphingobium* and unassigned genera belonging to the Babeliales and Rhodospirillales orders (Table S11).

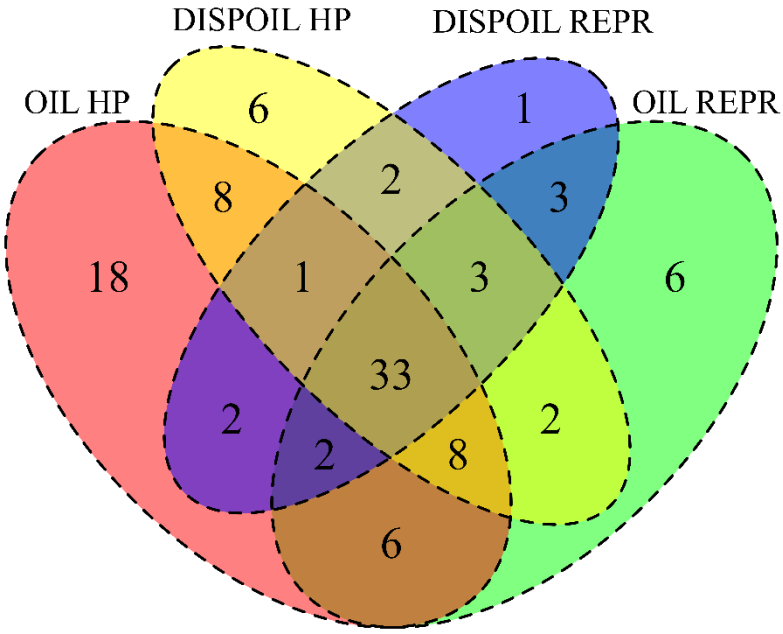

Figure 29. *Venn diagram of shared and unique ASVs enriched under the four different experimental conditions.*

5.1.4. Microbial taxa abundance

The acclimatised to oil communities that did not undergo depressurisation during sample retrieval (HP inocula) were more diverse in both OIL and DISPOIL treatments compared to their respective REPRESS that experienced the decompression/re-compression effect (Figure 30, Inoc). Several genera, including well-known HC-degrading bacteria such as *Oleispira*, *Marinomonas* and members of the family *Sphingomonadaceae*, were lost during the 1st enrichment period. The transition of acclimatised inocula to the ONR7 enrichment medium

resulted in the selection of *Pseudoalteromonas*, *Halomonas* and *Alcanivorax* as dominant taxa in all tested conditions. *Thalassomonas* was also present in all enrichments at steadily low abundance levels (Figure 30). *Pseudoalteromonas* and *Halomonas* dominated the community at the end of the 1st transfer under HP in both OIL and DISPOIL, while *Alcanivorax* replaced both during the subsequent enrichment steps becoming the most dominant genus until the end of the experiment under all pressure and oil treatments tested.

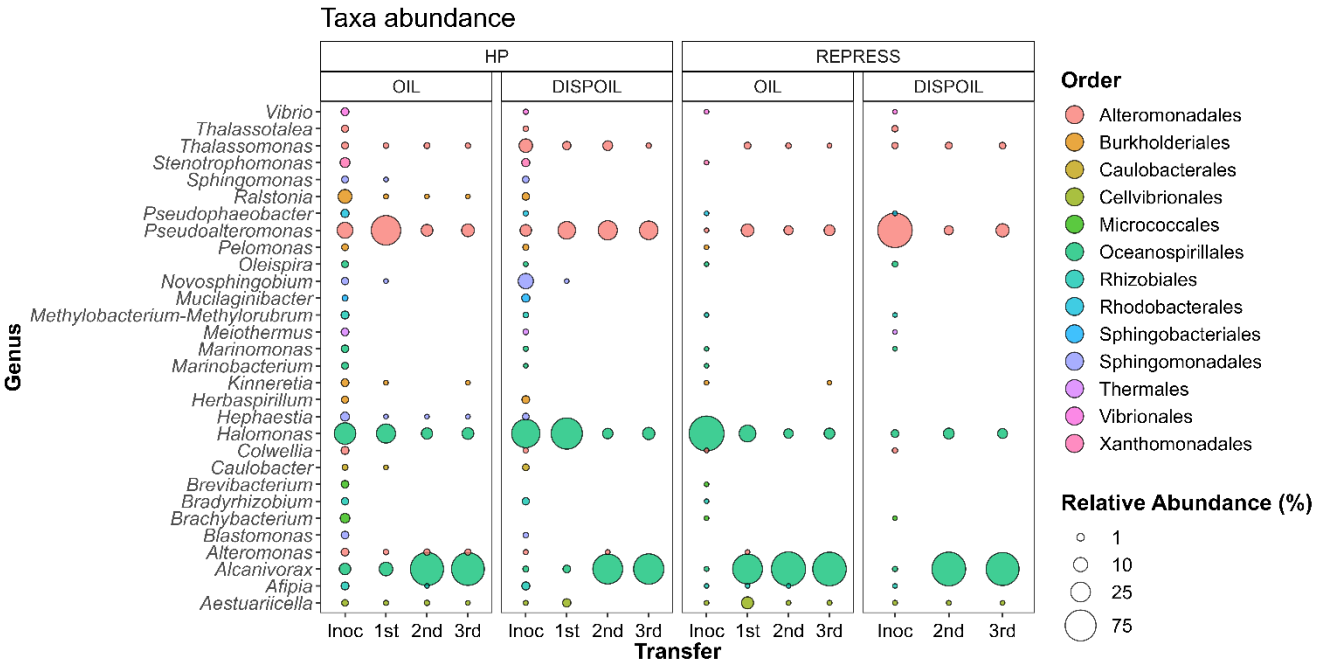

Figure 30. *Relative abundance of microbial taxa (Top 30 ASVs) at the Genus level of the acclimatised inocula ("Inoc") and their enrichment transfers under all treatments tested.*

5.2. HC degradation capacity

Due to the absence of dispersant, sub-sampling to determine total measured hydrocarbons (TMHs) in the OIL samples led to inconsistent values between T0, acclimatised and enriched samples and these were not further assessed. Therefore, the determination of HC concentrations for each inoculum and after each transfer step was performed solely for the DISPOIL samples, except for the DISPOIL-REPRESS 1st transfer due to loss of the sample (Figure 31). A complete removal of light alkanes was observed at the end of the acclimatisation phase in the HP-Inoc sample with the degradation capacity being up to 2-fold higher for TMHs and almost 3 times higher for the PAHs (Figure 31). This efficiency was further enhanced at the end of the 1st

transfer where the total measured alkanes and aromatic hydrocarbons were degraded almost completely (~92%) (Figure 31A). Approximately 95 % of heavy alkanes and PAHs were degraded during this incubation period indicating a very robust oil-degrading microbial community (Figure 31C-D). This extraordinary degradation capacity of heavy alkanes and PAHs was lost during the 2nd and 3rd transfer periods whereas the degradation of light alkanes was maintained. Interestingly, the -resistant to biodegradation- branched n-alkane biomarkers, pristane (PR) and phytane (PH), were highly degraded in the 1st and 2nd transfers of DISPOIL-HP treatment while this capacity was lost in the final enrichment step (Table S8). The internal standard used in our GC–MS analysis (17a21b-hopane) was also highly degraded, especially during the 1st enrichment period (~90 % decrease compared to the initial concentration). This is why we did not use these recalcitrant compounds as normalisation factors for biodegradation. High biodegradation percentage of PR and PH has been observed previously in enrichment cultures of oil-degrading consortia from sediments collected from a deep-sea hydrothermal area [242]. Overall, the artificial seawater medium ONR7 with HCs as the only carbon source selected for an alkane-degrading community of low diversity. This community was resistant to depressurisation-repressurisation based on the comparable degradation capacity between HP and REPRESS in the 2nd and 3rd transfers.

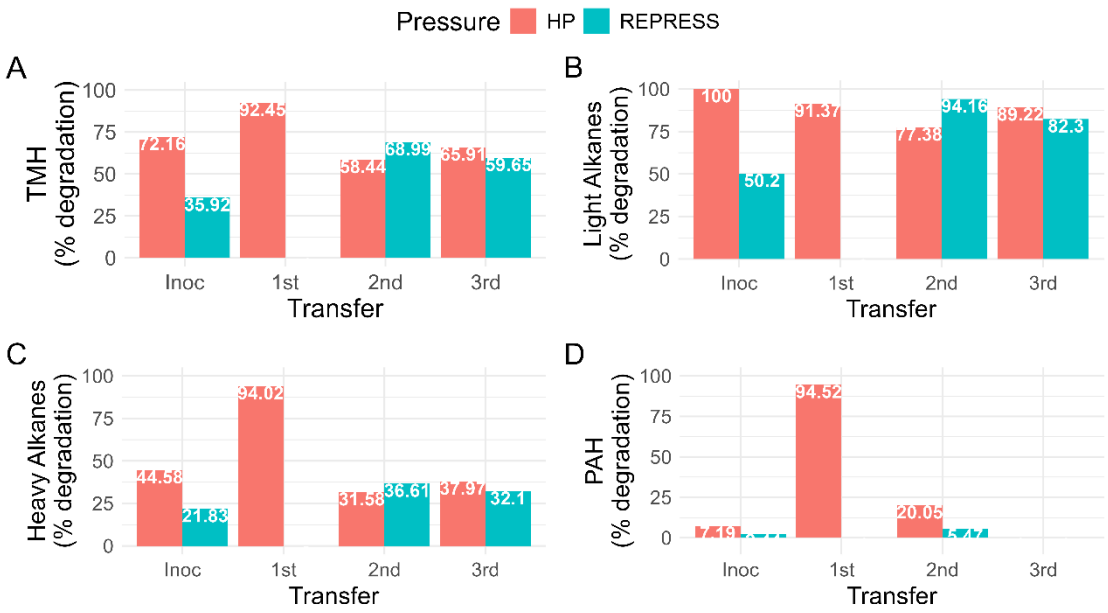

Figure 31. *HC degradation rates of the dispersed oil (DISPOIL) acclimatised inocula ("Inoc") and enriched samples under HP and REPRESS conditions for A) Total Measured Hydrocarbons (TMH), B) Light Alkanes (C14-C25), C) Heavy Alkanes (C26-C35) and D) Polyaromatic Hydrocarbons (PAH).*

5.3 Isolation of individual microbial strains

Table 4 lists the isolated strains, the conditions under which each strain was grown, the closest match and the sequence similarity to reference strains using BLAST alignment. All isolates were highly similar (97–100 %) to the BLAST-identified reference strains with the exception of the *Halomonas* EMDW-5 (<95 %). Most isolates showed >99 % sequence similarity to *Alloalcanivorax venustensis ISO4* (NR_025145.1), until recently classified as *Alcanivorax venustensis* (Rai et al., 2023).

Table 4. *List of isolated strains obtained from the deep EMS under all enrichment conditions. Sequences were BLASTed and the closest relatives are given along with their similarity percentage. The first part of the Isolate ID denotes the enrichment of origin (OIL-HP, DISPOIL-HP, OIL-REPRESS, DISPOIL-REPRESS), the second part mentions the solid medium the colony grew on (MA, CO) and the third part refers to the pressure conditions (10 or 0.1 MPa).*

Isolate ID	Strain No	Tentative species name	Similarity (%)
OIL-HP_MA_10	EMDW-1	H.meridiana (NR_042066.1)	99.64
OIL-HP_CO_10	EMDW-2	A. venustensis ISO4 (NR_025145.1)	100
OIL-REPRESS_CO_10	EMDW-3	A. venustensis ISO4 (NR_025145.1)	99.86
DISPOIL-REPRESS_CO_10	EMDW-4	A. venustensis ISO4 (NR_025145.1)	97.37
OIL-HP_CO_0.1	EMDW-5	H.meridiana (NR_042066.1), H.aquamarina (NR_042063.1)	93.24
DISPOIL-HP_CO_0.1	EMDW-6-1	A. venustensis ISO4 (NR_025145.1)	99.86
DISPOIL-HP_CO_0.1	EMDW-6-2	A. venustensis ISO4 (NR_025145.1)	99.79
OIL-REPRESS_CO_0.1	EMDW-8	A. venustensis ISO4 (NR_025145.1)	100
DISPOIL-REPRESS_CO_0.1	EMDW-9	A. venustensis ISO4 (NR_025145.1)	100
OIL-HP_MA_10	EMDW-1	A. venustensis ISO4 (NR_025145.1)	99.64

5.5 Discussion

5.5.1. Decompression during sample retrieval and loss of bacterial diversity

The impact of decompression upon retrieval and dispersant application on the microbial community structure and oil-degradation capacity was studied in deep waters of the EMS using a high-pressure sampling and experimentation system. The incubation of un-decompressed deep

water (collected with a pressure-retaining sampler) with crude oil at HHP resulted in a highly diverse HC-degrading microbial community (HP inocula). In contrast, the REPRESS inocula, which derived from decompressed water samples, resulted in oil-acclimatised microbial communities of much lower alpha diversity, despite the fact that seawater was re-compressed to *in situ* pressure 6 days after retrieval and incubated for 1 week at HHP. Our results showed that a relatively short-term decompression of deep-seawater samples may result in the permanent loss of microbial diversity. Taxa that were lost with decompression (based on differences between HP vs REPRESS inocula) belonged mainly to Burkholderiales (*Ralstonia*, *Herbaspirillum*) and Sphingomonadales (*Novosphingobium*, *Sphingomonas*, *Hephaestia*, *Blastomonas*). The majority of these taxa have been correlated with HC degradation but their piezo-behaviour requires further investigation. However, *Sphingomonas* and *Novosphingobium* have been isolated from deep-sea sediments in the abyssal Marianna Trench and a seamount in the Pacific Ocean respectively [243, 244]. Even though decompression has been linked with shifts in community composition, research studies do not directly correlate it with biodiversity loss [100, 245, 246]. Nonetheless, in a recent study by Liu et al., higher microbial diversity was observed when the Challenger Deep-collected sediments were enriched with HC at 100 MPa than at 0.1 MPa [247]. Similarly, in enrichment experiments with an iron-reducing microbial community, obtained from a deep petroleum reservoir, a higher microbial diversity was observed at 40 MPa than at 0.1 MPa [248]. In contrast to our experiments, however, decompressed samples in the above studies were incubated at atmospheric pressure instead of being re-pressurised in the lab. This work is the first to underline the importance of maintaining in situ pressure during sample retrieval to avoid loss in microbial diversity.

5.5.2. Loss of biodiversity by decompression and selective enrichment connected to reduced hydrocarbon degradation capacity.

The negative effect of decompression on microbial diversity was reflected on biodegradation rates of hydrocarbons having a higher impact on the removal of PAHs compared to the undisturbed HP inoculum. Transitioning of the acclimatised seawater communities (HP and REPRESS inocula) to ONR7, with crude oil or dispersed crude oil as the sole source of carbon caused a further drastic decrease in microbial diversity. The decrease was more apparent in the undisturbed HP-incubated samples that had higher initial diversity in the inoculum however, after the 2nd transfer both HP and REPRESS communities were comparable in diversity. This means that the observed negative effect of decompression during retrieval was

attenuated in the nutrient-rich growth conditions of the ONR7 medium. Highly efficient HC removal was observed only under undisturbed conditions (DISPOIL-HP, 1st transfer) with >90 % degradation of both light alkanes (C14 to C25) and recalcitrant compound classes, such as PAHs and heavy alkanes (C26-C35). The successive decrease in HC degradation with transfer steps within the HP treatment occurred concomitantly to biodiversity loss, despite an increase in microbial cell counts (Table S8-

Table S10, Figure S15). The increase of functional capacity, in a diverse microbial ecosystem, is attributed to the complex cooperative interactions which take place between

	Concentration (ppm)				Degradation (%)		
PAHs	**T0**	**1st**	**2nd**	**3rd**	**1st**	**2nd**	**3rd**
Napthalene	0.000598	0.000015	0.000355	0.000422	97.490	40.609	29.321
Fluorene	0.000350	0.000129	0.000065	0.000277	63.220	81.375	20.752
Dibenzothiophene	0.008260	0.001007	0.008019	0.011556	87.811	2.919	0.000
Phenanthrene	0.006785	0.001266	0.001330	0.005965	81.340	80.396	12.088
Anthracene	0.003379	0.001311	0.001344	0.006214	61.188	60.233	0.000
Fluoranthene	0.065067	0.003259	0.064697	0.064907	94.991	0.569	0.247
Chrysene	0.043387	0.002265	0.040208	0.041351	94.779	7.327	4.694
Pyrene	0.066423	0.003377	0.064916	0.065275	94.916	2.270	1.728
Benzo(b)fluoranthene	0.249529	0.012496	0.124647	0.249424	94.992	50.047	0.042
Benzo(k)fluoranthene	0.198530	0.009944	0.099134	0.198434	94.991	50.066	0.048
Benzo(e)pyrene	0.169935	0.008530	0.169236	0.169497	94.980	0.411	0.258
Benzo(a)pyrene	0.169991	0.008499	0.169919	0.169920	95.000	0.042	0.041
Perylene	0.153657	0.007684	0.153573	0.153557	95.000	0.055	0.065
Indeno(1,2,3-cd)pyrene	0.053796	0.005381	0.053795	0.053797	89.997	0.002	0.000
Dibenzo(a,h)anthracene	0.000024	0.000007	0.000009	0.000010	69.622	61.696	56.593
Benzo(g,h,i)perylene	0.000094	0.000030	0.000011	0.000033	68.040	88.279	64.370

members of the community, such as the exchange of secondary metabolites or other intermediates in a species-specific manner [41, 249, 250]. Here, microbial diversity loss in the enrichment cultures affected primarily the degradation of heavy alkanes and PAHs, which decreased by ~75 % and 100 % during the 2nd and 3rd enrichment period respectively. Several studies, using soil or sediment microbiota, have linked high microbial diversity to specialised

functions like heavy metal detoxification and HC degradation [251–254]. In Bell et al., a diverse soil microbial community degraded more crude oil than assemblages of selected specialised HC-degrading bacteria. This result was contrary to their original hypothesis that limiting microbial taxa, which compete for resources with HC-degrading bacteria, would enhance crude-oil biodegradation [251]. A similar conclusion was reached by Dell'Anno et al. who suggested that bioremediation strategies that can sustain high levels of bacterial diversity rather than the selection of specific taxa could lead to a higher HC degradation in contaminated marine sediments [252]. Key specialised functions that are carried out by few specific taxa, as is the degradation of PAHs, are more susceptible to diversity loss compared to generic functions that remain unaffected due to the presence of similarly performing species [254, 255]. Considering PAHs, the number and diversity of microbial groups capable of degrading them decreases as the number of rings in aromatic compounds increases [256]. Several of the low abundance taxa that were lost with decompression and transition from seawater to ONR7 medium are potential PAH degraders (e.g. *Novosphingobium*, *Sphingomonas*, *Marinomonas*, *Colwellia*, *Caulobacter*, *Stenotrophomonas*, *Ralstonia* and *Herbaspirillum*) and their absence may explain the eventual collapse in PAH degradation [257–262].

5.5.3. Composition of enriched oil-degrading microbial communities and the effect of dispersant

The enrichment in ONR7 favored similar HC degrading taxa under all treatments tested. *Thalassomonas*, *Pseudoalteromonas*, *Halomonas* and *Alcanivorax* were the genera that persisted or increased in abundance in the artificial seawater medium. *Pseudoalteromonas* and *Halomonas*, both considered as generic, non-specific oil degraders, were more abundant after the 1st transfer but were replaced by the obligate hydrocarbonoclastic genus *Alcanivorax* which became dominant in the 2nd and 3rd enrichments. The composition of our final-stage enrichment cultures is similar to that obtained from a 530-m-deep cold seep in the Gulf of Cadiz by Van Landuyt et al. who also performed enrichments in ONR7/dodecane medium at HHP [263]. The predominance of *Alcanivorax* in our HP enrichment cultures is in contrast with previous studies which generally reported an inhibition of specialised, hydrocarbonoclastic bacteria at HHP [264].

The application of Corexit9500A dispersant did not significantly affect the community structure in either the acclimatisation or the enrichment phase. Strains which were enhanced to a small degree by dispersant during the acclimatisation phase (inocula) were the HP-unique *Novosphingobium* and *Thalassomonas* which increased in abundance regardless of pressure

treatment. *Novosphingobium* has been previously associated with the biodegradation of aromatic compounds of oil [213, 265], which may explain its enrichment in the presence of dispersant that increases the bioavailability of these recalcitrant compounds. *Thalassomonas* was also enriched in the DWH deep plume, where dispersant was extensively used in the deep sea [83].

Alcanivorax was the most dominant genus in all enrichment consortia, irrespective of oil and pressure treatment. The increase in the relative abundance of *Alcanivorax*, a known short- to medium-chain alkane degrader, in successive enrichments was correlated with the lower degradation rates of PAHs and heavy alkanes. The presence of *Alcanivorax* in the deep EMS has also been reported by Liu et al. in oil-amended microcosm experiments with seawater from 824 to 1210 m depth [141] and our previous ONR7/crude-oil enrichment studies at atmospheric pressure [154]. *Alcanivorax* strains have been previously isolated from deep-sea environments [216, 217, 263, 266]. However, the absence of *Alcanivorax* species from the DWH deep plume and HHP laboratory tests with several *Alcanivorax* species (*A. borkumensis*, *A. jadensis* and *A. dieselolei*) led to the perception that *Alcanivorax* might lack proper adaptation mechanisms to hydrostatic pressure [112–114]. However, none of these studies included *A. venustensis*, which was the identified strain in seven out of ten sequenced colonies in this study. This species was recently emended as *Alloalcanivorax venustensis* based on a phylotaxogenomic analysis [267]. *A. venustensis* was isolated under all our experimental conditions (OIL-HP, DISPOIL-HP, OIL-REPRESS, DISPOIL-REPRESS) while it was also identified as the most abundant *Alcanivorax* ASV (99 % of the genus) in the enrichment cultures, having a 100 % similarity with *A. venustensis ISO4* based on BLAST analysis. The type strain *A. venustensis ISO4*, which is able to degrade aliphatic compounds, was isolated from the Mediterranean Sea at 280 m depth [268]. *A. venustensis* was also the dominant species in ONR7/dodecane cultures with cold seep sediments as inoculum under all three pressure conditions tested (0.1, 10, 30 MPa) showing promising piezotolerance in axenic cultures [263]. Unpublished data from our work with deep EMS HC-degrading consortia revealed the presence of *A. venustensis* at 0.1 MPa albeit in low abundance whereas *A. borkumensis* was the dominant *Alcanivorax* (unpublished data from experiments in Charalampous et al., 2021 [154]. Combined with the results of this study, our data suggest that *A. venustensis* may have a competitive advantage at elevated pressure over the piezosensitive *A. borkumensis* which dominates oil-contaminated surface waters and coastlines [112].

5.6. Conclusions

Our study highlights the importance of maintaining in situ pressure when performing experiments with deep-water microbial communities. Decompression during retrieval and recompression to in situ pressure after 6 days resulted in considerable loss of biodiversity that was not restored after a week-long incubation with oil or dispersed oil at HHP. The transfer of acclimatised-to-oil communities from natural seawater to ONR7 medium led to the enrichment of specific taxa belonging to the genera of *Alcanivorax*, *Halomonas*, *Pseudoalteromonas* and *Thalassomonas*, which were not sensitive to short decompression/compression cycles. The considerable loss in biodiversity, due to decompression upon sampling, decreased substantially the overall degradation efficiency of the deep consortium. Further decrease in biodiversity in ONR7 enrichments was accompanied by a near halt of specialised functions, such as long-chain alkane and PAH degradation. Several of the low abundance taxa that could not compete in the high-nutrient conditions of the enrichment medium were known marine PAH-degraders (e.g. *Marinomonas*, *Colwellia*), with a fraction of them also sensitive to decompression (e.g. *Novosphingobium*, *Sphingomonas*, *Caulobacter*, *Ralstonia*, *Herbaspirillum*). *Alcanivorax venustensis* was the dominant species in the end-point enrichment cultures. This species of *Alcanivorax* is the first to demonstrate piezotolerant traits and recently its phylogenetic classification has been emended to the new genus *Alloalcanivorax*. Overall, our results showed that diverse, undisturbed microbial communities can degrade more crude oil, and particularly the recalcitrant fractions of oil, compared to enriched consortia of HC-degrading bacteria. This outcome may partly explain the lack of success in several cases of bioremediation by bioaugmentation, where the addition of specialised bacterial strains to an established highly-diverse natural population in a contaminated environment has failed to enhance pollutant degradation.

CHAPTER 6.

Microbial succession patterns in a hydrocarbon plume emulation scenario in the deep Eastern Mediterranean Sea

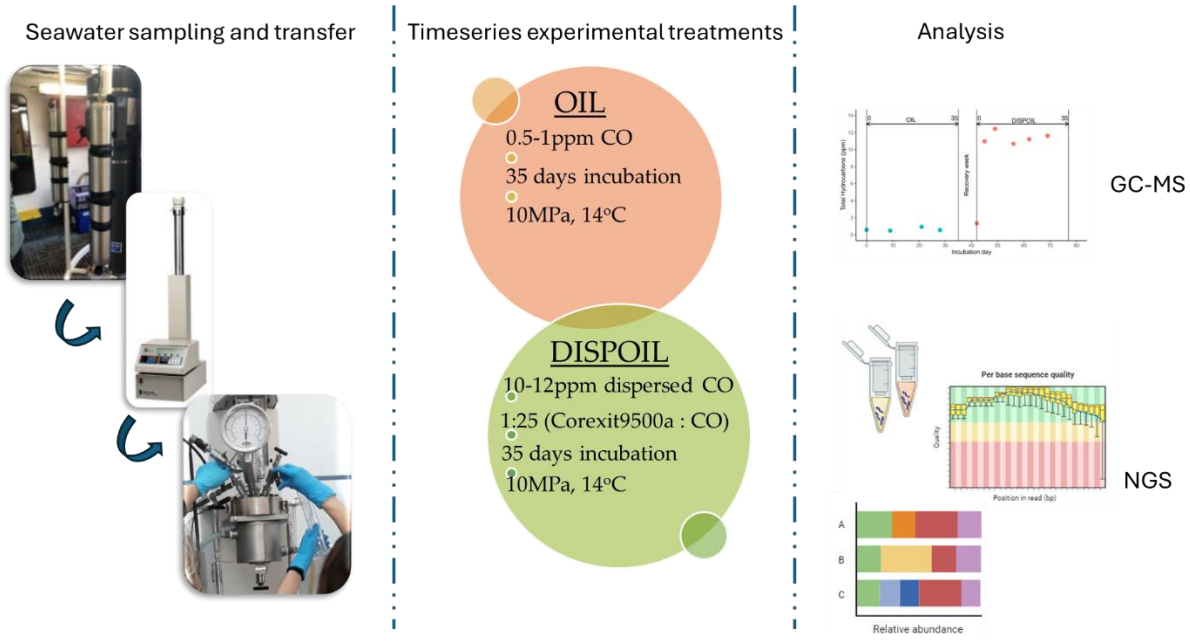

6.1 Abstract

During the DWH accident, a large proportion of the discharged oil and gas were entrapped in the water column forming the deep hydrocarbon plume. Studies in the aftermath of the accident elucidated the microbial response to hydrocarbons however, the effect of pressure was not properly evaluated or totally bypassed. In this work, we emulated a deep hydrocarbon plume at *in situ* conditions of the Eastern Mediterranean (EMS) basin, an area of increased interest for oil and gas activities yet understudied in terms of hydrocarbon bioremediation. The microbial composition and succession patterns of site-specific bacterial communities were monitored in the presence and absence of chemical dispersants, for a total of 77 days. Similarly to the DWH, results indicated members of γ-proteobacteria as first responders to the oil plume including *Oleispira, Alcanivorax* and *Marinobacter* whereas the addition of Corexit 9500A led to the dominance of *Alcanivorax* in the consortium and in the enrichment of Alphaproteobacteria and Flavobacteriales. To our knowledge, this is the first study that examines the response of un-decompressed microbial communities in the case of an oil spill and deep plume formation in the EMS.

6.2 Introduction

The discharge of oil and gas hydrocarbons in the deep sea causes the jetting effect due to pressure and temperature differences between the reservoir and the seafloor [63]. This familiar -for well blowouts- phenomenon leads to the dispersion of oil into smaller, neutrally buoyant droplets causing their accumulation in the water column and the formation of deep-water plumes [91, 269].

During the Deepwater Horizon (DWH) accident in the Gulf of Mexico (GoM) in 2010, uncontrolled leakage of oil and gas occurred at 1500 meters below sea level for a total of 87 days, marking it as the largest disaster in the history of oil spills [61]. It is estimated that all of the released gas (170.000 tonnes) and approximately half of the discharged oil (265.000 tonnes) were entrapped in the GoM's deep waters with the deepest expanding between 900-1300m for at least 35 km in distance [3, 60, 91].

This increase of sequestered hydrocarbons in the GoM's deep plume was attributed to the application of unprecedented amounts of chemical dispersants both at the sea surface (4,1 million litters) and for the first time, by subsea dispersant injection (SSDI) at the wellhead (2,9 million litters) at pressures of ~15MPa [27]. The decision to use dispersants was driven by safety

concerns for the responders, as the jetting effect alone proved insufficient to mitigate the oil from reaching the surface at large quantities. Furthermore, dispersant application was decided to lower the surface-to-volume ratio of the oil and create smaller oil droplets thereby enhancing hydrocarbon (HC) biodegradation [62, 63].

Microbial degradation remains, until today, the only available option for hydrocarbon remediation in the deep sea since any other oil recovery technology is technically infeasible [21, 36, 61]. In the DWH accident, approximately the 43-61% of the oil and gas that was entrained in the deep plume was biodegraded by specialised microorganisms capable of using hydrocarbons as carbon and energy source [60]. These microorganisms exist in low abundance as part of the rare biosphere, a microbial "seed bank" that becomes competitive upon exposure to hydrocarbons [35, 36, 191]. Moreover, these microbial taxa thrive in a harsh environment and are capable of oil mitigation under extreme pressure conditions that affect cellular and metabolic processes [6, 102].

In the aftermath of DWH accident and despite the fact that ~30% of the discharged hydrocarbons was biodegraded in the deep-water layers, only a limited number of studies have been performed to address the impact of high hydrostatic pressure (HHP) on HC degradation. Furthermore, these laboratory experiments have several frailties, and their results are not indicative of microbial response to an *in situ* deep oil release. For example, a work by Prince, Nash and Hill observed a 33% decrease in biodegradation of European crude oil at 15MPa compared to 0.1MPa however they performed their experiments with surface seawater [270]. Similarly, Fasca et al observed variations in structure and diversity of surface bacterial communities in the presence of low temperature, high pressure and oil contamination [108]. HHP studies with deep microbial communities have been performed however, to our knowledge, they all experienced decompression upon retrieval. [107, 109, 271].

The necessity for site-specific research under *in situ* pressure and temperature conditions was one of the major lessons learned from the DWH accident in order to provide accurate and representative results for both HC biodegradation rates and microbial response to an oil release in the deep sea [63]. The Eastern Mediterranean Sea (EMS) presents unique environmental parameters that differ significantly to those in the GoM. Deep waters are warmer in the EMS (14 ^{o}C) compared to the GoM (4 ^{o}C) and are considered as ultraoligotrophic with a severe limitation in phosphorus [121, 126]. The warmer EMS deep waters might facilitate HC biodegradation rates and mitigate the effect of pressure on microbial communities as the combination of low

temperature and high pressure has been previously found to slow microbial growth and thus oil metabolism [107].

In this study, a hydrocarbon plume simulation experiment was performed using un-decompressed deep EMS microbial communities at *in situ* pressure and temperature as described by Antoniou et al [237]. Deep seawater was collected using a high-pressure sampling device (HP-Sampler) and was exposed to crude oil (OIL treatment) and dispersed crude oil (DISPOIL treatment) for a total of 77 days with monitoring of HC levels and recording of microbial community shifts at specific time intervals. This work aims to assess the microbial response and to identify the primary key microorganisms involved in hydrocarbon degradation, in the case of an accidental oil release scenario and deep plume formation in the deep EMS.

6.3. Materials and Methods

6.3.1 Seawater sampling

Seawater samples were retrieved on board the R/V Aegaeo, on the 29th of February 2019 from a sampling station located in southern Crete, Greece (Gavdos station: coordinates 34°41'58.6"N 24°07'36.2"E). A high-pressure sampling unit (HP-Sampler), attached to a CTD rosette, was deployed to collect seawater from a depth range of 600-1000 m [237]. The seawater was maintained in the HP-Sampler for 4 days at *in situ* pressure and temperature until use in the laboratory. Seawater temperature and salinity was on average 13.83 ^{o}C/38.81 psu. Microbial community composition at the sampling depth range was highly similar based on Principal Component Analysis (PCoA) on Bray-Curtis distance matrix (Figure S16) Moreover, decompressed seawater was also collected from 1000 m depth in Niskin bottles and was immediately stored at 14 ^{o}C in the dark.

6.3.2 Emulation of a deep hydrocarbon plume in a high-pressure reactor

Timeseries experiments were conducted in a high-pressure reactor (HP-Reactor, Parr Instrument Company, IL, USA) at *in situ* pressure and temperature (10MPa, 14 ^{o}C), without pressure disruption at any stage of the experimental process that lasted, in total, 77 days (Figure 32). For the initial phase of the experiment (OIL treatment), 300 mL of un-decompressed seawater from the HP-Sampler was transferred via a high-pressure piston pump into the HP-Reactor which was prefilled with 300mL Niskin-collected deep seawater in the presence of 0.5-1 ppm of Iranian Light Crude Oil (CO; density ~0.7821 g mL^{-1}). Bioremediation was monitored

for 35 days by withdrawal of 100 mL for DNA extraction, GC-MS, dissolved organic carbon (DOC), cell counts and pH at indicated timepoints. This was substituted by addition of 100 mL filter-sterilized depressurized seawater from 1000 m to maintain the operating volume (600 mL) while, CO was replenished regularly to preserve hydrocarbon plume levels. At the end of the OIL treatment, ~450 mL were removed from the HP-Sampler for metagenomic analysis which will not be discussed here. The remaining volume, enriched in HC-degraders, acted as inoculum for the second phase of the experiment (DISPOIL treatment). Prior to the start of DISPOIL treatment, the volume within the HP-Reactor was raised at 600 mL with filter-sterilized deep seawater amended with CO and the HC-enriched microbial community was left to regenerate for 7 days. On day 42, crude oil and dispersant (1:25 *v/v* COREXIT™ EC9500A, COREXIT Environmental Solutions LLC, Sugar Land, TX, USA) were added at a concentration ranging between 10-12 ppm and replenished weekly. Sampling was performed on days 3, 7, 14, 21, 28, 35 for both treatments (t0 for DISPOIL treatment was Day 42).

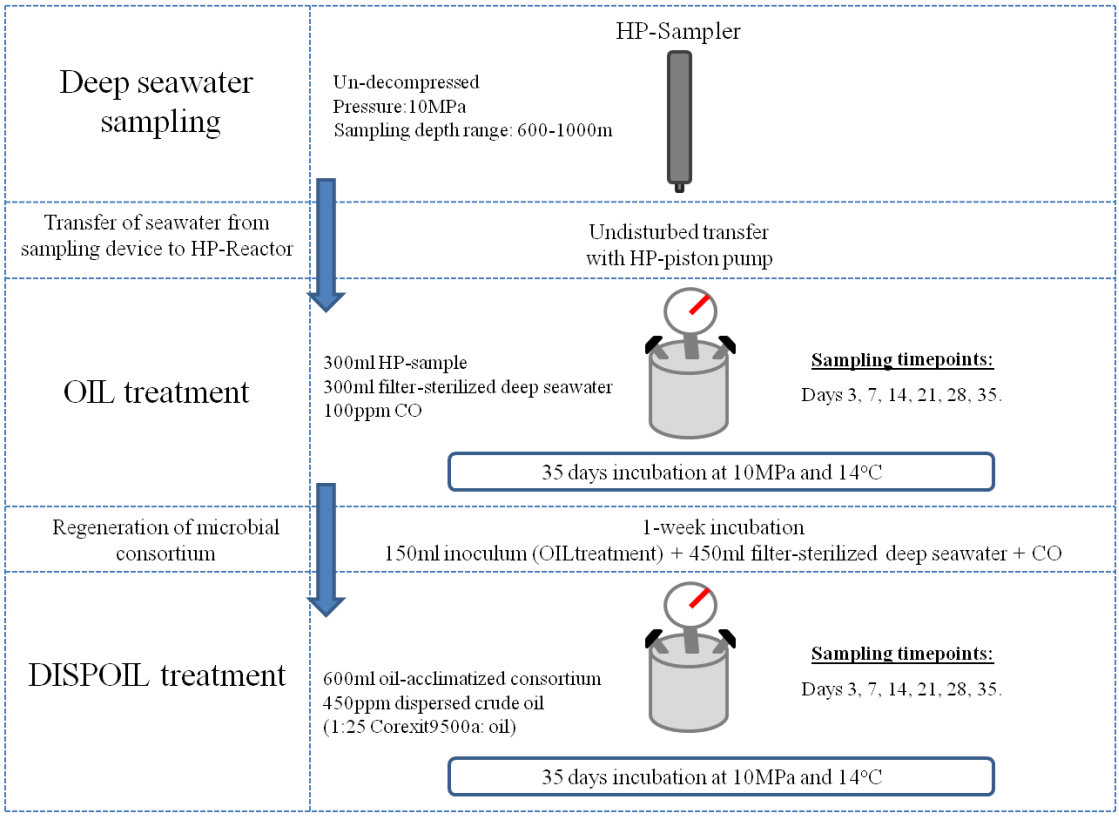

Figure 32. *Schematic representation of experimental workflow followed for deep-seawater sampling and timeseries experiments performed in the HP-Reactor at* in situ *pressure and temperature conditions. CO: crude oil, OIL: Oil-only treatment, DISPOIL: dispersed oil treatment.*

6.3.3 GC-MS analysis of hydrocarbons

Liquid-liquid extraction was performed to determine hydrocarbon levels as described in [237]. Briefly, 20 mL of dichloromethane (DCM Suprasolv®, Merck KGaA, Darmstadt, Germany) were added in a separation funnel containing 20 mL of sample and extracted by manual shaking. The organic phase was retained, and the aqueous phase was re-extracted twice. The solvent was removed in a hot plate with simultaneous nitrogen blow and the concentrated samples were transferred to 4 mL chromatography vials. Solid extracts were then separated into saturated and aromatic hydrocarbons by elution through SPE columns (Bond Elute TPH, Agilent Technologies, Inc., Santa Clara, CA, USA) using n-hexane Suprasolv® (Merck KGaA, Darmstadt, Germany) and DCM Suprasolv® respectively. GC-MS analysis was performed on an Agilent GC-MS HP 7890/5975C system, with an Agilent HP-5MS 5% phenyl methyl siloxane column (60 m × 250 μm × 0.25 μm). The HC mixture consisted of an Oil Analysis Standard (Absolute Standards Inc.®, Hamden, CT, USA) containing 44 compounds, and 17a(H),21b(H)-hopane (Chiron AS®, Trondheim, Norway). The standard composition of the HC mixture was normal alkanes from C10 to C35, pristane and phytane and 16 polycyclic aromatic hydrocarbons (PAHs).

6.3.4 Dissolved Organic Carbon (DOC) and pH determination

Aliquots of 10 mL were taken from each sampling timepoint, filtered through a 0.2μM PES membrane filter and stored at -20 ^{o}C until analysis. The samples were acidified to a pH < 2 using 5% hydrochloric acid (HCl) and were purged with nitrogen gas for 10 minutes to remove inorganic carbon compounds. DOC samples were measured on a Total Organic Carbon Analyzer (TOC-VCPN, Shimadzu, Japan) using a standard curve (TOC standard solution, 1000μg/L, Merck & Co., Inc., Kenilworth, NJ, USA). The pH was recorded using a HQD portable meter (HQ30d) and IntelliCAL PHC101 pH probe both purchased from Hach-LANGE.

6.3.5 Cell count determination-Flow cytometry

Microbial cell counts were determined on a CytoFlex Flow Cytometer (Beckman Coulter Inc, USA). The cells were fixed with 1% paraformaldehyde (PFA, 4% stock) and 0.025% glutaraldehyde (GA, 25% stock). The samples were diluted with filter-sterilized deionized water (DI) to a final concentration of 10^6-10^7 cells and were stained with 1x thiazole green stain (1000x stock in DMSO, BIOTIUM, USA) for 15min in the dark at room temperature. For the analysis of

samples, side-scatter (SSC) threshold was set to automatic (10,000) with a slow flow rate of 10μL min^{-1}.

6.3.6 DNA extraction and sequencing

Approximately, 70 mL from each sampling timepoint were passed through a 0.2μM PES membrane filter and extracted based on a protocol by [194] as modified in [154]. Briefly, the membranes were soaked in CTAB extraction buffer (1 M Tris-HCl (pH 8), 0.5 M EDTA (pH 8), 1M NaH2PO4 (pH 8), 5 M NaCl and 5% cetyltrimethylammonium bromide) and vortexed thoroughly for 2 minutes. The samples were then subjected to three freeze-thaw cycles (liquid nitrogen to 65 ºC). Lysozyme (10 mg/mL) and Proteinase K (20 mg/mL) were subsequently added, and the samples were incubated for 30 min at 37 ºC prior to SDS addition and further incubation at 65 ºC for 2 hours. The supernatant obtained after centrifugation (10,000g, 10min) was mixed with an equal volume of phenol:chloroform:isoamylalcohol (25:24:1) followed by another centrifugation step. Further purification was performed by mixing the aqueous phase with chloroform:isoamylalcohol (24:1) and the DNA was left to precipitate overnight by adding ice-cold isopropanol. The precipitated DNA obtained after centrifugation was washed with 70% molecular-grade ethanol. Finally, after another spin, the supernatant was discarded, and the DNA pellets were left to dry at room temperature. TE buffer was used for resuspending the DNA pellets and Qubit dsDNA high-sensitivity assay was used to measure the DNA concentration on a Qubit 4.0 fluorometer. The V3-V4 region of 16S rRNA gene sequence was amplified using the universal primers 341F and 806R [155, 241]. Sequencing was done on an Illumina MiSeq using V3 (2 x 300 bp) chemistry at Biosearch Technologies, LGC Genomics GmbH (Berlin, Germany).

6.3.7 Bioinformatic analysis

The bioinformatic analysis of the primer-clipped V3-V4 16S rRNA sequences was performed in R (version 4.3.2) using the *DADA2* package [157]. Following inspection of the quality read profiles, the 16S rRNA paired-end reads were quality-trimmed (max. 2 allowed expected errors per read) and reads >250 bp were retained. Afterwards the paired-end reads were dereplicated, denoised, merged to generate amplicon sequence variants (ASVs) and screened for chimeras. Taxonomy assignment up to Genus level was performed using the SILVA 16S rRNA gene database (Silva version 138) [159]. A single object including the ASV abundance and taxonomy tables, the experimental metadata and a neighbor-joining phylogenetic tree was

created with the *phyloseq* package [198] and was used in downstream analysis. The DISPOIL sample from Day 28 was excluded due to low number of reads. Overall, the dataset consisted of 13 samples (12 from the HP-Reactor plus the background seawater sample from 1000 m). ASVs that could not be taxonomically ranked at the phylum level were removed. After discarding zero abundance ASVs and single singletons (ASVs occurring only once in one sample), we applied a supervised prevalence filtering step to exclude ASVs with low biological meaning. In total, the dataset consisted of 188,654 reads with an average of 14,512 reads per sample (min: 2684, max: 28736) and a total of 2113 ASVs which were distributed among 30 phyla. 712 ASVs were assigned to 28 phyla.

6.3.8 Statistical analysis

All statistical analysis were performed in the R environment (version 4.3.2) using Rstudio software (version 2023.12.1) [158]. Figures were generated using the *ggplot2* package unless otherwise stated. Beta-diversity analysis was performed via Principal Component Analysis (PCoA) on Bray-Curtis dissimilarity distances using the cumulative sum scaling (CSS)-normalized dataset (*ordinate* function). The effect of explanatory variables was evaluated via distance-based redundancy analysis (dbRDA) based on Bray-Curtis dissimilarity matrix using the *vegan* package (*capscale* function). For this analysis, Day 0 samples were excluded from the dataset and the remaining samples were categorized into a new categorical variable according to the experimental stage (Early: days 3-7, Late: days 14-35). The two experimental variables (Treatment, Stage) were used and the significance of the dbRDA model was tested using permutation test for constrained correspondence analysis (*anova.cca* function). Alpha diversity analysis was applied on the dataset prior to any normalization. Microbial succession patterns were visualised on a heatmap with row and column dendrogams using *vegan* and *Heatplus* packages. Finally, differentially abundant taxa between the two treatments (OIL, DISPOIL) were identified using the *DESeq2* package and an alpha value of 0.05.

6.4 Results

6.4.1 Beta diversity

Principal Coordinate Analysis (PCoA) using Bray-Curtis dissimilarity distances indicated a drastic shift in microbial community composition immediately after exposure to hydrocarbons (Figure 33A). In order to assess the effect of experimental variables on data variation, distance-

based RDA (dbRDA) analysis was performed (Figure 33B). The dbRDA linear model including the two variables (Treatment, Stage) was statistically significant (R2-adj. = 0.567, p = 0.001) explaining the 65.35% of the total variation. Microbial communities were primarily separated by treatment (OIL, DISPOIL) on the first axis while the second axis separated only the OIL samples based on the experimental stage.

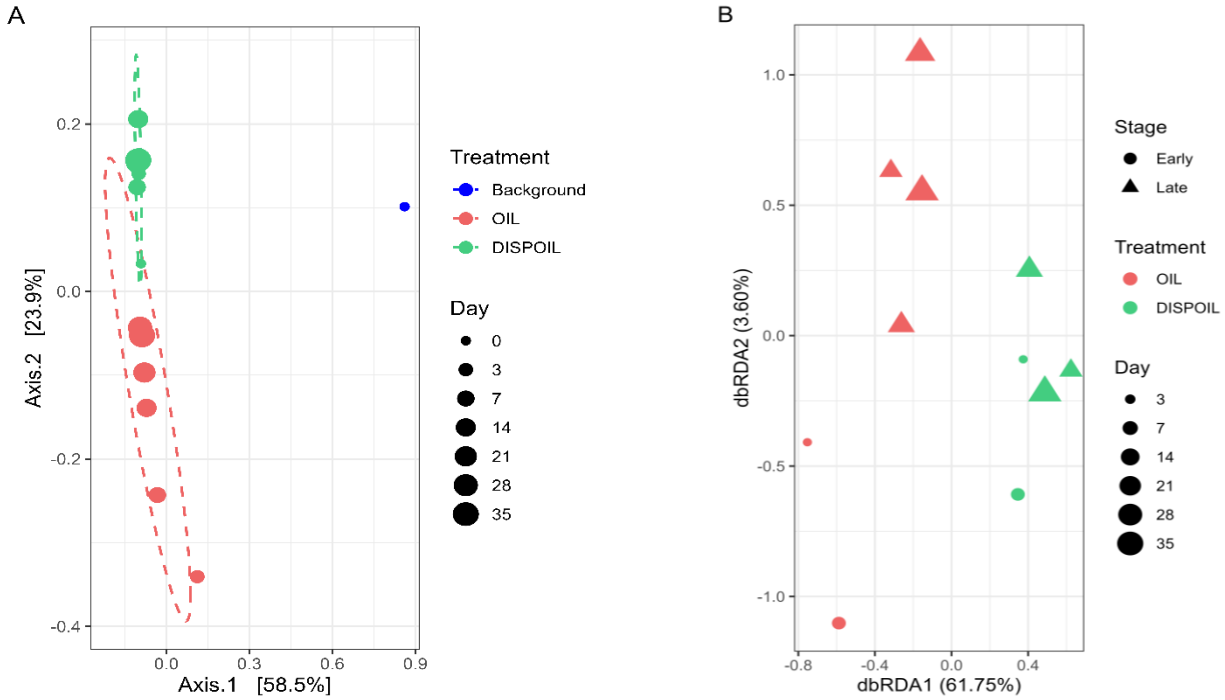

Figure 33. *Beta-diversity analysis using (A) Principal Coordinate Analysis (PCoA) and (B) distance-based Redundancy Analysis (dbRDA) based on Bray-Curtis dissimilarity matrix. Day 0 samples were excluded from the dbRDA analysis.*

6.4.2 Alpha diversity

Addition of crude oil caused a drastic decrease in microbial diversity levels within the first seven days of the experiment (Table 5). Furthermore, in the presence of dispersant, a lower number of unique ASVs was recorded however, the diversity levels remained relatively steady between the two treatments.

Treatment	**Observed ASVs**	**Diversity index**		
		Shannon	**Chao1**	**Simpson**
Background	570	5.32	576.5	0.99
OIL	116.5 ±27.16	2.92 ± 0.24	136.96 ±27.48	0.9 ± 0.02

DISPOIL	88.67 ±11.81	2.96 ± 0.11	115 ±27.22	0.92 ± 0.01

Table 5. *Alpha diversity indices measured for the two treatments (OIL, DISPOIL) and the natural seawater microbial community (Background).*

6.4.3 Microbial community composition and succession patterns

Microbial taxa belonging to Archaea (mainly Crenarchaeota), representing approximately the 34% of pristine seawater community (Backgr), were nearly depleted in the OIL treatment and entirely diminished in the DISPOIL treatment (Figure S17). On the other hand, Proteobacteria and Bacteroidota were the most enriched phyla in both treatments. Proteobacteria, dominated all sample timepoints (Backgr, OIL, DISPOIL), increasing from ~35% in the background community to ~92% and ~80% in OIL and DISPOIL treatments respectively. On the other hand, Bacteroidota were enriched in the later stages of the OIL treatment, presenting a 30-fold increase in abundance compared to the background sample however, they were favored in the presence of dispersant, comprising approximately the 20% of the DISPOIL community (~3 times higher than the OIL treatment).

Gammaproteobacteria were among the first responders to oil contamination while Alphaproteobacteria and Bacteroidia increased in abundance in the later stages of the OIL treatment and in the presence of dispersant (Figure S18). Particularly, within the first 3 days of incubation with crude oil, genera belonging to *Oleispira* (Oceanospirillales), *Thalassomonas*, *Thalassotalea* (Alteromonadales) and *Ralstonia* (Burkholderiales) were enriched in abundance (Figure 34, Figure S19). These were replaced in the next sampling timepoint with *Alcanivorax* (Oceanospirillales) and *Methylophaga* (Nitrosococcales) (Figure 34; O7). Further successional changes were observed in the late phase of the OIL experiment with enrichment of *Marinobacter* and *Thalassospira* (Alphaproteobacteria) that remained abundant until the end of this treatment (Figure 34; O14-O35). Following dispersant addition, *Alcanivorax* was enriched, dominating the microbial community throughout the DISPOIL treatment. Alphaproteobacteria genera belonging to *Thalassospira* (Rhodospirillales) *Hyphomonas* (Caulobacterales), *Nisaea* (Thalassobaculales) *Erythrobacter* (Sphingomonadales) and *Parvibaculum* (Parvibaculales) were also increased in abundance (Figure S19). Moreover, the addition of Corexit dispersant favored members of Flavobacteriales such as *Mesonia, Muricauda* and *Winogradskyella* (Figure S20).

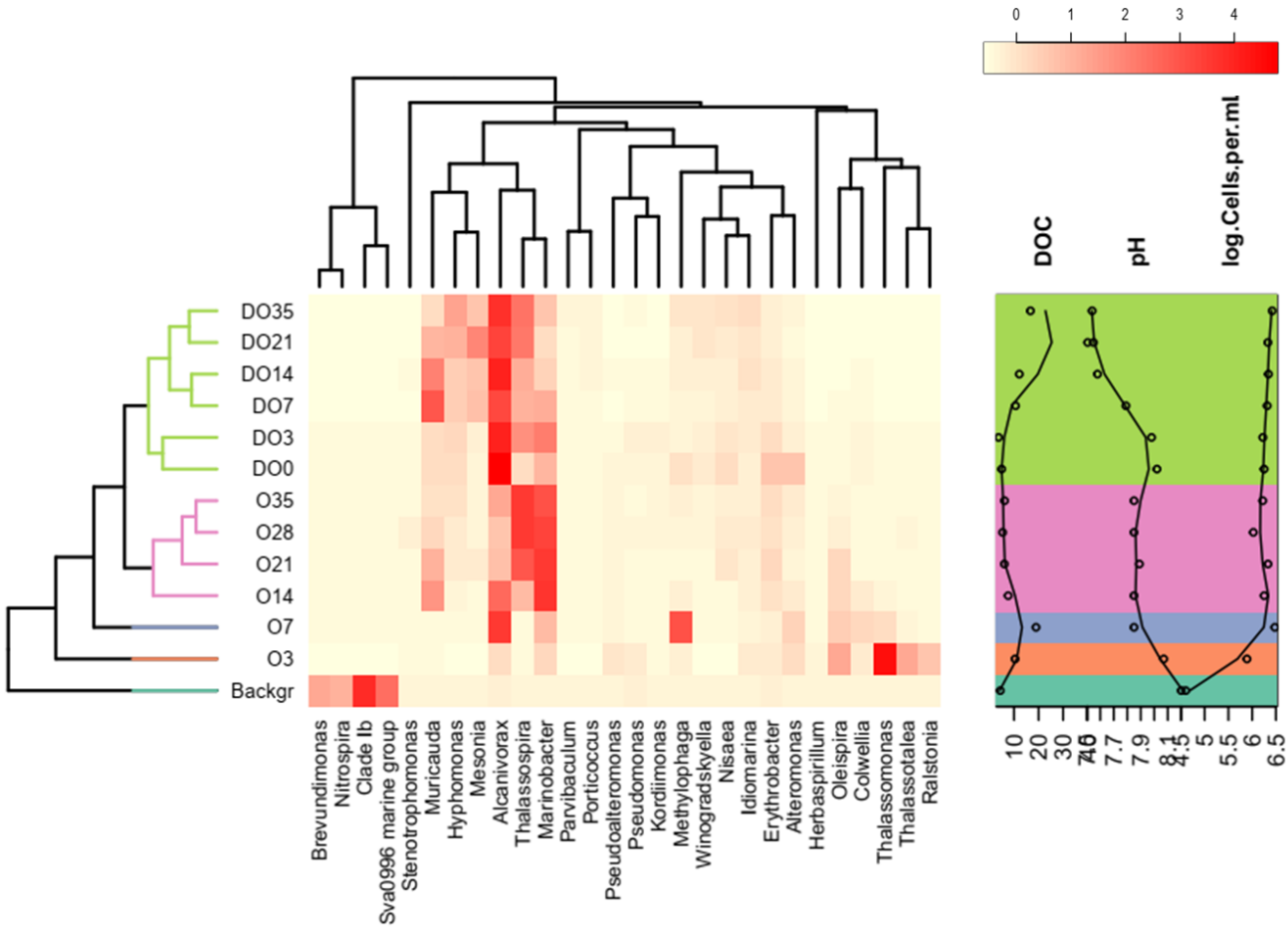

Figure 34. *Heatmap of relative abundance indicating the microbial succession patterns at the Genus level. Row dendrogram presents the clustering of samples based on Bray-Curtis dissimilarity. Column dendrogram presents the clustering of genera that occurred more often together. Genera with less than 1% relative abundance were discarded for plotting purposes. The right plot presents metadata of cell counts (cells mL^{-1}), DOC (mg L^{-1}) and pH in each sample.*

6.4.4 Identification of influential taxa

Differential abundance analysis (DESeq2) was applied to identify significantly enriched species between the two oil treatments. DESeq2 revealed 25 ASVs which were significantly higher in abundance in the OIL treatment (Figure 35, Table S13). Those belonged to 7 genera and were mainly members of Gammaproteobacteria such as *Oleispira* (Oceanospirillaceae), *Thalassomonas*, *Colwellia* (Colwelliaceae), *Marinobacter* and *Pseudoalteromonas*. In addition,

two ASVs belonging to the Alphaproteobacteria genera *Thalassospira* and *Kordiimonas* were also significantly influenced in this treatment. Interestingly, from the 13 ASVs linked with DISPOIL treatment, 3 belonged to *Oceanospirillaceae* however they were not classified as *Oleispira* at the genus level. Moreover, other genera with significantly higher abundance in DISPOIL treatment belonged to *Pseudomonas, Parvibaculum, Aestuariicella*, *Acinetobacter, Porticoccus* and *Magnetospira* (Figure 35, Table S13).

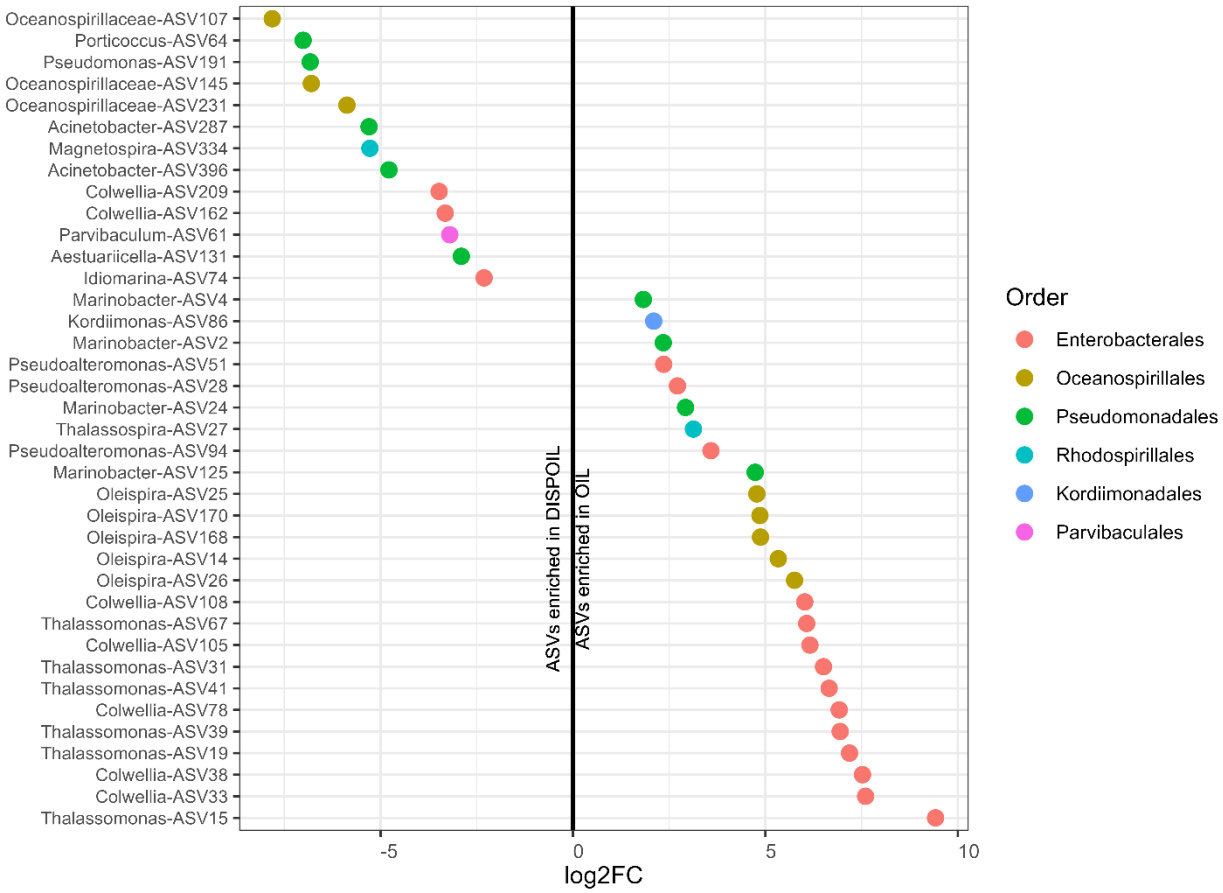

Figure 35. *DESeq2 analysis indicating the ASVs that were significantly influenced by OIL and DISPOIL treatment (p-adj < 0.05). Log2FC is the logarithmic fold change of taxa abundance between the two treatments (OIL-DISPOIL).*

6.5 Discussion

6.5.1 Emulation of a deep EMS plume

In this study we emulated a deep-sea oil plume at *in situ* environmental conditions of the EMS based on knowledge obtained from the DWH plume in the GoM. Using a low-cost HHP sampling apparatus, seawater was collected from the deep EMS water mass (EMDW) and was transferred under undisturbed pressure conditions to a HHP reactor [237]. A 77-day experiment was conducted, divided in two phases, using oil or dispersed oil at low concentrations to simulate

realistic hydrocarbon plume levels in the field. For the first phase of the experiment (OIL treatment), hydrocarbon concentrations ranged from 0.5-1 ppm while in the second (DISPOIL treatment) were between 10-12 ppm (Figure S21). These were comparable to the concentrations found in the DWH oil plume which spanned from ppb up to the highest concentration of 10 ppm recorded within 1 km distance from the MC-252 discharging well [189, 272]. During the experimental procedure, sub-samplings of 1/6 of the total volume (100 mL) and subsequent substitutions of the retrieved culture were also performed without any pressure disruption. The refilling with filter-sterilized deep seawater after every sub-sampling step ensured the preservation of inorganic nutrients and oxygen, while the frequent oil replenishment, allowed the constant supply of carbon to the microbial community throughout the experiment.

6.5.2 Hydrocarbon-biodegradation rates in the EMS plume

The regular addition of hydrocarbons in our study, resembled the deepwater circulation near the MC-252 well where certain water fractions were repeatedly exposed to fresh oil as predicted by Valentine et al model [68]. Dispersant was added in the second phase of the experiment (DISPOIL), after acclimatization of the microbial community to oil, to imitate the DWH accident response where Corexit 9500A was injected after 25 days from the start of the oil spill [62]. GC-MS analysis indicated higher oil concentrations in the presence of dispersant (DISPOIL treatment) which has been related with increased hydrocarbon levels in subsurface waters [70]. Nonetheless, elevated oil concentrations might also be attributed to the lower attachment of dispersed oil on equipment parts and surfaces (wall effect) during sub-sampling and substitution procedures. A thorough analysis of the high-pressure sampling apparatus, experimental workflow and hydrocarbon-biodegradation rates in the emulated oil plume are described and presented by Antoniou et al [237]. Briefly, in both OIL and DISPOIL treatments, the degradation of light alkanes (C14-C25) was a matter of few days ($t_{1/2}$ = 0.6-3.2 days) whereas dispersant addition enhanced the biodegradation of more recalcitrant compounds such as heavy alkanes (C26-C35) and PAHs. For example, half-life ($t_{1/2}$) of heavy alkanes were lowered by more than 50% in DISPOIL ($t_{1/2}$ = 2.1-2.8 days) compared to OIL ($t_{1/2}$ = 3.4-7.7 days) and PAH biodegradation reached more than 90% efficiency in the presence of dispersant (DISPOIL), 265 times higher than in the OIL treatment. Even though PAH bioavailability was initially low to begin with in the OIL treatment (61 ppb) and biodegradation efficiency could not be evaluated with certainty however, the notable decrease in the half-life of PAHs in DISPOIL between the

days 0-3 ($t_{1/2}$ = 19.4) and the end of the experiment ($t_{1/2}$ = 2.2-2.9) suggests that dispersant application enhanced PAH degradation [237].

6.5.3 Primary microbial response to hydrocarbon exposure

Early response to the presence of hydrocarbons involved the transitioning from a diverse microbial community comprised of species participating in nitrogen and carbon cycling towards a low-diverse consortium enriched in members of γ-proteobacteria similarly to the DWH plume [81, 193]. Among the first responders to oil contamination were *Thalassomonas, Thalassotalea, Oleispira* and *Ralstonia* which comprised ~75% of the microbial community and reached their highest levels on day 3 of the OIL treatment. *Oleispira,* a known marine obligate hydrocarbonoclastic bacterium (OHCB) was significantly enriched in the OIL treatment based on differential abundance analysis (DESeq2). Nucleotide BLAST analysis of the most abundant *Oleispira* 16S rRNA sequences (ASV14, ASV25, ASV26) indicated a similarity of 97.95% and 97.7% to the type strain *Oleispira antarctica* RB-8 isolated from the Antarctic coastal waters [273]. This psychrophilic strain with a broad growth range optimum (1-15 ºC) has been previously demonstrated to have an ecological competitiveness at low temperatures and can achieve similar growth rates at 4 ºC and 16 ºC in the presence of linear alkanes (C10-C24) [43, 274, 275]. Yet, *O. antarctica* utilizes a very restrict fraction of hydrocarbons compared to other OHCB and is unable to grow on longer-chain alkanes. This might explain why *Oleispira,* despite its fast response to oil contamination, it is rapidly outcompeted in the warmer deep EMS waters (14 ºC) [275]. A similar observation was made by Thomas et al in oil-amended seawater microcosms incubated at 16 ºC [276].

Thalassomonas and *Thalassotalea,* both members of the *Colwelliaceae* family were among the enriched genera in OIL treatment that declined rapidly after day 3. *Thalassomonas,* has been previously found in the DWH plume, increasing in abundance together with *Colwellia, Cycloclasticus* and *Pseudoalteromonas* after partial capture of the well [83]. In addition, *Thalassotalea* has also participated in HC biodegradation as important member of the microbial consortium in the DWH plume [85]. *Thalassotalea sp.* strain ND16A, isolated from the EMS at 1055 m depth, contains a chatechol 2,3 dioxygenase and two ring-hydroxylating dioxygenase gene clusters in its genome, which are important in aromatic hydrocarbon degradation [277].

6.5.4 Succession patterns in later stages of the EMS deep plume

Following the decrease of these primary responders, the microbial community was enriched in the OHCB, *Alcanivorax* and in *Methylophaga* (OIL; day 7). *Alcanivorax* is a

ubiquitous n-alkane degrader in surface oil-contaminated waters [38, 49]. The absence of *Alcanivorax* from the DWH plume [81–83] in combination with the reduced growth and impaired metabolic rates of isolated strains (*A. borkumensis, A.jadensis, A.dieselolei*) at elevated pressures, registered this genus as sensitive to HHP [112, 113]. However, several *Alcanivorax* strains have been isolated from deep-sea environments [217, 218, 263]. In addition, in previous oil studies by our group, *Alcanivorax* was among the dominant taxa in microbial consortia from the deep EMS while Liu et al also identified members of *Alcanivoraceae* in oil-amended microcosm experiments with deep EMS seawater [141, 154, 278]. This might be attributed to the warmer deep-water temperatures of the EMS (14 ºC) which may reduce the effect of high pressure thus allowing the presence of *Alcanivorax* here as opposed to other oceans at equal depths (4 ºC) [107]. The most abundant *Alcanivorax* ASVs in our dataset belonged to *A. borkumensis* SK2 (ASV3; 99.74% similarity), *A.venustensis* ISO4 (ASV6, 100% similarity) and *A. jadensis* T9 (ASV34, ASV10; 99.23% similarity) (Figure S22). *A. venustensis* was the dominant genus in our previous oil enrichment experiments under HHP, presenting piezotolerant traits, whereas *A. borkumensis* was enriched in our atmospheric incubations with oil-amended deep seawater [154, 278].

Methylophaga were recorded only at day 7 of the OIL treatment in our experiments. Interestingly, these methylotrophs were initially not detected in DWH plume studies during the active phase of the oil spill, prior to the use of dispersants [81, 279]. However crude-oil enrichment studies by Mishamandani et al indicated the short-lived bloom of *Methylophaga* which might have been missed during the early stages of the DWH blowout [280, 281].

The succession of *Alcanivorax* by *Marinobacter* (OIL; days 14-35), another obligate hydrocarbonoclastic species, and *Thalassospira* (OIL; days 21-35) indicates the transition towards metabolically more versatile genera [43]. The two most abundant *Marinobacter* ASVs had a similarity to *M. adhaerens* HP15 (ASV2-99,74%, ASV4-100% similarity). A different *M. adhaerens* strain (t76_800) has been previously associated with long-chain alkane degradation [282]. On the other hand, members of *Thalassospira* have been linked with PAH degradation [214, 283].

The addition of Corexit 9500A led to the dominance of *Alcanivorax* throughout the second phase of our experiment. Increased levels of Bacteroidia (*Flavobacteriaceae*) were also recorded in post-spill DWH plume after the well was completely shut [83]. *Flavobacteriaceae* have been previously associated with degradation of high molecular organic matter in marine environments, were favored in the presence of dispersant [83, 284]. The increased DOC levels

during this experimental phase are probably attributed to the release of organic compounds by the metabolic activities of *Flavobacteriaceae*. Furthermore, unclassified Oceanospirillaceae were significantly enriched in DISPOIL treatment similarly to the results following the DWH blowout in the GoM. Nonetheless, microbial community composition in an oil plume simulation study by Hu et al enabled the recovery of near-complete genomes including the previously unidentified DWH Oceanospirillales now registered as *Bermanella* species, a novel alkane degrader [85].

6.6 Conclusions

A deep oil plume was successfully emulated under *in situ* pressure and temperature conditions of the Eastern Mediterranean Sea. For a total of 77-days, microbial succession patterns and hydrocarbon levels were monitored in the presence of oil and dispersed oil to assess the microbial response in the case of an oil spill and deep plume formation in the EMS. Primary hydrocarbon degraders belonged to the class of γ-proteobacteria and included the OHCB *Oleispira* followed by *Alcanivorax* and *Marinobacter*. Similarly to the DWH blowout, dispersant was added after 35 days from the initial exposure to hydrocarbons, when the microbial community was already acclimatised to oil. In the presence of Corexit 9500A, members of Alphaproteobacteria (*Hyphomonas*) and Flavobacteriales (*Mesonia, Muricauda, Winogradskyella*) were favored however, the microbial community was dominated by *Alcanivorax*. Furthermore, distinct microbial taxa were significantly enriched in the two treatments with the most intriguing difference observed in *Oceanospirillaceae* members between OIL (*Oleispira*) and DISPOIL (unclassified). Overall, our results highlight the crucial role of the hydrocarbonoclastic *Oleispira, Alcanivorax* and *Marinobacter* in hydrocarbon bioremediation in the deep EMS.

CHAPTER 7.

Conclusions and Future perspectives

This dissertation attempts to address the microbial community structure in areas of interest for oil and gas activities, evaluate its response to hydrocarbon inputs and examine successional changes in the case of a deep oil spill accident in the Eastern Mediterranean Sea. The main conclusions drawn from this study are given below:

- The pristine waters of the deep EMS in the examined stations present notable levels of known hydrocarbon-degrading strains therefore a microbial "seed bank" of species that is ready to respond upon exposure to hydrocarbon pollution.
- A rapid response, within a week, to crude oil contamination was observed by the deep microbial consortium, despite the lower *in situ* temperature, indicating a community with an increased potential in HC biodegradation compared to the surface consortium.
- Decompression of microbial communities upon deep seawater retrieval resulted in the loss of biodiversity which has been linked to decreased hydrocarbon-degradation rates especially for the more recalcitrant PAHs.
- Corexit 9500A dispersant increased the solubility of Iranian light crude oil and the bioavailability of its hydrocarbon substrates.
- Dispersant had no effect on the selection of hydrocarbon degraders in the presence of the nutrient-rich enrichment medium ONR7.
- Taken together, the data on microbial community in combination with hydrocarbon degradation rates from the emulated plume described in Antoniou et al [237], suggest that dispersant does not have an inhibitory effect and can induce HC removal in the deep EMS.

- The combination of the nutrient-rich ONR7 medium and crude oil as C-source formed the conditions that led to the antagonistic emergence of *Alcanivorax* which outcompeted other key hydrocarbon degraders.
- The ubiquitous in surface oil spills, *Alcanivorax*, appears to have an important role in bioremediation of hydrocarbon pollution in the warmer deep waters of the EMS in contrast to the DWH plume where it was not detected in the microbial consortium responding to the oil contamination.
- This work highlights the presence of an *Alcanivorax* strain recently emended in the *Alloalcanivorax* genus (*A. venustensis*) that has the ability to grow and degrade hydrocarbons under high pressure in the deep EMS.
- Besides *Alcanivorax,* other hydrocarbonoclastic bacteria like *Oleispira* and *Marinobacter* were also enriched under HHP and were among the early responders to a deep EMS plume.

While this thesis contributes towards the understanding of how microbial communities will respond to an oil pollution in the deep EMS however, there are many more that need to be done in order to fully elucidate the self-healing capability of this basin. In particular:

- Further work could be performed towards the examination of the eukaryotic microbial fraction that is actively involved in hydrocarbon bioremediation in the deep EMS. In particular, fungi are probably the most diversified group of unicellular eukaryotes with known genera involved in hydrocarbon bioremediation (mycoremediation). However, the majority of studies have been performed for terrestrial taxa whereas marine fungal diversity and oil removal capabilities remain unexplored.
- The metabolic pathways and genes triggered in the presence of hydrocarbons, dispersant and high-pressure conditions could be elucidated for the deep EMS hydrocarbon-degrading consortium via metagenomic functional profiling. Moreover, genome sequence analysis of the isolated *Alloalcanivorax venustensis* could provide insight in the bacterium's capacity to remove hydrocarbons under high pressure.
- Since the future drilling marine areas near Crete are located in extreme depths of >3500 m below sea-level, high-pressure experiments need to be performed using seawater samples from greater depths (3000 m, 4000 m, 5000 m) to study the microbial response and HC degradation capacity under *in situ* environmental conditions. Furthermore,

through these experiments novel piezophilic hydrocarbon-degrading strains may be identified that thrive in the warmer waters of the EMS.

- In the context of energy transition and the use of natural gas in the energy mix due to its lower net carbon dioxide emission rate, the exploration and exploitation activities in the EMS marine region focus mainly on gas-rich fields. Therefore, further high-pressure studies could be conducted using methane and/or other hydrocarbon gases (ethane, propane, butane) as substrates to the deep EMS community and evaluate their response and gas fate.

About the author

Georgia Charalampous (GC) received her biology diploma from the Biology department (University of Crete, Greece) and her Master's degree in Protein Biotechnology from the same department. As part of her MSc studies, her master thesis was completed at the Institute of Molecular Cell & Systems Biology at the University of Glasgow, Scotland where she continued as a graduate researcher (2014-2015). In 2016, GC became involved as a scientific associate in the Horizon 2020 project, "INMARE" (2016-2019) at the Chemical and Environmental Engineering (CHENVENG) department of the Technical University of Crete (TUC). She started her PhD in 2019 as part of the "HEALMED" research project and since 2022 she is involved as a scientific associate in the "X-PRESS" project both funded by H.F.R.I, at the Institute of Geoenergy, FORTH.

Journal Publications

PhD Journal Publications

Charalampous G, Fragkou E, Kalogerakis N, Antoniou E, Gontikaki E. Diversity links to functionality: Unraveling the impact of pressure disruption and culture medium on crude oil-enriched microbial communities from the deep Eastern Mediterranean Sea. *Mar Pollut Bull*. 2024; 202:116275.

Charalampous G, Fragkou E, Kormas KA, Menezes ABD, Polymenakou PN, Pasadakis N, Kalogerakis N, Antoniou E, Gontikaki E. Comparison of Hydrocarbon-Degrading Consortia from Surface and Deep Waters of the Eastern Mediterranean Sea: Characterization and Degradation Potential. *Energies*. 2021; 14(8):2246.

Other Journal Publications

Antoniou E; Fragkou E; **Charalampous G**; Marinakis D; Kalogerakis N; Gontikaki E. Emulating Deep-Sea Bioremediation: Oil Plume Degradation by Undisturbed Deep-Sea Microbial Communities Using a High-Pressure Sampling and Experimentation System. *Energies* 2022; 15:4525.

Kritsiligkou P; Chatzi A; **Charalampous G**; Mironov A; Grant CM; Tokatlidis K Unconventional Targeting of a Thiol Peroxidase to the Mitochondrial Intermembrane Space Facilitates Oxidative Protein Folding. *Cell Rep.* 2017; 18(11):2729-2741.

International and National Conference Presentations

Composition of prokaryotic and eukaryotic microbial communities across the water column of the Eastern Mediterranean Sea, *10th International Conference of Mikrobiokosmos*, Larissa 30-2 December 2023 (poster presentation).

Enrichment and isolation of piezotolerant hydrocarbon degraders from the deep waters of the Eastern Mediterranean Sea, *13th International Congress on Extremophiles*, Loutraki 18-22 September 2022 (poster presentation).

Comparison of Hydrocarbon‐Degrading Consortia from Surface and Deep Waters of the Eastern Mediterranean Sea, *8th European Bioremediation Conference (EBC-VIII)*, Chania 12-17 June 2022 (poster-flash presentation).

Enrichment of Piezotolerant Hydrocarbon Degraders from Deep Water Communities of the Eastern Mediterranean Sea, *8th European Bioremediation Conference (EBC-VIII)*, Chania 12-17 June 2022 (oral presentation).

Comparison of Hydrocarbon‐Degrading Consortia from Surface and Deep Waters of the Eastern Mediterranean Sea: Characterization and Degradation Potential Characterization and Degradation Potential of Hydrocarbon-Degrading, *9th International Conference of Mikrobiokosmos*, Athens 16-18 December 2021 (e-poster).

Consortia from Surface and Deep Waters of the Eastern Mediterranean Sea, *8th International Symposium on applied Microbiology and molecular biology in Oil Systems (ISMOS)*, online symposium 8-11 June 2021 (poster presentation).

References

1. National Academies of Sciences Engineering and Medicine (2023) Inputs: Sources of Oil in the Ocean. In: Oil in the Sea IV. National Academies Press, Washington, D.C.

2. Overton EB, Wade TL, Radović JR, et al (2016) Chemical Composition of Macondo and Other Crude Oils and Compositional Alterations During Oil Spills. Oceanography 29:50–63

3. Rullkötter J, Farrington J (2021) What Was Released? Assessing the Physical Properties and Chemical Composition of Petroleum and Products of Burned Oil. Oceanography 34:44–57. https://doi.org/10.5670/oceanog.2021.116

4. Overton EB, Wetzel DL, Wickliffe JK, Adhikari PL (2020) Spilled Oil Composition and the Natural Carbon Cycle: The True Drivers of Environmental Fate and Effects of Oil Spills BT - Scenarios and Responses to Future Deep Oil Spills: Fighting the Next War. In: Murawski SA, Ainsworth CH, Gilbert S, et al (eds). Springer International Publishing, Cham, pp 33–56

5. Kvenvolden KA, Cooper CK (2003) Natural seepage of crude oil into the marine environment. Geo-Marine Lett 23:140–146. https://doi.org/10.1007/s00367-003-0135-0

6. Scoma A, Yakimov MM, Boon N (2016) Challenging Oil Bioremediation at Deep-Sea Hydrostatic Pressure. Front Microbiol 7:1203; 10.3389/fmicb.2016.01203. https://doi.org/10.3389/fmicb.2016.01203

7. Soto LA, Botello A V, Licea-Durán S, et al (2014) The environmental legacy of the Ixtoc-I oil spill in Campeche Sound, southwestern Gulf of Mexico. Front Mar Sci 1:. https://doi.org/10.3389/fmars.2014.00057

8. Beyer J, Trannum HC, Bakke T, et al (2016) Environmental effects of the Deepwater Horizon oil spill: A review. Mar Pollut Bull 110:28–51. https://doi.org/https://doi.org/10.1016/j.marpolbul.2016.06.027

9. National Academies of Sciences Engineering and Medicine (2023) Changes in Offshore Safety Since 2010. In: Advancing Understanding of Offshore Oil and Gas Systemic Risk

in the U.S. Gulf of Mexico. National Academies Press, Washington, D.C., pp 39–72

10. Dong J, Asif Z, Shi Y, et al (2022) Climate Change Impacts on Coastal and Offshore Petroleum Infrastructure and the Associated Oil Spill Risk: A Review. J. Mar. Sci. Eng. 10

11. Muehlenbachs L, Cohen MA, Gerarden T (2013) The impact of water depth on safety and environmental performance in offshore oil and gas production. Energy Policy 55:699–705. https://doi.org/10.1016/j.enpol.2012.12.074

12. Murawski SA, Hollander DJ, Gilbert S, Gracia A (2020) Deepwater Oil and Gas Production in the Gulf of Mexico and Related Global Trends. In: Murawski SA, Ainsworth CH, Gilbert S, et al (eds) Scenarios and Responses to Future Deep Oil Spills: Fighting the Next War. Springer International Publishing, Cham, pp 16–32

13. Kostianoy AG, Carpenter A (2018) History, Sources and Volumes of Oil Pollution in the Mediterranean Sea. In: Carpenter A, Kostianoy AG (eds) Oil Pollution in the Mediterranean Sea: Part I: The International Context. Springer International Publishing, Cham, pp 9–31

14. UNEP/MAP and Plan Bleu (2020) State of the Environment and Development in the Mediterranean

15. Kostianoy AG, Carpenter A (2018) Oil and Gas Exploration and Production in the Mediterranean Sea. In: Carpenter A, Kostianoy AG (eds) Oil Pollution in the Mediterranean Sea: Part I. Springer International Publishing, Cham, pp 53–77

16. Piante C and, Ody D (2015) Blue Growth in the Mediterranean Sea: the Challenge of Good Environmental Status. MedTrends Project. WWF-France.

17. Ratner M (2016) Natural Gas Discoveries in the Eastern Mediterranean. Washington, DC

18. Mohammad N, Mohamad Ishak WW, Mustapa SI, Ayodele BV (2021) Natural Gas as a Key Alternative Energy Source in Sustainable Renewable Energy Transition: A Mini Review. Front Energy Res 9:. https://doi.org/10.3389/fenrg.2021.625023

19. National Academies of Sciences Engineering and Medicine (2023) Oil Spill Response. In: Oil in the Sea IV: Quick Guide for Practitioners and Researchers. National Academies

Press, Washington, D.C., pp 21–33

20. Li P, Cai Q, Lin W, et al (2016) Offshore oil spill response practices and emerging challenges. Mar Pollut Bull 110:6–27. https://doi.org/https://doi.org/10.1016/j.marpolbul.2016.06.020

21. Mapelli F, Scoma A, Michoud G, et al (2017) Biotechnologies for Marine Oil Spill Cleanup: Indissoluble Ties with Microorganisms. Trends Biotechnol 35:860–870. https://doi.org/https://doi.org/10.1016/j.tibtech.2017.04.003

22. Etkin DS, Nedwed TJ (2021) Effectiveness of mechanical recovery for large offshore oil spills. Mar Pollut Bull 163:111848. https://doi.org/10.1016/j.marpolbul.2020.111848

23. National Academies of Sciences Engineering and Medicine (2020) The Use of Dispersants in Marine Oil Spill Response. National Academies Press, Washington, D.C.

24. Prince RC (2015) Oil Spill Dispersants: Boon or Bane? Environ Sci Technol 49:6376–6384. https://doi.org/10.1021/acs.est.5b00961

25. Merlin F, Zhu Z, Yang M, et al (2021) Dispersants as marine oil spill treating agents: a review on mesoscale tests and field trials. Environ Syst Res 10:37. https://doi.org/10.1186/s40068-021-00241-5

26. Zhu Z, Merlin F, Yang M, et al (2022) Recent advances in chemical and biological degradation of spilled oil: A review of dispersants application in the marine environment. J Hazard Mater 436:129260. https://doi.org/https://doi.org/10.1016/j.jhazmat.2022.129260

27. Quigg A, Farrington J, Gilbert S, et al (2021) A Decade of GoMRI Dispersant Science: Lessons Learned and Recommendations for the Future. Oceanography 34:98–111. https://doi.org/10.5670/oceanog.2021.119

28. Ortmann AC, Anders J, Shelton N, et al (2012) Dispersed oil disrupts microbial pathways in pelagic food webs. PLoS One 7:e42548. https://doi.org/10.1371/journal.pone.0042548

29. Péquin B, Cai Q, Lee K, Greer CW (2022) Natural attenuation of oil in marine environments: A review. Mar Pollut Bull 176:113464. https://doi.org/https://doi.org/10.1016/j.marpolbul.2022.113464

30. Dalby AP, Kormas KA, Christaki U, Karayanni H (2008) Cosmopolitan heterotrophic microeukaryotes are active bacterial grazers in experimental oil-polluted systems. Environ Microbiol 10:47–56. https://doi.org/10.1111/j.1462-2920.2007.01428.x

31. Kostka JE, Teske AP, Joye SB, Head IM (2014) The metabolic pathways and environmental controls of hydrocarbon biodegradation in marine ecosystems. Front Microbiol 5:. https://doi.org/10.3389/fmicb.2014.00471

32. Atlas RM, Hazen TC (2011) Oil Biodegradation and Bioremediation: A Tale of the Two Worst Spills in U.S. History. Environ Sci Technol 45:6709–6715. https://doi.org/10.1021/es2013227

33. Prince R, Atlas RM (2005) Bioremediation of Marine Oil Spills. In: Bioremediation. pp 269–292

34. Farrington JW, Overton EB, Passow U (2021) BIOGEOCHEMICAL PROCESSES AFFECTING THE FATE OF DISCHARGED DEEPWATER HORIZON GAS AND OIL. Oceanography 34:76–97

35. Gibbons SM, Caporaso JG, Pirrung M, et al (2013) Evidence for a persistent microbial seed bank throughout the global ocean. Proc Natl Acad Sci 110:4651–4655. https://doi.org/10.1073/pnas.1217767110

36. Joye S, Kleindienst S, Gilbert J, et al (2016) Responses of Microbial Communities to Hydrocarbon Exposures. Oceanography 29:136–149. https://doi.org/10.5670/oceanog.2016.78

37. Leahy JG, Colwell RR (1990) Microbial degradation of hydrocarbons in the environment. Microbiol Rev 54:305–315. https://doi.org/10.1128/mr.54.3.305-315.1990

38. Head IM, Jones DM, Röling WFM (2006) Marine microorganisms make a meal of oil. Nat Rev Microbiol 4:173–182. https://doi.org/10.1038/nrmicro1348

39. Widdel F, Knittel K, Galushko A (2010) Anaerobic Hydrocarbon-Degrading Microorganisms: An Overview. In: Timmis KN (ed) Handbook of Hydrocarbon and Lipid Microbiology. Springer Berlin Heidelberg, Berlin, Heidelberg, pp 1997–2021

40. Bacosa HP, Ancla SMB, Arcadio CGLA, et al (2022) From Surface Water to the Deep

Sea: A Review on Factors Affecting the Biodegradation of Spilled Oil in Marine Environment. J Mar Sci Eng 10:426–441. https://doi.org/10.3390/jmse10030426

41. McGenity TJ, Folwell BD, McKew BA, Sanni GO (2012) Marine crude-oil biodegradation: a central role for interspecies interactions. Aquat Biosyst 8:10. https://doi.org/10.1186/2046-9063-8-10

42. Hazen TC, Prince RC (2016) Marine Oil Biodegradation. https://doi.org/10.1021/acs.est.5b03333

43. Yakimov MM, Timmis KN, Golyshin PN (2007) Obligate oil-degrading marine bacteria. https://doi.org/10.1016/j.copbio.2007.04.006

44. Ganesh Kumar A, Manisha D, Sujitha K, et al (2021) Genome sequence analysis of deep sea Aspergillus sydowii BOBA1 and effect of high pressure on biodegradation of spent engine oil. Sci Rep 11:9347. https://doi.org/10.1038/s41598-021-88525-9

45. Birolli WG, de A. Santos D, Alvarenga N, et al (2018) Biodegradation of anthracene and several PAHs by the marine-derived fungus Cladosporium sp. CBMAI 1237. Mar Pollut Bull 129:525–533. https://doi.org/https://doi.org/10.1016/j.marpolbul.2017.10.023

46. Wang W, Shao Z (2013) Enzymes and genes involved in aerobic alkane degradation. Front Microbiol 4:116. https://doi.org/10.3389/fmicb.2013.00116

47. Ladino-Orjuela G, Gomes E, da Silva R, et al (2016) Metabolic Pathways for Degradation of Aromatic Hydrocarbons by Bacteria. In: de Voogt WP (ed) Reviews of Environmental Contamination and Toxicology Volume 237. Springer International Publishing, Cham, pp 105–121

48. Wanpeng Wang and Zongze Shao (2013) Enzymes and genes involved in aerobic alkane degradation. 4:1–7. https://doi.org/10.3389/fmicb.2013.00116

49. Wang W, Shao Z (2014) The long-chain alkane metabolism network of Alcanivorax dieselolei. Nat Commun 5:5755. https://doi.org/10.1038/ncomms6755

50. Sharma I (2020) Bioremediation Techniques for Polluted Environment: Concept, Advantages, Limitations, and Prospects. In: Murillo-Tovar MA, Saldarriaga-Noreña H, Saeid A (eds). IntechOpen, Rijeka, p Ch. 12

51. Nikolopoulou M, Kalogerakis N (2010) Biostimulation Strategies for Enhanced Bioremediation of Marine Oil Spills Including Chronic Pollution BT - Handbook of Hydrocarbon and Lipid Microbiology. In: Timmis KN (ed). Springer Berlin Heidelberg, Berlin, Heidelberg, pp 2521–2529

52. Mapelli F, Scoma A, Michoud G, et al (2017) Biotechnologies for Marine Oil Spill Cleanup : Indissoluble Ties with Microorganisms. Trends Biotechnol 35:860–870. https://doi.org/10.1016/j.tibtech.2017.04.003

53. Ueno A, Ito Y, Yumoto I, Okuyama H (2007) Isolation and characterization of bacteria from soil contaminated with diesel oil and the possible use of these in autochthonous bioaugmentation. World J Microbiol Biotechnol 23:. https://doi.org/10.1007/s11274-007-9423-6

54. Nikolopoulou M, Eickenbusch P, Pasadakis N, et al (2013) Microcosm evaluation of autochthonous bioaugmentation to combat marine oil spills. N Biotechnol 30:734–742. https://doi.org/https://doi.org/10.1016/j.nbt.2013.06.005

55. Pereira E, Napp AP, Allebrandt S, et al (2019) Biodegradation of aliphatic and polycyclic aromatic hydrocarbons in seawater by autochthonous microorganisms. Int Biodeterior Biodegradation 145:104789. https://doi.org/https://doi.org/10.1016/j.ibiod.2019.104789

56. Dehvari M, Ghafari S, Haghighifard NJ, Jorfi S (2021) Petroleum Contaminated Seawater Detoxification in Microcosm by Halotolerant Consortium Isolated from Persian Gulf. Curr Microbiol 78:95–106. https://doi.org/10.1007/s00284-020-02267-x

57. Radwan SS, Al-Mailem DM, Kansour MK (2019) Bioaugmentation failed to enhance oil bioremediation in three soil samples from three different continents. Sci Rep 9:19508. https://doi.org/10.1038/s41598-019-56099-2

58. Zimmermann LA, Feldman MG, Benoit DS, et al (2021) FROM DISASTER TO UNDERSTANDING. Oceanography 34:16–29

59. Reddy CM, Arey JS, Seewald JS, et al (2012) Composition and fate of gas and oil released to the water column during the Deepwater Horizon oil spill. 109:20229–20234. https://doi.org/10.1073/pnas.1101242108

60. Joye SB (2015) Deepwater Horizon, 5 years on. Science (80-) 349:592–593. https://doi.org/10.1126/science.aab4133

61. Kujawinski EB, Reddy CM, Rodgers RP, et al (2020) The first decade of scientific insights from the Deepwater Horizon oil release. Nat Rev Earth Environ 1:237–250. https://doi.org/10.1038/s43017-020-0046-x

62. Kujawinski EB, Kido Soule MC, Valentine DL, et al (2011) Fate of Dispersants Associated with the Deepwater Horizon Oil Spill. Environ Sci Technol 45:1298–1306. https://doi.org/10.1021/es103838p

63. Hazen TC (2020) Lessons from the 2010 Deepwater Horizon Accident in the Gulf of Mexico. In: Wilkes H (ed) Hydrocarbons, Oils and Lipids: Diversity, Origin, Chemistry and Fate. Springer International Publishing, Cham, pp 847–864

64. Bacosa HP, Erdner DL, Liu Z (2015) Differentiating the roles of photooxidation and biodegradation in the weathering of Light Louisiana Sweet crude oil in surface water from the Deepwater Horizon site. Mar Pollut Bull 95:265–272. https://doi.org/https://doi.org/10.1016/j.marpolbul.2015.04.005

65. Passow U, Overton EB (2021) The Complexity of Spills: The Fate of the Deepwater Horizon Oil. Ann Rev Mar Sci 13:109–136. https://doi.org/https://doi.org/10.1146/annurev-marine-032320-095153

66. Ryerson TB, Camilli R, Kessler JD, et al (2012) Chemical data quantify Deepwater Horizon hydrocarbon flow rate and environmental distribution. Proc Natl Acad Sci 109:20246–20253. https://doi.org/10.1073/pnas.1110564109

67. McNutt MK, Camilli R, Crone TJ, et al (2012) Review of flow rate estimates of the Deepwater Horizon oil spill. Proc Natl Acad Sci 109:20260–20267. https://doi.org/10.1073/pnas.1112139108

68. Valentine DL, Mezić I, Maćešić S, et al (2012) Dynamic autoinoculation and the microbial ecology of a deep water hydrocarbon irruption. Proc Natl Acad Sci 109:20286–20291. https://doi.org/10.1073/pnas.1108820109

69. French-McCay DP, Jayko K, Li Z, et al (2021) Oil fate and mass balance for the

Deepwater Horizon oil spill. Mar Pollut Bull 171:112681. https://doi.org/10.1016/j.marpolbul.2021.112681

70. Spier C, Stringfellow WT, Hazen TC, Conrad M (2013) Distribution of hydrocarbons released during the 2010 MC252 oil spill in deep offshore waters. Environ Pollut 173:224–230. https://doi.org/https://doi.org/10.1016/j.envpol.2012.10.019

71. Joye SB, MacDonald IR, Leifer I, Asper V (2011) Magnitude and oxidation potential of hydrocarbon gases released from the BP oil well blowout. Nat Geosci 4:160–164. https://doi.org/10.1038/ngeo1067

72. Du M, Kessler JD (2012) Assessment of the Spatial and Temporal Variability of Bulk Hydrocarbon Respiration Following the Deepwater Horizon Oil Spill. Environ Sci Technol 46:10499–10507. https://doi.org/10.1021/es301363k

73. Kessler JD, Valentine DL, Redmond MC, et al (2011) A persistent oxygen anomaly reveals the fate of spilled methane in the deep Gulf of Mexico. Science 331:312–315. https://doi.org/10.1126/science.1199697

74. Lubchenco J, McNutt M, Lehr B (2011) BP deepwater Horizon oil budget: What happened to the oil? 225–230

75. Passow U, Ziervogel K, Asper V, Diercks A (2012) Marine snow formation in the aftermath of the Deepwater Horizon oil spill in the Gulf of Mexico. Environ Res Lett 7:035301. https://doi.org/10.1088/1748-9326/7/3/035301

76. Daly KL, Passow U, Chanton J, Hollander D (2016) Assessing the impacts of oil-associated marine snow formation and sedimentation during and after the Deepwater Horizon oil spill. Anthropocene 13:18–33. https://doi.org/10.1016/j.ancene.2016.01.006

77. Edwards BR, Reddy CM, Camilli R, et al (2011) Rapid microbial respiration of oil from the Deepwater Horizon spill in offshore surface waters of the Gulf of Mexico. Environ Res Lett 6:035301. https://doi.org/10.1088/1748-9326/6/3/035301

78. Ziervogel K, Mckay L, Rhodes B, et al (2012) Microbial Activities and Dissolved Organic Matter Dynamics in Oil-Contaminated Surface Seawater from the Deepwater Horizon Oil Spill Site. 7:. https://doi.org/10.1371/journal.pone.0034816

79. Chakraborty R, Borglin SE, Dubinsky EA, et al (2012) Microbial Response to the MC-252 Oil and Corexit 9500 in the Gulf of Mexico. Front Microbiol 3:357. https://doi.org/10.3389/fmicb.2012.00357

80. Redmond MC, Valentine DL (2012) Natural gas and temperature structured a microbial community response to the Deepwater Horizon oil spill. Proc Natl Acad Sci 109:20292–20297. https://doi.org/10.1073/pnas.1108756108

81. Hazen TC, Dubinsky EA, DeSantis TZ, et al (2010) Deep-Sea Oil Plume Enriches Indigenous Oil-Degrading Bacteria. Science (80-) 330:204–208. https://doi.org/10.1126/science.1195979

82. Mason OU, Hazen TC, Borglin S, et al (2012) Metagenome, metatranscriptome and single-cell sequencing reveal microbial response to Deepwater Horizon oil spill. ISME J 6:1715–1727. https://doi.org/10.1038/ismej.2012.59

83. Dubinsky EA, Conrad ME, Chakraborty R, et al (2013) Succession of Hydrocarbon-Degrading Bacteria in the Aftermath of the Deepwater Horizon Oil Spill in the Gulf of Mexico. Environ Sci Technol 47:10860–10867. https://doi.org/10.1021/es401676y

84. Yang T, Nigro LM, Gutierrez T, et al (2016) Pulsed blooms and persistent oil-degrading bacterial populations in the water column during and after the Deepwater Horizon blowout. Deep Sea Res Part II Top Stud Oceanogr 129:282–291. https://doi.org/10.1016/j.dsr2.2014.01.014

85. Hu P, Dubinsky EA, Probst AJ, et al (2017) Simulation of Deepwater Horizon oil plume reveals substrate specialization within a complex community of hydrocarbon degraders. Proc Natl Acad Sci 114:7432–7437. https://doi.org/10.1073/pnas.1703424114

86. Kleindienst S, Seidel M, Ziervogel K, et al (2015) Chemical dispersants can suppress the activity of natural oil-degrading microorganisms. Proc Natl Acad Sci 112:14900–14905. https://doi.org/10.1073/pnas.1507380112

87. Ziervogel K, Joye SB, Arnosti C (2016) Microbial enzymatic activity and secondary production in sediments affected by the sedimentation pulse following the Deepwater Horizon oil spill. Deep Sea Res Part II Top Stud Oceanogr 129:241–248. https://doi.org/https://doi.org/10.1016/j.dsr2.2014.04.003

88. Steen A, Findlay A (2008) FREQUENCY OF DISPERSANT USE WORLDWIDE. Int Oil Spill Conf Proc 2008:645–649. https://doi.org/10.7901/2169-3358-2008-1-645

89. Gros J, Socolofsky SA, Dissanayake AL, et al (2017) Petroleum dynamics in the sea and influence of subsea dispersant injection during Deepwater Horizon. Proc Natl Acad Sci U S A 114:10065–10070. https://doi.org/10.1073/pnas.1612518114

90. Murawski SA, Schlüter M, Paris CB, Aman ZM (2019) Resolving the dilemma of dispersant use for deep oil spill response. Environ Res Lett 14:91002. https://doi.org/10.1088/1748-9326/ab3aa0

91. Camilli R, Reddy CM, Yoerger DR, et al (2010) Tracking Hydrocarbon Plume Transport and Biodegradation at Deepwater Horizon. Science (80-) 330:201–204. https://doi.org/10.1126/science.1195223

92. Place BJ, Perkins MJ, Sinclair E, et al (2016) Trace analysis of surfactants in Corexit oil dispersant formulations and seawater. Deep Res Part II 129:273–281. https://doi.org/10.1016/j.dsr2.2014.01.015

93. Bælum J, Borglin S, Chakraborty R, et al (2012) Deep-sea bacteria enriched by oil and dispersant from the Deepwater Horizon spill. Environ Microbiol 14:2405–2416. https://doi.org/10.1111/j.1462-2920.2012.02780.x

94. Campo P, Venosa AD, Suidan MT (2013) Biodegradability of Corexit 9500 and Dispersed South Louisiana Crude Oil at 5 and 25 °C. Environ Sci Technol 47:1960–1967. https://doi.org/10.1021/es303881h

95. Prince RC, McFarlin KM, Butler JD, et al (2013) The primary biodegradation of dispersed crude oil in the sea. Chemosphere 90:521–526. https://doi.org/10.1016/j.chemosphere.2012.08.020

96. National Academies of Sciences Engineering and Medicine (2020) The Use of Dispersants in Marine Oil Spill Response. The National Academies Press, Washington, DC

97. Techtmann SM, Zhuang M, Campo P, et al (2017) Corexit 9500 Enhances Oil Biodegradation and Changes Active Bacterial Community Structure of Oil-Enriched

Microcosms. Appl Environ Microbiol 83:e03462-16. https://doi.org/10.1128/AEM.03462-16

98. Brakstad OG, Nordtug T, Throne-Holst M (2015) Biodegradation of dispersed Macondo oil in seawater at low temperature and different oil droplet sizes. Mar Pollut Bull 93:144–152. https://doi.org/10.1016/j.marpolbul.2015.02.006

99. Kostka JE, Prakash O, Overholt W a, et al (2011) Hydrocarbon-Degrading Bacteria and the Bacterial Community Response in Gulf of Mexico Beach Sands Impacted by the Deepwater Horizon Oil Spill. Appl Environ Microbiol 77:7962–7974. https://doi.org/10.1128/AEM.05402-11

100. Garel M, Bonin P, Martini S, et al (2019) Pressure-Retaining Sampler and High-Pressure Systems to Study Deep-Sea Microbes Under in situ Conditions. Front Microbiol 10:453. https://doi.org/10.3389/fmicb.2019.00453

101. Cario A, Oliver GC, Rogers KL (2019) Exploring the Deep Marine Biosphere: Challenges, Innovations, and Opportunities. Front Earth Sci 7:225. https://doi.org/10.3389/feart.2019.00225

102. Oger PM, Jebbar M (2010) The many ways of coping with pressure. Res Microbiol 161:799–809. https://doi.org/https://doi.org/10.1016/j.resmic.2010.09.017

103. Tamburini C, Boutrif M, Garel M, et al (2013) Prokaryotic responses to hydrostatic pressure in the ocean – a review. Environ Microbiol 15:1262–1274. https://doi.org/10.1111/1462-2920.12084

104. Amano C, Zhao Z, Sintes E, et al (2022) Limited carbon cycling due to high-pressure effects on the deep-sea microbiome. Nat Geosci 15:1041–1047. https://doi.org/10.1038/s41561-022-01081-3

105. Fang J, Zhang L, Bazylinski DA (2010) Deep-sea piezosphere and piezophiles : geomicrobiology and biogeochemistry. Trends Microbiol 18:413–422. https://doi.org/10.1016/j.tim.2010.06.006

106. Yayanos A, Dietz AS (1981) Obligately barophilic bacterium from the Mariana Trench Microbiology : 78:5212–5215

107. Marietou A, Chastain R, Beulig F, et al (2018) The Effect of Hydrostatic Pressure on Enrichments of Hydrocarbon Degrading Microbes From the Gulf of Mexico Following the Deepwater Horizon Oil Spill. Front Microbiol 9:808. https://doi.org/10.3389/fmicb.2018.00808

108. Fasca H, de Castilho LVA, de Castilho JFM, et al (2018) Response of marine bacteria to oil contamination and to high pressure and low temperature deep sea conditions. Microbiologyopen 7:e00550; 10.1002/mbo3.550. https://doi.org/10.1002/mbo3.550

109. Perez Calderon LJ, Gontikaki E, Potts LD, et al (2019) Pressure and temperature effects on deep-sea hydrocarbon-degrading microbial communities in subarctic sediments. Microbiologyopen 8:e00768; 10.1002/mbo3.768. https://doi.org/10.1002/mbo3.768

110. Nguyen UT, Lincoln SA, Valladares Juárez AG, et al (2018) The influence of pressure on crude oil biodegradation in shallow and deep Gulf of Mexico sediments. PLoS One 13:e0199784; 10.1371/journal.pone.0199784. https://doi.org/10.1371/journal.pone.0199784

111. Schedler, M., Hiessl, R., Valladares Juárez AG (2014) Effect of high pressure on hydrocarbon-degrading bacteria. AMB Express

112. Scoma A, Barbato M, Borin S, et al (2016) An impaired metabolic response to hydrostatic pressure explains Alcanivorax borkumensis recorded distribution in the deep marine water column. Sci Rep 6:31316. https://doi.org/10.1038/srep31316

113. Scoma A, Barbato M, Hernandez-Sanabria E, et al (2016) Microbial oil-degradation under mild hydrostatic pressure (10 MPa): which pathways are impacted in piezosensitive hydrocarbonoclastic bacteria? Sci Rep 6:23526. https://doi.org/10.1038/srep23526

114. Scoma A, Boon N (2016) Osmotic Stress Confers Enhanced Cell Integrity to Hydrostatic Pressure but Impairs Growth in Alcanivorax borkumensis SK2. Front Microbiol 7:. https://doi.org/10.3389/fmicb.2016.00729

115. Grossi V, Yakimov MM, Ali B Al, et al (2010) Hydrostatic pressure affects membrane and storage lipid compositions of the piezotolerant hydrocarbon-degrading Marinobacter hydrocarbonoclasticus strain #5. Environ Microbiol 12:2020–2033. https://doi.org/10.1111/j.1462-2920.2010.02213.x

116. Hackbusch S, Noirungsee N, Viamonte J, et al (2020) Influence of pressure and dispersant on oil biodegradation by a newly isolated Rhodococcus strain from deep-sea sediments of the gulf of Mexico. Mar Pollut Bull 150:110683. https://doi.org/10.1016/j.marpolbul.2019.110683

117. Antoniou E, Kalogerakis N (2023) Laboratory testing of dispersant effectiveness at high pressures. Can J Chem Eng 101:772–781. https://doi.org/https://doi.org/10.1002/cjce.24707

118. Noirungsee N, Hackbusch S, Viamonte J, et al (2020) Influence of oil, dispersant, and pressure on microbial communities from the Gulf of Mexico. Sci Rep 10:7079. https://doi.org/10.1038/s41598-020-63190-6

119. Cario A, Oliver GC, Rogers KL (2022) Characterizing the Piezosphere: The Effects of Decompression on Microbial Growth Dynamics. Front Microbiol 13:867340. https://doi.org/10.3389/fmicb.2022.867340

120. UNEP/MAP (2023) Mediterranean Quality Status

121. Skliris N (2014) Past, Present and Future Patterns of the Thermohaline Circulation and Characteristic Water Masses of the Mediterranean Sea. In: Goffredo S, Dubinsky Z (eds) The Mediterranean Sea: Its history and present challenges. Springer Netherlands, Dordrecht, pp 29–48

122. Ozer T, Gertman I, Kress N, et al (2017) Interannual thermohaline (1979–2014) and nutrient (2002–2014) dynamics in the Levantine surface and intermediate water masses, SE Mediterranean Sea. Glob Planet Change 151:60–67. https://doi.org/10.1016/j.gloplacha.2016.04.001

123. Skliris N, Zika JD, Herold L, et al (2018) Mediterranean sea water budget long-term trend inferred from salinity observations. Clim Dyn 51:2857–2876. https://doi.org/10.1007/s00382-017-4053-7

124. Theocharis A, Klein B, Nittis K, Roether W (2002) Evolution and status of the Eastern Mediterranean Transient (1997–1999). J Mar Syst 33–34:91–116. https://doi.org/https://doi.org/10.1016/S0924-7963(02)00054-4

125. Velaoras D, Papadopoulos VP, Kontoyiannis H, et al (2019) Water masses and hydrography during April and June 2016 in the Cretan Sea and Cretan Passage (Eastern Mediterranean Sea). Deep Sea Res Part II Top Stud Oceanogr 164:25–40. https://doi.org/10.1016/j.dsr2.2018.09.005

126. Krom MD, Emeis K-C, Van Cappellen P (2010) Why is the Eastern Mediterranean phosphorus limited? Prog Oceanogr 85:236–244. https://doi.org/10.1016/j.pocean.2010.03.003

127. Powley HR, Cappellen P Van, Krom MD (2017) Nutrient Cycling in the Mediterranean Sea: The Key to Understanding How the Unique Marine Ecosystem Functions and Responds to Anthropogenic Pressures. In: Fuerst-Bjelis B (ed) Mediterranean Identities - Environment, Society, Culture. InTech, Rijeka

128. Ben Ezra T, Krom MD, Tsemel A, et al (2021) Seasonal nutrient dynamics in the P depleted Eastern Mediterranean Sea. Deep Sea Res Part I Oceanogr Res Pap 176:103607. https://doi.org/10.1016/j.dsr.2021.103607

129. Krom M, Kress N, Berman-Frank I, Rahav E (2014) Past, Present and Future Patterns in the Nutrient Chemistry of the Eastern Mediterranean. In: Goffredo S, Dubinsky Z (eds) The Mediterranean Sea. Springer Netherlands, Dordrecht, pp 49–68

130. Yokokawa T, De Corte D, Sintes E, Herndl G (2010) Spatial patterns of bacterial abundance, activity and community composition in relation to water masses in the eastern Mediterranean Sea. Aquat Microb Ecol 59:185–195. https://doi.org/10.3354/ame01393

131. Hazan O, Silverman J, Sisma-Ventura G, et al (2018) Mesopelagic Prokaryotes Alter Surface Phytoplankton Production during Simulated Deep Mixing Experiments in Eastern Mediterranean Sea Waters. Front Mar Sci 5:1–11. https://doi.org/10.3389/fmars.2018.00001

132. Reich T, Ben-Ezra T, Belkin N, et al (2022) A year in the life of the Eastern Mediterranean: Monthly dynamics of phytoplankton and bacterioplankton in an ultra-oligotrophic sea. Deep Sea Res Part I Oceanogr Res Pap 182:103720. https://doi.org/10.1016/j.dsr.2022.103720

133. Rahav E, Berman-Frank I (2023) Temporal and vertical dynamics of diatoms and

dinoflagellates in the southeastern Mediterranean Sea. J Plankton Res 45:614–624. https://doi.org/10.1093/plankt/fbad025

134. Haber M, Roth Rosenberg D, Lalzar M, et al (2022) Spatiotemporal Variation of Microbial Communities in the Ultra-Oligotrophic Eastern Mediterranean Sea. Front Microbiol 13:. https://doi.org/10.3389/fmicb.2022.867694

135. Techtmann SM, Fortney JL, Ayers KA, et al (2015) The Unique Chemistry of Eastern Mediterranean Water Masses Selects for Distinct Microbial Communities by Depth. PLoS One 10:e0120605. https://doi.org/10.1371/journal.pone.0120605

136. Santi I, Kasapidis P, Psarra S, et al (2020) Composition and distribution patterns of eukaryotic microbial plankton in the ultra-oligotrophic Eastern Mediterranean Sea. Aquat Microb Ecol 84:155–173. https://doi.org/10.3354/ame01933

137. Siokou-Frangou I, Christaki U, Mazzocchi MG, et al (2010) Plankton in the open Mediterranean Sea: a review. Biogeosciences 7:1543–1586. https://doi.org/10.5194/bg-7-1543-2010

138. Sarmento H, Montoya JM, Vázquez-Domínguez E, et al (2010) Warming effects on marine microbial food web processes: how far can we go when it comes to predictions? Philos Trans R Soc London Ser B, Biol Sci 365:2137–2149. https://doi.org/10.1098/rstb.2010.0045

139. Lelieveld J, Hadjinicolaou P, Kostopoulou E, et al (2012) Climate change and impacts in the Eastern Mediterranean and the Middle East. Clim Change 114:667–687. https://doi.org/10.1007/s10584-012-0418-4

140. Rahav E, Silverman J, Raveh O, et al (2019) The deep water of Eastern Mediterranean Sea is a hotspot for bacterial activity. Deep Sea Res Part II Top Stud Oceanogr 164:135–143. https://doi.org/10.1016/j.dsr2.2019.03.004

141. Liu J, Techtmann SM, Woo HL, et al (2017) Rapid Response of Eastern Mediterranean Deep Sea Microbial Communities to Oil. Sci Rep 7:5762. https://doi.org/10.1038/s41598-017-05958-x

142. Steele JA, Countway PD, Xia L, et al (2011) Marine bacterial, archaeal and protistan

association networks reveal ecological linkages. ISME J 5:1414–1425. https://doi.org/10.1038/ismej.2011.24

143. Kirchman DL (2018) Community structure of microbes in natural environments. In: Processes in Microbial Ecology. Oxford University PressOxford, pp 53–72

144. Gostel MR, Kress WJ (2022) The Expanding Role of DNA Barcodes: Indispensable Tools for Ecology, Evolution, and Conservation. Diversity 14:213. https://doi.org/10.3390/d14030213

145. Caron DA, Alexander H, Allen AE, et al (2017) Probing the evolution, ecology and physiology of marine protists using transcriptomics. Nat Rev Microbiol 15:6–20. https://doi.org/10.1038/nrmicro.2016.160

146. Nagata T, Tamburini C, Arístegui J, et al (2010) Emerging concepts on microbial processes in the bathypelagic ocean – ecology, biogeochemistry, and genomics. Deep Sea Res Part II Top Stud Oceanogr 57:1519–1536. https://doi.org/10.1016/j.dsr2.2010.02.019

147. Stoecker DK, Hansen PJ, Caron DA, Mitra A (2017) Mixotrophy in the Marine Plankton. Ann Rev Mar Sci 9:311–335. https://doi.org/10.1146/annurev-marine-010816-060617

148. Pitta P, Giannakourou A, Christaki U (2001) Planktonic ciliates in the oligotrophic Mediterranean Sea: longitudinal trends of standing stocks, distributions and analysis of food vacuole contents. Aquat Microb Ecol 24:297–311. https://doi.org/10.3354/ame024297

149. Christaki U (2001) Nanoflagellate predation on auto- and heterotrophic picoplankton in the oligotrophic Mediterranean Sea. J Plankton Res 23:1297–1310. https://doi.org/10.1093/plankt/23.11.1297

150. Belkin N, Guy-Haim T, Rubin-Blum M, et al (2022) Influence of cyclonic and anticyclonic eddies on plankton in the southeastern Mediterranean Sea during late summertime. Ocean Sci 18:693–715. https://doi.org/10.5194/os-18-693-2022

151. Van Wambeke F, Christaki U, Bianchi M, et al (2000) Heterotrophic bacterial production in the Cretan Sea (NE Mediterranean). Prog Oceanogr 46:205–216. https://doi.org/10.1016/S0079-6611(00)00019-7

152. Meziti A, Kormas K (2022) Microbial Life in the Aegean Sea. Springer Berlin Heidelberg, Berlin, Heidelberg, pp 1–11

153. Reygondeau G, Irisson J, Ayata S-D, et al (2015) Definition of the Mediterranean Eco-regions and Maps of Potential Pressures in These Eco-regions. In: Perseus Deliverable

154. Charalampous G, Fragkou E, Kormas KA, et al (2021) Comparison of Hydrocarbon-Degrading Consortia from Surface and Deep Waters of the Eastern Mediterranean Sea: Characterization and Degradation Potential. Energies 14:2246. https://doi.org/10.3390/en14082246

155. Klindworth A, Pruesse E, Schweer T, et al (2013) Evaluation of general 16S ribosomal RNA gene PCR primers for classical and next-generation sequencing-based diversity studies. Nucleic Acids Res 41:e1–e1. https://doi.org/10.1093/nar/gks808

156. Comeau AM, Li WKW, Tremblay J-É, et al (2011) Arctic Ocean Microbial Community Structure before and after the 2007 Record Sea Ice Minimum. PLoS One 6:e27492. https://doi.org/10.1371/journal.pone.0027492

157. Callahan BJ, McMurdie PJ, Rosen MJ, et al (2016) DADA2: High-resolution sample inference from Illumina amplicon data. Nat Methods 13:581–583. https://doi.org/10.1038/nmeth.3869

158. R Development Core Team (2023) R: a language and environment for statistical computing

159. Quast C, Pruesse E, Yilmaz P, et al (2012) The SILVA ribosomal RNA gene database project: improved data processing and web-based tools. Nucleic Acids Res 41:D590–D596. https://doi.org/10.1093/nar/gks1219

160. Guillou L, Bachar D, Audic S, et al (2012) The Protist Ribosomal Reference database (PR2): a catalog of unicellular eukaryote Small Sub-Unit rRNA sequences with curated taxonomy. Nucleic Acids Res 41:D597–D604. https://doi.org/10.1093/nar/gks1160

161. Paulson JN, Stine OC, Bravo HC, Pop M (2013) Differential abundance analysis for microbial marker-gene surveys. Nat Methods 10:1200–1202. https://doi.org/10.1038/nmeth.2658

162. Oksanen J, Blanchet FG, Friendly M, et al (2022) vegan: Community Ecology Package

163. Lozada M, Marcos MS, Commendatore MG, et al (2014) The bacterial community structure of hydrocarbon-polluted marine environments as the basis for the definition of an ecological index of hydrocarbon exposure. Microbes Environ 29:269–276. https://doi.org/10.1264/jsme2.me14028

164. Wickham H (2016) ggplot2: Elegant Graphics for Data Analysis. Springer-Verlag New York

165. Harrell Jr. F, Dupont C (2020) Hmisc: Harrell Miscellaneous. R Package Version 5.1-1

166. Mitra A, Flynn KJ, Burkholder JM, et al (2014) The role of mixotrophic protists in the biological carbon pump. Biogeosciences 11:995–1005. https://doi.org/10.5194/bg-11-995-2014

167. Kirchman DL (2018) Microbial primary production and phototrophy. In: Processes in Microbial Ecology. Oxford University PressOxford, pp 92–112

168. Fuhrman JA, Cram JA, Needham DM (2015) Marine microbial community dynamics and their ecological interpretation. Nat Rev Microbiol 13:133–146. https://doi.org/10.1038/nrmicro3417

169. Callieri C, Coci M, Corno G, et al (2013) Phylogenetic diversity of nonmarine picocyanobacteria. FEMS Microbiol Ecol 85:293–301. https://doi.org/10.1111/1574-6941.12118

170. Jeong HJ, Park JY, Nho JH, et al (2005) Feeding by red-tide dinoflagellates on the cyanobacterium Synechococcus . Aquat Microb Ecol 41:131–143

171. Meziti A, Smeti E, Daniilides D, et al (2023) Increased contribution of parasites in microbial eukaryotic communities of different Aegean Sea coastal systems. PeerJ 11:e16655. https://doi.org/10.7717/peerj.16655

172. Unrein F, Gasol JM, Not F, et al (2014) Mixotrophic haptophytes are key bacterial grazers in oligotrophic coastal waters. ISME J 8:164–176. https://doi.org/10.1038/ismej.2013.132

173. Koppelle S, López-Escardó D, Brussaard CPD, et al (2022) Mixotrophy in the bloom-

forming genus Phaeocystis and other haptophytes. Harmful Algae 117:102292. https://doi.org/10.1016/j.hal.2022.102292

174. Giovannoni SJ (2017) SAR11 Bacteria: The Most Abundant Plankton in the Oceans. Ann Rev Mar Sci 9:231–255. https://doi.org/10.1146/annurev-marine-010814-015934

175. Bolaños LM, Tait K, Somerfield PJ, et al (2022) Influence of short and long term processes on SAR11 communities in open ocean and coastal systems. ISME Commun 2:116. https://doi.org/10.1038/s43705-022-00198-1

176. Šantić D, Stojan I, Matić F, et al (2023) Picoplankton diversity in an oligotrophic and high salinity environment in the central Adriatic Sea. Sci Rep 13:7617. https://doi.org/10.1038/s41598-023-34704-9

177. Sen K, Sen B, Wang G (2022) Diversity, Abundance, and Ecological Roles of Planktonic Fungi in Marine Environments. J Fungi 8:491. https://doi.org/10.3390/jof8050491

178. Gladfelter AS, James TY, Amend AS (2019) Marine fungi. Curr Biol 29:R191–R195. https://doi.org/10.1016/j.cub.2019.02.009

179. Liu R, Wei X, Song W, et al (2022) Novel Chloroflexi genomes from the deepest ocean reveal metabolic strategies for the adaptation to deep-sea habitats. Microbiome 10:75. https://doi.org/10.1186/s40168-022-01263-6

180. Biard T (2022) Diversity and ecology of Radiolaria in modern oceans. Environ Microbiol 24:2179–2200. https://doi.org/https://doi.org/10.1111/1462-2920.16004

181. Mitra A, Flynn KJ, Tillmann U, et al (2016) Defining Planktonic Protist Functional Groups on Mechanisms for Energy and Nutrient Acquisition: Incorporation of Diverse Mixotrophic Strategies. Protist 167:106–120. https://doi.org/10.1016/j.protis.2016.01.003

182. Rizos I, Debeljak P, Finet T, et al (2023) Beyond the limits of the unassigned protist microbiome: inferring large-scale spatio-temporal patterns of Syndiniales marine parasites. ISME Commun 3:16. https://doi.org/10.1038/s43705-022-00203-7

183. Wang Y-T, Xue Y-R, Liu C-H (2015) A Brief Review of Bioactive Metabolites Derived from Deep-Sea Fungi. Mar Drugs 13:4594–4616. https://doi.org/10.3390/md13084594

184. King GM, Smith C, Tolar B, Hollibaugh JT (2013) Analysis of Composition and Structure of Coastal to Mesopelagic Bacterioplankton Communities in the Northern Gulf of Mexico. Front Microbiol 3:. https://doi.org/10.3389/fmicb.2012.00438

185. Mascle J, Mary F, Praeg D, et al (2014) Distribution and geological control of mud volcanoes and other fluid/free gas seepage features in the Mediterranean Sea and nearby Gulf of Cadiz. Geo-Marine Lett 34:89–110. https://doi.org/10.1007/s00367-014-0356-4

186. MacDonald IR, Garcia-Pineda O, Beet A, et al (2015) Natural and unnatural oil slicks in the Gulf of Mexico. J Geophys Res Ocean 120:8364–8380. https://doi.org/https://doi.org/10.1002/2015JC011062

187. Roller BRK, Stoddard SF, Schmidt TM (2016) Exploiting rRNA operon copy number to investigate bacterial reproductive strategies. Nat Microbiol 1:16160. https://doi.org/10.1038/nmicrobiol.2016.160

188. Stoddard SF, Smith BJ, Hein R, et al (2015) rrnDB: improved tools for interpreting rRNA gene abundance in bacteria and archaea and a new foundation for future development. Nucleic Acids Res 43:D593-8. https://doi.org/10.1093/nar/gku1201

189. Hazen TC, Techtmann SM (2018) Oil Biodegradation in Deep Marine Basins. In: Steffan R (ed) Consequences of Microbial Interactions with Hydrocarbons, Oils, and Lipids: Biodegradation and Bioremediation. Springer International Publishing, Cham, pp 1–18

190. Alves TM, Kokinou E, Zodiatis G, et al (2016) Multidisciplinary oil spill modeling to protect coastal communities and the environment of the Eastern Mediterranean Sea. Sci Rep 6:36882. https://doi.org/10.1038/srep36882

191. Kleindienst S, Grim S, Sogin M, et al (2016) Diverse, rare microbial taxa responded to the Deepwater Horizon deep-sea hydrocarbon plume. ISME J 10:400–415. https://doi.org/10.1038/ismej.2015.121

192. Yergeau E, Maynard C, Sanschagrin S, et al (2015) Microbial Community Composition, Functions, and Activities in the Gulf of Mexico 1 Year after the Deepwater Horizon Accident. Appl Environ Microbiol 81:5855–5866. https://doi.org/10.1128/AEM.01470-15

193. King GM, Kostka JE, Hazen TC, Sobecky PA (2015) Microbial Responses to the

Deepwater Horizon Oil Spill: From Coastal Wetlands to the Deep Sea. Ann Rev Mar Sci 7:377–401. https://doi.org/10.1146/annurev-marine-010814-015543

194. Natarajan VP, Zhang X, Morono Y, et al (2016) A Modified SDS-Based DNA Extraction Method for High Quality Environmental DNA from Seafloor Environments. Front Microbiol 07: https://doi.org/10.3389/fmicb.2016.00986

195. Sundberg C, Al-Soud WA, Larsson M, et al (2013) 454 pyrosequencing analyses of bacterial and archaeal richness in 21 full-scale biogas digesters. FEMS Microbiol Ecol 85:612–626. https://doi.org/10.1111/1574-6941.12148

196. Schliep KP (2011) phangorn: phylogenetic analysis in R. Bioinformatics 27:592–593. https://doi.org/10.1093/bioinformatics/btq706

197. Wright, Erik S (2016) Using DECIPHER v2.0 to Analyze Big Biological Sequence Data in R. R J 8:352. https://doi.org/10.32614/RJ-2016-025

198. McMurdie PJ, Holmes S (2013) phyloseq: An R Package for Reproducible Interactive Analysis and Graphics of Microbiome Census Data. PLoS One 8:e61217. https://doi.org/10.1371/journal.pone.0061217

199. Zuur AF, Ieno EN, Smith GM (2007) Analysing Ecological Data. Springer New York, New York, NY

200. Love MI, Huber W, Anders S (2014) Moderated estimation of fold change and dispersion for RNA-seq data with DESeq2. Genome Biol 15:550. https://doi.org/10.1186/s13059-014-0550-8

201. McMurdie PJ, Holmes S (2014) Waste Not, Want Not: Why Rarefying Microbiome Data Is Inadmissible. PLoS Comput Biol 10:e1003531. https://doi.org/10.1371/journal.pcbi.1003531

202. Finn DR, Yu J, Ilhan ZE, et al (2020) MicroNiche: an R package for assessing microbial niche breadth and overlap from amplicon sequencing data. FEMS Microbiol Ecol 96:1–12. https://doi.org/10.1093/femsec/fiaa131

203. Warnes GR, Bolker B, Bonebakker L, et al (2022) gplots: Various R Programming Tools for Plotting Data

204. Zahed MA, Aziz HA, Isa MH, Mohajeri L (2010) Effect of Initial Oil Concentration and Dispersant on Crude Oil Biodegradation in Contaminated Seawater. Bull Environ Contam Toxicol 84:438–442. https://doi.org/10.1007/s00128-010-9954-7

205. Liu J, Bacosa HP, Liu Z (2017) Potential Environmental Factors Affecting Oil-Degrading Bacterial Populations in Deep and Surface Waters of the Northern Gulf of Mexico. Front Microbiol 7:2131. https://doi.org/10.3389/fmicb.2016.02131

206. Bacosa HP, Kang A, Lu K, Liu Z (2021) Initial oil concentration affects hydrocarbon biodegradation rates and bacterial community composition in seawater. Mar Pollut Bull 162:111867. https://doi.org/10.1016/j.marpolbul.2020.111867

207. Potts LD, Perez Calderon LJ, Gontikaki E, et al (2018) Effect of spatial origin and hydrocarbon composition on bacterial consortia community structure and hydrocarbon biodegradation rates. FEMS Microbiol Ecol 94:fiy127. https://doi.org/10.1093/femsec/fiy127

208. Bargiela R, Mapelli F, Rojo D, et al (2015) Bacterial population and biodegradation potential in chronically crude oil-contaminated marine sediments are strongly linked to temperature. Sci Rep 5:11651. https://doi.org/10.1038/srep11651

209. Duran R, Cravo-Laureau C (2016) Role of environmental factors and microorganisms in determining the fate of polycyclic aromatic hydrocarbons in the marine environment. FEMS Microbiol Rev 40:814–830. https://doi.org/10.1093/femsre/fuw031

210. Ferguson RMW, Gontikaki E, Anderson JA, Witte U (2017) The Variable Influence of Dispersant on Degradation of Oil Hydrocarbons in Subarctic Deep-Sea Sediments at Low Temperatures (0–5 °C). Sci Rep 7:2253. https://doi.org/10.1038/s41598-017-02475-9

211. Bagi A, Pampanin DM, Brakstad OG, Kommedal R (2013) Estimation of hydrocarbon biodegradation rates in marine environments: A critical review of the Q10 approach. Mar Environ Res 89:83–90. https://doi.org/10.1016/j.marenvres.2013.05.005

212. Miller JI, Techtmann S, Joyner D, et al (2020) Microbial Communities across Global Marine Basins Show Important Compositional Similarities by Depth. MBio 11:10.1128/mbio.01448-20. https://doi.org/10.1128/mBio.01448-20

213. Yuan J (2015) The diversity of PAH-degrading bacteria in a deep-sea water column above the Southwest Indian Ridge. Front Microbiol 6:. https://doi.org/10.3389/fmicb.2015.00853

214. Zhao B, Wang H, Li R, Mao X (2010) Thalassospira xianhensis sp. nov., a polycyclic aromatic hydrocarbon-degrading marine bacterium. Int J Syst Evol Microbiol 60:1125–1129. https://doi.org/10.1099/ijs.0.013201-0

215. Thomas GE, Cameron TC, Campo P, et al (2020) Bacterial Community Legacy Effects Following the Agia Zoni II Oil-Spill, Greece. Front Microbiol 11:. https://doi.org/10.3389/fmicb.2020.01706

216. Yang S, Li M, Lai Q, et al (2018) Alcanivorax mobilis sp. nov., a new hydrocarbon-degrading bacterium isolated from deep-sea sediment. Int J Syst Evol Microbiol 68:1639–1643. https://doi.org/10.1099/ijsem.0.002612

217. Lai Q, Wang J, Gu L, et al (2013) Alcanivorax marinus sp. nov., isolated from deep-sea water. Int J Syst Evol Microbiol 63:4428–4432. https://doi.org/10.1099/ijs.0.049957-0

218. Lai Q, Zhou Z, Li G, et al (2016) Alcanivorax nanhaiticus sp. nov., isolated from deep sea sediment. Int J Syst Evol Microbiol 66:3651–3655. https://doi.org/10.1099/ijsem.0.001247

219. Gontikaki E, Potts LD, Anderson JA, Witte U (2018) Hydrocarbon-degrading bacteria in deep-water subarctic sediments (Faroe-Shetland Channel). J Appl Microbiol 125:1040–1053. https://doi.org/10.1111/jam.14030

220. Imron MF, Titah HS (2018) Optimization of diesel biodegradation by <italic>Vibrio alginolyticus</italic> using Box-Behnken design. Environ Eng Res 23:374–382. https://doi.org/10.4491/eer.2018.015

221. Hedlund BP, Staley JT (2001) Vibrio cyclotrophicus sp. nov., a polycyclic aromatic hydrocarbon (PAH)-degrading marine bacterium. Int J Syst Evol Microbiol 51:61–66. https://doi.org/10.1099/00207713-51-1-61

222. Liu Z, Liu J (2013) Evaluating bacterial community structures in oil collected from the sea surface and sediment in the northern Gulf of Mexico after the Deepwater Horizon oil spill. Microbiologyopen 2:492–504. https://doi.org/10.1002/mbo3.89

223. Tao Z, Bullard S, Arias C (2011) High Numbers of Vibrio vulnificus in Tar Balls Collected from Oiled Areas of the North-Central Gulf of Mexico Following the 2010 BP Deepwater Horizon Oil Spill. Ecohealth 8:507–511. https://doi.org/10.1007/s10393-011-0720-z

224. Suja LD, Summers S, Gutierrez T (2017) Role of EPS, Dispersant and Nutrients on the Microbial Response and MOS Formation in the Subarctic Northeast Atlantic. Front Microbiol 8:676. https://doi.org/10.3389/fmicb.2017.00676

225. Sun X, Kostka JE (2019) Hydrocarbon-Degrading Microbial Communities Are Site Specific, and Their Activity Is Limited by Synergies in Temperature and Nutrient Availability in Surface Ocean Waters. Appl Environ Microbiol 85:. https://doi.org/10.1128/AEM.00443-19

226. Mas-Lladó M, Piña-Villalonga JM, Brunet-Galmés I, et al (2014) Draft Genome Sequences of Two Isolates of the Roseobacter Group, Sulfitobacter sp. Strains 3SOLIMAR09 and 1FIGIMAR09, from Harbors of Mallorca Island (Mediterranean Sea). Genome Announc 2:e00350-14. https://doi.org/10.1128/genomeA.00350-14

227. (2013) Directive 2013/30/EU on safety of offshore oil and gas operations. Off J Eur Union 178:66–106

228. Cordes EE, Jones DOB, Schlacher TA, et al (2016) Environmental Impacts of the Deep-Water Oil and Gas Industry: A Review to Guide Management Strategies. Front Environ Sci 4:58; 10.3389/fenvs.2016.00058. https://doi.org/10.3389/fenvs.2016.00058

229. Scoma A, Yakimov MM, Daffonchio D, Boon N (2017) Self-healing capacity of deep-sea ecosystems affected by petroleum hydrocarbons. EMBO Rep 18:868–872. https://doi.org/10.15252/embr.201744090

230. Bartlett DH (2002) Pressure effects on in vivo microbial processes. Biochim Biophys Acta - Protein Struct Mol Enzymol 1595:367–381. https://doi.org/10.1016/S0167-4838(01)00357-0

231. Wannicke N, Frindte K, Gust G, et al (2015) Measuring bacterial activity and community composition at high hydrostatic pressure using a novel experimental approach: a pilot study. FEMS Microbiol Ecol 91:fiv036. https://doi.org/10.1093/femsec/fiv036

232. Fasca H, de Castilho LVA, de Castilho JFM, et al (2018) Response of marine bacteria to oil contamination and to high pressure and low temperature deep sea conditions. Microbiologyopen 7:e00550. https://doi.org/10.1002/mbo3.550

233. Hassanshahian M, Cappello S (2013) Crude Oil Biodegradation in the Marine Environments. In: Chamy R, Rosenkranz F (eds) Biodegradation - Engineering and Technology. InTech, Rijeka, pp 101–136

234. Prince RC, Nash GW, Hill SJ (2016) The biodegradation of crude oil in the deep ocean. MPB 111:354–357. https://doi.org/10.1016/j.marpolbul.2016.06.087

235. Seidel M, Kleindienst S, Dittmar T, et al (2016) Biodegradation of crude oil and dispersants in deep seawater from the Gulf of Mexico: Insights from ultra-high resolution mass spectrometry. Deep Sea Res Part II Top Stud Oceanogr 129:108–118. https://doi.org/10.1016/j.dsr2.2015.05.012

236. Murawski SA, Schlüter M, Paris CB, Aman ZM (2020) Summary of Contemporary Research on the Use of Chemical Dispersants for Deep-Sea Oil Spills. In: Murawski SA, Ainsworth CH, Gilbert S, et al (eds) Scenarios and Responses to Future Deep Oil Spills: Fighting the Next War. Springer International Publishing, Cham, pp 494–512

237. Antoniou E, Fragkou E, Charalampous G, et al (2022) Emulating Deep-Sea Bioremediation: Oil Plume Degradation by Undisturbed Deep-Sea Microbial Communities Using a High-Pressure Sampling and Experimentation System. Energies 15:4525. https://doi.org/10.3390/en15134525

238. Dyksterhouse SE, Gray JP, Herwig RP, et al (1995) Cycloclasticus pugetii gen. nov., sp. nov., an Aromatic Hydrocarbon-Degrading Bacterium from Marine Sediments. Int J Syst Bacteriol 45:116–123. https://doi.org/10.1099/00207713-45-1-116

239. Heuer H, Krsek M, Baker P, et al (1997) Analysis of actinomycete communities by specific amplification of genes encoding 16S rRNA and gel-electrophoretic separation in denaturing gradients. Appl Environ Microbiol 63:3233–3241. https://doi.org/10.1128/aem.63.8.3233-3241.1997

240. Stucky BJ (2012) SeqTrace: A Graphical Tool for Rapidly Processing DNA Sequencing Chromatograms. J Biomol Tech 23:90–93. https://doi.org/10.7171/jbt.12-2303-004

241. Thijs S, Op De Beeck M, Beckers B, et al (2017) Comparative Evaluation of Four Bacteria-Specific Primer Pairs for 16S rRNA Gene Surveys. Front Microbiol 8:. https://doi.org/10.3389/fmicb.2017.00494

242. Ma M, Zheng L, Yin X, et al (2021) Reconstruction and evaluation of oil-degrading consortia isolated from sediments of hydrothermal vents in the South Mid-Atlantic Ridge. Sci Rep 11:1456. https://doi.org/10.1038/s41598-021-80991-5

243. Yang S, Li X, Xiao X, et al (2020) Sphingomonas profundi sp. nov., isolated from deep-sea sediment of the Mariana Trench. Int J Syst Evol Microbiol 70:3809–3815. https://doi.org/10.1099/ijsem.0.004235

244. Zhang D-C, Liu Y-X, Huang H-J (2017) Novosphingobium profundi sp. nov. isolated from a deep-sea seamount. Antonie Van Leeuwenhoek 110:19–25. https://doi.org/10.1007/s10482-016-0769-3

245. La Cono V, Smedile F, La Spada G, et al (2015) Shifts in the meso- and bathypelagic archaea communities composition during recovery and short-term handling of decompressed deep-sea samples. Environ Microbiol Rep 7:450–459. https://doi.org/10.1111/1758-2229.12272

246. Yanagibayashi M, Nogi Y, Li L, Kato C (1999) Changes in the microbial community in Japan Trench sediment from a depth of 6292 m during cultivation without decompression. FEMS Microbiol Lett 170:271–279. https://doi.org/10.1111/j.1574-6968.1999.tb13384.x

247. Liu Y, Chen S, Xie Z, et al (2023) Influence of Extremely High Pressure and Oxygen on Hydrocarbon-Enriched Microbial Communities in Sediments from the Challenger Deep, Mariana Trench. Microorganisms 11:630. https://doi.org/10.3390/microorganisms11030630

248. Dong H, Yu L, Xu T, et al (2023) Cultivation and biogeochemical analyses reveal insights into biomineralization caused by piezotolerant iron-reducing bacteria from petroleum reservoirs and their application in MEOR. Sci Total Environ 903:166465. https://doi.org/10.1016/j.scitotenv.2023.166465

249. Nawaz MZ, Subin Sasidharan R, Alghamdi HA, Dang H (2022) Understanding Interaction Patterns within Deep-Sea Microbial Communities and Their Potential

Applications. Mar Drugs 20:108. https://doi.org/10.3390/md20020108

250. Peter H, Beier S, Bertilsson S, et al (2011) Function-specific response to depletion of microbial diversity. ISME J 5:351–361. https://doi.org/10.1038/ismej.2010.119

251. Bell TH, Stefani FOP, Abram K, et al (2016) A Diverse Soil Microbiome Degrades More Crude Oil than Specialized Bacterial Assemblages Obtained in Culture. Appl Environ Microbiol 82:5530–5541. https://doi.org/10.1128/AEM.01327-16

252. Dell'Anno A, Beolchini F, Rocchetti L, et al (2012) High bacterial biodiversity increases degradation performance of hydrocarbons during bioremediation of contaminated harbor marine sediments. Environ Pollut 167:85–92. https://doi.org/10.1016/j.envpol.2012.03.043

253. Maron P-A, Sarr A, Kaisermann A, et al (2018) High Microbial Diversity Promotes Soil Ecosystem Functioning. Appl Environ Microbiol 84:e02738-17. https://doi.org/10.1128/AEM.02738-17

254. Singh BK, Quince C, Macdonald CA, et al (2014) Loss of microbial diversity in soils is coincident with reductions in some specialized functions. Environ Microbiol 16:2408–2420. https://doi.org/10.1111/1462-2920.12353

255. Xun W, Li W, Xiong W, et al (2019) Diversity-triggered deterministic bacterial assembly constrains community functions. Nat Commun 10:3833. https://doi.org/10.1038/s41467-019-11787-5

256. Somee MR, Amoozegar MA, Dastgheib SMM, et al (2022) Genome-resolved analyses show an extensive diversification in key aerobic hydrocarbon-degrading enzymes across bacteria and archaea. BMC Genomics 23:690. https://doi.org/10.1186/s12864-022-08906-w

257. Al-Thukair AA, Malik K (2016) Pyrene metabolism by the novel bacterial strains Burkholderia fungorum (T3A13001) and Caulobacter sp (T2A12002) isolated from an oil-polluted site in the Arabian Gulf. Int Biodeterior Biodegradation 110:32–37. https://doi.org/10.1016/j.ibiod.2016.02.005

258. Elufisan TO, Rodríguez-Luna IC, Oyedara OO, et al (2020) The Polycyclic Aromatic

Hydrocarbon (PAH) degradation activities and genome analysis of a novel strain Stenotrophomonas sp . Pemsol isolated from Mexico. PeerJ 8:e8102. https://doi.org/10.7717/peerj.8102

259. Lyu Y, Zheng W, Zheng T, Tian Y (2014) Biodegradation of Polycyclic Aromatic Hydrocarbons by Novosphingobium pentaromativorans US6-1. PLoS One 9:e101438. https://doi.org/10.1371/journal.pone.0101438

260. Prince RC, Gramain A, McGenity TJ (2010) Prokaryotic Hydrocarbon Degraders. In: Handbook of Hydrocarbon and Lipid Microbiology. Springer Berlin Heidelberg, Berlin, Heidelberg, pp 1669–1692

261. Xu HX, Wu HY, Qiu YP, et al (2011) Degradation of fluoranthene by a newly isolated strain of Herbaspirillum chlorophenolicum from activated sludge. Biodegradation 22:335–345. https://doi.org/10.1007/s10532-010-9403-7

262. Xu H, Li X, Sun Y, et al (2016) Biodegradation of Pyrene by Free and Immobilized Cells of Herbaspirillum chlorophenolicum Strain FA1. Water, Air, Soil Pollut 227:120. https://doi.org/10.1007/s11270-016-2824-0

263. Van Landuyt J, Cimmino L, Dumolin C, et al (2020) Microbial enrichment, functional characterization and isolation from a cold seep yield piezotolerant obligate hydrocarbon degraders. FEMS Microbiol Ecol 96:1–15. https://doi.org/10.1093/femsec/fiaa097

264. Scoma A, Heyer R, Rifai R, et al (2019) Reduced TCA cycle rates at high hydrostatic pressure hinder hydrocarbon degradation and obligate oil degraders in natural, deep-sea microbial communities. ISME J 13:1004–1018. https://doi.org/10.1038/s41396-018-0324-5

265. Wang W, Li Z, Zeng L, et al (2020) The oxidation of hydrocarbons by diverse heterotrophic and mixotrophic bacteria that inhabit deep-sea hydrothermal ecosystems. ISME J 14:1994–2006. https://doi.org/10.1038/s41396-020-0662-y

266. Lai Q, Wang L, Liu Y, et al (2011) Alcanivorax pacificus sp. nov., isolated from a deep-sea pyrene-degrading consortium. Int J Syst Evol Microbiol 61:1370–1374. https://doi.org/10.1099/ijs.0.022368-0

267. Rai A, Suresh G, Ria B, et al (2023) Phylogenomic analysis of the genus Alcanivorax: proposal for division of this genus into the emended genus Alcanivorax and two novel genera Alloalcanivorax gen. nov. and Isoalcanivorax gen. nov. Int J Syst Evol Microbiol 73:. https://doi.org/10.1099/ijsem.0.005672

268. Fernández-Martínez J, Pujalte MJ, García-Martínez J, et al (2003) Description of Alcanivorax venustensis sp. nov. and reclassification of Fundibacter jadensis DSM 12178T (Bruns and Berthe-Corti 1999) as Alcanivorax jadensis comb. nov., members of the emended genus Alcanivorax. Int J Syst Evol Microbiol 53:331–338. https://doi.org/10.1099/ijs.0.01923-0

269. French-McCay DP, Horn M, Li Z, et al (2018) Modeling Distribution, Fate, and Concentrations of Deepwater Horizon Oil in Subsurface Waters of the Gulf of Mexico. In: Stout SA, Wang Z (eds) Oil Spill Environmental Forensics Case Studies. Elsevier, pp 683–735

270. Prince RC, Nash GW, Hill SJ (2016) The biodegradation of crude oil in the deep ocean. Mar Pollut Bull 111:354–357. https://doi.org/10.1016/j.marpolbul.2016.06.087

271. Liu J, Zheng Y, Lin H, et al (2019) Proliferation of hydrocarbon-degrading microbes at the bottom of the Mariana Trench. Microbiome 7:47. https://doi.org/10.1186/s40168-019-0652-3

272. Lee K, Nedwed T, Prince RC, Palandro D (2013) Lab tests on the biodegradation of chemically dispersed oil should consider the rapid dilution that occurs at sea. Mar Pollut Bull 73:314–318. https://doi.org/10.1016/j.marpolbul.2013.06.005

273. Yakimov MM, Giuliano L, Gentile G, et al (2003) Oleispira antarctica gen. nov., sp. nov., a novel hydrocarbonoclastic marine bacterium isolated from Antarctic coastal sea water. Int J Syst Evol Microbiol 53:779–785. https://doi.org/https://doi.org/10.1099/ijs.0.02366-0

274. Kube M, Chernikova TN, Al-Ramahi Y, et al (2013) Genome sequence and functional genomic analysis of the oil-degrading bacterium Oleispira antarctica. Nat Commun 4:2156. https://doi.org/10.1038/ncomms3156

275. Gregson BH, Metodieva G, Metodiev M V, et al (2020) Protein expression in the obligate hydrocarbon-degrading psychrophile Oleispira antarctica RB-8 during alkane degradation

and cold tolerance. Environ Microbiol 22:1870–1883. https://doi.org/https://doi.org/10.1111/1462-2920.14956

276. Thomas GE, Brant JL, Campo P, et al (2021) Effects of Dispersants and Biosurfactants on Crude-Oil Biodegradation and Bacterial Community Succession. Microorganisms 9:1200. https://doi.org/10.3390/microorganisms9061200

277. Stelling SC, Techtmann SM, Utturkar SM, et al (2014) Draft Genome Sequence of Thalassotalea sp. Strain ND16A Isolated from Eastern Mediterranean Sea Water Collected from a Depth of 1,055 Meters. Genome Announc 2:. https://doi.org/10.1128/genomeA.01231-14

278. Charalampous G, Fragkou E, Kalogerakis N, et al (2024) Diversity links to functionality: Unraveling the impact of pressure disruption and culture medium on crude oil-enriched microbial communities from the deep Eastern Mediterranean Sea. Mar Pollut Bull 202:116275. https://doi.org/https://doi.org/10.1016/j.marpolbul.2024.116275

279. Valentine DL, Kessler JD, Redmond MC, et al (2010) Propane Respiration Jump-Starts Microbial Response to a Deep Oil Spill. Science (80-) 330:208–211. https://doi.org/10.1126/science.1196830

280. Mishamandani S, Gutierrez T, Aitken MD (2014) DNA-based stable isotope probing coupled with cultivation methods implicates Methylophaga in hydrocarbon degradation. Front Microbiol 5:76. https://doi.org/10.3389/fmicb.2014.00076

281. Gutierrez T, Aitken MD (2014) Role of methylotrophs in the degradation of hydrocarbons during the Deepwater Horizon oil spill. ISME J 8:2543–2545. https://doi.org/10.1038/ismej.2014.88

282. Lopes EM, Fernandes CC, de Macedo Lemos EG, Kishi LT (2020) Reconstruction and in silico analysis of new Marinobacter adhaerens t76_800 with potential for long-chain hydrocarbon bioremediation associated with marine environmental lipases. Mar Genomics 49:100685. https://doi.org/https://doi.org/10.1016/j.margen.2019.04.010

283. Kodama Y, Stiknowati LI, Ueki A, et al (2008) Thalassospira tepidiphila sp. nov., a polycyclic aromatic hydrocarbon-degrading bacterium isolated from seawater. Int J Syst Evol Microbiol. https://doi.org/10.1099/ijs.0.65476-0

284. Tonteri O, Reunamo A, Nousiainen A, et al (2023) Effects of Dispersant on the Petroleum Hydrocarbon Biodegradation and Microbial Communities in Seawater from the Baltic Sea and Norwegian Sea. Microorganisms 11:. https://doi.org/10.3390/microorganisms11040882

APPENDIX I-Supplementary Figures

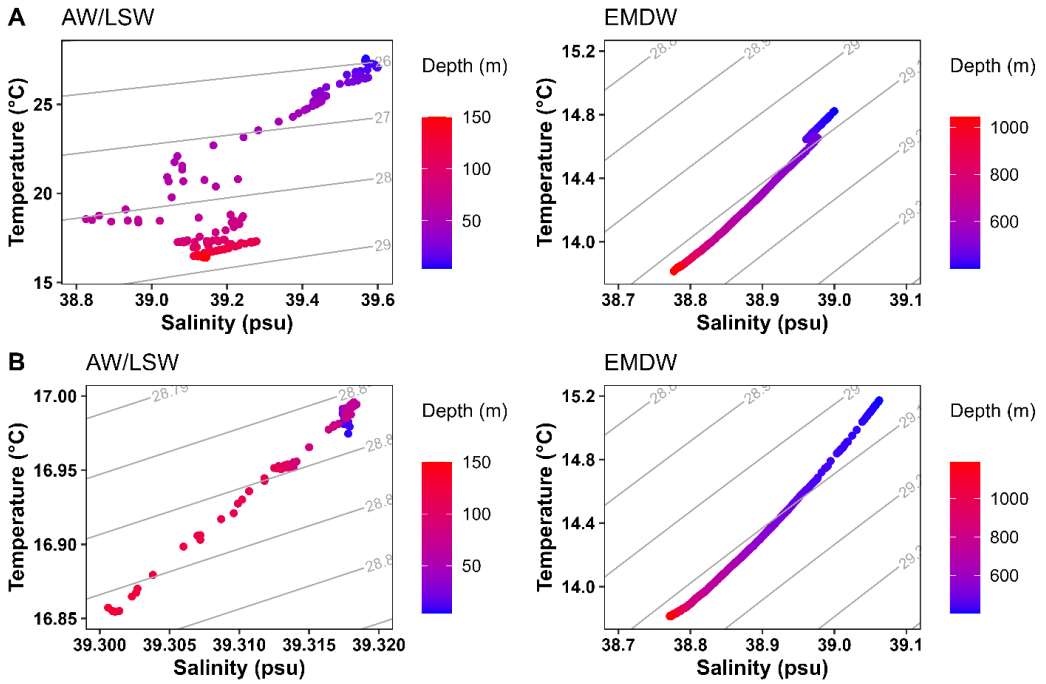

Figure S1. *Temperature-Salinity diagrams for surface (AW/LSW) and deep (EMDW) water masses of A) Summer and B) Winter sampling. Thin grey lines represent isopycnals of density in kg* m^{-3}.

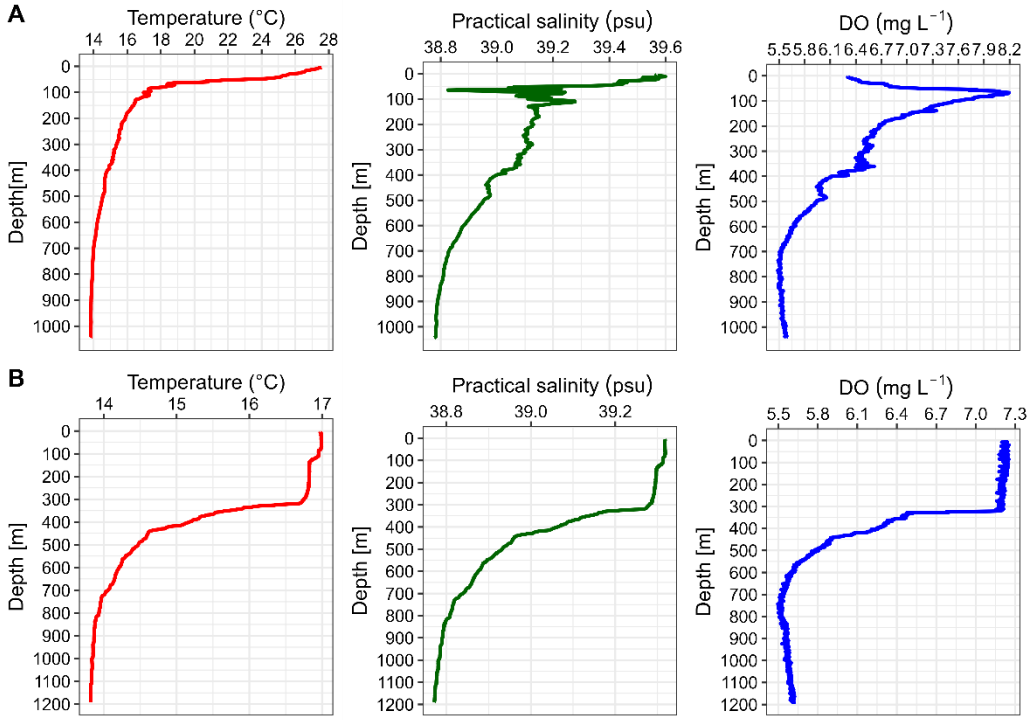

Figure S2. *Temperature, salinity and dissolved oxygen profiles for A) Summer and B) Winter sampling. Winter water perturbation is obvious reaching depths down to 300 m.*

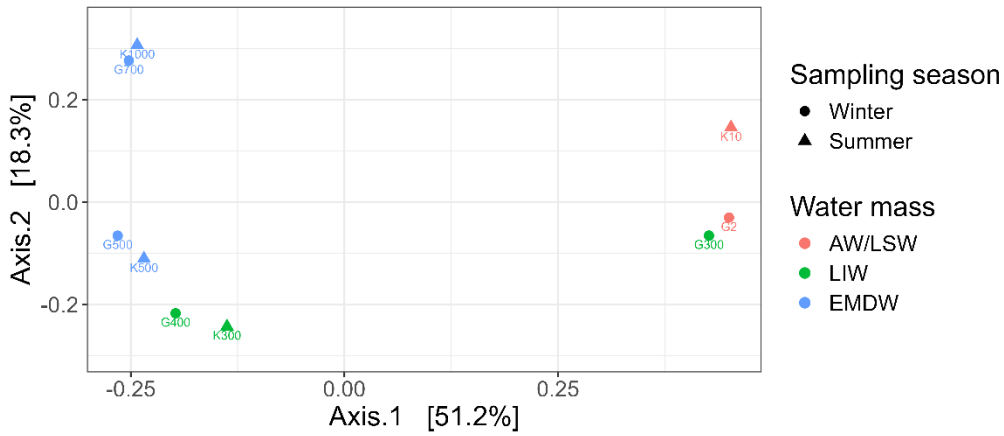

Figure S3*. Principal coordinate analysis of unicellular eukaryotic samples based on Bray-Curtis dissimilarity distances. Samples are separated according to the water mass from which they were retrieved.*

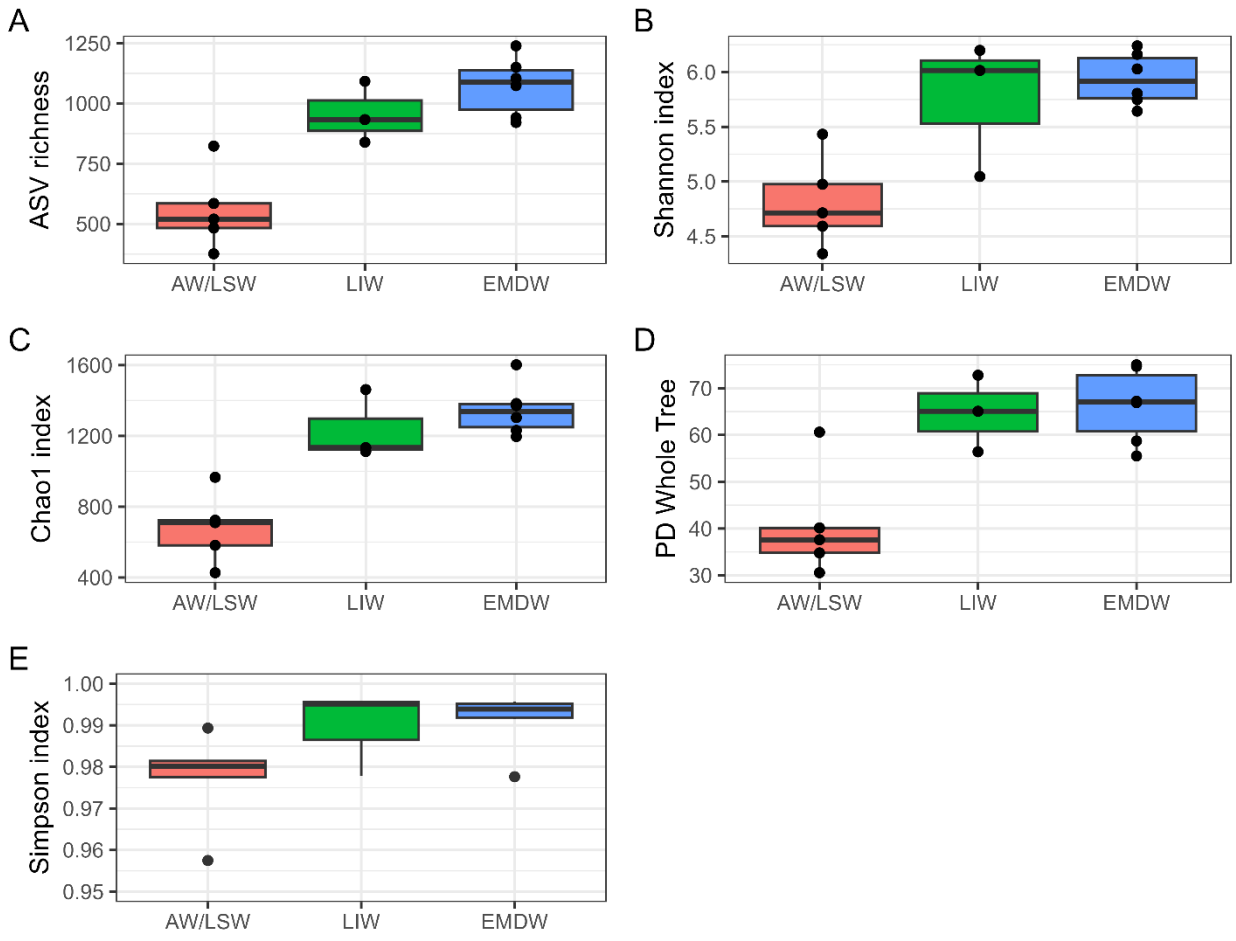

Figure S4. *Boxplot of alpha diversity indices of bacterial samples for each water mass. The deepest (EMDW) water layer presented higher diversity levels while the surface (AW/LSW) samples had the lowest.*

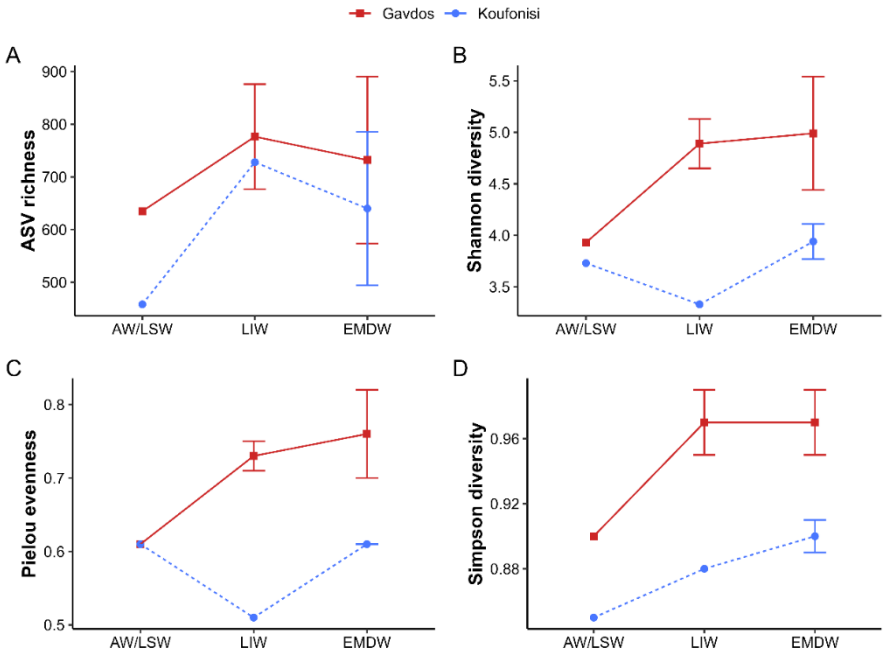

Figure S5. *Alpha-diversity metrics of unicellular eukaryotes in each water mass for every sampling station. Diversity levels were notably higher at Gavdos (winter) station compared to Koufonisi (summer) station across all three water layers, with the largest disparity observed in the intermediate (LIW) layer between the two sampling sites.*

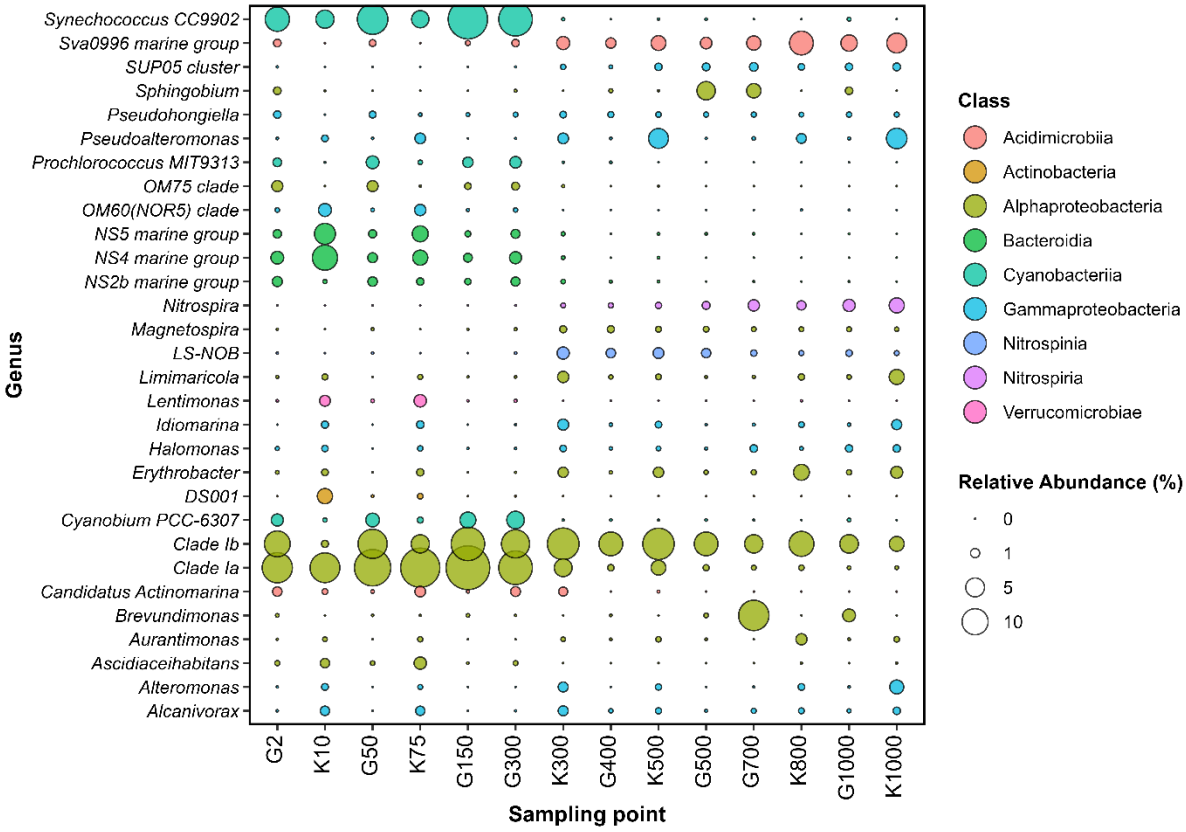

Figure S6. *Relative abundance bubbleplot of Top30 genera. Known hydrocarbon-degrading taxa are present throughout the water column in Koufonisi and in the deep waters of Gavdos station.*

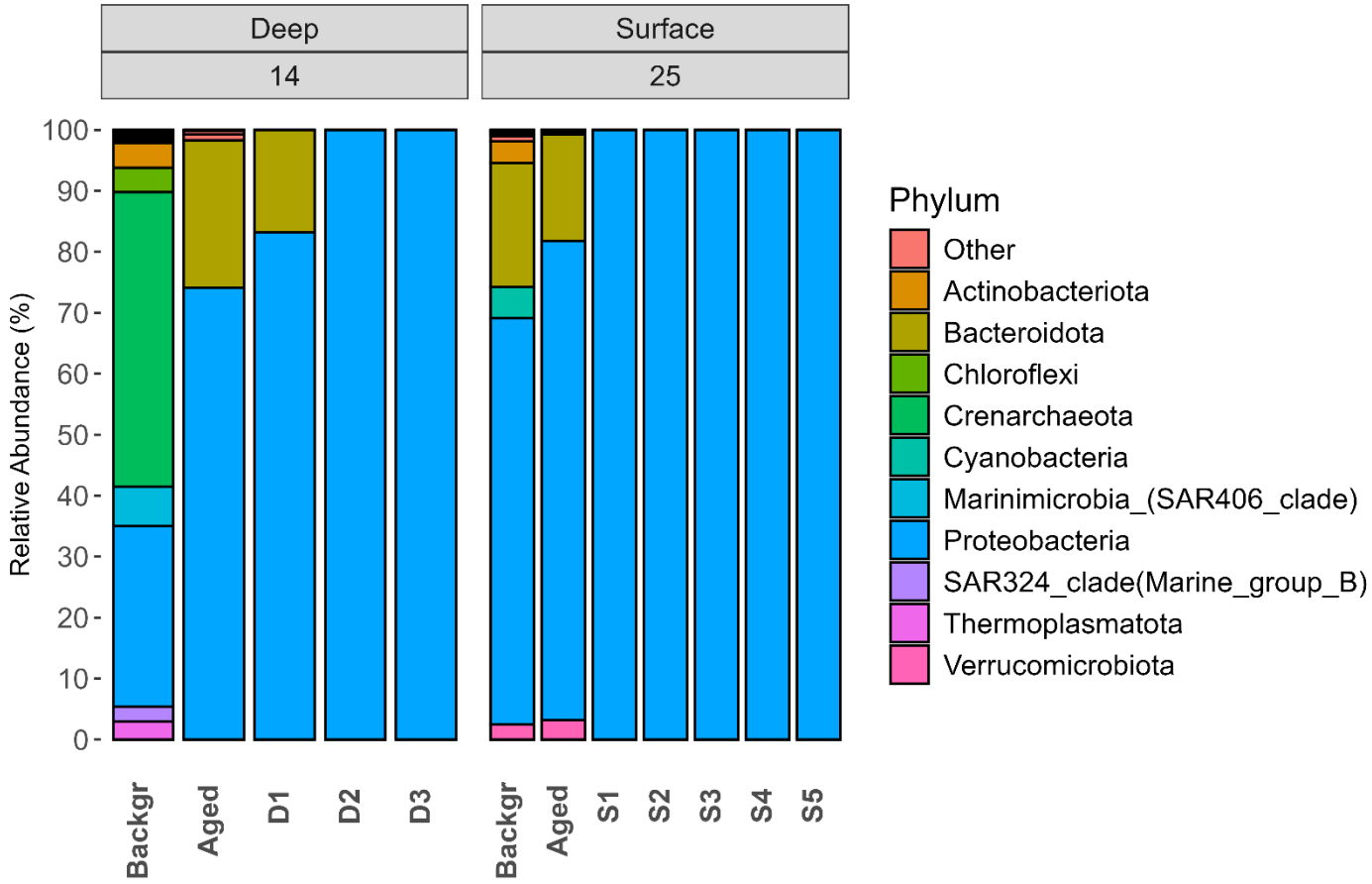

Figure S7*. Relative abundance of bacterial taxa at the phylum level for Surface and Deep enrichments.*

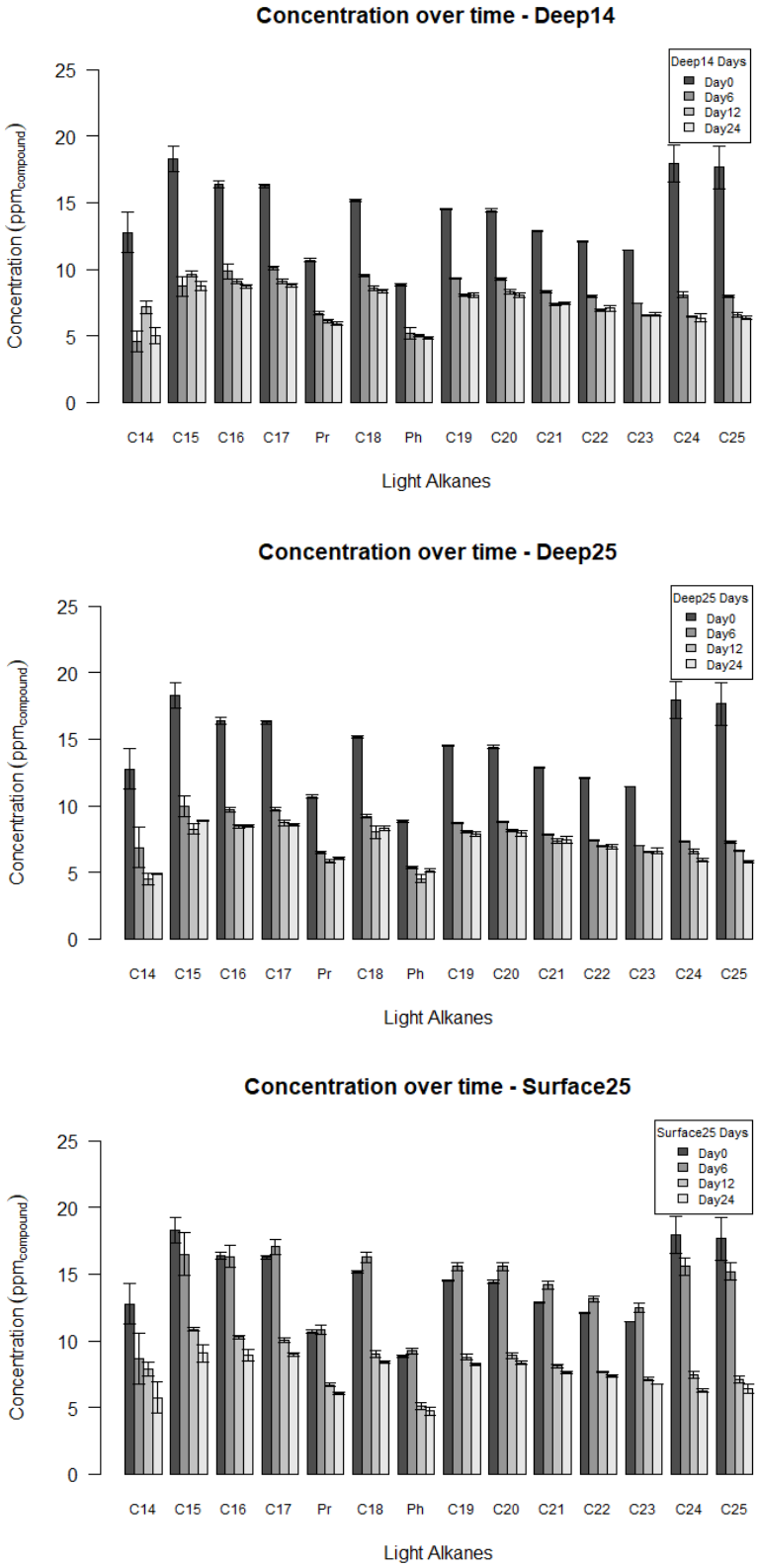

Figure S8.*Concentration changes of the light alkanes over time in treatments Deep14, Deep25, and Surface25. Error bars represent standard deviation (n=3).*

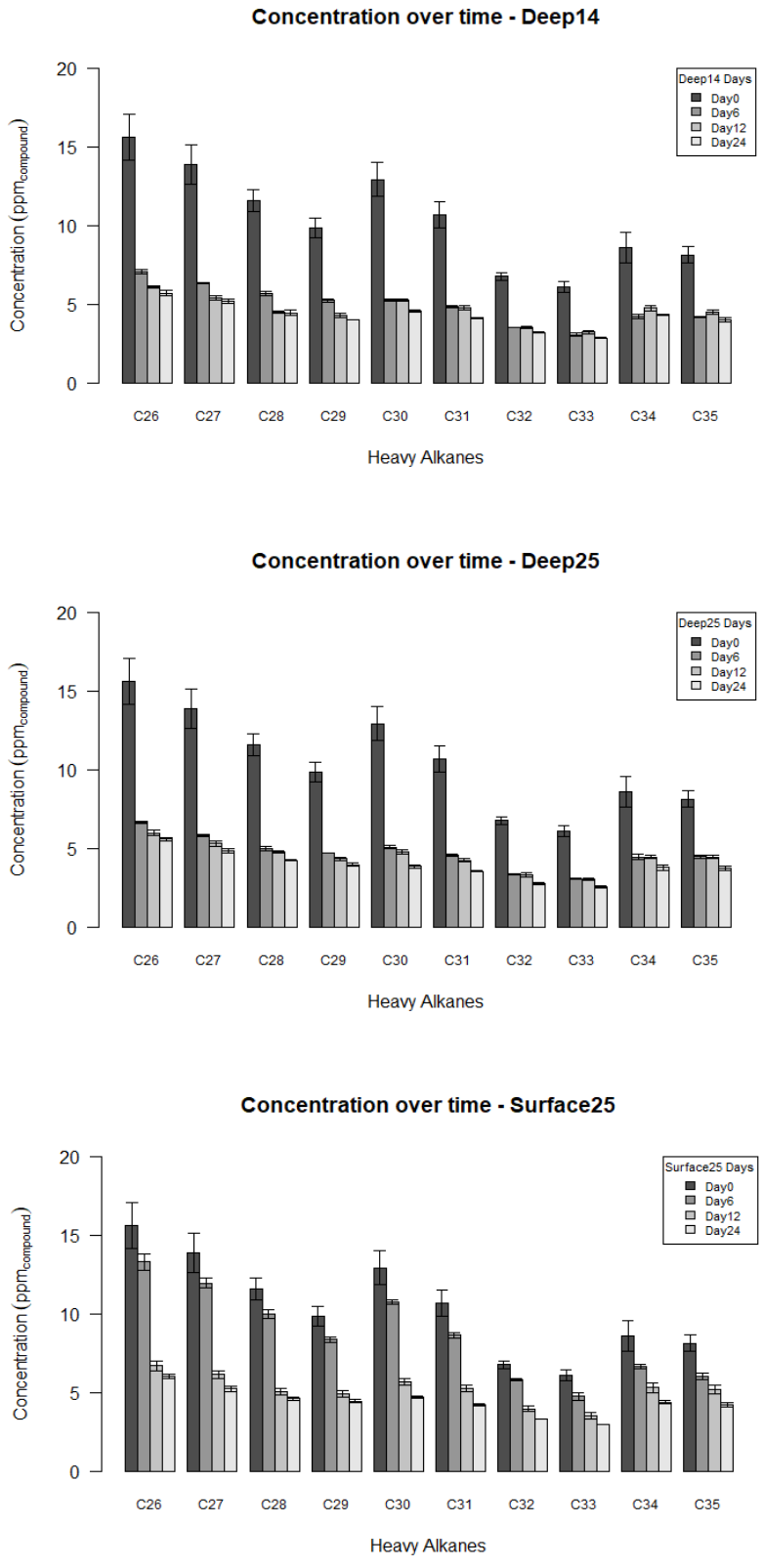

Figure S9*.Concentration changes of the heavy alkanes over time in treatments Deep14, Deep25, and Surface25. Error bars represent standard deviation (n=3).*

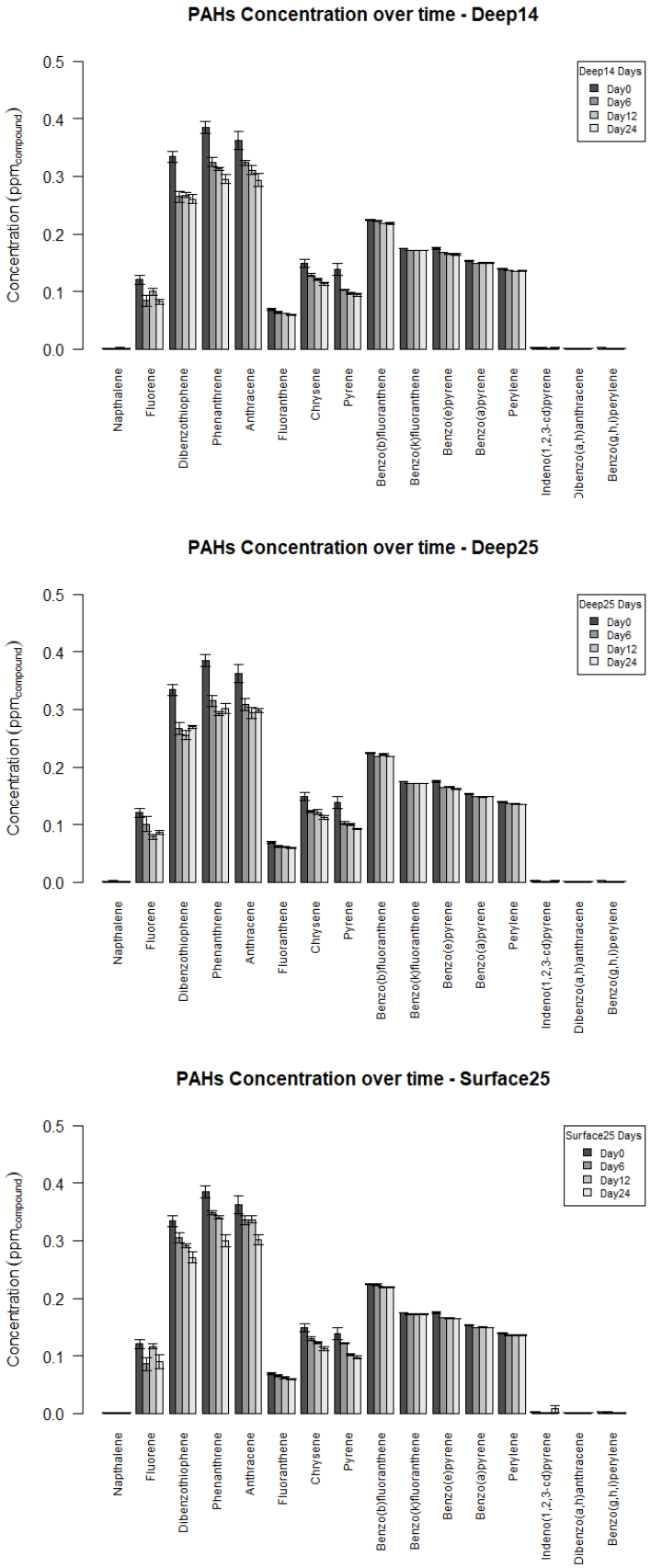

Figure S10 *Concentration changes of the PAHs over time in treatments Deep14, Deep25, and Surface25. Error bars represent standard deviation (n=3).*

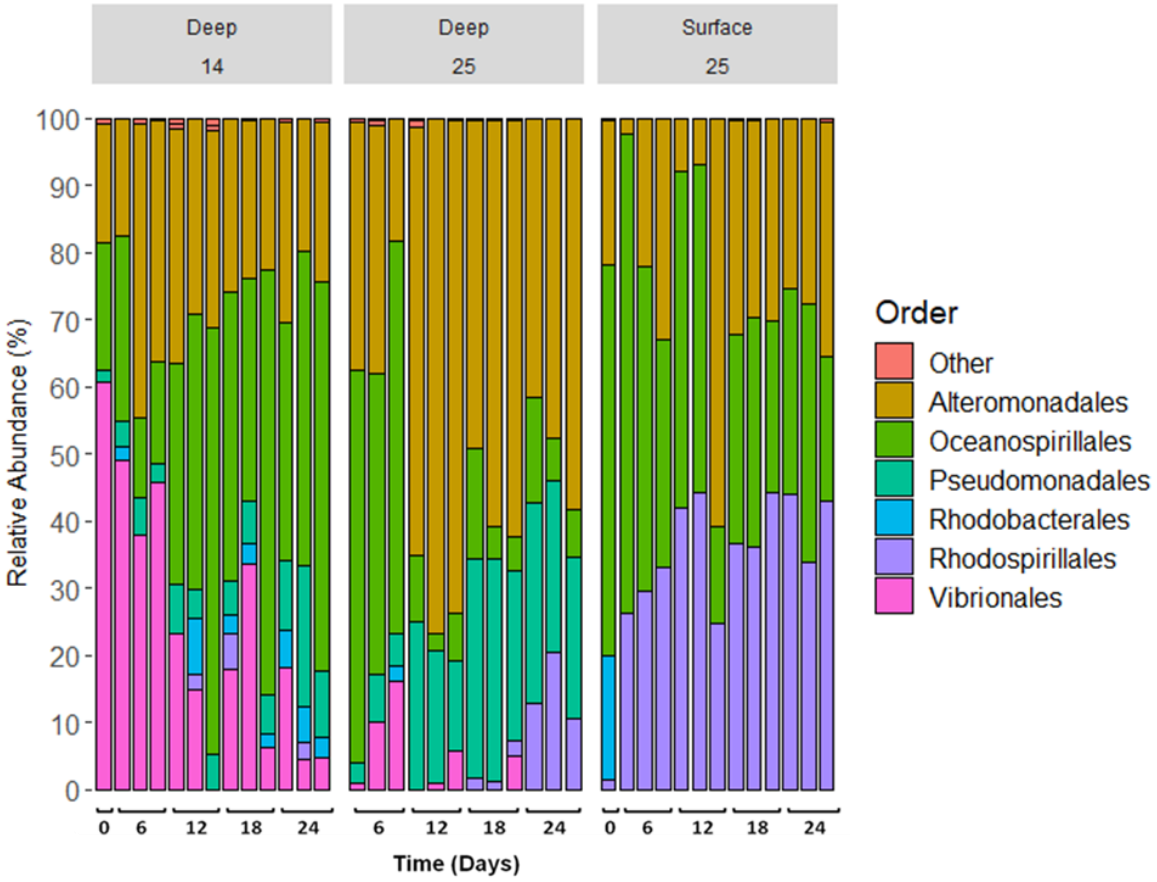

Figure S11. *Relative abundance of bacterial taxa at the Order level plotted against time (days) and grouped by treatment (Deep14, Deep25, Surface25). Brackets on the x-axis correspond to the triplicate samples for the given timepoint.*

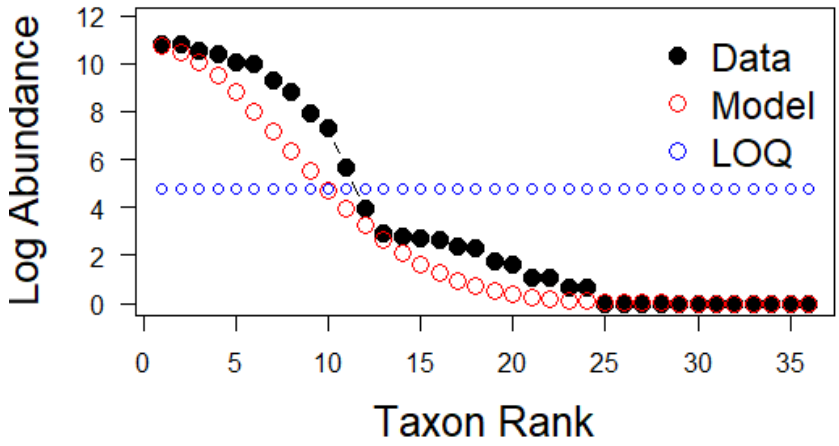

Figure S12. *Rank distribution of Genus taxa. The limit of quantification (LOQ), shown in blue circles, is 1.3 standard deviation from zero in order to address false positive results. Taxa are displayed in black while the lognormal rank distribution model is given in red circles.*

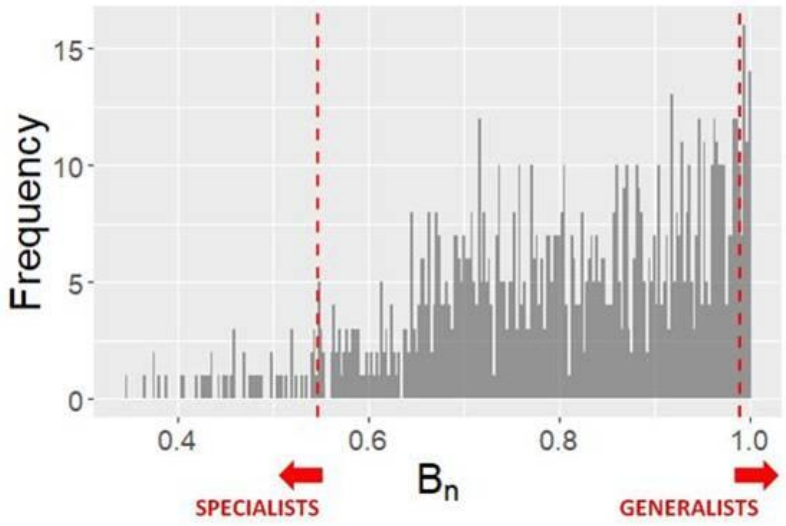

Figure S13. *Null model distribution of Levin's BN niche. On the x-axis, the Levin's BN distribution across the three different treatments (Deep14, Deep25, Surface25) versus the frequency of random BN values on the y-axis. The red dotted lines indicate the 0.05 and 0.95 quantiles. Samples below the 5th quantile are considered specialists while those above the 95th are generalists.*

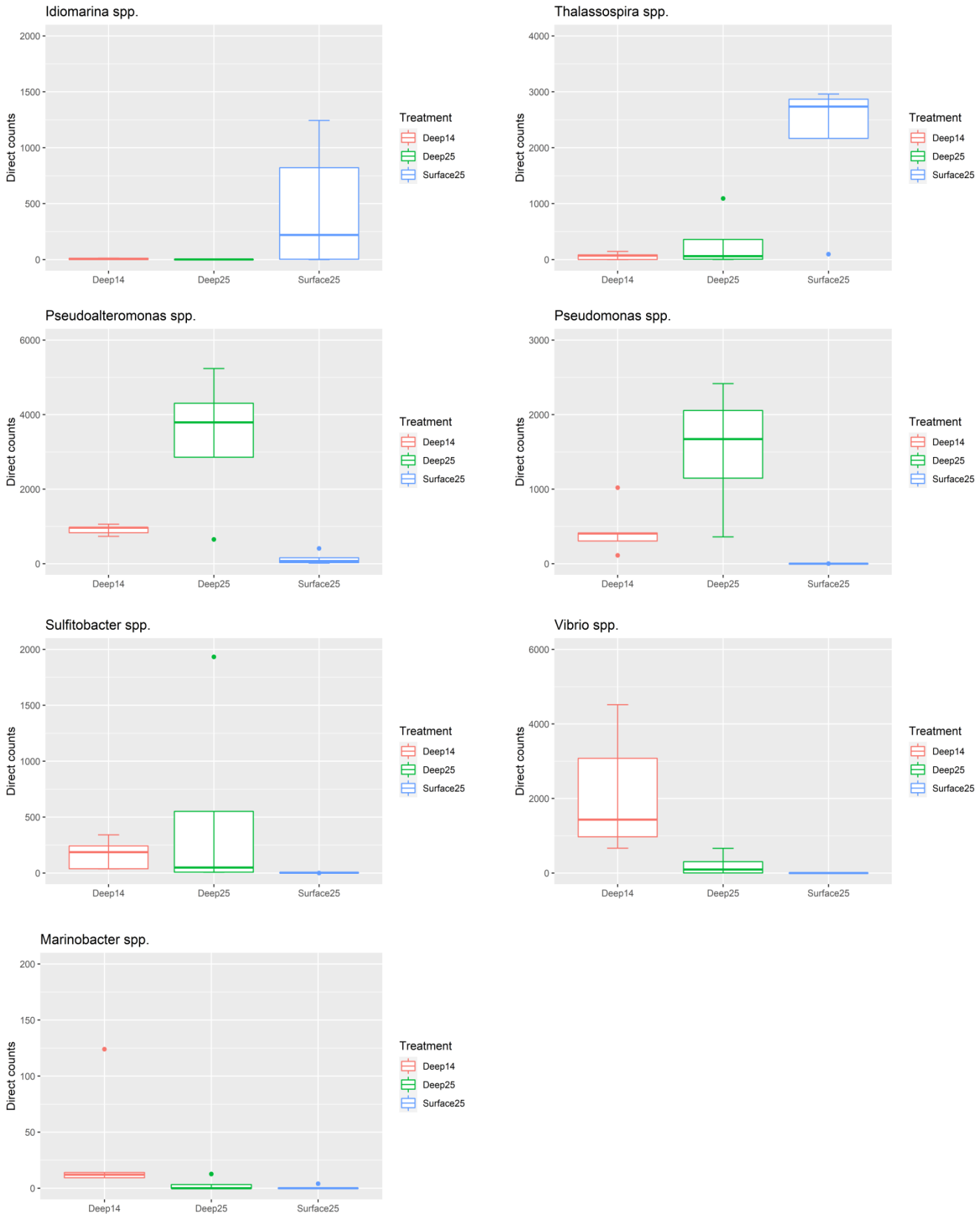

Figure S14. *Direct counts from rarefied data of specialist taxa, identified by Levin's BN niche, by Treatment.*

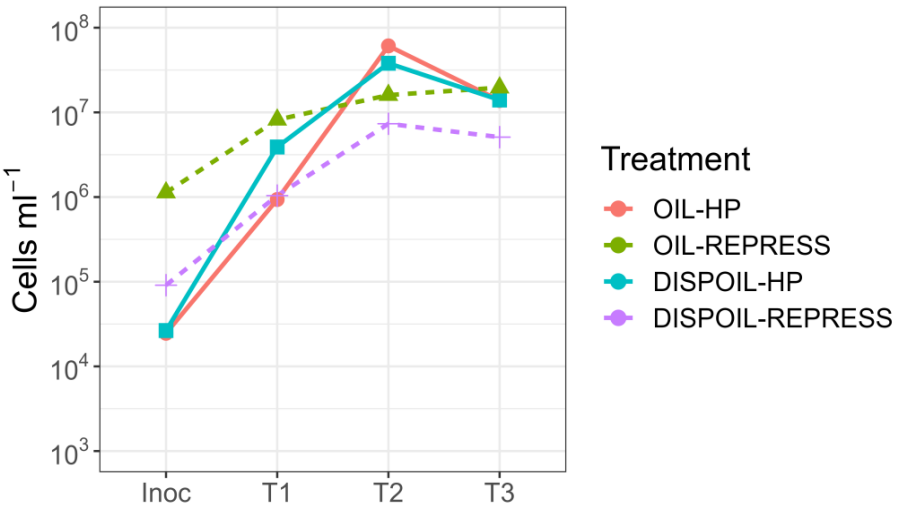

Figure S15. *Microbial cell counts measured for acclimatised (Inoc) and enrichment transfers (T1-T3) for each treatment of the experiment under HP (solid lines) and REPRESS (dashed lines) pressure conditions.*

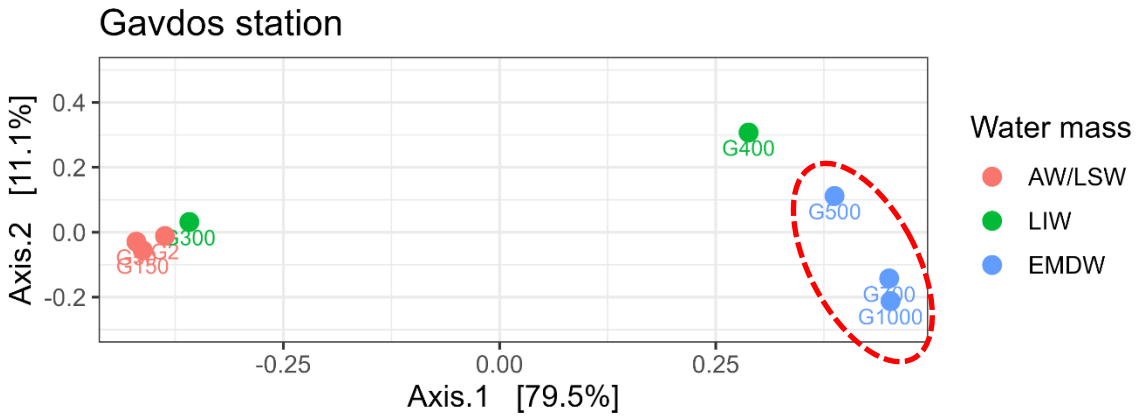

Figure S16. *Distribution of microbial samples collected from various depths at Gavdos station based on Principal Coordinate Analysis (PCoA). The red ellipse encircles the samples collected from the deepest EMDW layer indicating the similarity in microbial composition.*

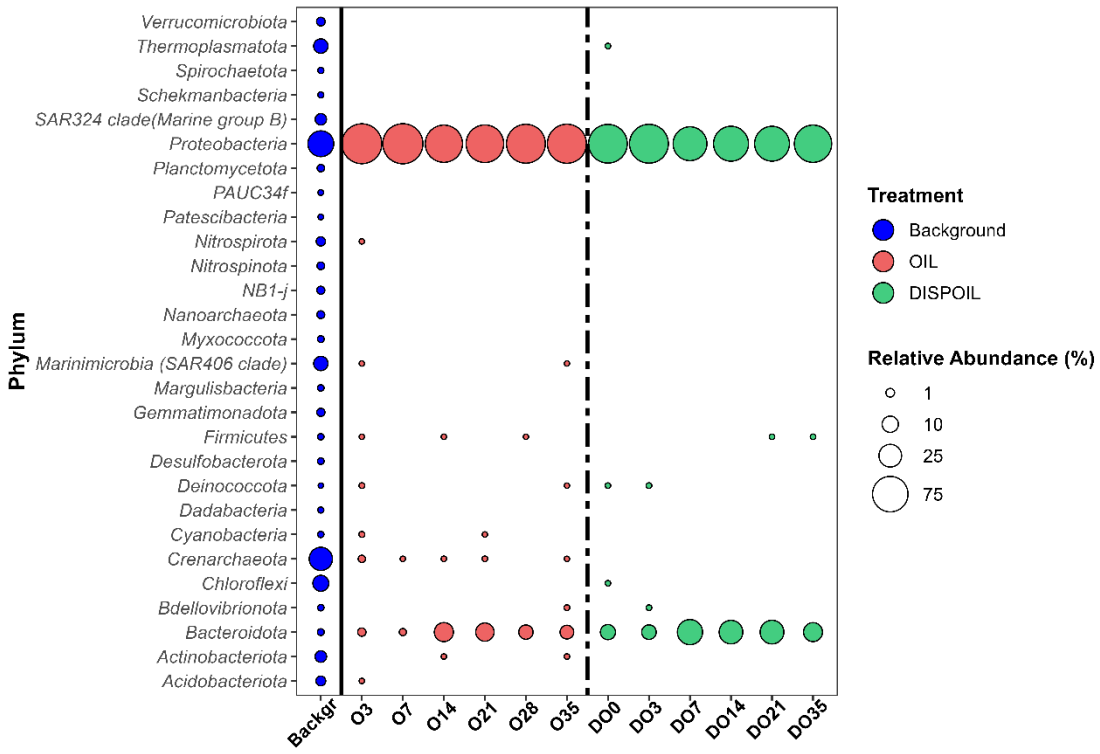

Figure S17. *Bubbleplot of relative abundance of species at the Phylum level indicating the drop in microbial diversity between the background sample and the oil-amended treatments (OIL, DISPOIL). Proteobacteria and Bacteroidota were the dominant phyla in the presence of hydrocarbons. The x-axis characters correspond to Treatments (Backgr= Background, O=OIL, DO=DISPOIL) and the numbers indicate the sampling day.*

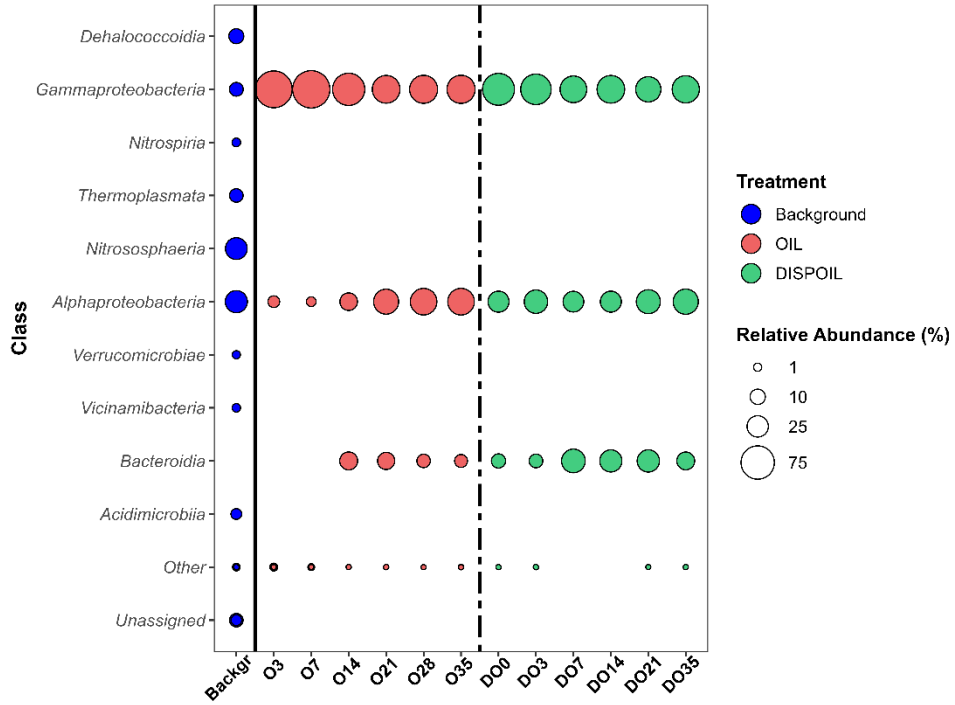

Figure S18. *Relative abundance bubbleplot of taxa at the Class level. Taxa with relative abundance below 1% are classified as "Other". The x-axis characters correspond to Treatments (Backgr= Background, O=OIL, DO=DISPOIL) and the numbers indicate the sampling day.*

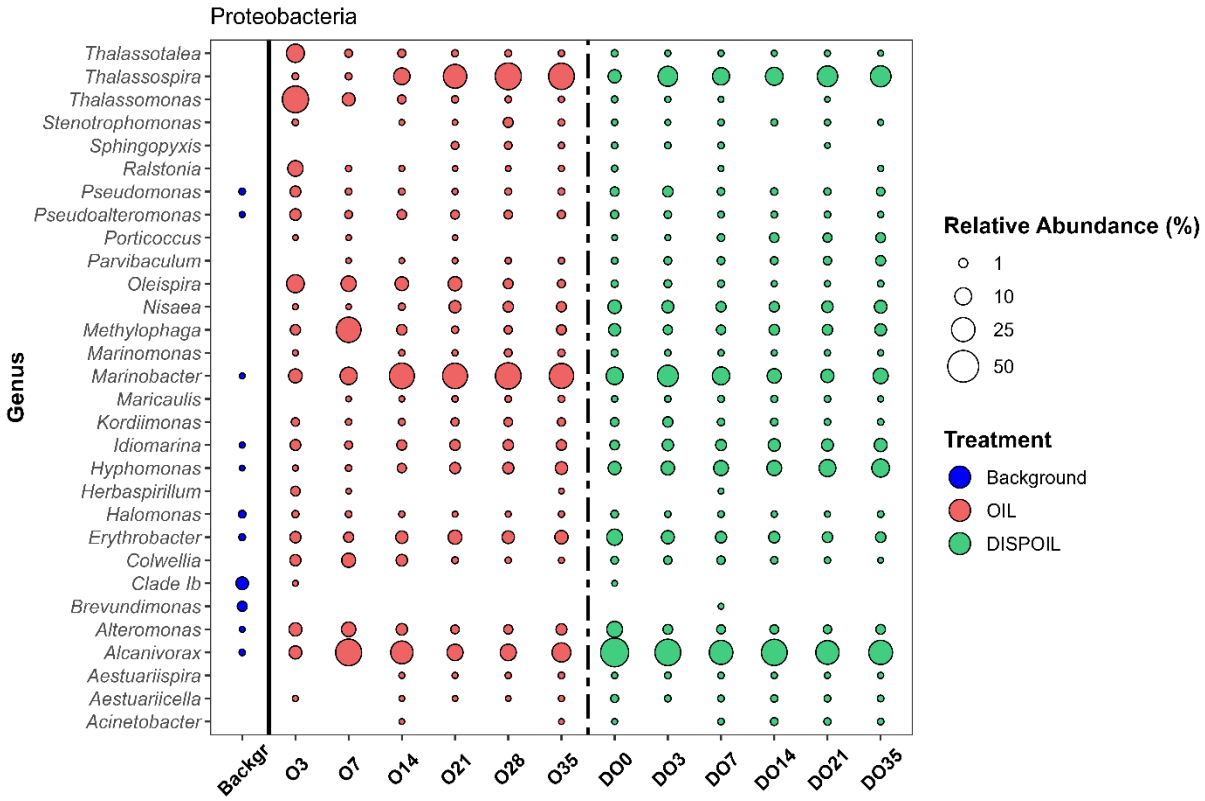

Figure S19. *Relative abundance bubbleplot of Proteobacteria at the Genus level. The x-axis characters correspond to Treatments (Backgr= Background, O=OIL, DO=DISPOIL) and the numbers indicate the sampling day.*

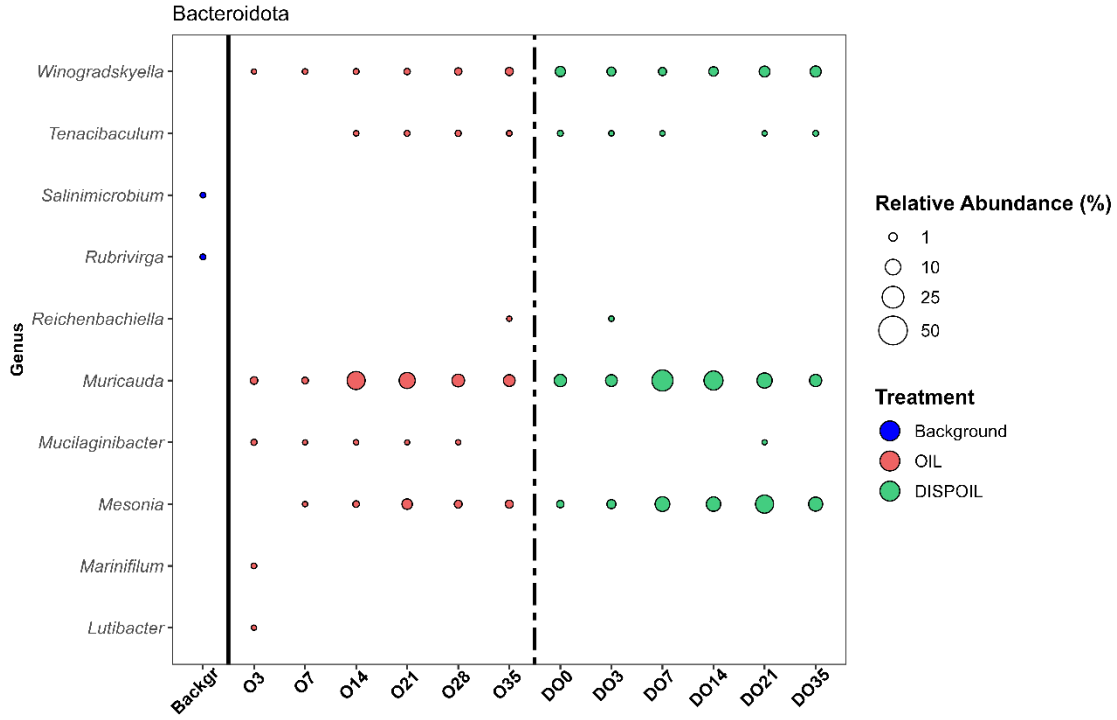

Figure S20. *Relative abundance bubbleplot of Bacteroidota at the Genus level. The x-axis characters correspond to Treatments (Backgr= Background, O=OIL, DO=DISPOIL) and the numbers indicate the sampling day.*

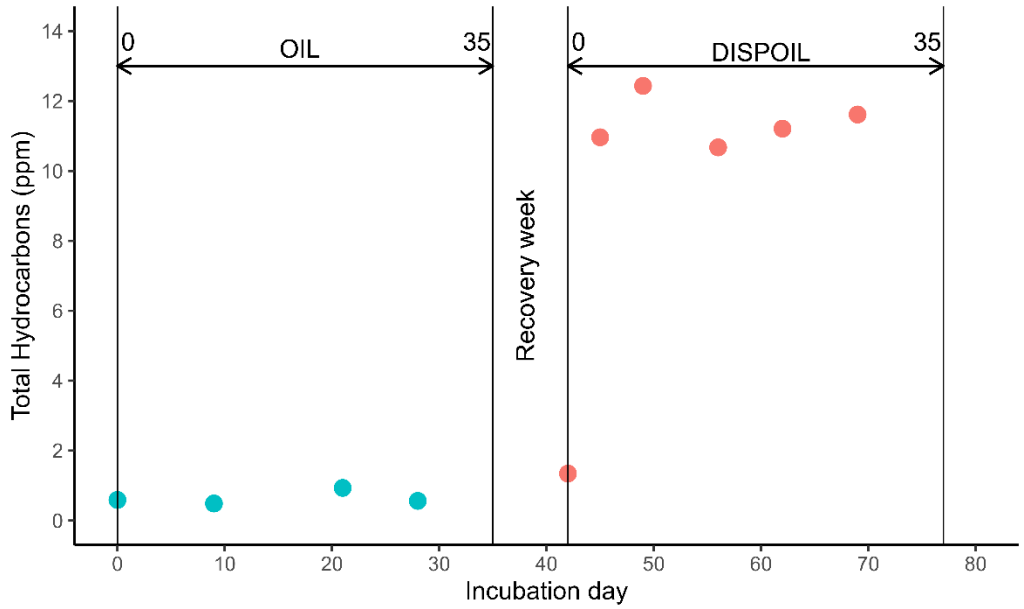

Figure S21.*Total concentration of hydrocarbons (ppm) measured at indicated timepoints after subsampling and substitution of the retrieved volume with filter-sterilized deep seawater amended with oil or dispersed oil. During the OIL treatment, crude oil was added on days 0, 9, 21 and 28 while during the DISPOIL treatment, dispersed oil was added on days 0, 3, 7, 14, 21 and 28 (corresponding to days 42, 45, 49, 56, 63 and 70 of the DISPOIL treatment).*

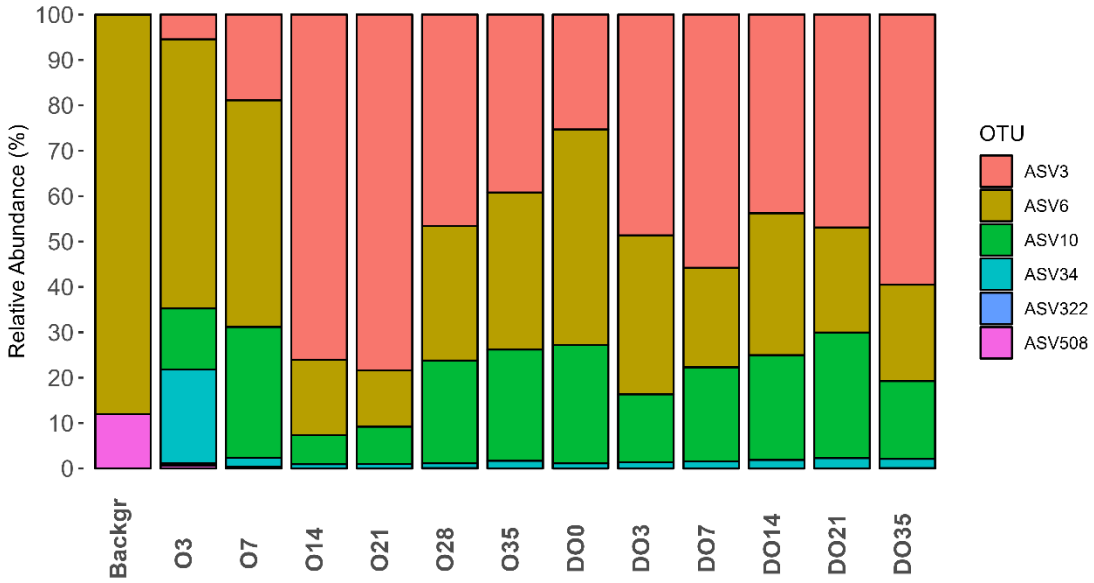

Figure S22. *Relative abundance barplot of Alcanivorax ASVs in each sampling timepoint .*

APPENDIX II-Supplementary Tables

Table S1. *ANOVA and Tukey HSD significance test of differences in alpha-diversity of bacterial communities between the three water masses.*

Diversity metric	ANOVA		Tukey HSD test		
	p-value	F-value	AW/LSW-LIW	LIW-EMDW	AW/LSW-EMDW
Shannon	0.00189	11.69	0.01994	0.79	0.00181
Simpson	0.0777	3.25	0.22189	0.97	0.07825
PD whole tree	0.00226	11.14	0.01382	0.97	0.00264

Table S2. *ANOVA significance results of differences in alpha-diversity of unicellular eukaryotic communities between the two sampling locations (season) and the three water masses.*

Diversity metric	Location (season)		Water mass	
	p-value	F-value	*p*-value	F-value
Shannon	0.018	12.11	0.300	1.54
Simpson	0.001	46.92	0.012	12.14
PD whole tree	0.212	2.041	0.121	3.31

Table S3. *Characteristic parameters of surface and deep co-occurrence networks.*

Network	SURFACE	DEEP
Number of nodes	51	63
Number of edges	1122	237
Positive correlation (%)	53	61
Avg. number of neighbors	44	11.5
Network diameter	2	4
Network radius	1	2
Characteristic path length	1.12	1.35
Clustering coefficient	0.923	0.861
Network density	0.88	0.767

Network heterogenity	0.173	0.317
Network centralization	0.125	0.114
Connected components	1	9

Table S4. *% Degradation by Day24 for each of the 16 EPA priority PAHs examined in this study, in treatments Deep14, Deep25, and Surface25. Empty values correspond to non-detectable peaks.*

PAH	Surface25	Deep14	Deep25
Naphthalene	45.48	46.26	41.24
Fluorene	25.27	31.39	28.39
Dibenzothiophene	18.81	21.89	19.21
Phenanthrene	22.24	23.37	21.75
Anthracene	16.69	18.93	17.47
Fluoranthene	13.91	13.53	14.18
Chrysene	24.72	23.47	24.88
Pyrene	29.52	31.50	33.10
Benzo(b)fluoranthene	2.39	2.40	2.98
Benzo(k)fluoranthene	1.55	2.09	1.84
Benzo(e)pyrene	5.82	6.07	7.50
Benzo(a)pyrene	2.22	2.17	2.35
Perylene	2.67	2.90	2.98
Indeno(1,2,3-cd)pyrene	—	—	—
Dibenzo(a,h)anthracene	0.76	—	3.87
Benzo(g,h,i)perylene	64.23	59.06	51.22

	ASV Richness	Shannon diversity

	Deep14	Deep25	Surface25	Deep14	Deep25	Surface25
Background	364	—	248	4.54	—	4.44
Aged	159	—	179	2.98	—	2.97
0	50	—	72	2.36	—	1.68
6	94.33 ± 14.01	70.67 ± 21.78	39.33 ± 3.06	2.62 ± 0.05	2.3 ± 0.32	1.5 ± 0.25
12	87.33 ± 24.66	70.67 ± 29.02	49.33 ± 8.08	2.45 ± 0.57	1.9 ± 0.24	1.44 ± 0.15
18	85.33 ± 19.86	63.67 ± 17.01	48.33 ± 6.03	2.55 ± 0.42	2.09 ± 0.18	1.74 ± 0.09
24	80.33 ± 10.02	64 ± 6.24	51 ± 9.54	2.63 ± 0.27	2.1 ± 0.13	1.66 ± 0.14
	Chao1 index			**InvSimpson diversity**		
	Deep14	**Deep25**	**Surface25**	**Deep14**	**Deep25**	**Surface25**
Background	522.91	—	262.44	27.28	—	50.73
Aged	199.62	—	219.07	10.41	—	8.69
0	59.75	—	157	7.01	—	4.65
6	387.06 ± 77.19	180.9 ± 192.74	54.06 ± 11.5	8.9 ± 0.65	5.75 ± 1.99	3.6 ± 0.97
12	220.42 ± 112.77	126.97 ± 108.88	91.39 ± 15.56	7.47 ± 4.02	3.54 ± 0.74	3.21 ± 0.6
18	147.23 ± 36.41	169.03 ± 139.99	62.17 ± 4.38	7.87 ± 3.77	4.79 ± 1.08	4.17 ± 0.41
24	177.37 ± 30.86	193.83 ± 83.99	80.44 ± 36.57	9.4 ± 3.87	5.33 ± 0.8	3.85 ± 0.3

Table S5. *Alpha diversity indices of microbial communities in treatments Deep14, Deep25, and Surface25 at each time-point.*

Table S6. *DESeq2 analysis results.*

DESeq2 by Depth. Most influential ASVs in enriched in Surface samples (positive log2FC)

	log2FoldChange	padj	Order	Family	Genus
ASV80	7.240484	3.42E-21	Oceanospirillales	Halomonadaceae	Halomonas
ASV4	5.972842	6.05E-21	Oceanospirillales	Halomonadaceae	Halomonas

	log2FoldChange	padj	Order	Family	Genus
ASV82	6.643629	4.94E-19	Oceanospirillales	Halomonadaceae	Halomonas
ASV19	6.962857	5E-19	Alteromonadales	Alteromonadaceae	Alteromonas
ASV16	5.889541	8.55E-19	Oceanospirillales	Halomonadaceae	Halomonas
ASV48	5.700159	1.32E-17	Oceanospirillales	Halomonadaceae	Halomonas
ASV30	8.462	3.42E-14	Alteromonadales	Idiomarinaceae	Idiomarina
ASV87	4.304216	4.82E-14	Oceanospirillales	Halomonadaceae	Halomonas
ASV15	7.97939	7.5E-14	Alteromonadales	Idiomarinaceae	Idiomarina
ASV111	5.159446	6.27E-13	Oceanospirillales	Halomonadaceae	Halomonas
ASV125	4.543738	1.2E-11	Oceanospirillales	Halomonadaceae	Halomonas
ASV247	4.750055	3E-09	Oceanospirillales	Halomonadaceae	Halomonas
ASV24	4.570913	1.86E-05	Caulobacterales	Hyphomonadaceae	Hyphomonas
ASV83	3.473179	3.35E-05	Rhodospirillales	Thalassospiraceae	Thalassospira
ASV23	2.511715	4.96E-05	Rhodobacterales	Rhodobacteraceae	Sulfitobacter
ASV299	3.780624	0.000166	Rhodospirillales	Thalassospiraceae	Thalassospira
ASV1	3.56691	0.00021	Rhodospirillales	Thalassospiraceae	Thalassospira
ASV77	3.340557	0.000389	Rhodospirillales	Thalassospiraceae	Thalassospira
ASV289	4.250027	0.000631	Alteromonadales	Alteromonadaceae	Alteromonas
ASV320	3.399414	0.001117	Oceanospirillales	Halomonadaceae	Halomonas

DESeq2 by Temperature. Most influential ASVs enriched at 14oC (Deep14 treatment) (negative log2FC).

ASV25	-4.19424	3.13E-06	Rhodobacterales	Rhodobacteraceae	Sulfitobacter
ASV44	-4.80003	9.14E-05	Alteromonadales	Marinobacteraceae	Marinobacter
ASV257	-4.15966	0.000319	Oceanospirillales	Alcanivoracaceae1	Alcanivorax
ASV240	-3.99691	0.000649	Oceanospirillales	Alcanivoracaceae1	Alcanivorax
ASV7	-2.16424	0.004031	Oceanospirillales	Alcanivoracaceae1	Alcanivorax
ASV41	-4.07133	0.005807	Vibrionales	Vibrionaceae	Vibrio
ASV21	-4.06944	0.006391	Vibrionales	Vibrionaceae	Vibrio
ASV27	-4.02641	0.007581	Vibrionales	Vibrionaceae	Vibrio

Table S7 *Successional patterns in the microbial community structure as shown in DESeq2 analysis by Time and Treatment.*

		Enriched ASVs					Depleted ASVs				
			log2FoldChange	padj	Order	Genus		log2FoldChange	padj	Order	Genus
Deep14	**Day 0-6**	No ASVs enriched					No ASVs depleted				
	Day 6-12	ASV1	6.866	<0.001	Rhodospirillales	Thalassospira	No ASVs depleted				
		ASV4	4.823	0.001	Oceanospirillales	Halomonas					
	Day 12-18	No ASVs enriched					No ASVs depleted				
	Day 18-24	ASV22	1.858529319	<0.001	Pseudomonadales	Pseudomonas	No ASVs depleted				
		ASV25	1.165912144	<0.001	Rhodobacterales	Sulfitobacter					
		ASV9	1.559843895	<0.001	Pseudomonadales	Pseudomonas					
		ASV12	1.367002217	0.004	Oceanospirillales	Alcanivorax					
		ASV18	1.515809692	0.006	Pseudomonadales	Pseudomonas					
		ASV14	1.279769589	0.008	Oceanospirillales	Alcanivorax					
Deep25	**Day 0-6**	No ASVs enriched					No ASVs depleted				
	Day 6-12	ASV2	3.681	<0.001	Alteromonadales	Pseudoalteromonas	ASV26	-10.423	<0.001	Alteromonadales	Alteromonas
		ASV10	3.864	<0.001	Alteromonadales	Pseudoalteromonas	ASV5	-5.964	<0.001	Alteromonadales	Alteromonas
		ASV53	4.751	<0.001	Alteromonadales	Pseudoalteromonas	ASV3	-3.896	<0.001	Oceanospirillales	Alcanivorax
		ASV8	4.596	<0.001	Oceanospirillales	Alcanivorax	ASV44	-7.297	<0.001	Alteromonadales	Marinobacter
		ASV79	3.392	0.001	Alteromonadales	Pseudoalteromonas	ASV34	-4.670	0.001	Alteromonadales	Alteromonas
		ASV213	5.962	0.002	Alteromonadales	Pseudoalteromonas	ASV97	-4.616	0.001	Oceanospirillales	Alcanivorax
		ASV91	3.442	0.002	Alteromonadales	Pseudoalteromonas	ASV121	-4.838	0.002	Oceanospirillales	Alcanivorax
		ASV94	3.215	0.004	Alteromonadales	Pseudoalteromonas	ASV25	-3.263	0.004	Rhodobacterales	Sulfitobacter
		ASV98	3.332	0.004	Alteromonadales	Pseudoalteromonas	ASV7	-2.945	0.004	Oceanospirillales	Alcanivorax
							ASV19	-5.443	0.006	Alteromonadales	Alteromonas
	Day 12-18	ASV1	7.678	<0.001	Rhodospirillales	Thalassospira	ASV8	-8.540	<0.001	Oceanospirillales	Alcanivorax
		ASV178	6.524	<0.001	Rhizobiales	Aurantimonas	ASV23	-5.824	0.006	Rhodobacterales	Sulfitobacter
	Day 18-24	ASV1	3.824	<0.001	Rhodospirillales	Thalassospira	No ASVs depleted				
Surface25	**Day 0-6**	ASV4	5.786	<0.001	Oceanospirillales	Halomonas	ASV7	-10.529	<0.001	Oceanospirillales	Alcanivorax
		ASV1	3.371	<0.001	Rhodospirillales	Thalassospira	ASV8	-14.463	<0.001	Oceanospirillales	Alcanivorax
		ASV16	5.659	<0.001	Oceanospirillales	Halomonas	ASV23	-10.258	<0.001	Rhodobacterales	Sulfitobacter
		ASV20	5.694	<0.001	Oceanospirillales	Halomonas	ASV6	-10.613	<0.001	Oceanospirillales	Alcanivorax
		ASV48	5.035	<0.001	Oceanospirillales	Halomonas	ASV24	-8.262	0.001	Caulobacterales	Hyphomonas
	Day 6-12	ASV15	6.453	<0.001	Alteromonadales	Idiomarina					
		ASV30	8.988	<0.001	Alteromonadales	Idiomarina					
	Day 12-18	No ASVs enriched					No ASVs depleted				
	Day 18-24	No ASVs enriched					No ASVs depleted				

Table S8. *Concentration (ppm) and degradation (%) of light alkanes at each transfer step of DISPOIL treatment under constant high pressure (HP treatment).*

	Concentration (ppm)				Degradation (%)		
Light Alkanes	**T0**	**1st**	**2nd**	**3rd**	**1st**	**2nd**	**3rd**
C10	0.003	0.000	0.002	0.003	89.956	19.532	1.431
C11	0.005	0.000	0.002	0.003	98.069	58.530	42.152
C12	0.011	0.000	0.006	0.008	97.274	46.587	29.252
C13	0.007	0.001	0.004	0.004	91.667	47.228	39.489
C14	0.013	0.001	0.004	0.005	92.897	65.193	61.551
C15	0.048	0.004	0.003	0.004	90.849	93.500	92.252
C16	0.235	0.023	0.013	0.014	90.108	94.460	93.869
C17	0.209	0.059	0.029	0.015	71.549	86.306	92.809
Pristane	0.263	0.029	0.005	0.163	89.066	98.229	37.940
C18	0.836	0.076	0.129	0.034	90.855	84.574	95.922
Phytane	0.341	0.034	0.088	0.215	90.158	74.259	37.009
C19	1.019	0.084	0.182	0.031	91.799	82.109	96.966
C20	1.168	0.128	0.275	0.075	89.044	76.460	93.589
C21	1.115	0.079	0.249	0.041	92.942	77.702	96.306
C22	1.030	0.070	0.241	0.049	93.228	76.591	95.254
C23	0.905	0.068	0.212	0.037	92.486	76.555	95.903
C24	0.829	0.052	0.281	0.104	93.783	66.117	87.493

Table S9. *Concentration (ppm) and degradation (%) of heavy alkanes at each transfer step of DISPOIL treatment under constant high pressure (HP treatment).*

	Concentration (ppm)				Degradation (%)		
Heavy Alkanes	**T0**	**1st**	**2nd**	**3rd**	**1st**	**2nd**	**3rd**
C25	0.754	0.051	0.272	0.158	93.302	63.896	79.089
C26	0.636	0.043	0.234	0.157	93.256	63.180	75.387
C27	0.533	0.040	0.227	0.177	92.420	57.334	66.780
C28	0.387	0.027	0.168	0.133	93.021	56.622	65.746
C29	0.415	0.026	0.257	0.232	93.636	38.112	43.945
C30	0.572	0.033	0.466	0.451	94.171	18.429	21.124
C31	0.544	0.026	0.463	0.454	95.144	14.755	16.563
C32	0.504	0.027	0.454	0.453	94.543	9.893	10.185
C33	0.365	0.017	0.330	0.332	95.350	9.447	8.892
C34	0.308	0.013	0.270	0.276	95.657	12.108	10.381
C35	0.207	0.013	0.188	0.109	93.671	9.505	47.598

Table S10. *Concentration (ppm) and degradation (%) of PAH compounds at each transfer step of DISPOIL treatment under constant high pressure (HP treatment).*

	Concentration (ppm)				Degradation (%)		
PAHs	**T0**	**1st**	**2nd**	**3rd**	**1st**	**2nd**	**3rd**
Napthalene	0.000598	0.000015	0.000355	0.000422	97.490	40.609	29.321
Fluorene	0.000350	0.000129	0.000065	0.000277	63.220	81.375	20.752
Dibenzothiophene	0.008260	0.001007	0.008019	0.011556	87.811	2.919	0.000
Phenanthrene	0.006785	0.001266	0.001330	0.005965	81.340	80.396	12.088
Anthracene	0.003379	0.001311	0.001344	0.006214	61.188	60.233	0.000
Fluoranthene	0.065067	0.003259	0.064697	0.064907	94.991	0.569	0.247
Chrysene	0.043387	0.002265	0.040208	0.041351	94.779	7.327	4.694
Pyrene	0.066423	0.003377	0.064916	0.065275	94.916	2.270	1.728
Benzo(b)fluoranthene	0.249529	0.012496	0.124647	0.249424	94.992	50.047	0.042
Benzo(k)fluoranthene	0.198530	0.009944	0.099134	0.198434	94.991	50.066	0.048
Benzo(e)pyrene	0.169935	0.008530	0.169236	0.169497	94.980	0.411	0.258
Benzo(a)pyrene	0.169991	0.008499	0.169919	0.169920	95.000	0.042	0.041
Perylene	0.153657	0.007684	0.153573	0.153557	95.000	0.055	0.065
Indeno(1,2,3-cd)pyrene	0.053796	0.005381	0.053795	0.053797	89.997	0.002	0.000
Dibenzo(a,h)anthracene	0.000024	0.000007	0.000009	0.000010	69.622	61.696	56.593
Benzo(g,h,i)perylene	0.000094	0.000030	0.000011	0.000033	68.040	88.279	64.370

Table S11. *Taxonomic classification of amplicon sequence variants (ASVs) identified from the Venn diagram analysis as unique under undisturbed conditions (HP treatment). Eighteen ASVs are unique for the OIL treatment, six for DISPOIL and eight are common between the two treatments.*

	ID	Class	Order	Family	Genus
OIL	ASV400	Alphaproteobacteria	Caulobacterales	Caulobacteraceae	Caulobacter
	ASV430	Alphaproteobacteria	Sphingomonadales	Sphingomonadaceae	Hephaestia
	ASV508	Alphaproteobacteria	Sphingomonadales	Sphingomonadaceae	Hephaestia
	ASV53	Alphaproteobacteria	Thalassobaculales	Nisaeaceae	Nisaea
	ASV1633	Alphaproteobacteria	Sphingomonadales	Sphingomonadaceae	Novosphingobium
	ASV1106	Alphaproteobacteria	Sphingomonadales	Sphingomonadaceae	Sphingomonas
	ASV790	Alphaproteobacteria	Caulobacterales	Caulobacteraceae	Unassigned
	ASV16	Gammaproteobacteria	Oceanospirillales	Alcanivoracaceae1	Alcanivorax
	ASV73	Gammaproteobacteria	Oceanospirillales	Alcanivoracaceae1	Alcanivorax
	ASV87	Gammaproteobacteria	Oceanospirillales	Alcanivoracaceae1	Alcanivorax
	ASV237	Gammaproteobacteria	Alteromonadales	Alteromonadaceae	Alteromonas
	ASV642	Gammaproteobacteria	Alteromonadales	Alteromonadaceae	Alteromonas
	ASV486	Gammaproteobacteria	Burkholderiales	Burkholderiaceae	Cupriavidus
	ASV19	Gammaproteobacteria	Alteromonadales	Marinobacteraceae	Marinobacter
	ASV3033	Gammaproteobacteria	Alteromonadales	Pseudoalteromonadaceae	Pseudoalteromonas
	ASV59	Gammaproteobacteria	Burkholderiales	Burkholderiaceae	Ralstonia
	ASV2574	Gammaproteobacteria	Burkholderiales	Burkholderiaceae	Ralstonia
	ASV465	Gammaproteobacteria	Burkholderiales	Comamonadaceae	Unassigned
DISPOIL	ASV43	Alphaproteobacteria	Sphingomonadales	Sphingomonadaceae	Novosphingobium
	ASV2571	Alphaproteobacteria	Rhodospirillales	Unassigned	Unassigned
	ASV2658	Babeliae	Babeliales	Unassigned	Unassigned
	ASV262	Gammaproteobacteria	Oceanospirillales	Halomonadaceae	Halomonas
	ASV477	Gammaproteobacteria	Oceanospirillales	Halomonadaceae	Halomonas
	ASV607	Gammaproteobacteria	Oceanospirillales	Halomonadaceae	Halomonas
COMMON	ASV774	Gammaproteobacteria	Oceanospirillales	Alcanivoracaceae1	Alcanivorax
	ASV1716	Gammaproteobacteria	Oceanospirillales	Alcanivoracaceae1	Alcanivorax
	ASV2738	Gammaproteobacteria	Oceanospirillales	Halomonadaceae	Halomonas
	ASV620	Gammaproteobacteria	Alteromonadales	Pseudoalteromonadaceae	Pseudoalteromonas
	ASV1013	Gammaproteobacteria	Alteromonadales	Pseudoalteromonadaceae	Pseudoalteromonas
	ASV1260	Gammaproteobacteria	Alteromonadales	Pseudoalteromonadaceae	Pseudoalteromonas
	ASV2655	Gammaproteobacteria	Alteromonadales	Pseudoalteromonadaceae	Pseudoalteromonas
	ASV2737	Gammaproteobacteria	Alteromonadales	Pseudoalteromonadaceae	Pseudoalteromonas

Table S12. *Taxonomic classification of amplicon sequence variants (ASVs) identified from the Venn diagram analysis as common between undisturbed and disrupted pressure conditions (HP-REPRESS).*

	ID	Class	Order	Family	Genus
COMMON HP-REPPRESS & OIL-DISPOIL	ASV14	Gammaproteobacteria	Cellvibrionales	Cellvibrionaceae	Aestuariicella
	ASV35	Gammaproteobacteria	Cellvibrionales	Cellvibrionaceae	Aestuariicella
	ASV122	Gammaproteobacteria	Cellvibrionales	Cellvibrionaceae	Aestuariicella
	ASV1	Gammaproteobacteria	Oceanospirillales	Alcanivoracaceae1	Alcanivorax
	ASV116	Gammaproteobacteria	Oceanospirillales	Alcanivoracaceae1	Alcanivorax
	ASV149	Gammaproteobacteria	Oceanospirillales	Alcanivoracaceae1	Alcanivorax
	ASV177	Gammaproteobacteria	Oceanospirillales	Alcanivoracaceae1	Alcanivorax
	ASV336	Gammaproteobacteria	Oceanospirillales	Alcanivoracaceae1	Alcanivorax
	ASV493	Gammaproteobacteria	Oceanospirillales	Alcanivoracaceae1	Alcanivorax
	ASV572	Gammaproteobacteria	Oceanospirillales	Alcanivoracaceae1	Alcanivorax
	ASV849	Gammaproteobacteria	Oceanospirillales	Alcanivoracaceae1	Alcanivorax
	ASV1105	Gammaproteobacteria	Oceanospirillales	Alcanivoracaceae1	Alcanivorax
	ASV1241	Gammaproteobacteria	Oceanospirillales	Alcanivoracaceae1	Alcanivorax
	ASV1605	Gammaproteobacteria	Oceanospirillales	Alcanivoracaceae1	Alcanivorax
	ASV510	Gammaproteobacteria	Oceanospirillales	Alcanivoracaceae1	Alcanivorax
	ASV573	Gammaproteobacteria	Oceanospirillales	Alcanivoracaceae1	Alcanivorax
	ASV1427	Gammaproteobacteria	Oceanospirillales	Alcanivoracaceae1	Alcanivorax
	ASV1439	Gammaproteobacteria	Oceanospirillales	Alcanivoracaceae1	Alcanivorax
	ASV1470	Gammaproteobacteria	Oceanospirillales	Alcanivoracaceae1	Alcanivorax
	ASV2	Gammaproteobacteria	Alteromonadales	Alteromonadaceae	Alteromonas
	ASV3	Gammaproteobacteria	Oceanospirillales	Halomonadaceae	Halomonas
	ASV4	Gammaproteobacteria	Oceanospirillales	Halomonadaceae	Halomonas
	ASV9	Gammaproteobacteria	Oceanospirillales	Halomonadaceae	Halomonas
	ASV11	Gammaproteobacteria	Oceanospirillales	Halomonadaceae	Halomonas
	ASV295	Gammaproteobacteria	Oceanospirillales	Halomonadaceae	Halomonas
	ASV311	Gammaproteobacteria	Oceanospirillales	Halomonadaceae	Halomonas
	ASV345	Gammaproteobacteria	Oceanospirillales	Halomonadaceae	Halomonas
	ASV389	Gammaproteobacteria	Oceanospirillales	Halomonadaceae	Halomonas
	ASV492	Gammaproteobacteria	Oceanospirillales	Halomonadaceae	Halomonas
	ASV2575	Gammaproteobacteria	Oceanospirillales	Halomonadaceae	Halomonas
	ASV1060	Gammaproteobacteria	Oceanospirillales	Halomonadaceae	Halomonas
	ASV5	Gammaproteobacteria	Alteromonadales	Pseudoalteromonadaceae	Pseudoalteromonas
	ASV6	Gammaproteobacteria	Alteromonadales	Pseudoalteromonadaceae	Pseudoalteromonas
	ASV7	Gammaproteobacteria	Alteromonadales	Pseudoalteromonadaceae	Pseudoalteromonas
	ASV17	Gammaproteobacteria	Alteromonadales	Pseudoalteromonadaceae	Pseudoalteromonas
	ASV21	Gammaproteobacteria	Alteromonadales	Pseudoalteromonadaceae	Pseudoalteromonas
	ASV32	Gammaproteobacteria	Alteromonadales	Pseudoalteromonadaceae	Pseudoalteromonas
	ASV55	Gammaproteobacteria	Alteromonadales	Pseudoalteromonadaceae	Pseudoalteromonas
	ASV656	Gammaproteobacteria	Alteromonadales	Pseudoalteromonadaceae	Pseudoalteromonas
	ASV929	Gammaproteobacteria	Alteromonadales	Pseudoalteromonadaceae	Pseudoalteromonas
	ASV516	Gammaproteobacteria	Alteromonadales	Pseudoalteromonadaceae	Pseudoalteromonas
	ASV792	Gammaproteobacteria	Alteromonadales	Pseudoalteromonadaceae	Pseudoalteromonas
	ASV1561	Gammaproteobacteria	Alteromonadales	Pseudoalteromonadaceae	Pseudoalteromonas
	ASV495	Gammaproteobacteria	Alteromonadales	Pseudoalteromonadaceae	Pseudoalteromonas
	ASV690	Gammaproteobacteria	Alteromonadales	Pseudoalteromonadaceae	Pseudoalteromonas
	ASV1730	Gammaproteobacteria	Pseudomonadales	Pseudomonadaceae	Pseudomonas
	ASV36	Gammaproteobacteria	Alteromonadales	Colwelliaceae	Thalassomonas
	ASV54	Gammaproteobacteria	Alteromonadales	Colwelliaceae	Thalassomonas
	ASV67	Gammaproteobacteria	Alteromonadales	Colwelliaceae	Thalassomonas
	ASV47	Gammaproteobacteria	Alteromonadales	Colwelliaceae	Thalassomonas
	ASV637	Gammaproteobacteria	Alteromonadales	Colwelliaceae	Thalassomonas
COMMON HP-REPRESS (OIL ONLY)	ASV24	Alphaproteobacteria	Rhodospirillales	Thalassospiraceae	Thalassospira
	ASV37	Alphaproteobacteria	Caulobacterales	Hyphomonadaceae	Hyphomonas
	ASV40	Bacteroidia	Flavobacteriales	Flavobacteriaceae	Mesonia
	ASV179	Alphaproteobacteria	Rhizobiales	Xanthobacteraceae	Afipia
	ASV733	Gammaproteobacteria	Burkholderiales	Comamonadaceae	Kinneretia
	ASV831	Gammaproteobacteria	Alteromonadales	Pseudoalteromonadaceae	Pseudoalteromonas
COMMON HP-REPRESS (DISPOIL ONLY)	ASV31	Alphaproteobacteria	Sphingomonadales	Sphingomonadaceae	Erythrobacter
	ASV130	Gammaproteobacteria	Pseudomonadales	Pseudomonadaceae	Pseudomonas

Table S13. *Identification of influential taxa based on DESeq2 analysis.*

OIL			
Genus	**ASV**	**Log2FC**	**padj**
Oleispira	ASV14	5.334195	1.16594E-11
Oleispira	ASV26	5.757119	4.3175E-10
Thalassomonas	ASV15	9.419697	1.1008E-07
Oleispira	ASV25	4.777223	2.85677E-07
Thalassomonas	ASV19	7.184695	1.85479E-06
Colwellia	ASV33	7.602275	1.85479E-06
Colwellia	ASV38	7.521535	2.30907E-05
Thalassomonas	ASV31	6.508855	2.52455E-05
Marinobacter	ASV24	2.924966	2.52455E-05
Thalassomonas	ASV39	6.942485	2.52455E-05
Thalassomonas	ASV67	6.072257	9.18221E-05
Pseudoalteromonas	ASV94	3.585154	0.000295635
Marinobacter	ASV2	2.34706	0.000584916
Colwellia	ASV105	6.156315	0.000596955
Pseudoalteromonas	ASV28	2.71617	0.000761618
Marinobacter	ASV125	4.73436	0.001221027
Colwellia	ASV108	6.021856	0.00227757
Oleispira	ASV170	4.857417	0.00227757
Pseudoalteromonas	ASV51	2.356853	0.002716096
Thalassospira	ASV27	3.130199	0.005678403
Marinobacter	ASV4	1.829085	0.01138753
Oleispira	ASV168	4.872285	0.017391177
Colwellia	ASV78	6.917348	0.017391177
Thalassomonas	ASV41	6.65573	0.024677618
Kordiimonas	ASV86	2.098709	0.035673

DISPOIL			
Genus	**ASV**	**Log2FC**	**padj**
Oceanospirillaceae	ASV107	-7.81065	1.56E-10
Pseudomonas	ASV191	-6.82477	8.85E-08
Porticoccus	ASV64	-7.00913	2.86E-07
Oceanospirillaceae	ASV145	-6.79653	4.86E-07
Oceanospirillaceae	ASV231	-5.87032	1.85E-06
Parvibaculum	ASV61	-3.19996	0.002278
Aestuariicella	ASV131	-2.8995	0.002278
Acinetobacter	ASV287	-5.29672	0.003131
Colwellia	ASV209	-3.4767	0.004148
Colwellia	ASV162	-3.31873	0.011388
Magnetospira	ASV334	-5.27469	0.011783
Acinetobacter	ASV396	-4.77981	0.026522
Idiomarina	ASV74	-2.30758	0.040955

This page was intentionally left blank